
UNIVERSITY OF BIRMINGHAM

# RELIABILITY OF POWER SYSTEMS WITH CLIMATE CHANGE EFFECTS ON PV AND WIND POWER GENERATION

By

**Abdullah Altamimi**

A thesis submitted to

The University of Birmingham for the degree of

**DOCTOR OF PHILOSOPHY**

Department of Electronic, Electrical and Systems Engineering
College of Engineering and Physical Sciences
University of Birmingham

**To my parents**

UNIVERSITY OF BIRMINGHAM

## University of Birmingham Research Archive

### E-theses repository

This unpublished thesis/dissertation is copyright of the author and/or third parties. The intellectual property rights of the author or third parties in respect of this work are as defined by The Copyright Designs and Patents Act 1988 or as modified by any successor legislation.

Any use made of information contained in this thesis/dissertation must be in accordance with that legislation and must be properly acknowledged. Further distribution or reproduction in any format is prohibited without the permission of the copyright holder.

# Acknowledgements

I would like to express my sincere and deepest gratitude to my supervisor Dr. Dilan Jayaweera, for his continuous guidance and putting his enlightening experience at my disposal. His patience, time, technical depth and contributions to the success of my studies, and full support are deeply appreciated.

I would like to acknowledge the financial support of Majmaah University and Saudi Arabian Cultural Bureau. Without their support, studying at one of the world's leading universities (University of Birmingham), would have only been a dream.

I would like also to extend my thanks to my colleagues and friends at Power System and Control Research Group for their support, sharing their knowledge with me and encouragement throughout my PhD. In particular, I wish to thank Dr. Zafar A. Khan, Bader Alharbi, Daniel Donaldson, Waleed Alabri, Dr. Manuel Alvarez-Alvarado, Dr. Hasan Gunduz, and Wilson Vasquez. I would also to thank Dr. Hamed Almutiri, Dr. Hasan Almahroug, Dr. Mohammed Alharbi for their help and support.

I would express my gratitude to my parents, Saleh and Sara, and siblings, for their endless belief in me. Words cannot express how grateful I am to them for all of the sacrifices that they have made for me. My deepest appreciation for their love, patience, understanding, and inspiration and their prayer for me was what sustained me thus far.

Special thanks to my wife Khulud and my children Sara, Nawaf and Khalid for their support, belief, love and for being there for me, even during some of the most stressful times. Without their support, unconditional love, encouragement this journey would have been very difficult.

# ABSTRACT

Concerns over global climate change has led utilities to reduce greenhouse gas (GHG) emissions by decarbonising the power sector. The accelerating rate of climate change is likely to expose a decarbonised power system to climate related stresses. In particular, Photo Voltaic (PV) and wind power generation systems comprise a significant share in the power grid, which is potentially vulnerable to climate change, and therefore may impact the reliability of power systems with their integrations. Typical reliability assessments do not consider the climate effects and related stresses either on the PV or wind power generating systems or at their component levels. Therefore, this thesis investigates and addresses the challenges of reliability assessment of power grid with the interaction of climate changes and renewable power generation systems.

As a part of the investigation, the thesis proposes a novel systematic framework to assess the PV system components' availability with the interaction of future changes in climate. The framework is developed to quantify the climate related stresses on the hierarchical levels of a PV system, which include component, subsystem, PV system and the grid. The framework was formed by considering multiple elements including thermal stress, bathtub curve, ageing and degradation level and operated on Markov chain embedded Monte Carlo simulation. The uniqueness of the framework is its ability to identify the critical components in a PV system that lead to climate-associated failures. Thesis also proposes a comprehensive framework to assess the reliability of a PV and wind power integrated power system accounting climate change impacts by deploying diverse levels of GHG emission scenarios. Uncertainties in the future climate scenarios were established by proposing an advanced stochastic model considering likelihood-based Markov chain method for generating future climate scenario. The proposed model is integrated to the reliability assessment framework to assess realistic impacts on the reliability of a power system.

Investigations were suggested the impacts of climate change effects on PV and wind power generation system were true and in quantitative terms PV systems are more vulnerable to climate change effects than wind power generating systems. The climate change related true impacts on PV and wind power generating systems could be mitigated by quantifying change in impacts quantitatively and then systematic replacement of vulnerable sub system components in time before their end of life. Further investigations suggest that IGBTs and capacitors are key components that are more sensitive to thermal stresses of climate change effects resulting a considering impacts on their availability and on the power system reliability with their presence. Further assessments also revealed that the impacts on power system reliability due to the climate change effects on PV and wind power generation system were not uniform over the long run which further emphasises the need of a quantitative and system assessment in order to expose true impacts of climate change on PV and wind power generation system extending to the entire power system reliability. The thesis provides a solid foundation of frameworks required in the quantitative assessment.

# List of Publications

Part of the above contribution were published in international journal and conferences. The list of the papers are as follows:

1- **Altamimi, Abdullah,** and Jayaweera, D., 2020. *Reliability of power systems with climate change impacts on hierarchical levels of PV systems*. Electric Power Systems Research, vol. 190, 2021.

2- **Altamimi, Abdullah**, and Dilan Jayaweera. "*Reliability performances of grid-integrated PV systems with varying climatic conditions*." (2017): 17-6. The paper was presented on IET International Conference on Resilience of Transmission and Distribution Networks (RTDN 2017) September 2017.

3- **Altamimi, Abdullah**, and Dilan Jayaweera. "*Long-Term Reliability Impacts of a Power System with Climate Change Effects on Wind Farms*.". The paper was presented on *2018 IEEE PES Innovative Smart Grid Technologies Conference Europe (ISGT-Europe)*. IEEE, October 2018.

4- Gunduz, H., Khan, Z. **Altamimi, Abdullah**, & Jayaweera, D. (2018, August). *An Innovative Methodology for Load and Generation Modelling in a Reliability Assessment with PV and Smart Meter Readings*. In *2018 IEEE Power & Energy Society General Meeting (PESGM)* (pp. 1-5). IEEE.

5- **Altamimi, Abdullah**, Peju Oyewole, and Dilan Jayaweera. "*Future Power System Study Models With Stochastic Climate Changes Imposed on Wind and PV Power generation*.". The paper was presented on *2018 IEEE PES Saudi Arabia Smart Grid Technologies Conference (SASG)*. IEEE, December 2018.

# Table of Contents

# List of Figures

# List of Tables

# Nomenclature

| | |
|---|---|
| GHG | Greenhouse Gas |
| RCMs | Regional Climate Models |
| WFs | Wind farms |
| MCS | Monte Carlo Simulation |
| LBMC | likelihood-Based Markov Chain |
| IEEE-RTS | IEEE Reliability Test System |
| RBTS | Roy Billinton Test System |
| WG | Weather Generator |
| PV | Photovoltaic |
| NERC | North American Electric Reliability Council |
| LOLE | Loss of Load Expectation |
| LOEE | Loss of Energy Expectation |
| LOLF | Loss of Load Frequency |
| LOLD | Loss of Load Duration |
| PLC | Probability of Load Curtailment |
| EDLC | Expected Duration of Load Curtailment |
| ELC | Expected Load Curtailment |
| EDNS | Expected Demand Not Supplied |
| EENS | Expected Energy Not Supplied |

| | |
|---|---|
| SAIFI | System Average Interruption Frequency Index |
| SAIDI | System Average Interruption Duration Index |
| CAIDI | Customer Average Interruption Duration Index |
| ENS | Energy Not Supplied |
| LLU | Loss of the Largest Unit |
| CRM | Capacity Reserve Margin |
| COPT | Capacity Outage Probability Table |
| RESs | Renewable Energy Sources |
| WTG | Wind Turbine Generation |
| IG | Induction Generator |
| DFIG | Doubly-Fed Induction Generator |
| PMG | Permanent Magnet Generator |
| RCPs | Representative Concentration Pathways |
| TFRCD | Task Force for Regional Climate Downscaling |
| AR5 | Fifth Assessment Report |
| SRES | Special Report on Emission Scenarios |
| IPCC | Intergovernmental Panel on Climate Change |
| FOR | Forced Outage Rate |
| PV | Photovoltaic |
| *Pdf* | Probability Density Function |

| | |
|---|---|
| $R$ | Reliability [%] |
| $P$ | Probability [%] |
| $\lambda$ | Failure rate [1/yr] |
| $\lambda_{Base}$ | Base failure rate [1/yr] |
| $\lambda_I$ | Failure in the infant period |
| $\lambda_C$ | Failure during both useful life and wear out stages |
| $\lambda_K$ | Failure of component K |
| $\lambda f$ | Degradation rate (1/yr) |
| $\prod_N$ | Number of stress factors |
| $T_U$ | Useful life of the components |
| $T_W$ | Wear out stages of the components |
| $a$ | Failure rate displacement parameter (1/yr) |
| δ | Failure rate scale |
| β | Failure rate scale during infant period |
| η | Failure rate location parameter |
| $\pi_T$ | Thermal stress factor |
| $\pi_Q$ | Quality factor |
| $\pi_S$ | Electrical stress factor |
| $\pi_E$ | Environmental factor |
| $\pi_C$ | Contact construction factor |
| $\pi_{SR}$ | Series resistance factor |
| $\pi_v$ | Voltage stress factor |
| $\pi_A$ | Application stress factor |
| $T_J$ | Junction temperature (°C) |
| $T_c$ | Case temperature (°C) |

| | |
|---|---|
| $\Delta T$ | Linear heat transfer (°C) |
| $T_{HS}$ | Hot spot temperature (°C) |
| $T_{cell}$ | PV cell temperature |
| $T_{amb}$ | Ambient temperature |
| $T_{STC}$ | Temperature at standard test condition |
| $\theta_a$ | Thermal resistance from ambient to case |
| $P_{S-loss}$ | Power dissipations in the switch |
| $P_{D-loss}$ | Power dissipations in the diode |
| $\theta_{11,22}$ ,$\theta_{12,21}$ | Thermal resistance coefficients |
| $D$ | Diode |
| $IGBT$ | Insulated-gate bipolar transistor |
| $V$ | Eigenvalues |
| $\bar{V}$ | Eigenvector |
| $G$ | Matrix |
| $i$ | Row index for matrices (p.u.) |
| $j$ | Column index for matrices (p.u.) |
| $P_{pv}$ | PV output power (MW) |
| $Eff_{pv}$ | PV efficiency |
| $R_c$ | Irradiation point ($W/m^{2)}$ |
| $G_{bi}$ | Global solar irradiation ($W/m^2$) |
| $P_{STC}$ | Rated power (MW) |
| $A_i$ | Availability of subsystem $i$ (%) |
| $U_i$ | Unavailability of subsystem $i$ (%) |
| $C_i$ | Load curtailment in system state $i$, |

# Chapter 1: Introduction

This chapter introduces the concepts of power system reliability and climate change, sets out the motivation, aim, and objectives of the research, and identifies the contributions of the PhD work to the body of knowledge. The structure of the thesis is also outlined.

## 1.1 Thesis Background

The power system is a complex electrical network and its primary function is to provide its consumers with a safe, continuous, and reliable supply of electrical energy as economically as possible. In fact, this is challenging due to random failures of equipment, which is characterized by a multitude of factors beyond the utility's control [1]. This leads to power system failures ranging from interruptions in a component at a small area to widespread blackout. Severe major power supply disturbance events have occurred frequently in recent years. The unplanned outage resulting from failures occurs due to a number of reasons including adverse climatic and server weather. For example, in June 2019, a major power outage occurred Dallas County, Texas due to a severe thunderstorm where 350,000 households were affected [2]. In July 2018, a large system outage occurred in the whole of Azerbaijan due to increase in summer temperature which resulted in enhancing the combinatorial effect of temperature and system congestion resulting in unmanageable stress on the electrical power system [3]. Climate change predictions specify that the frequency and severity of weather pattern might arise in the future, and consequently probability of failure of power system can potentially rise due to such changes in weather patterns [4]. Therefore, power system utilities need to be resilient and reliable against climate change by accounting these factors in power system studies.

Climate change poses a huge threat to power system infrastructure. Several power system components are exposed to weather related events that can lead to an adverse effect on reliability of power system [5]. For instance, the increase in temperatures induced by climate change can have significant implications in power components thermal stress. The uncertain erratic weather-related stress can pose a challenge to the existing power system infrastructure as it designed on the past or current climate conditions with limited insight into future climate change scenarios. Changes in future climate could adversely affect electric utilities, power system components and electricity demand with impacts propagating to consumers, industries and national/global economies. The weather-related events cause more than 78% of major interruptions to the U.S. power grid [6]. Random and unexpected outages make it hard for system operators to meet the power system objectives, which can have severe consequences for the consumers [1]. Apart from the extreme weather events, a gradual change in the climate is evident and is likely to adversely impact the power system [4]. Therefore, flexibility and reliability assessments are essential to mitigate the impact of the climate change.

Climate change is characterised by a change in atmospheric Greenhouse Gas (GHG) concentration level and change in weather patterns including air temperature, wind speed, sea levels storm, cloud cover, river flows, precipitation and solar irradiation, etc. According to independent analyses by National Aeronautics and Space Administration (NASA) and the National Oceanic and Atmospheric Administration (NOAA), the year 2018 was the fourth warmest year since 1880 with regard to the earth's global temperature [7]. The contemporary conventional power generation has been a major source GHG emissions [4]. Thus, policymakers are urging to decarbonise the power generation to confront the challenges of global warm and mitigate climate change. This intensified the need for the integration of renewable energy (RE) in power systems [8]. According to [9], in 2019, the share of RE integrated into the UK grid had risen to 35.5 %. In 2025, it is expected that roughly 50 % of

the total UK power consumption will be supplied by RE [9]. Among these RE sources, the most prominent are Photovoltaics (PVs) and wind power generation system due to the technological development and their unending nature.

Renewable energy generation is also subject to physical impacts of climate change with implications for the reliability and performance of the power system [10]. Wind and PV are more sensitive to climate change as they have a very high correlation with weather and a small change in weather pattern can have a substantial impact on them and consequently on the loads supplied by them [4, 11]. The effect of long-term climate change on PV and wind integrated power system can lead to additional stresses on power systems reliability due to failure in the components. Therefore, assessing the influence of RE on overall reliability has become extremely intricate due to the involvement of a multitude of factors such as degradation, aging, thermal and environmental stress. It is crucial to evaluate the reliability performance of existing PV and wind technologies integrated power system in future climate scenarios to consider any measures that can be adapted to mitigate the possible effect of climate change. The climate-related stress could also adversely impact the availability of RE components (such as PV cells or diodes), leading to a reduction of the entire system reliability. The climate-related stress may also be compounded by long-term availability losses- owing to equipment degradation. Incorporating such facets together with future climate scenarios in reliability assessment is critical, to enable power system planners and operators to measure the potential impacts of climate change and develop relevant strategies to mitigate the impact to power system components

## 1.2 Thesis Motivation and the Scope of the Research

Rising levels of GHGs are known to be causing irreversible changes in the earth's climate, an effect referred to as "climate change", which is raising global temperatures and creating other consequent alterations in weather patterns. Weather-sensitive energy sources such as PV and wind resources are expected to be influenced by the effects of climate change [12-15]. The impact of climate change on the reliability assessment of a power system comprising integrated renewable energy is a factor often ignored in long-term studies. Most power system utilities exclude impacts of climate change and unplanned outages caused by server weather from reliability indices due to the uncertainties associated with future climate and its consequences. Including climate change impact studies can potentially allow the utilities to respond to the real changes in the reliability of the power system and adopting measures to mitigate the possible effect of climate change on reliability of the power system.

The PV and wind power generation system could be exposed to more frequently adverse climate conditions than those for which they were designed, and might not function as intended to be. Due to the stochasticity of them, the reliability assessment of large-scale PV and wind-integrated power systems has become essential for establishing strategies for their planning, operation, and management. To address these challenges, an innovative framework is required to investigate the reliability performance of PV and wind integrated power system climate change effect under future different climate scenarios. Furthermore, future climate change associated failure in the existing PV system components is not usually taken into account [12]. The availability of the components is also subjected to climate stress and associated impacts such as effect of thermal stress in components. A systematic framework considering the future climate effect on the reliability of PV system components' lifespan together with degradation needs to be considered to develop a holistic assessment. An understanding of this effect on the reliability of renewable energy resources and systematic

reliability evaluation of their actual capability to supply demand is therefore essential. Therefore, to maintain the existing levels of power system reliability, quality, and continuity of supply, the power utilities should incorporate effects of future climate change by including all relevant direct and indirect effects in the design of the components in future technologies.

The best available climate projections should be used to develop a suitable model of system reliability. This can be achieved by incorporating climate change characteristics and future climate scenarios based on different GHG emission scenarios produced by regional climate models (RCMs) at high resolution. Developing a suitable assessment technique to capture the impacts of different GHG scenarios in a future scenario is imperative to reveal power grid risks and facilitate to the decision making within a design, maintenance and planning of the power system.

It is evident from the above that the effects of climate change on the reliability of RE integrated power systems are essential and often ignored. Therefore, the need for incorporating impacts of climate change on the reliability of renewable energy, their components and power system is essential to maintain the reliability of the future power system to acceptable standards. This requires developing innovative frameworks and incorporating appropriate climate model for ascertaining the impacts of climate change on the individual RE sources and impacts on the integrated power systems while considering the associated factors impacting the availability of components.

## 1.1 Aim and Objectives of the Research

The aim of the research is to develop an innovative framework to investigate the long-term impact of climate change on the reliability performance of wind and PV integrated power

systems, and hierarchical levels of a PV system. The following specific project objectives were crafted to achieve this aim:

- To review and select the most appropriate global and regional climate models relevant to the assessment of renewable power generation, particularly PV and wind power generation system.
- To develop and simulate future climate for a variety of years and GHG emission scenarios.
- To propose a probabilistic approach to assess the long-term impact of climate change on the reliability performance of a PV-integrated power system.
- To propose a novel availability approach for quantifying the impact of climate change on PV system components, PV subsystems, the entire PV system, and the grid-level system.
- To develop a new methodology for assessing the reliability of PV-system that incorporates failure resulting from thermal stress, aging, and degradation as well as the effects of climate change to identify the critical components and subsystems in a PV system that lead to climate-associated failure.
- To propose a framework for assessing the long-term impact of climate change on the reliability of a (wind farm) WF-integrated power system.
- To establish a stochastic model for generating future climate scenarios with the goal of gauging their impact on PV- and WF-integrated power systems.

## 1.2 Research Contributions

The main contributions of the research presented in this thesis can be summarized as follows:

- An innovative framework is proposed for evaluating the reliability performance of interaction of integrated PV system with the impact of future climate change. The framework incorporates the UKCP09 climate change model output for various emission scenarios, a PV power generation model, and an MCS technique. The framework enables an examination of the influence of the effects of climate change under three different scenarios and PV system aging with respect to the reliability of the overall power system. The effect of climate change on PV integrated power system increase with the rise of GHG emission. (Chapter. 4)
- A new methodology for assessing the reliability of power system with substantial WF integration was proposed. The methodology take into account URO-CORDEX climate change model under different emission scenarios, a wind power generation system model, and an MCS technique. The method can be used to quantify the potential impacts of future climate change on wind energy integrated power system to develop relevant strategies to mitigate the impact. The climate change would potentially have a considerable impact on power system reliability particularly at RCP8.5 emission scenario over long-term. (Chapter.5)
- A new likelihood-based Markov chain (LBMC)-based stochastic climate model is proposed for establishing an impact assessment through the generation of possible future climate scenarios derived from GHG scenarios. The proposed method can be used to obtain optimum strategies considering possible future scenario to improve the power system reliability performance with optimal integration of renewable energy. (Chapter. 6)
- An innovative framework is proposed for the impact of climate on reliability assessment of the hierarchical level of PV systems using analytical, MCS and Markov Chain methods. This framework contributed to the system reliability

assessment methods in integrating PV system as it considers the added PV system components' failure initiated by the climate related stress. It enhances the understanding of the effect of climate factors on system reliability. (Chapter. 7)

- A developments method for evaluating the availability and reliability of the PV array by using Markov chain model. The developed method is scalable which can be applied for both large and small PV array systems, and it used to calculate the availability, unavailability and the de-rated states of the PV array. (Chapter. 7)
- A mathematical model has been developed for estimating the availability of a PV component given the effects of PV degradation, aging, and climate. This method could be practically useful to understand the behaviour of the PV system with degradation rate during both the components' useful life and end of life. (Chapter. 7)
- Identification of critical components and subsystems within a PV system that lead to climate-associated failure. This is a vital toward reliability enhancement by mitigate the effect of future climate in critical components and considering the effect on components' design. (Chapter. 7)

## 1.3 Thesis Outline

The thesis is divided into eight chapters. After this introductory chapter, chapter 2 and 3 respectively present the literature review on power system reliability and climate change, with emphasis on renewable power generation systems. Chapter 4 and 5 propose novel comprehensive frameworks that address and investigate the impact of climate change on the reliability assessment of power system with PV and wind power generation systems, respectively. Within these frameworks, different types of climate models are used in each chapter. The climate models presented in chapter 4 and 5 were used to develop a stochastic

model to generate future emission scenarios based on GHG emission in chapter 6. The stochastic model is further used for reliability assessment of both PV and wind power generation system over long-term. Chapter 7 presents a novel framework by developing the framework given in chapter 4 to quantify the climate related stresses on the hierarchical levels of a PV system, which include component, subsystem, PV system and the grid. The developed framework formed by considering multiple elements including thermal stress, bathtub curve, ageing and degradation level and operated on Markov chain embedded Monte Carlo simulation. Finally, chapter 8 presents the conclusion of the entire research. The details of the chapters are as follow

**Chapter 2** presents the theory and literature review of power system reliability, along with an overview of the way power system reliability is affected by the integration of renewables. The concepts and definitions associated with reliability and availability are first introduced, followed by a description of the hierarchical levels associated with power system reliability: generation, transmission, and distribution. The most commonly used reliability indices and reliability evaluation methods are detailed, and the chapter also includes a review of the latest research and remaining gaps related to the reliability of integrated renewable power generation. The closing discussion explores the performance of PV- and WF-integrated power systems with respect to reliability.

**Chapter 3** highlights the concepts relevant to climate change and the emission scenarios produced by the latest climate models along with their influence on renewable energy technologies. It begins with the fundamentals of climate change: definition, causes, and supporting evidence. A critical evaluation of the literature review related to climate change is also presented, including an analysis of a number of emission scenarios and different climate models. The risks related to climate change with respect to renewable energy, power systems,

and reliability are identified. The final element discussed is the impact of climate change on renewable energy and its resources.

**Chapter 4** introduces the proposed framework for assessing the long-term impact of climate change on the performance of a large-scale integrated PV system. Also described are the UKCP09 climate change model, the simulations performed, the UKCP09 Weather Generator (WG), and the emission scenarios, along with key findings and output samples. PV system modelling and the IEEE-RTS are also reviewed, along with an analysis of PV system reliability and the case studies conducted.

**Chapter 5** covers the assessment of the effects of climate change on the reliability performance of a power system comprising integrated large onshore WFs. The methodology is defined: the WF and wind power generation system models as well as the CORDEX and EURO-CORDEX climate change models, along with their simulations, emission scenarios, structures, timescales, and output samples. Also introduced are the adapted RBTS and the reliability of wind power generation system under the effects of climate change. The chapter ends with the parameters of the case studies conducted for the validation of the proposed framework.

**Chapter 6** describes the development of a proposed a stochastic model for generating future climate scenarios enabling determination of their impact to power systems that contain renewable power generation. The chapter sets out the methodology; the LBMC method; the PV and wind power generation system model; and the climate change simulation, including emission scenarios and the steps in the simulation. It concludes with a discussion of reliability performance and the results of each case study.

**Chapter 7** explains the proposed approach for the long-term reliability assessment of PV-integrated power systems, which includes consideration of the effects of climate change on PV

system hierarchical levels. The proposed framework is examined, including weather simulation and the reliability of the hierarchical model. Details of the component, subsystem, PV system, and grid hierarchical levels are also spelled out. Further elements presented are the proposed Markov Chain model, the availability and reliability of the specifics of the PV system components, and the power generation model. The chapter finishes with an analysis of the reliability evaluation and discussion of the case studies.

**Chapter 8** provides a summary of the thesis findings, the conclusions that can be drawn out of the investigations, and the main contributions of the research. Potential future investigations and recommendations are also suggested.

# Chapter 2: Power System Reliability: Literature Review

## 2.1 Introduction

Electrical power is the main pillar on which so many aspects of life are centred and modern power industries find it very challenging to meet customer expectations at all times. A power system consists of three main subsystems, i.e. generation, transmission and distribution systems. Their objectives are to provide an uninterrupted, reliable supply of quality electricity to all types of customers [1]. However, random and unforeseen outages make it hard for them to meet all of these objectives. The substantial social and environmental consequences associated with outages have intensified the need for more thorough reliability assessment. While redundant equipment constitutes a way to improve the reliability of power supply to end-users, this philosophy might result in additional supply costs for customers [16]. For these reasons, power system reliability assessment methods and reliability indices to quantify the performances of the systems have been proposed and further developed as a means of assessing power system segments and components. In developed countries, power system planning, design, and operating criteria have evolved over a number of years due to continuing growth in renewable power integration, growth in electricity demand, and ongoing climate change [4]. These factors have led to additional stresses on power systems, and assessing their influence has become extremely difficult and complex.

With respect to the climate change factor, the anticipated changes in power demand over the coming decades may pose numerous challenges for the power system sector, including all three of its main subsystems: generation, transmission, and distribution [4]. On the generation side, a greater share of renewables in the energy mix is necessary for mitigating climate change and strengthening energy security and system resilience [4, 17]. The integration

of renewable power generation into a power system may lead to protect against the failure of the entire power system [16]. Even a mix of supplies, including conventional and renewable power generation, are themselves vulnerable to impacts of climate changes, which include global warming, extreme events, changes in weather patterns, and in the availability of wind, solar, and hydropower resources [18]. Current transmission and distribution systems/networks have been developed taking into account historical climate data - a method that fails to take into account probable changes in the frequency and intensity of climatic conditions, including wind, lightning, ice storms and global warming [19]. Such weather-related uncertainties may lead to substantial mismatches in supply and demand. On the demand side, rises in temperature can influence the balance of heating and cooling patterns, having a substantial negative effect on power demand and supply, thus leading to reliability issues [20]. The key point is that, in combination with population increases, future global climate change will pose new challenges with respect to electricity demand [20].

Power system reliability has emerged as a powerful platform for grasping the impact of climate change on a power system and its components [4], thus making this factor vital for ensuring that electricity supplies can always meet the load demand adequately under all conditions. New platforms for the evaluation of power system reliability must be developed so that the effects of weather on power system components can be measured.

This chapter introduces the basic reliability concept and gives an overview of power system reliability, along with an explanation of the impact associated with the integration of photovoltaic (PV) systems and wind power generation system with respect to the evaluation of power system reliability. The concepts and definitions associated with reliability and availability are presented in section 2.2. Section 2.3 describes the basic hierarchical levels of power system reliability: generation, transmission, and distribution. Sections 2.4 and 2.5 detail the most commonly used reliability indices and reliability evaluation methods, respectively.

Section 2.6 provides a review of the latest research and remaining gaps related to the reliability of integrated renewable power generation. The performance of a PV integrated power system is discussed with respect to reliability in section 2.6.1, while the reliability evaluation of a power system containing wind generation is outlined in section 2.6.2.

## 2.2 Attributes of System Reliability and Availability

Reliability is defined as the probability that an item/component/system will continue to function and to achieve the required level of performance under specified conditions and periods of time [1]. In the context of power systems, reliability is the ability of a system to deliver electricity to customers in order to meet the required demand at an acceptable level at all times. Power system reliability is defined by the North American Electric Reliability Council (NERC) as "the degree to which the performances of the electrical system elements result in power being delivered to consumers within the accepted standard and in the amount desired" [21] .Reliability $R(t)$ can be defined mathematically as given in (2.1), which is related to the probability density function $f(t)$ [1].

$$R(t) = \int_{t}^{\infty} f(t)\, dt \tag{2.1}$$

Availability *A(t)*, is the characteristic probability of the performance of power system facilities/ elements that will provide a required operation under a specific condition during a specific period, as measured in percentage [21]. In contrast, unavailability is the antithesis of availability. Availability can be defined mathematically as [22]

$$A(t) = \frac{Total\ system\ operating\ time\ (Uptime)}{Total\ simulation\ time\ (operting\ cycle)} \tag{2.2}$$

As illustrated in **Figure 2.1,** power system reliability analysis is normally divided into two basic concepts: system **adequacy** and system **security** [22-24]. In general, the concept of system adequacy is related to the sufficiency of the existing generation to supply the electricity demand and includes the ability of the transmission and distribution segments to deliver the generated power to the load point [25]. The concept is thus associated with all steady-state conditions that do not include the dynamic conditions of the system. On the other hand, the concept of system security is related to the ability of the system to react and to survive any transients disturbances that occur within the system. In particular, it refers to random and unforeseen disturbances and the avoidance of system failure as a result of such disturbances.

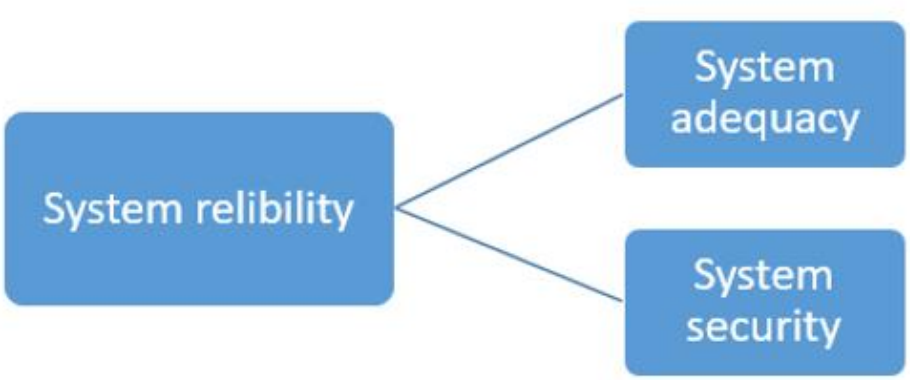


**Figure 2.1.** Main subdivisions of power system reliability

## 2.3 Hierarchical Levels of Power System Reliability

As illustrated in **Figure 2.2**, to some extent, the hierarchical levels involved in an evaluation of power system reliability comprises of the three common segments of in a power system: generation, transmission, and distribution [22, 26-28]. The first hierarchical level (HL I) is related to the reliability of generation facilities with respect to their ability to meet the desired demand, which is generally called "generating capacity reliability evaluation". HL I studies are based on the assumption that the ability of both the transmission and distribution systems to deliver electricity to the load point is fully reliable and can therefore be ignored

[24]. **Figure 2.3** represents the basic HL I generating system model, in which the total load is supplied by the generation of the entire system. At the second hierarchical level (HL II), the reliability assessment of both the generation and transmission networks is considered, along with an assessment of their ability to meet requirements at the grid supply points. These include the operational constraints of the transmission system (thermal limits and voltage limits, etc.) which are the targets of most power utility assessments [24].

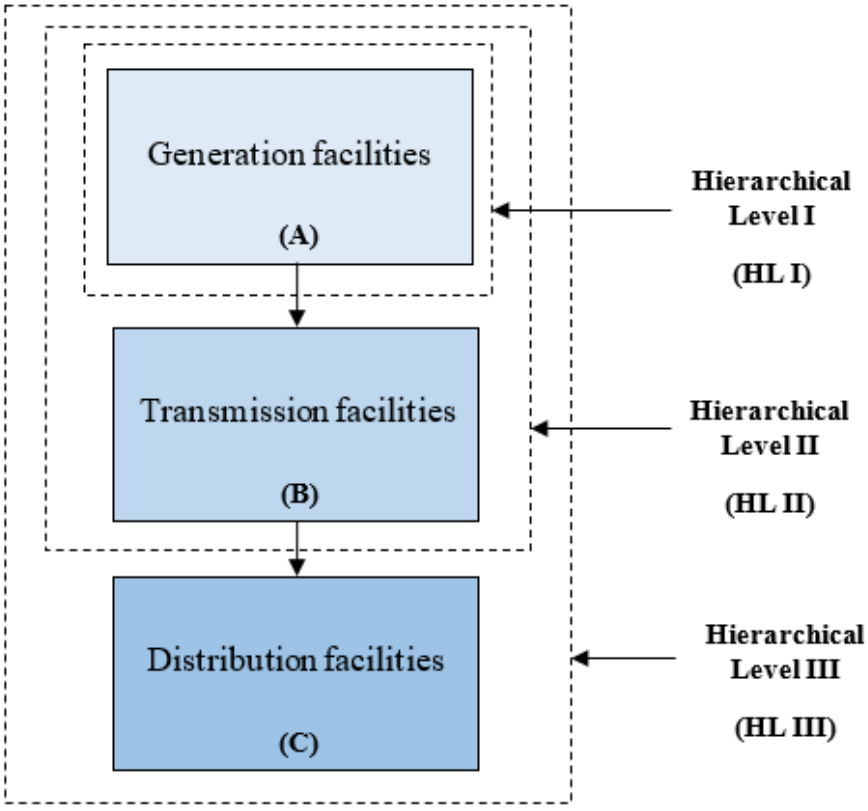


**Figure 2.2** Hierarchal levels of power system reliability [24]

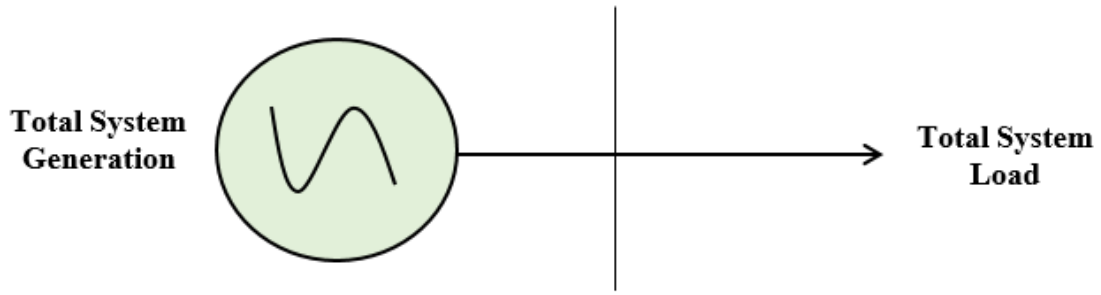


**Figure 2.3**. Basic HL I generating system model

The third and final hierarchical level (HL III) represents the most complex assessment level because it is associated with the ability of the power system to meet the electricity demands of individual customers. It is thus related to the ability of all three power system segments, from the supply point to the customer point, including generation, transmission, and distribution, to meet "end-use customer" demand. To reduce the complexity of this level, an assessment of HL II output is employed as input for HL III studies [22, 29]. A variety of reliability indices can be used as metrics for assessing system performance at each hierarchical level, as explained in the next section.

## 2.4 Reliability Indices

The reliability indices used for quantifying the expected statistical value of the future reliability level of a power system. The power utility industry has developed a number of reliability indices for measuring the duration of an outage, the response time, the frequency of occurrence, and the number of customers who lost power [1]. The existing literature includes reference to numerous reliability indices designed for different uses at the three hierarchical levels [22, 24, 30]. The main significant reliability indices can be classified as indicators of probability, expectation, duration, and frequency [31]. Probability and expectation indices measure the manner in which an expected event will occur and its consequences; the duration

and frequency indices measure the anticipated length of time the event will last and how often it might recur [31].

The following subsections explain the most common indices employed for each of the hierarchical levels.

### 2.4.1 HL I Reliability Indices

The most common indices for assessing the adequacy of a generation system at HL I are Loss of Load Expectation (LOLE), Loss of Energy Expectation (LOEE), Loss of Load Frequency (LOLF), and Loss of Load Duration (LOLD). These indices can be described mathematically as follows [22].

1) Loss of load expectation**:** LOLE represents the probability that the cumulative power supply will be unable to cover power consumption. For reliable generation, the LOLE limit value is 10 h per year [32]. A higher LOLE number thus indicates outages in existing units. LOLE can be described mathematically as follows:

$$LOLE = \sum_{i \in S} P_i \, T_i \tag{2.3}$$

where $LOLE$ is measured in (h/year), $P_i$ indicates the individual probability associated with the system state, $T_i$ represents the duration of the loss of the power supply of system state $i$, and $S$ denotes the set of all system states related to the loss of load.

2) Loss of energy expectation**:** LOEE is used for calculating the expected energy not supplied due to insufficient installed capacity or to outages in the capacity, as follows:

$$LOEE = \sum_{i \in S} 8760 \; P_i \; C_i \tag{2.4}$$

where LOEE is measured in (MWh/year), $P_i$ denotes the individual probability associated with the system state, and $C_i$ represents the loss of load for system state $i$. The LOEE index indicates the expected energy not supplied by the generating system as a result of an imbalance between the load demand and the available generation capacity [22].

3) Loss of load frequency**:** LOLF represents the expected frequency of future generation occurrence in a given period [23].

$$LOLF = \sum_{i \in S} F_i - f_i \tag{2.5}$$

where $LOLF$ is measured in (occ./year), $F_i$ indicates the frequency of the departing system state $i$, and $f_i$ refers to a portion of $F_i$.

4) Loss of load duration**:**

$$LOLD = \frac{LOLE}{LOLF} \tag{2.6}$$

where $LOLD$ is measured in (h/disturbance).

### 2.4.2 HL II Reliability Indices

In HL II studies, additional indices are required for the assessment of the composite system adequacy that characterizes a transmission system. The most common indices used for assessing transmission system adequacy at HL II are Probability of Load Curtailment (PLC), Expected Duration of Load Curtailment (EDLC), Expected Load Curtailment (ELC), Expected Demand Not Supplied (EDNS), and Expected Energy Not Supplied (EENS). These indices can be described mathematically as follows [22]:

1) Probability of load curtailment**:**

$$PLC = \sum_{i \in S} P_i \tag{2.7}$$

where $P_i$ represents the probability associated with system state $i$, and $S$ refers to the set of all system states related to load curtailment.

2) Expected duration of load curtailment:

$$EDLC = PLC \times 8760 \tag{2.8}$$

where $EDLC$ is measured in (h/year).

3) Expected load curtailment:

$$ELC = \sum_{i \in S} C_i \ F_i \tag{2.9}$$

where $ELC$ is measured in (MW/year), $C_i$ denotes the load curtailment in system state $i$, and $F_i$ represents the frequency of departing system state $i$.

4) Expected demand not supplied:

$$EDNS = \sum_{i \in S} C_i \ P_i \tag{2.10}$$

where $EDNS$ is measured in (MW), $C_i$ indicates the load curtailment in system state $i$, and $P_i$ denotes the probability associated with system state $i$.

5) Expected energy not supplied:

$$EENS = \sum_{i \in S} C_i \ F_i \ D_i = \sum_{i \in S} 8760 \ C_i \ P_i \tag{2.11}$$

$$EENS = EDNS \times 8760 \tag{2.12}$$

where $EENS$ is measured in (MWh/year), $D_i$ represents the duration of system state $i$, $C_i$ denotes the load curtailment in system state $i$, and $F_i$ indicates the frequency of departing system state $i$. The EENS index is very common and is similar to LOEE in HL I studies.

### 2.4.3 HL III Reliability Indices

HL III studies, on the other hand, require different adequacy indices in order to reflect the composite nature of a distribution system. These indices can be used for measuring future and past system performance. The most common ones employed for assessing distribution system adequacy at HL III are the System Average Interruption Frequency Index (SAIFI), the System Average Interruption Duration Index (SAIDI), the Customer Average Interruption Duration Index (CAIDI), and Energy Not Supplied (ENS). These indices can be described mathematically as follows [22]:

1) System Average Interruption Frequency Index:

$$SAIFI = \frac{\sum_{i \in R} \lambda_i \ N_i}{\sum_{i \in R} N_i} \tag{2.13}$$

where $SAIFI$ is measured in (interruptions/customer/year), $R$ represents the set of load points in the system, $\lambda_i$ denotes the failure rate at load point $i$, and $N_i$ indicates the number of customers at load point $i$.

2) System Average Interruption Duration Index:

$$SAIDI = \frac{\sum_{i \in R} U_i \ N_i}{\sum_{i \in R} N_i} \tag{2.14}$$

where $SAIDI$ is measured in (h/customer/year), $U_i$ refers to the unavailability of the system in (h/year) at load point $i$, $\lambda_i$ denotes the failure rate at load point $i$, $N_i$ indicates the number of customers at load point $i$, and $R$ represents the set of load points in the system.

3) Customer Average Interruption Duration Index:

$$CAIDI = \frac{\sum_{i \in R} U_i \ N_i}{\sum_{i \in R} \lambda_i N_i} = \frac{SAIDI}{SAIFI} \tag{2.15}$$

where $CAIDI$ is measured in (h/customer interruption), $U_i$ represents the unavailability of the system in (h/year) at load point $i$, $\lambda_i$ indicates the failure rate at load point $i$, $N_i$ denotes the number of customers at load point $i$, and $R$ refers to the set of load points in the system.

4) Energy not supplied:

$$ENS = \sum_{i \in R} L_i \;\; U_i \tag{2.16}$$

where $ENS$ is measured in (kWh/year), $L_i$ indicates the average load in kW not supplied to load point $i$, and $U_i$ represents the unavailability of the system in (h/year) at load point $i$.

The adequacy indices presented above for the three hierarchical levels are the expected values of probability distributions, which are not deterministic values. Although each hierarchical level involves different adequacy indices, they are essentially similar from a probabilistic logic perspective [22]. Details of additional adequacy indices, including more extensive descriptions of the indices related to each hierarchical level, are given in [22, 24, 30, 33]. The calculations of the indices involve at least one of the reliability approaches, which are described in the next section.

## 2.5 Approaches to Reliability Evaluation

Reliability assessment methods for evaluating the performance of a power system are typically divided into two main categories: deterministic and probabilistic [1]. Deterministic methods, such as loss of the largest unit (LLU) and capacity reserve margin (CRM) evaluations, are used for maintaining the adequacy of a power system under most system outages, with the exception of low-probability outages in the generation or transmission subsystem [32, 34]. One major drawback of this approach is that it cannot deal appropriately with renewable generation due to the high degree of intermittency and uncertainty associated with renewable energy [35]. In probabilistic approaches, on the other hand, power system behaviour and performance are modelled more comprehensively and include consideration of a variety of factors that impact

the system. These techniques can be classified into two streams: analytical and simulation-based (e.g. Monte Carlo simulation (MCS)) or can be hybrid methods [1, 22].

Analytical approaches are based primarily on the concept of mathematical models as a means of evaluating system reliability: they lead to numerical solutions [36]. In contrast, simulation approaches provide comprehensive solutions for assessing system reliability by simulating system behaviour and the actual processes of the system with the use of statistical approaches based on historical data.

A number of analytical techniques have been proposed and applied in studies such as [37, 38]; among the common examples is a generation model, which is used for calculating a capacity outage probability table (COPT) [33]. Other analytical techniques in common use for evaluating the reliability of power systems include a fuzzy fault tree [39], fault tree analysis [40-42], event tree analysis [43], a binary decision diagram [44], a reliability block diagram [45], the state-space method [46], and a Markov process [47].

For studies of large systems, an MCS is employed for assessing power system reliability [48-50]. Both the analytical and MCS techniques provide advantages and disadvantages. Analytical methods are simple, efficient in reliability analysis, relatively fast with respect to computation time, and accurate for a small grid for a specific time, but they are complex for large grids due to the long computation time required and the difficulty inherent in developing representations of a physical system model [32, 51]. In fact, analytical methods fail to evaluate a real system process effectively because they are based on predefined probabilities. Another disadvantage of an analytical method is that it cannot deal with sequentially time-dependent events [5]. The main advantage of a simulation-based method over an analytical method, in contrast, is that it enables the simulation of a real and complex power system in order to quantify the reliability indices [52]. Simulation-based methods are thus more appropriate for

complex and larger power systems, especially given the intermittent nature of renewable integration and the stochasticity of failure and environmental conditions [35]. The work presented in this thesis involved the use of a simulation method based MCS and a hybrid reliability method that combines both an analytical and a simulation technique, as explained in a later in the chapter.

### 2.5.1 Monte Carlo Simulation

Because of the associated increased system state space, simulation methods are generally used with a large power grid and also often for consideration of complex system input, such as the impact of weather [5]. A simulation method is based on MCS and enables an evaluation of power system reliability in a stochastic framework in which the system states are selected randomly. As an alternative to analytical methods, MCS is often applied for determining how random component failures disrupt system performance [32]. Historical component behaviour, such as failure and recovery times, is an essential element in MCS [8].

MCS can be classified into two methods: sequential and non-sequential [53]. Moreover, a hybrid model that combines both techniques can also be developed. In sequential MCS, the system state is sampled chronologically according to the components of historical system operation, so that time-related events can be considered [53, 54]. The sequential version is also referred to as a state duration sampling technique since it is reliant on a sampling of the probability distribution of the state durations of the components. On the other hand, in non-sequential MCS, or state sampling techniques, the system state is obtained from a random selection of time intervals through the random sampling of component states, load states, and the network state. This method is thus independent of chronological time [22].

However, as mentioned earlier, MCS is a type of sampling process used for estimating indicators of system reliability, such as demand not supplied or energy not supplied. These indicators represent expected statistical values that denote prospective performance with respect to power system reliability. The accuracy of the reliability indicators is dependent on the number of iterations of MCS and meeting convergence criteria [32]. Thus, for accurate estimates of reliability indices, the simulations must include a large number of iterations and may also need to meet other specific criteria[51, 55].

### 2.5.2 Markov Chains

One analytical method of evaluating the performance of a power system with respect to reliability is based on a numerical algorithm called a Markov chain. A Markov chain is a stochastic model in which future states are restricted based only on the current state rather than on the entire history [1]. A Markov chain method can be used to evaluate the reliability, availability and maintainability of systems [1, 56, 57]. Each component in a system is represented by possible states, for example by two states: either up or down. This example is also called a binary-state model. The probabilities of being in either an up or a down state are termed the availability and unavailability of the component. For reliability assessment purposes, availability and unavailability are vital elements of component performance. The two-state model can also be extended to take into account other specific state dependencies, based on the operating conditions associated with the components, such as aging and degradation.

The probability of a process moving between states describes the transition from a current to a future state and is defined using a transition rate matrix. A future state is then dependent only on the present state as input, instead of previous state. A Markov chain technique uses the failure and repair rate of the components for calculating the probability of a

transition as well as for computing the probability associated with each system state [47]. This method is accurate for systems with a small number of components and becomes additionally complicated as the number of components increases [1]. One disadvantage of this method is thus the difficulty of building a diagram for a huge system with a large number of components [5]. Numerous studies have involved the implementation of a Markov chain method for a variety of applications. For example, in [47], an analytical method based on a Markov chain was employed for the reliability assessment of the availability of wind farm generation. In [58], the author proposed a solar generation model based on a Markov Chain in order to estimate the power generated from a solar cell. As reported in [5, 59], a Markov chain has also been used for the reliability assessment of simple power system components.

## 2.6 Overview of Renewable Power Generation Reliability

Because renewable generation is intermittent, their behaviour differs from that of conventional power generation. According to the UK Department for Business, Energy and Industrial Strategy, in the UK, the share of electricity generation attributable to renewables had risen to 35.5 % for the second quarter of 2019 [9]. This amount includes renewable sources such as wind, solar PV, hydro, and bioenergy, but of these sources, PV and wind energy are the fastest growing. It is also expected that approximately 50 % of the total UK power consumption will be supplied by renewable energy by 2025 [9]. However, the variable and intermittent nature of renewable energy sources (RESs) makes consideration of RES integration a vital aspect of the reliability assessment of power systems. In cases involving such integration, the reliability performance of grid-connected renewable power generation should be carefully re-evaluated based on consideration of additional uncertain factors such as climate change. An extensive range of studies focusing on the reliability performance of power systems

and renewable power generation are available in the literature. However, very few studies are targeted at assessing the impact of climate change on RESs. Most previously published reports have failed to take into account the impact of climate change on the reliability of integrated renewable power systems, and none of these studies proposes a method of systematic and comprehensive reliability assessment. The following subsections discuss the studies most relevant to the reliability performance of two of the most common renewable generation technologies: PV systems and wind power.

### 2.6.1 Reliability of PV Power Generating Systems

The global contribution of PV power to the electricity mix is gradually increasing, but PV generation is highly variable due to its dependence on meteorological conditions. For these reasons, the reliability assessment of large-scale grid-connected PV systems as a basis for establishing their operation, planning, and management strategies has become vital. Reliability assessment is also essential for quantifying the risk associated with a PV system and for regulating effective measures for mitigating that risk [11]. The reliability performance of a PV system is affected by a range of factors: the type of configuration, the failure points of the PV system components, the lifetime and location of the system, and the ambient conditions [60, 61]. Some of these aspects might not result in the failure of the entire PV system, but they could still influence the variability and availability of the PV output [62]. In fact, these aspects can lead to the derating of PV system performance and therefore the degrading of the ability of the PV system to supply the load, which results in reliability issues. These concerns must be taken into consideration during the design stage in order to establish the appropriate level of reliability for the PV system and its components [63].

However, the existing state of the art with respect to integrated PV power system reliability is very broad and has included an examination of a variety of PV features, including system generation profiles with PV penetration, methods of evaluating PV system reliability, the failure rates of critical PV system components, the cyber-physical components that affect PV system reliability, and the reliability associated with different PV system configurations. Reliability assessment that incorporates consideration of environmental factors and the effects of ambient conditions on grid-integrated PV system reliability has, until now, not been a subject of in-depth investigation. In particular, the impact of long-term climate change on an integrated PV system has previously been an unexplored research avenue due to the uncertainties associated with climate change. This area is one of the aspects examined in the following chapters of this thesis.

PV systems can be designed to have a small- or large- scale capacity, from a few kW up to several MWs, and are normally configured as one of two possible connection structures: either stand-alone [64] or grid-connected [65, 66]. Large-scale grid-connected PV systems are structured as centralized topology, a string topology, or a multi-string topology [67]. The structure of these topologies is dependent mainly on the connections to the inverters, which convert power from DC to AC. The structural topologies and internal electronic parts of the inverter have an enormous impact on the reliability performance of a PV system [68]. In the study presented in [69], the reliability and sensitivity of an integrated PV system were determined for both string inverter and central inverter configurations. The proposed model incorporated ambient weather and the effects of aging into the PV system failure rates.

Researchers have suggested a number of analytical and simulation methods for evaluating reliability studies associated with PV systems: MCSs [70-72], Markov chains [73, 74], a block diagram [75], fault tree analysis [40], and fuzzy logic [76]. MCS methods are reported in [70, 71] for the assessment of the reliability of PV-integrated and isolated power

systems, with hourly solar irradiation constituting input for both the PV system [70] and battery storage [71]. The studies were aimed at applying the MCS for an investigation of the influence of solar irradiation and battery storage on reliability performance. A simplified reliability block diagram was proposed in [75] as a method of modelling PV system reliability, and the availability and failure rate of the system were identified. In [77, 78], the authors presented Markov chain models designed for evaluating the reliability performance of small-scale PV systems. A new mathematical model based on a Markov chain, which incorporated the effects of variations in insolation, was proposed in [79] for the assessment of PV system reliability. However, a Markov chain has limitations with respect to scope and applications, such as its inability to provide accurate estimates of some energy yield metrics [78].

The reliability of PV system components is highly uncertain due to the nature of the ambient conditions, which poses major challenges in regard to the design of a large-scale PV system. For this reason, most of the available studies published in the literature have been concentrated on the reliability of PV power conversion components [80, 81], while only a few studies have focused on the entire PV system. The consequent belief is that the majority of PV system failures are related to the power electronic components [82-84]. For example, the reliability performance of the subsystems has been evaluated for a PV module [85, 86], for a DC-AC inverter [83, 87], and for a DC-DC converter [80, 81]. Other studies have focused on component details, including insulated-gate bipolar transistors (IGBTs) [84, 88], capacitors [88], and diodes [87, 88]. In [88, 89], the researchers employed an analytical model based on the FIDES methodology for evaluating the reliability performance of a DC-DC converter and a DC-AC inverter and for estimating their failure rates. The FIDES methodology enables a prediction of the reliability of the components, based on consideration of different stress factors and time sequences. In the same way, other researchers [81, 83] have used Military Handbook MIL-HDBK-217F for estimating the reliability performance of power electronic components.

MIL-HDBK-217F is an analytical model employed for evaluating the inherent reliability of US military electronic components and thereby improving system reliability [90]. Considering PV subsystems and components in this way might enable identification of the weakest parts and indicate appropriate modifications that would enhance overall reliability [91].

The lifetime and location of a PV system and its components are also essential aspects that can influence PV system reliability. The effects of lifetime degradation and geographic location on an integrated PV system inverter were assessed as reported in [61], with the goal of evaluating their impact on the reliability performance of the inverter. The authors of [89] used the FIDES methodology to study the effects of different geographic locations on the PV generation profile and PV system reliability. Their study showed that geographic location and ambient weather have an enormous impact on overall PV system reliability. The reliability assessment of a PV system power inverter for design purposes was proposed in [92]; the goal of the study was to reduce the stress on the inverter in order to maximize its lifetime.

The effects of weather and ambient conditions are significant considerations that should be taken into account during the reliability assessment of a PV system due to the uncertainties associated with weather. Environmental factors and climate change pose additional challenges for grid-integrated PV systems [11]. A fuzzy c-means method was implemented by the authors of [93] as a method of estimating PV output power based on the use of historical weather data for the reliability assessment of a grid-connected PV system. Their method was based on a clustering technique, which is very sensitive, is characterized by low intrusion detection, and is therefore not preferred for this type of study [94]. An MCS-based reliability method was proposed for the assessment of normal and adverse weather effects on an electricity distribution system and a PV generation system [95]. Solar irradiation is the primary source of PV power generation [96], but other weather factors can also affect the power output from a PV system [97]. In the study reported in [96], solar irradiation was employed as the only main factor for

determining the profile of a solar cell generator farm, with temperature being neglected. The relation between the output power $P_{PV}$ in (MW) and solar irradiation can be expressed mathematically as follows [96]:

$$P_{PV} = \begin{cases} P_r \left({G_{act}}^2 \,/\, (G_{std}\, R_c)\right) & 0 \le G_{act} < R_c \\ P_r \ (G_{act} \,/\, G_{std}\,) & R_c \le G_{act} < G_{std} \\ P_r & G_{act} > G_{std} \end{cases} \quad (2.17)$$

where $G_{act}$, $G_{std}$ represent, respectively, the actual solar irradiation and the standard solar irradiation, usually set as 1,000 ($W/m^2$); $R_c$ indicates a specific irradiation point usually set at 150 ($W/m^2$); ; and $P_r$ denotes the rated power of the PV farm.

In a more recent study [40], fault tree analysis was used in order to include consideration of solar insolation and wind speed in an assessment of the reliability performance of a hybrid renewable energy system containing PV and wind energy. Similarly, MCS has been applied in order to take solar irradiation and ambient temperature into account for the evaluation of the reliability of a grid-connected PV system [97]. In these studies, the impact of the ambient weather was applied only as input to the PV generation model, while the impact of weather on the components was neglected. The influence of ambient weather and environmental conditions on grid-connected PV systems and their components has thus not previously received a great deal of attention. Prior to the work presented here, the uncertainties associated with the impact of future weather and climate change over the long term had not been very well captured, nor had any researchers examined the long-term impact of climate change on an integrated PV system. This topic constitutes one of the primary research areas targeted in this thesis.

An integrated PV system is also affected by and interacts with the impact of climate change, but until now, the level of that impact remained to be investigated [4]. Climate change

can affect a PV resource with respect to factors such as cloud cover and ambient temperature, which can cause variations in the amount of power generated [4]. The ambient temperature can also have an effect on PV components because it contributes to overall failure [18]. These variations in the power generated and in the occurrence of failures have an enormous influence on the voltage and power flow, with a resultant significant impact on grid reliability and PV system integration [18]. The application of regional climate models for the development of comprehensive models of the impact of climate change on integrated PV systems is therefore vital for obtaining estimates of the level of that impact.

Based on the above discussion, although the literature contains sufficient reports about reliability analyses of grid-connected PV systems, the studies available have focused on some aspects of reliability while others have been left unexamined. Only a few studies of an entire PV system have been conducted, and most of these have been focused on only one PV reliability level, such as the components level, the subsystem level, or the system level. Other work has been concentrated on a variety of PV factors, such as subsystem failure rates, location, the lifetime of the components, and ambient conditions. However, these studies were based on simplified assumptions, and the power system models were not highly detailed. In point of fact, according to the existing research, no comprehensive framework had previously been created for evaluating the reliability of an entire PV system while including consideration of the impact of climate change. Therefore, acquiring an understanding of the impact of climate change on the reliability of grid-connected renewable power generation represents a challenge that had not been addressed before this study.

### 2.6.2 Reliability of Wind Power Generating Systems

Over the past few decades, the penetration of wind power generation system has been growing rapidly because it provides clean energy and an alternative to thermal power

generation based on fossil fuels [8]. Replacing existing thermal power generation wind power generation system is challenging, but reduction targets for greenhouse gas (GHG) emissions is driving the increases in the penetration of wind generation [8]. In 2018, installed wind power generation system amounted to 51.3 GW, which brought the total global installation at that time up to 591 GW [8]. Wind power generation system is well known to be dependent on weather, thus rendering it a variable and intermittent form of energy. The uncertainties and fluctuations associated with wind speed and other weather factors can affect the reliability and operation of a power system integrated with wind power generation system, which presents significant challenges for grid operators [98]. Consequently, the reliability of a wind-integrated power system must be carefully assessed for both power system planning, operation, and additional considerations must be considered during a reliability assessment.

Because the high penetration of wind power has created ongoing concern, a considerable amount of research has been targeted at assessing the reliability of a power system with integrated wind power generation system, with an extensive range of studies having been focused on a variety of aspects related to this topic: wind turbine generation (WTG) characteristics and the wind speed regime, environmental concerns, geographic location, the contribution of wind generation to a power system, approaches to assessing the reliability of wind power generation system, and the reliability associated with different types of wind turbines. A number of issues have also arisen with respect to grid-integrated wind power generation system, such as the fact that wind power is highly random and intermittent in nature due to the uncertainty inherent in wind speed, which could affect capacity credit of wind [4, 99]. The capacity credit is also a vital indicator employed by some researchers for measuring the capacity of a conventional generator that can be replaced by a wind power generator while maintaining the same level of reliability [100, 101]. In contrast with conventional generation, the power output by a wind turbine is modelled as a function of the wind speed and is dependent

on variations in the wind speed and the nominal capacity of the turbine. The relationship between the output power and wind speed is nonlinear and is represented by a typical power curve, such as the one shown in **Figure 2.4** [102]. The curve is dependent on the primary parameters: the wind turbine capacity and the values of the cut-in, rated, and cut-out wind speeds [103]. The cut-in wind speed is the minimum speed at which the wind turbine will begin to generate power. The rated wind speed is the wind speed level at which the wind turbine reaches its nominal capacity and generates the rated power. The cut-out wind speed is the maximum speed beyond which the turbine will shut down. The power curve can thus be expressed in terms of these parameters, as follows [104]:

$$P = \begin{cases} (A + B \times U + C \times U^2) \times P_r & U_{ci} \leq U < U_r \\ P_r & U_r \leq U < U_{co} \\ 0 & U \geq U_{co} \end{cases} \quad (2.18)$$

where $U$ indicates the wind speed in (m/s); $U_{ci}$ represents the cut-in speed of the wind turbine in (m/s); $U_r$ denotes the rated speed of the turbine in (m/s); $U_{co}$ refers to the cut-out speed of the turbine in (m/s); $P_r$ stands for the rated power output of the WTG (MW); and A, B, and C are constant parameters that can be computed from the cut-in, rated, and cut-out wind speed, respectively, as presented in [104].

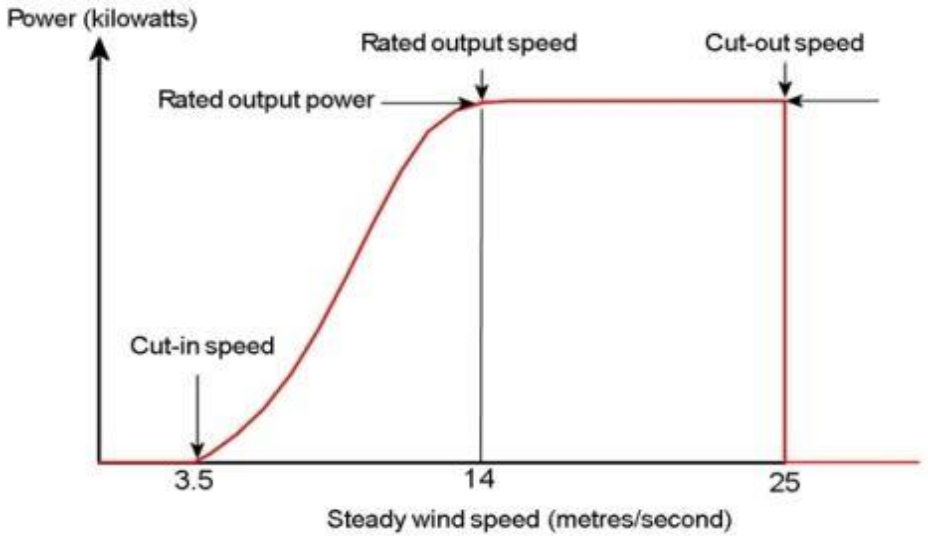


**Figure 2.4.** Typical power output curve for a wind turbine [102]

The literature provides reports of a number of methods for evaluating power system reliability in the presence of wind generators; most refer to probabilistic methods. Several probabilistic methods have therefore recently been designed for both analytical [105, 106] and simulation techniques [50, 107] for the measurement of the contribution of wind power to power system reliability. The creation of a multi-state model for predicting the output of a power grid connected to wind farms in order to examine power system adequacy was presented in [48, 108]. Optimal states have been determined from analytical methods using a fuzzy c-means clustering technique [109], initial K-means clustering [108], and a state-sampling simulation approach [48]. While the multistate method is fast, it might not be able to maintain sequential features and correlations between states. An analytical method based on discrete convolution was proposed in [110] for an examination of the impact of wind speed on wind farm reliability. The proposed reliability model incorporates consideration of the correlation between wind speed and the wind turbine failure rate, while the correlations between wind speeds and the wind turbine components are neglected. In the work presented in [111], a Markovian method was employed for estimating the availability of wind farms based on consideration of the stochastic nature of wind speed availability. The authors of [112] proposed

a large wind farm and a load data model as multi-dimensional clusters for reliability evaluation purposes and to maintain the correlation between them. These methods [111, 112] become more complicated with increasing numbers of wind farms [113]. A novel analytical method based on a discrete wind speed frame analysis was proposed in [114] for measuring the reliability indicators associated with a wind-diesel hybrid power system.

Geographic location is a key aspect of the evaluation of the reliability of wind power generation system because the weather system in a particular region has a direct impact on the wind regime [115]. For example, in the UK, storms tracking in from the Atlantic may help increase wind speeds in the northern part of the country [115]. In scenarios related to climate change and future emissions, the storm track paths could change wind speeds either positively or negatively, according to the geographic location. To create a common wind speed model, R. Billiton et al. [107, 116] simulated different levels of wind speeds at different geographical locations and used a sequential MCS for evaluating the reliability of a power system that included wind generation. The authors of [110] conducted non-sequential MCS in order to evaluate the correlation levels for a reliability assessment that included consideration of the impact of the geographical location. The developers of the reliability models presented in [117] took into account the geographical location of both offshore and onshore types of wind farms.

Various types of wind turbine generators have been adopted by manufacturers, with a determination of the optimal and most reliable still under study [118]. Among these types of generators are variable speed and fixed speed, such as a squirrel-cage induction generator (IG), a variable-speed doubly-fed induction generator (DFIG), an asynchronous induction generator, and a permanent magnet generator (PMG) [119, 120]. The DFIG and PMG versions are much more efficient than the IG because they run at variable speeds while the IG operates at a fixed speed [121]. The authors of [122] evaluated and compared the reliability performance of

different wind turbines including DFIGs and PMGs with the same capacity. The advantages of a PMGs over a DFIG are its simpler gearbox and fewer grid issues [123].

The uncertain and variable nature of wind could lead to fluctuations in the reliability of the turbine components and, therefore, in the output power profiles. A wind turbine contains several complex components connected to one another, including a generator, a hub, low- and high-speed drive shafts, a gearbox, a yaw system, and power electronics. All of these components are disposed to failure. A recent study suggests that power electronic components are one of the key items that cause the high failure rates in modern wind turbines based variables speed [124]. The authors of [125] performed reliability evaluations for an offshore wind turbine and found that after the power electronic components, the gearbox, generator, and pitch system are the main factors in turbine failure. Many researchers have indicated that gearboxes contribute to the overall failure of wind turbines due to the associated size, wind loads, and location making it harder to maintain, repair, and replace them [124-126]. The gearbox is responsible for speeding up the low-speed shaft so that it provides the speed required by the high-speed shaft to drive the generator [125]. Based on survey results, the three most critical components that contribute to wind turbine failure are the electrical control, the electrical system, and the sensors [127]. However, other studies have indicated that, along with the electrical controls and electrical systems, the most critical components are the rotor blades [128].

It should be pointed out that, because the energy produced by a wind turbine is weather dependent, ambient weather is an important element in the assessment of the reliability performance of wind turbines. Failure rates are also related to ambient conditions, including wind speed, which varies from season to season and from day to day [129, 130]. Recent studies have been conducted in order to estimate the influence of weather on the reliability of wind power and the associated components. For example, the results of the study presented in [131]

demonstrate that severe weather could cause the catastrophic failure of wind turbine components, thus affecting the maintenance process and the reliability of the turbine. An examination of optimal maintenance strategies for wind turbines under stochastic weather conditions was reported in [132]. The effects of weather conditions and geographical location on wind turbine failure have been studied, as presented in [133]. The researchers used three wind turbines during distinctly different weather conditions at different locations in order to estimate the impact of weather on the turbines. They found a cross-correlation between the failure of the components and the weather conditions at that location. The stochastic nature of weather thus makes wind power output complex to predict, a consideration that must be included in an assessment of wind turbine reliability.

A review of the existing literature reveals that reliability analyses of grid-connected wind power generation system have been addressed in many studies, which have been focused on some features while other aspects have been neglected. The majority of the research has been targeted at reliability methods as well as the geographical location, along with the different types of wind turbines and their components. Few studies have addressed the impact of weather-related factors on the reliability of wind power generation system. In fact, some of these studies have derived their conclusions from surveys, which do not involve modelling, while others have been based on small-scale, simplified modelling and not on detailed power modelling. To the best of the author's knowledge, very little or no previous research has involved consideration of the future impact of climate change on the reliability evaluation of realistic power systems connected to wind farms. In addition, until now, the impact of climate change on wind turbine components and their influence on a power system had not been investigated and still represented a significant challenge. The need to include consideration of the impact of climate change on wind-connected power system reliability represents a vital element in the success of power planning, operation, and maintenance strategies.

## 2.7 Summary

This chapter provides background about and a critical literature review of the assessment of the reliability of a composite power system and of a power system that includes PV and wind power generation system. The power system reliability and availability concepts, hierarchical levels of power system reliability, reliability indices, and basic reliability evaluation methods were briefly presented.

Adequacy evaluation methods can be divided into two main categories: deterministic and probabilistic. Probabilistic methods can be further classified as either analytical or simulation-based MCS. Reliability modelling is explored for each hierarchical level of a power system: generation, transmission, and distribution. The most common reliability indicators used in composite power system studies are described. Although different adequacy indices are used with each hierarchical level, their probabilistic logic is mostly similar. Also included are a discussion of reliability evaluation methods and explanations of the MCS and Markov chain methods. The latest studies related to these topics are reviewed critically.

The chapter also outlines the state of the art with respect to power system reliability that includes consideration of PV systems and wind turbines systems. Most of the research focused on factors such as component failure, the lifetime of the system, and the ambient conditions, geographic location, and the reliability of different types of configuration system. The chapter also highlighted the identification of research gaps missing from the literature and still in need of investigation. However, one of these areas, weather-related effects on both PV and wind power generation system, was already under study. The impact of climate change on the reliability performance of power systems that include wind and PV power generation has not previously been evaluated adequately but instead has been overlooked or ignored key features.

# Chapter 3: Literature Review of Climate Change and its Impact on Renewable Energy

## 3.1 Introduction

During 20th century, significant climate change has been observed, many aspects of which are unprecedented. The global mean surface temperature has risen, ice sheets and snow have decreased, the sea level has risen, and numerous extreme events have been recorded. All of these occurrences are due to the unparalleled rate of increase in the greenhouse gases (GHGs) emissions created by human influence. In 2018, the latest Intergovernmental Panel on Climate Change (IPCC) revealed that global warming has already produced temperature elevations of 1.5 $^{o}$C to 2 $^{o}$C as a result of past and current GHG emissions [134]. Just a small rise in global temperatures will have grave consequences because of the effect on weather patterns: floods, storms, heatwaves, wildfires, and drought [134].

From a climate change perspective, the expected shifts in power demand mean that operators of power systems, including generation, transmission, and distribution, will face serious challenges over the coming decades [4]. On the generation side, replacing existing generators with renewable power generation aimed at climate change mitigation is now a policy requirement [4]. Even a mix of conventional and renewable power generation supplies is itself subject to the impact of climate change, including global warming; changes in weather patterns; the availability of wind, solar, and hydropower resources; and extreme events [4, 135]. Transmission and distribution systems are also liable to suffer negative consequences due to global warming, lightning and storms, heat waves, drought and wildfires [135]. Climate change and extreme events can affect transmission lines by disrupting service and reducing efficiency, with a consequent mismatch of supply and demand [135]. On the demand side, temperature changes, reduced water availability, weather extremes, higher sea levels, and storm surges

could substantially influence the demand for energy and water [135]. Global warming also affects energy demand since elevated temperatures could affect the balance of cooling and heating patterns, having a variety of individual and combined effects on the power demand and supply, thus creating reliability issues [135].

This chapter provides an overview of concepts relevant to climate change and emission scenarios as well as their influence on renewable energy technologies. It begins with the fundamentals of climate change: definition, causes, and supporting evidence. A critical evaluation of the literature related to climate change is also presented, including an analysis of various emission scenarios and different climate models. The risks related to climate change with respect to renewable energy, power systems, and reliability are identified. The final element discussed is the impact of climate change on renewable energy and its resources.

## 3.2 Definition of Climate Change

Weather and climate differ. The first describes short-term atmospheric weather fluctuations that normally shift from hour to hour or day to day and are represented by weather elements such as temperature, air pressure, humidity, cloudiness, precipitation of various kinds, and wind [136]. In contrast, climate refers to the average weather or weather patterns for a specific geographical region, normally over the long term [136]. The IPCC *Fifth Assessment Report* (AR5) designates the average or prevailing weather as the 'Weather', as set out in [137]:

> Weather is measured in terms of such things as wind, temperature, humidity, atmospheric pressure, cloudiness and precipitation. In most places, weather can change from hour-to-hour, day-to-day, and season-to-season.

The term climate is defined as follows [137]:

> Climate in a narrow sense is usually defined as the average weather, or more rigorously, as the statistical description in terms of the mean and variability of relevant quantities over a period of time ranging from months to thousands or millions of years.

The Earth's energy balance is ultimately driven by the sun through the absorbed and reflected solar irradiation flux. Therefore, any change in the inward and outward solar irradiation flux to and from its surface and through space affects the Earth's energy balance, causing climate change. Shifts in climate have already occurred and are expected to increase in the future [136]. The term climate change, or climatic change, is defined in [137] as follows:

> Climate change refers to a change in the state of the climate that can be identified (e.g., by using statistical tests) by changes in the mean and/or the variability of its properties, and that persists for an extended period, typically decades or longer.

## 3.3 Evidence and Causes of Climate Change

Changes in the climate are due primarily to non-anthropogenic, or natural, and anthropogenic factors, i.e., caused by human expansion and activity. Non-anthropogenic effects result mainly from volcanic activity, modulations in solar cycles, and changes in ocean circulation [138]. On the other hand, human activity includes the burning of fossil fuels, which has increased significantly since the industrial revolution. Human activity had unequivocally increased the gases in the atmosphere known collectively as GHGs, notably carbon dioxide ($CO_2$), which has significantly increased global warming through trap radiation [139]. Atmospheric gases allow shortwave solar radiation to pass through to the Earth and heat its surface [140]. The Earth's surface radiates longwave radiation back into the atmosphere. However, GHGs, particularly carbon dioxide ($CO_2$) and water vapour ($H_2O$), are not transparent to longwave radiation, instead absorbing it and heating up the atmosphere. As well,

the atmosphere emits radiation both into space and toward the surface of the Earth, creating additional surface warming. This phenomenon is called the greenhouse effect [140].

In the IPCC assessment, for the purposes of evaluating climate change, the radiative forcing (RF) concept is used for measuring the intensity of a number of mechanisms ($W/m^2$) that affect the Earth's energy balance [138]. Any mechanism that can either positively or negatively impact the balance of radiative energy is designated as RF. Significant evidence exists that human influence has raised the land surface albedo, leading to a change in the RF. During the course of the industrial era, the average anthropogenic radiative force has been 2.3 $W/m^2$ [138]. The evidence for the existence of climate change and its impact on the energy demand are highlighted in [141]. For the period between 2015 and 2019, the average five-year global temperature was the warmest on record and is estimated to be 1.1 $^oC$ above pre-industrial levels [142]. This escalation is due to increases in GHG emissions, as explained in the next section.

## 3.4 Greenhouse Gases

GHGs refer to specific gases in the atmosphere that have an impact on global warming through their absorption of particular radiation and its emission to the surface of the Earth, thus creating the greenhouse effect [137]. The increased concentration of GHGs in the atmosphere is due mostly to human activity [138]. The most familiar gas of note is carbon dioxide ($CO_2$), which occurs naturally but also mostly anthropogenically from the burning of fossil fuels derived from fossil carbon deposits, such as coal, oil, gas, and biomass as well as from industrial processes such as cement production [137]. More than 90 % of $CO_2$ emissions come from fossil fuel burning and cement production, while roughly 70 % of the total GHGs emissions are produced from human activity [140]. The rate of growth in GHGs was 1.5 % per year from 2008 to 2017, with the highest point during that period being observed in 2017 [142].

$CO_2$ emissions have continued to increase, from 406.99 ppm in August 2018 to a new high point of 409.95 ppm in August 2019, and it is expected that $CO_2$ levels will continue to rise in the future [143]. **Figure 3.1** shows the outward RF due to monthly average global $CO_2$ emissions [143]. The results shown are based only on key components of climate forcing rather than on all components: only direct forcing from $CO_2$ was considered [143]. **Table 3.1** lists the primary GHGs along with their corresponding sources of emission [144].

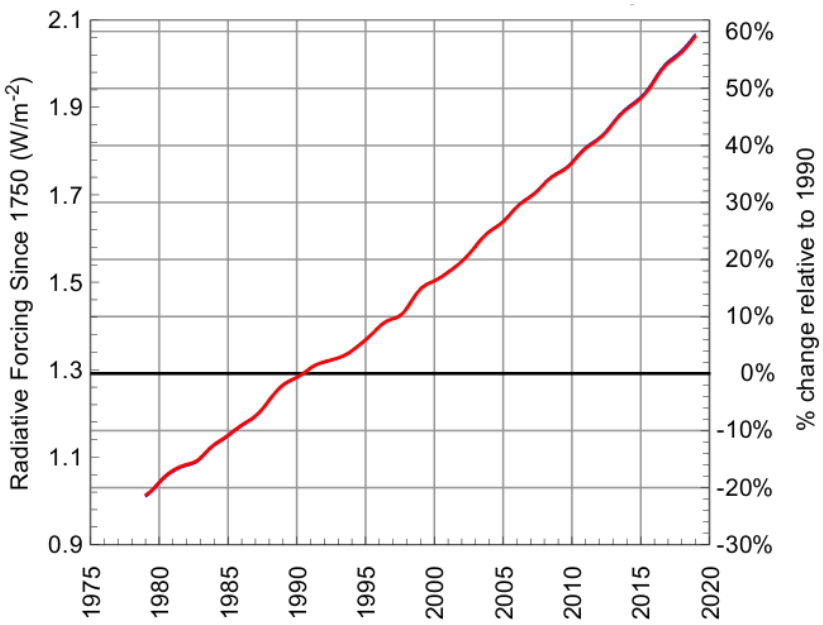


**Figure 3.1**. Radiative forcing due to CO2 alone with the percentage change indicated on the right-hand axis [143]

**Table 3.1.** Sources of Greenhouse Gases

| Greenhouse gas | Emission sources |
|---|---|
| Carbon dioxide ($CO_2$) | Fossil fuels, industrial processes, and deforestation |
| Water vapour ($H_2O$) | Increased evaporation from oceans and elsewhere with rising temperatures |
| Methane ($CH_4$) | Agricultural activities, biomass burning, and waste management |
| Nitrous oxide ($N_2O$) | Fertilizer use |
| Ozone ($O_3$) | Pollution from cars, fossil fuels, and industrial chemical processes |
| Other chlorofluorocarbons (CFCs), (HFCs), (PFCs), and ($SF_6$) | Industrial processes and refrigeration |

## 3.5 Emission Scenarios

Future climate change projections are reliant on GHG emissions which are, in turn, linked to factors such as population growth, human activity, industrial processes, and natural effects. The impact of these factors on climate change varies with the level of emissions associated with specific scenarios. Scientists from a variety of disciplines have collaborated to study these factors as a means of developing emission scenarios. It is vital to differentiate such scenarios so that the RF can be used for predicting future scenarios based on how human activities act on and respond to climate change. The IPCC has therefore provided special reports on emission scenarios (SRES), published in 1990, 1992, and 2000, in which they provide different climate change emission scenarios based on consideration of driving forces over the long term [145, 146].

The 2000 IPCC *Special Report on Emissions Scenarios* classified a number of emission scenarios with the goal of reflecting current understanding and knowledge about underlying uncertainties [145]. Emission scenarios are defined in the IPCC report as follows [145]:

> A set of scenarios was developed to represent a range of driving forces and emissions in the scenario literature so as to reflect current understanding and knowledge about underlying uncertainties.

The SRES emission scenarios are the most confident and the ones used most extensively by researchers and modellers for developing climate change projections, for example, in [147-149]. The SRES scenarios consider all related GHGs as well as different driving forces, including demographic, technological, and economic developments. Forty emission scenarios were developed, representing four sets of so-called ‘families’: Al, A2, Bl, and B2 [145]. Each family is dependent on future development and a driving forces storyline described according to two trends: the first involves increasing regionalisation or increasing

globalisation, and the second is associated with strong economic or strong environmental values, as illustrated in **Figure 3.2** [145].

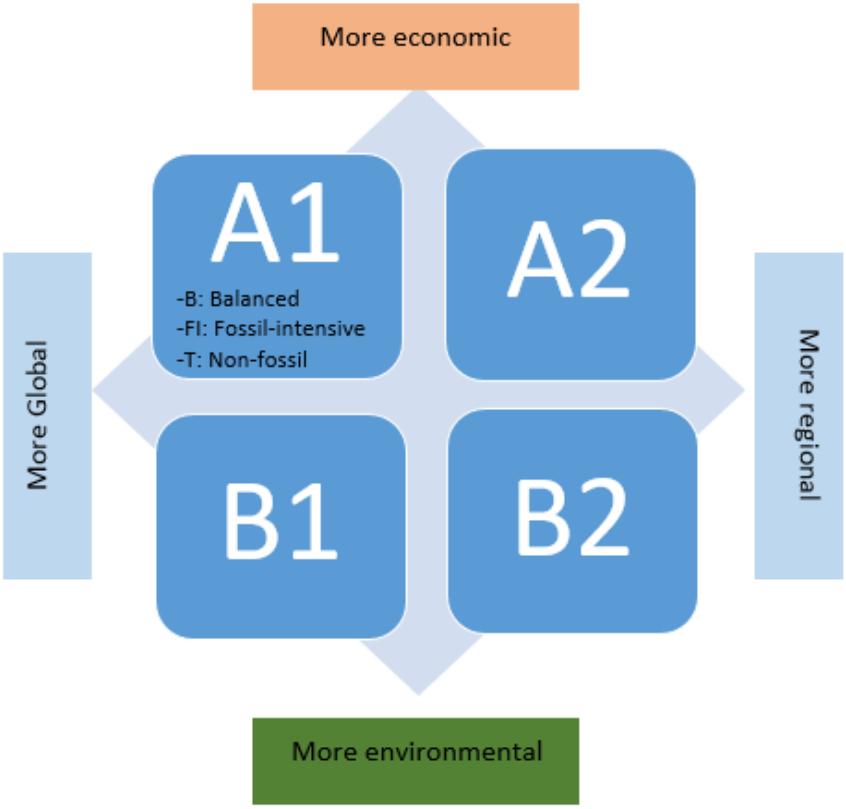


**Figure 3.2.** Main SRES storylines and scenario families

Six groups are drawn from the four family sets in order to provide additional sets of narratives, as indicted in **Figure 3.3** [145]. The six groups are composed of one each from A2, Bl, and B2, and three from within the Al family: AlB (balanced), A1FI (fossil fuel intensive), and AIT (predominantly non-fossil fuel). The Al family describes future scenarios with high-emission of GHGs, rapid economic growth and increasing global population. On the other hand, the A2 family describes future scenarios with lower emissions than with the A1 family but greater than with B1 or B2, with continuously increasing global population and regionally oriented economic development. Of the four families, the B2 one is associated with scenarios involving the lowest emission levels [145].

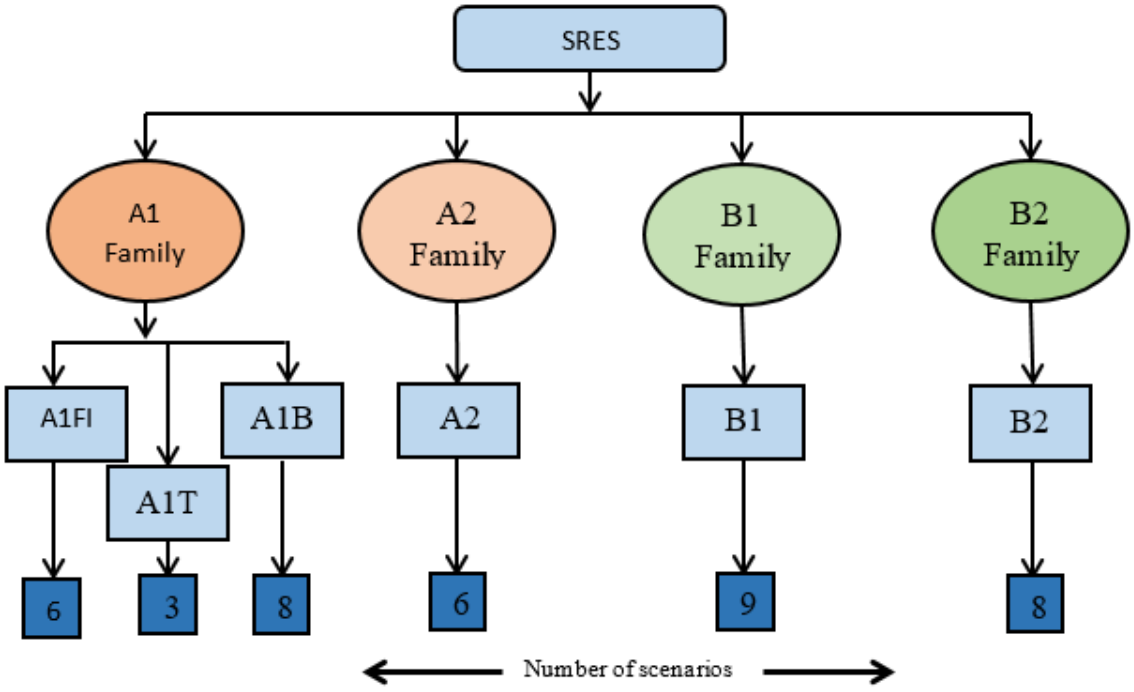


**Figure 3.3.** Extended characteristics of the four SRES storylines and scenarios

Four other new future scenarios that have been generated recently from the integrated assessment models (IAMs) are designated as representative concentration pathways (RCPs) [150]. The new RCP scenarios represent concentrations and corresponding emissions based on the existing literature but are not directly dependent on the four SRES scenario storylines. The four additional emission scenarios have been named based on the anticipated RF level for the year 2100. They are classified as one low-emission scenario (RCP2.6), two medium-emission scenarios (RCP4.5 and RCP6), and one high-emission scenario (RCP8.5) [151]. For the RCPs, the assumption is that the average global temperature will continue to increase and that it is strongly dependent on the level of the emissions in the specific scenario [151]. Additional information about climate change factors under RCP emission scenarios is available in [152, 153].

The studies published in the literature include examinations of a variety of emission scenarios for use in assessing the impact of climate on a number of areas, including power systems. A climate emission scenarios produced by the parallel climate model (PCM) and

regional climate model (RCM) used by the U.S. Department of Energy and the National Centre for Atmospheric Research were implemented for different future years in order to estimate the possible impact of climate change on water resources [154]. In the study reported in [155], the SRES A2 and B2 scenarios were simulated with the goal of evaluating the effects of climate on the energy supply and the heat demand. In other work [156], SRES emission scenarios, including A1FI, A2, and B1, were applied for assessing the influence of climate change on power demand and extreme demand. RCP 4.5 emission scenarios have been employed for estimating the impact of climate change on wind resources [157] and on the simulation of building energy [158]. The authors of [159] applied a combination of RCP 4.5 and SRES A1B in order to assess river flow and hydroelectric power under future changes in the climate. SRES A1B, A2, and RCP 2.6 have also been used for investigating the performance of a hydroelectric power plant and power market fluctuations under a variety of climatic conditions [160]. In [161], researchers reported the use of two emission scenarios, RCP 2.6 and RCP 8.5, for gauging the effects of future climate conditions on thermoelectric power generation.

## 3.6 Climate Model Overview

Climate models are mathematical models designed for simulating the interaction among climate force drivers, including land surfaces, oceans, and the atmosphere [140]. They are used for acquiring an understanding of climate systems and for projecting climate change in different ways based on the energy balance of the Earth. The simplest climate model, called a zero-dimensional global model [140], is based on simple physical interactions and can be applied for measuring the average global climate but does not enable the simulation of regional climate changes. However, location, key physical interactions, and all three-dimensions climate models, including zero, vertical, and horizontal, are required to be considered for the general circulation models (GCMs) [140, 162]. GCMs can supply climate change and climatic indications for the entire world since they are based on horizontal resolution, normally between

150 km and 300 km (i.e., a whole country rather than a specific location) [163]. The 2007 and 2014 IPCC reports provide a wide range of GCMs for estimating future climate change, given a variety of emission scenarios [137, 164]. In contrast, RCMs provide a climate and climate change overview for local and small areas at a higher resolution, commonly between 10 km and 50 km [165]. RCMs that are nested into GCMs are vital models that can produce an accurate reflection of climate change for a certain location [163]. One example of an RCM is the one used in the UK Climate Projections 2009 project (UKCP09) carried out by the Hadley Centre and designated HadRM3 [166]. A detailed review of different regional climate models is given in [167, 168]. At least two-thirds of climate models reveal extremely comparable signs of changes in the mean global temperature at the same grid point scale, with statistically minor differences in large regions [169].

The literature contains examples of several models used for assessing a variety of aspects of the impact of climate change, including the effects on power systems. For example, atmosphere-ocean general circulation model (AOGCM) projections were used in the work presented in [156] as a means of assessing the impact of climate change on power demands for different IPCC emission scenarios. The authors of [170] employed a number of climate models, such as IDEAM, AOGCM, and HadCM3, in order to examine the potential impact of climate change on the vulnerability of hydroelectric power plants. In the study reported in [171], a regional climate model based on a statistical analogue resampling scheme (STARS) was used for estimating the impact of climate change on variations in thermal, hydroelectric, and wind power plants. For the research presented in [172], an alternative technique was applied for predicting future weather data using a HadGEM2-CC model for evaluating the energy demand of a building. The technique was based on joining a forecast time series with climate periodicity analysis. Two climate models were combined in The Inter-Sectoral Impact Model Intercomparison Project (ISI-MIP) has been employed in order to analyse the performance of

a thermoelectric plant under varied climatic conditions [161]. An RCM from the Coupled Model Intercomparison Project 5 (CMIP5) GCMs for the Russian region has been used for gauging the climatic influence on the Russian power industry for a specific type of power equipment [173]. The authors of [174] implemented the Hadley Centre Central England Temperature (HadCET) dataset in order to examine temperature increases in the power supply and demand in the UK. In a final example, a PROMES-UCLM regional climate model was applied for estimating the impact of climate change on hydroelectric power [175].

## 3.7 Identification of the Power System Risks Associated with Climate Change

Climate change affects electricity, human health, water resources, agriculture, food security, and the economy. In the context of electricity, it has both a direct and an indirect impact on the reliability of an entire power system because of the way changes in weather patterns affect the performance of the components required for the system to operate [135]. The impact can vary depending on emission scenarios and climate drivers, such as temperature, wind speed, and extreme weather events. These factors can critically influence both the demand side and all facets of electric power systems, including generation, transmission, and distribution. Electric power infrastructure is also vulnerable to threats from extreme weather caused by climate change, such as wildfires, heatwaves, storms, droughts, flooding, and rising seas. Any of these risks could lead to power reductions, power outages, component failure, decreased reliability, increased maintenance, higher capital costs, and negative environmental consequences. While a number of these risks are currently under study, they are still insufficiently explored, and others are yet to be investigated. However, in the context of power

system reliability, the following are the risk issues that must be considered with respect to power grid planning:

- The efficiency and reliability of thermoelectric power generation are affected by temperature, drought, and extreme events [135, 176]. In addition, power generation stations, such as thermoelectric power generation and hydroelectric power are susceptible to potential disruption and reductions in efficiency due to weather events, diminished water availability, and temperature increases [135, 177].
- The generation, efficiency, and reliability of photovoltaic (PV) power are reliant on solar irradiation levels, temperature, cloud characteristics, wind speeds, and dust [12-15].
- Wind-generated power is sensitive to wind speed and direction as well as to variations in wind speed, air density, and air temperature [14, 15, 165]. Moreover, wind turbine components are vulnerable to high wind speeds that create stress in turbine components [14, 135]. Furthermore, wave power generation shifts according to wave power, which is sensitive to changes in wind speeds [10, 15]. In addition, tidal energy can be influenced by rising sea levels [178, 179].
- Hydroelectric power generation is affected by the availability of water, which is influenced by precipitation, higher temperatures, and river inflow levels [10, 135].
- Biomass power generation is impacted by precipitation, temperature, and drought [180, 181].
- Transmission efficiency and the available transmission capacity are governed by air temperature [182, 183]. Moreover, Transmission losses can rise due to increased demand resulting from climate change [182] while overhead transmission lines are affected by high winds, cold waves, heavy snow, and lightning strikes [184, 185]. Furthermore, Overhead distribution lines can be damaged by high winds, cold spells,

heavy snow, and lightning strikes [184, 185]. On the other hand, underground cable systems are affected by increases in ground temperature, which reduce ratings [182].

- Substation capacity could shift as a result of ambient temperature changes and extreme weather events [182, 185]. In case of components within substation, higher ambient temperatures can have negative consequences with respect to transformer capacity [13, 182]. Also transformer performance can be impaired by heat waves [182, 185]. In addition, switchgear is susceptible to rises in temperature, which reduce ratings [182].
- Electricity demand can be impacted by weather conditions on a daily basis [182]. It can shift with changes in temperature, cloud cover, wind speed, precipitation, and humidity [156, 182]. Additionally, heating and cooling demand is subject to changes in temperature [186, 187].

## 3.8 Influence of Climate Change on Renewable Power Generation

Since it produces very low GHG emissions, renewable energy is generally considered to be clean and green. Renewable energy resources can be both positively and negatively affected by changing climate conditions [185], which can affect them in ways that create problems for existing renewable power generation. This section emphasizes the significance of future changes in PV and wind power generation system resources under changing climate conditions, highlighting a variety of anticipated GHG emission scenarios that can, over the coming decades, have notable consequences for power systems that include integrated renewable power generation.

### 3.8.1 PV Power Generation

The globally increasing contribution of PV power to electricity generation is ultimately governed by climate drivers such as ambient temperature and cloud cover. As mentioned at the

beginning of this chapter, climate is determined mainly by the inward and outward balance of solar irradiation flux, which means that solar power is highly vulnerable to any changes in factors that affect that balance. This section presents an overview of studies published by researchers who have tackled issues related to the vulnerability and sensitivity of PV resources and power generation to the impact of climate change.

#### 3.8.1.1 Vulnerability and Sensitivity to Climate

PV power generation is dependent not only on weather but also on climate: any change in climate could affect power generation at the seasonal or annual time scale. The amount of power generated is vulnerable to the effects of climate change and ambient weather conditions, including changes in solar irradiation, temperature, snow cover, cloud cover, dust, wind velocity, precipitation, and extreme weather events [15, 165, 188, 189]. Any alterations in these weather patterns thus have the potential to affect the pattern of the generation profile. A rise in ambient temperature can impact PV efficiency by increasing the operating temperature of a cell and thus the eventual power output [190-192]. It has been shown that, depending on the technology used, increasing the ambient temperature by 1 $^{o}$C can reduce PV efficiency by about 0.5 % [165]. A change in cloud cover that has a direct impact on solar irradiation will alter PV efficiency and the amount of power generated [188, 193]. Shifts in atmospheric water vapour content and cloud characteristics could also influence the atmospheric transmission of solar irradiation [193]. The authors of [194] suggested that, by 2039, the reduction in global solar irradiation due to climate change will be 5 % for low-latitude regions, which will have a significant potential impact on solar power generation. A change in wind speed can affect the ambient environment around the PV system and, consequently, PV efficiency and output power [192, 195]. Rainfall can influence PV generation by reducing solar irradiation but might also help remove dust in dry regions [196]. Extreme weather, such as storms, snow, and heatwaves, has negative consequences for both PV-generated power and PV infrastructure [10, 197].

#### 3.8.1.2 Impact on Solar Energy Resources

Previous studies have assessed the impact of climate on solar energy, but most of these studies were focused on changes in PV resources rather than in PV generation. The study presented in [198] involved the examination and highlighting of US solar resources as a means of understanding future shifts in patterns related to those resources. By the end of the 2040s, mean US seasonal and daily solar irradiation values could decrease by up to 20 % [199]. In the case of the UK, average annual solar resources could increase in the southern UK and decrease in the northwest [12]. In the work reported in [200], the impact of and sensitivity to climate with respect to PV generation and concentrated solar power (CSP) were assessed for a range of regions, including the US, Europe, Australia, China, Algeria, and Saudi. HadGE1 and HadCM3 climate models were used, and only one emission scenario, SRES A1B, and one future year were presented. Their findings revealed a slight increase in solar irradiation in Europe and China and a small decrease in the amounts in the US and Saudi Arabia, with Arabia. This study could be improved with the use of additional representative emission scenarios, more climatic variables, and different future periods. In other studies, such as the one presented in [201], future hourly global irradiation data based on two emission scenarios were generated in order to estimate changes in solar irradiation for Greece . The impact of other climate variables was not considered. Long-term changes in solar irradiation have also been predicted using CMIP5 climate models, and their influence on PV systems has been evaluated [193]. Although, this study also involved only one future period, it demonstrated that PV output could decline in some parts of the world. The changes predicted in future solar resources encompassed eight world regions, with the greatest indication of negative repercussions due to climate change being found in parts of Europe, India, and northwestern China [193].. In the study described in [202], the effects of climate change on solar, wind, hydro, and thermoelectric power generation were assessed using five RCMs from the EURO-CORDEX model. Until

now, only a few researchers have employed climate models for estimating changes in PV generation profiles.

The above literature review reveals that several studies have been conducted with the goal of investigating the impact of climate change on PV energy, with a focus on a variety of aspects, such as region, emission scenarios, and climate models at different temporal and spatial scales. Most previous studies have been focused on a global climate model, a short timescale, and one emission scenario, which fail to show the real long-term impact at the regional level. In only a few past studies has a multi-emission scenario at a multidecadal timescale been applied in a comprehensive model for an examination of the further consequences of climate change with respect to PV applications.

### 3.8.2 Wind Power Generation System

Because it represents a clean energy source and an alternative to fossil-fuel-based thermal power generation, the implementation of wind power generation system has been growing quickly over the last few decades. While replacing existing thermal power generation with wind power generation system is challenging, this shift can perhaps help reduce GHG emissions, which constitute the primary cause of climate change [203]. However, the influence of climate on wind power generation system is substantial with respect to both power planning and the optimisation of development strategies. This section provides an insightful review of recent research related to the vulnerability and sensitivity of wind power generation system and resources under climate change.

#### 3.8.2.1 Vulnerability and Sensitivity to Climate

Based on the risks associated with the effect of climate change on power systems are identified in section 3.7, wind power generation system is subjected to the consequences of climate change. A number of studies have been conducted with the goal of determining critical

weather factors that affect wind power generation system. The risks associated with climate change have a potential impact on wind-based electricity production because they can influence wind speed patterns, which constitute the most vital driver of wind energy [204]. An additional factor is that, since wind speed is measured according to atmospheric circulation [205], changes in global warming, atmospheric flow, and storm climates can affect wind resource indexes [205]. Changes in wind speed due to climate change over the last few decades have been reported in [206]. Other climate-related factors also have an effect on wind power generation system, such as wind direction, changes in temperature, and rises in sea levels [196, 207]. Wind direction also plays a minor role in wind power generation system, but the statistical analysis of wind direction is difficult [10, 208]. Additional relevant climate-related factors include air density, which can influence the power generated from wind turbines [209] because air density has an inverse relationship with regional air temperature, which means that increases in air temperature lead to decreases in air density and hence the power output from wind turbines [209].

Few previous studies have included consideration of the detrimental impact of climate change and weather factors on turbine components. Extremely low temperatures and large amounts of ice accretion have negative effects on these components [203]. Ice accretion on wind turbine blades can reduce the performance and durability of the turbine [210, 211]. Extremely low or high temperatures are liable to change the physical properties of the materials that comprise turbine components [209]. Lightening can also damage both the blades and the mechanical and electrical components [212], and extreme wind speeds can be detrimental to blades and other turbine components [213]. Increasing the size and capacity of wind turbines makes them even more vulnerable to the uncertainty associated with climate. Since the power produced by wind generation is proportional to the cube of the wind speed, a small shift in that speed can have an enormous impact on the amount of power generated [214], with the result

that wind power generation system varies substantially in response to altered wind speeds. While specific changes in wind speed are dependent on the geographic location and season, in general, a 10 % shift in wind speed leads to a 13 % to 25 % change in the energy yield [215]. Because turbines cannot function below or above cut-in and cut-off speeds, respectively, changing wind speeds can thus reduce the amount of power generated [204].

#### 3.8.2.2 Impact on Wind Energy Resources

A number of studies have been carried out, primarily in developed countries, in order to explore the impact of climate on wind power generation system [214, 216-220]. The projected results of these studies exhibit negative and positive variations, but at seasonal or annual time scales, most of the variations are negative and are highly dependent on GHG emission scenarios. The research reported in [217, 218] demonstrated the possibility of decreased average summer wind speeds and increased average winter wind speeds for the European region, which has a direct impact on power system generation at seasonal and annual timescales. With respect to the UK, wind power generation system is estimated to grow in the north and diminish in the south [204, 221]. However, other researchers have found that, for a future period (2020–2049), climate change will result in moderate reductions in annual wind power generation system in different part of the world [222, 223]. Most of these investigations have been conducted using large-scale GCM features rather than reginal-scale ones (e.g., wind farms), which are associated with a high degree of uncertainty[218]. The potential impact of climate change on wind energy resources was assessed for the European region using a multi-model ensemble of 21 CMIP5 GCMs [202]. The authors of [205] evaluated the effects of climate change on the stability of wind energy resources but for only one future emission scenario, SRES A2, and only for the United States.

wind power generation system will likely be influenced by climate change, thus significantly affecting power systems with high penetrations of wind energy. The above

literature review demonstrates that several researchers have studied the impact of climate change on wind energy with respect to a variety of aspects, such as location, emission scenarios, and timescale and climate models. Most of the studies have addressed the influence of the climate using a GCM and representing only one emission scenario for a short forecasting timescale. Very few previous integration and planning studies of wind power and climate change have included comprehensive consideration of RCM, different emission scenarios over multidecadal. For these reasons, a more exhaustive study that is aimed at assessing the further implications of potential future changes in climate elements with respect to wind energy and that employs the latest climate change projections and multi-emission scenarios at the multidecadal scale would therefore be indispensable for planning and guiding the effective utilization of a power system that encompasses integrated wind energy.

## 3.9 Summary

This chapter has presented a basic overview of concepts relevant to climate change and emission scenarios as well as their influence on renewable energy technologies. Climate change fundamentals, including its definition and causes as well as evidence of its existence have been briefly introduced. Human activity increases the levels of atmospheric gases known collectively as GHGs, which have been significantly implicated in climate change. The chapter has included further information about GHGs, emission scenarios, and climate models as well as an introduction to different climate models and a number of emission scenarios. The risks associated with climate change with respect to renewable energy, power systems, have also been identified.

The chapter outlines the state of the art related to renewable energy, including PV and wind power and resources, with respect to the impact of climate change. The literature review presented in this chapter has highlighted research gaps that need to be considered. Weather-

related effects on renewable energy were already under study, with several researchers studying the impact of climate change on renewable energy and focusing on a variety of aspects such as location, emission scenarios, and timescale and climate models. Most previous studies have involved the use of GCMs, single emission scenarios, and short to medium timescales. These limitations prevent a determination of the real long-term impact of climate change on renewable energy. The review showed that further investigation of additional complications introduced by potential future changes in climatic elements with respect to renewable energy would therefore be vital. Such research must involve the use of the latest climate change projections and multi-emission scenarios at the multidecadal scale.

# Chapter 4: Modelling, Simulation and Impact Assessment of Effects of Climate Change on PV Systems

## 4.1 Introduction

The primary goal of the work presented in this chapter was to assess the long-term impact of climate change on the performance of a large-scale integrated photovoltaic (PV) system. The chapter presents a comprehensive analysis of the modelling framework of the ambient climatic conditions pertinent to a centralized and a decentralized grid-integrated PV system, along with an explanation of the application of Monte Carlo simulation (MCS) for quantifying the influences on each type of system and for evaluating the extent of the impact of PV integration on operating conditions of future power grids. The impact assessments for this study are based on the incorporation of the most recent regional climate models (RCMs) at high resolution and for different emission scenarios.

The adoption of power generation from renewable resources such as wind, hydropower, waves, and PV has been driven by global warming and the accompanying need to mitigate greenhouse gas (GHG) emissions. GHGs are produced predominantly as a result of the worldwide consumption of energy produced from fossil fuels. As explored in Chapter 3, these emissions have already damaged the environment, with further environmental changes expected resulting from ongoing amounts of GHG emissions. PV systems are being developed globally as an alternative clean energy source that entails no fossil fuels and releases near-zero $CO_2$ emissions [224].

However, PV power generation is highly vulnerable to climate change: greater uncertainty and variability in the weather due to atmospheric changes directly affect a PV system, its components, and their performance, with negative consequences for grid reliability [225]. Temperature shifts can alter the operating voltages of PV cells, variations in the levels

of irradiance can impact power output, and changes in shading can affect the flow of current in a cell [226].

PV power generation differs from power generation from conventional units: it is associated with both a high degree of uncertainty and numerous variables, making it completely stochastic in nature since the power output from PV units can be impaired by environmental variables and component failures [11, 72]. An investigation of the ways in which future climate change can potentially impact the operability of PV systems over the long run is vital for the planning, operation, and maintenance of modern power systems [224]. A framework for assessing the reliability of a PV-integrated power system can therefore effectively establish its future impact on a power system.

Ambient temperature, operating temperature, and solar irradiation can negatively affect the output of a PV system and thus its reliability. Other weather factors such as precipitation, wind, cloud cover, and snow also impact PV output and generation resources derived from solar irradiation. For example, increased precipitation reduces direct irradiation, leading to lower efficiency. In climate models, such weather factors are considered with respect to their effects on the resources available, such as temperature and solar irradiation, rather than taking into account their direct impact on the PV system itself. Variations in ambient weather conditions thus entail significant ramifications in the case of a high penetration of PV power generation, which then have consequences for the distribution segment of a power system. A resulting major reverse power flow might lead to a serious power interruption due to instabilities in grid performance, such as increases in grid voltage [226]. Such overvoltage can shift the power flow, inducing problematic voltage fluctuations as a result of the failure of PV power generation systems, with possible additional effects on PV components [11, 227]. Grid-connected PV systems are highly sensitive to operating states, power loss, temperature, and ambient conditions, all of which can reduce overall system reliability [225].

The following sections of this chapter explore the effects of variations in climate on the operating temperature, irradiance, and shading of a PV system, along with their impact on the aging spectrum of the PV module. For this study, long-term climate change simulations and a variety of emission scenarios were incorporated into models of centralized and decentralized large-scale integrated PV systems. The influences of these scenarios into the simulations are captured through the use of non-sequential MCS applied as a means of assessing the impact on the reliability performance of the grid. The experimental work incorporated probabilistic climate change projections from the UKCP09 climate change model under low-, medium-, and high-emission scenarios (based on 30-year historical weather observation data) for three time frames: 2020s (2010-2039), 2050s (2040-2069), and 2080s (2070-2099). The IEEE Reliability Test System (IEEE-RTS) was utilized for case studies that were conducted as a means of illustrating the functioning of the proposed frameworks. Parts of this chapter have been published previously [228] during the course of this Ph.D. work.

The chapter is structured as follows. The main methodology is introduced in section 4.2. The UKCP09 climate change model, its description, the simulations conducted, the UKCP09 Weather Generator (WG), and the emission scenarios, along with key findings and output samples are presented in section 4.3. The PV system modelling and the PV power and generation model are detailed in section 4.4. IEEE-RTS is described in section 4.5, and the analysis of the reliability of the PV system is explained in section 4.6. Sections 4.7 and 4.8, respectively, report on the case studies and summarize the chapter

## 4.2 Methodology

The objective of this section was to communicate the main steps involved in the framework created for assessing the impact of climate change on an integrated PV system and

ultimately on power system reliability. The framework encompasses four main steps: climate change simulation, PV power generation system model development, power system model simulation, and reliability assessment. The first step entailed the simulation of a stochastic climate change model for low, medium, and high emission scenarios over a variety of timescales through the adoption of the UK Climate Projections 2009 (UKCP09) based on different circulation climate models (CCMs) and regional climate models (RCMs) [229].The simulation results were fed in as input for the second step: the development of the PV power generation system model. In the third step, the influence of climate on the characteristics of the PV-integrated power system was modelled in order to develop the fourth-step reliability assessment and to quantify the level of the long-term impact. **Figure 4.1** illustrates the key elements of the methodology presented in this chapter.

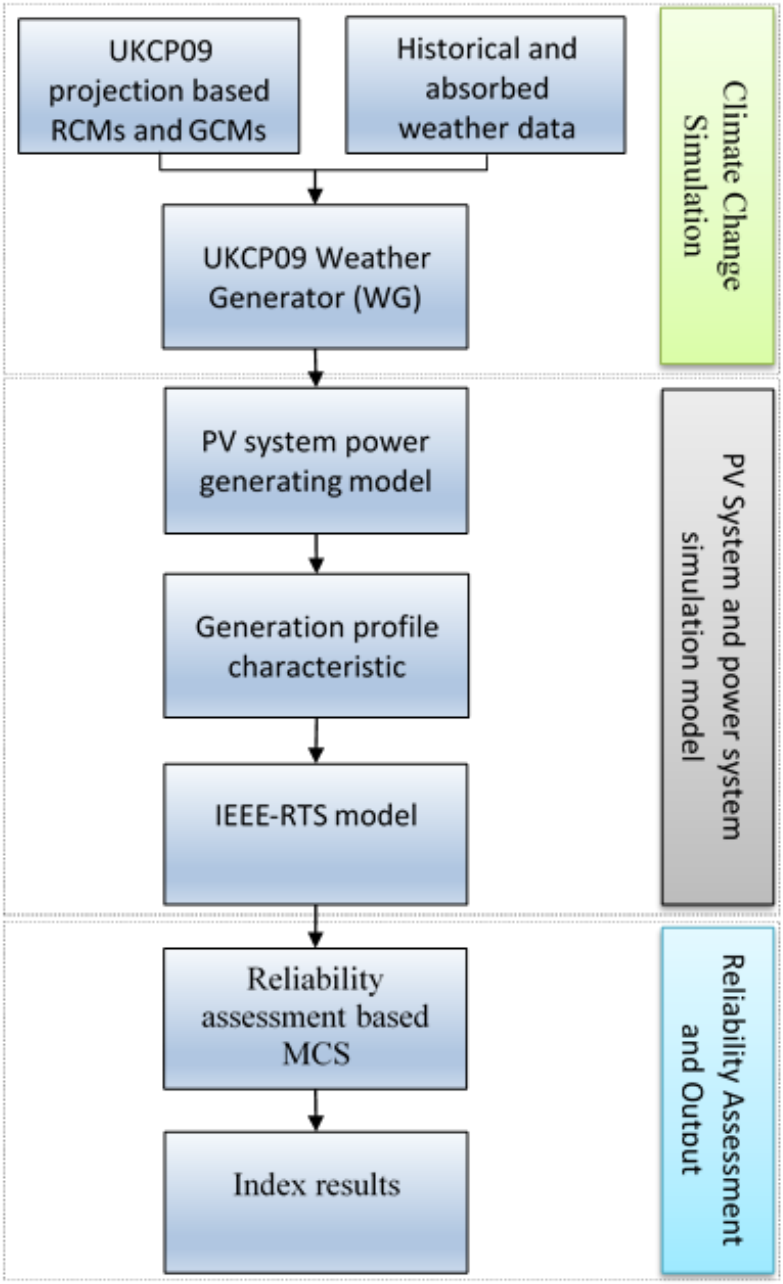


**Figure 4.1.** Overview of the main methodology for determining the impact of climate change on an integrated PV system

## 4.3 Climate Change Simulation

This section introduces the climate change simulations and describes one of the climate change models applied in the research presented in this thesis. As mentioned in Chapter 3, a number of climate change models are available for simulating future changes in climate based on different 'storylines' at varied resolution levels. In this thesis, high-resolution climate models were employed for investigating the impact of climate change on PV power generation:

UKCP09 projections and WG results [229, 230]. Within these models, a number of global climate models (GCMs) and RCMs are employed to cover a wide range of future climate projections and scenarios. Climate change simulations enable the use of sets of future meteorological data as a means of examining the impact of climate on the performance reliability of a PV-integrated power system. The next subsections introduce the UKCP09 Climate Projections and the UKCP09 WG. Steps in the climate change simulation, and WG sample outcomes that highlight climate change are also presented.

### 4.3.1 UKCP09 Climate Projections

The UKCP09 climate model is based on advanced scientific methods provided by the Met Office Hadley Centre Climate Programme, which is an updated version of UKCP02 [166]. The development of UKCP09 involved contributions from more than 34 organizations and support from UK departments that included the Department for Environment, Food & Rural Affairs (Defra) and the Department of Business, Energy & Industrial Strategy (BEIS) [166]. The model can simulate future climate data projections for UK land and marine regions for the 21st century. It offers superior spatial and temporal information as well as extended statistics related to uncertainty. Thirty years of climate observation data for the UK are also used for simulating future climate conditions. These features can enable an assessment of the potential impact of climate change on a power system, which can help in the determination of appropriate adaptation planning that will enable that impact to be addressed in ways that could minimise negative consequences.

### 4.3.2 UKCP09 Projection Structure

UKCP09 climate variables are simulated based on data derived from the Hadley Centre Coupled Climate Model (HadCM3), the GCM, and the RCM at a spatial resolution of 25 km. The UKCP09 structure involves the running of three main climate models: two GCMs

(HadSM3 and HadCM3) and one RCM (HadRM3). These climate models also include other models, such as the HadAM3 atmospheric CCM model and the HadOM3 ocean model [166]. The GCMs are downscaled from a horizontal resolution of 295 km to a higher resolution of 25 km for the examination of regional features such as mountains, lakes, and land surface properties. The output from UKCP09 consists of climate variables in the form of probability distributions over a selected timescale of seven overlapping 30-year periods. To modify the model simulation so that the adapted version meets the requirements for this study, the outcomes, including timescales, emission scenarios, climate variables, spatial resolution, temporal resolution, and geographic location, as well as the WG model needed additional adjustments, as described in the next sections.

#### 4.3.2.1 UKCP09 Weather Generator

The WG model can provide a synthetic daily/hourly time series of climate variables within the UK based on the UKCP09 projections and on historical and absorbed local geographical data [166, 230]. It can give local geographical information such as details about hills and valleys that facilitate the expansion of the resolution from 25 km to 5 km. The key procedures for simulating hourly weather data are indicated in **Figure 4.2**. The synthetic hourly time series variables featured in the WG climate model are precipitation, air temperature, vapour pressure, relative humidity, and hours of sunshine; other variables are added for the synthetic daily time series, such as sea-level air pressure. The model does not simulate some climate variables, such as lightning and wind speed, due to the high degree of uncertainty associated with them. The model is suitable for a number of purposes, it can be implemented with varied adjustments, thus it used to enable consideration of different timescales, emission scenarios, climate variables, spatial resolutions, temporal resolutions, and geographic locations.

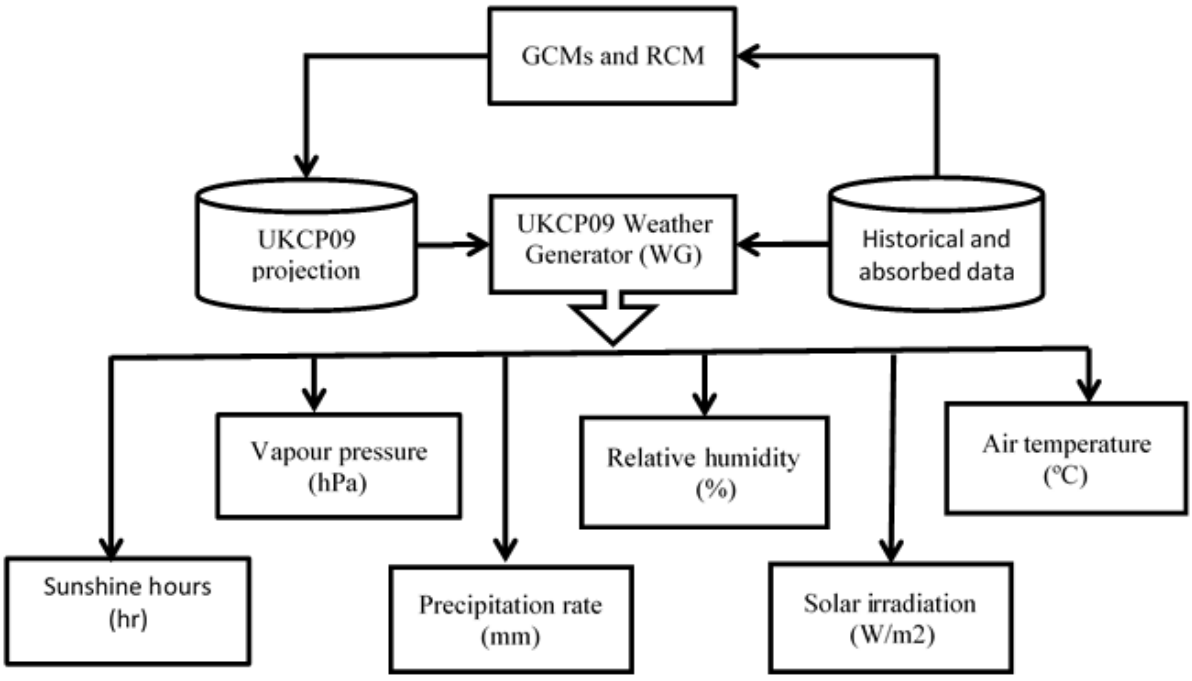


**Figure 4.2.** Main UKCP09 WG methodology for simulating future hourly climate variables

#### 4.3.2.2 UKCP09 Emission Scenarios

As discussed in section 3.5 in Chapter 3, over the long run, the weather is expected to change from time to time due to anthropogenic and non-anthropogenic effects. The anthropogenic, or so-called 'human effect', has been studied and modelled by researchers and scientists and is believed to be perhaps the greatest cause of substantial future climate change [138]. Since the UKCP09 model is based on an assumption of no significant changes in future non-anthropogenic effects, any changes in the climate variables considered are therefore due primarily to human activity [166]. The emission scenarios incorporated into the UKCP09 are taken from the Intergovernmental Panel on Climate Change (IPCC) *Special Report on Emissions Scenarios* (SRES): A1FI, A1B, and B. These scenarios are categorised based on the level of GHG emissions associated with each one: a high level of emissions for A1FI, a medium level for A1B, and a low level for B1, as indicated in **Figure 4.3.**

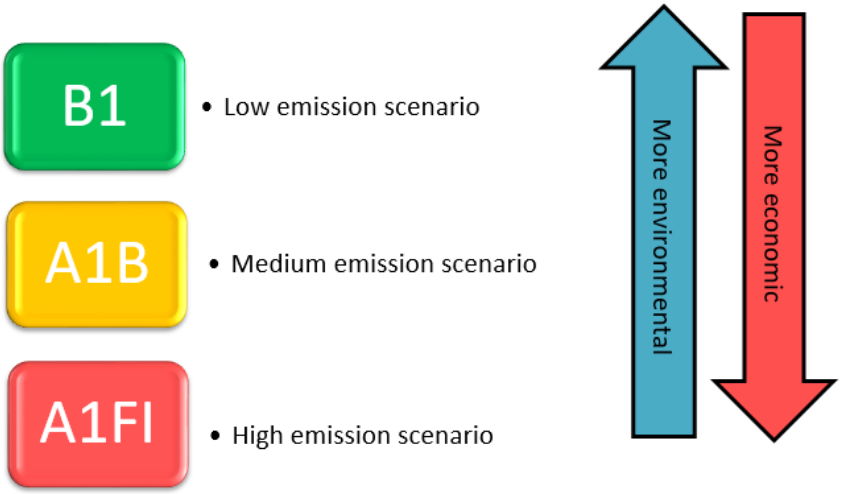


**Figure 4.3**. Main climate change emission scenarios

All of these emission scenarios were explored in the work presented in this thesis. They are dependent on a number of storylines, predominantly environmental and economic development, as detailed in section 3.5 of Chapter 3. For example, high- and medium-emission scenarios would result from rapid global economic development that entails substantial future energy demand while a low-emission scenario represents a more sustainable future in which environmental concerns are addressed. In this theoretical context, the greater the GHG emissions, the more serious would be the expected changes in climate and the less attention would be devoted to the environment.

#### 4.3.2.3 UKCP09 Timescale

The UKCP09 WG model can simulate climate variables for seven future overlapping 30-year periods based on historical and absorbed data (baseline data). **Table 4.1** gives the seven overlapping future periods starting from 2010 and ending with 2099. For simplicity, each 30-year period is designated according to its middle decade, such as the 2020s, and is therefore referred to by the middle decade in this thesis. A further three non-overlapping future 30-year periods have also been selected: the 2020s, 2050s, and 2080s. These periods have been employed for the specific time-horizon-based reliability assessment of a power system in order

to investigate and compare the impact of climate change over the long term and for different time spans.

**Table 4.1.** The seven 30-year overlapping future periods

| No. | 1960 | 1980 | 2010 | 2020 | 2030 | 2040 | 2050 | 2060 | 2070 | 2080 | 2090 |
|---|---|---|---|---|---|---|---|---|---|---|---|
| 1 | Baseline | | 2020s (2010-2039) | | | | | | | | |
| 2 | | | | 2030s (2020-2049) | | | | | | | |
| 3 | | | | | 2040s (2030-2059) | | | | | | |
| 4 | | | | | | 2050s (2040-2069) | | | | | |
| 5 | | | | | | | 2060s (2050-2079) | | | | |
| 6 | | | | | | | | 2070s (2060-2089) | | | |
| 7 | | | | | | | | | 2080s (2070-2099) | | |

#### 4.3.2.4 Steps in the Climate Change Simulation

The first stage of the climate change simulation involved an analysis of the UKCP09 climate change projections and the UKCP09 WG interactions. **Figure 4.4** outlines the main approach employed for simulating long-term climate change with the goal of establishing its impact on the reliability assessment of a PV-integrated power system. The climate variables most relevant for this investigation were air temperature and solar irradiation, which were examined for all three emission scenarios. In the same way, spatial resolution, temporal resolution, and geographic location were determined based on the study requirements. The WG model was then applied for estimating at a high 12 km resolution the hourly climate data for the identified climate zone: Birmingham, UK. The temporal resolution which was selected for this study is for three non-overlapping 30-year periods: the 2020s, the 2050s, and the 2080s. The historical and absorbed data cover the 30 years from 1960 to 1990. Based on these specifications, output samples were then simulated for use in the climate assessment.

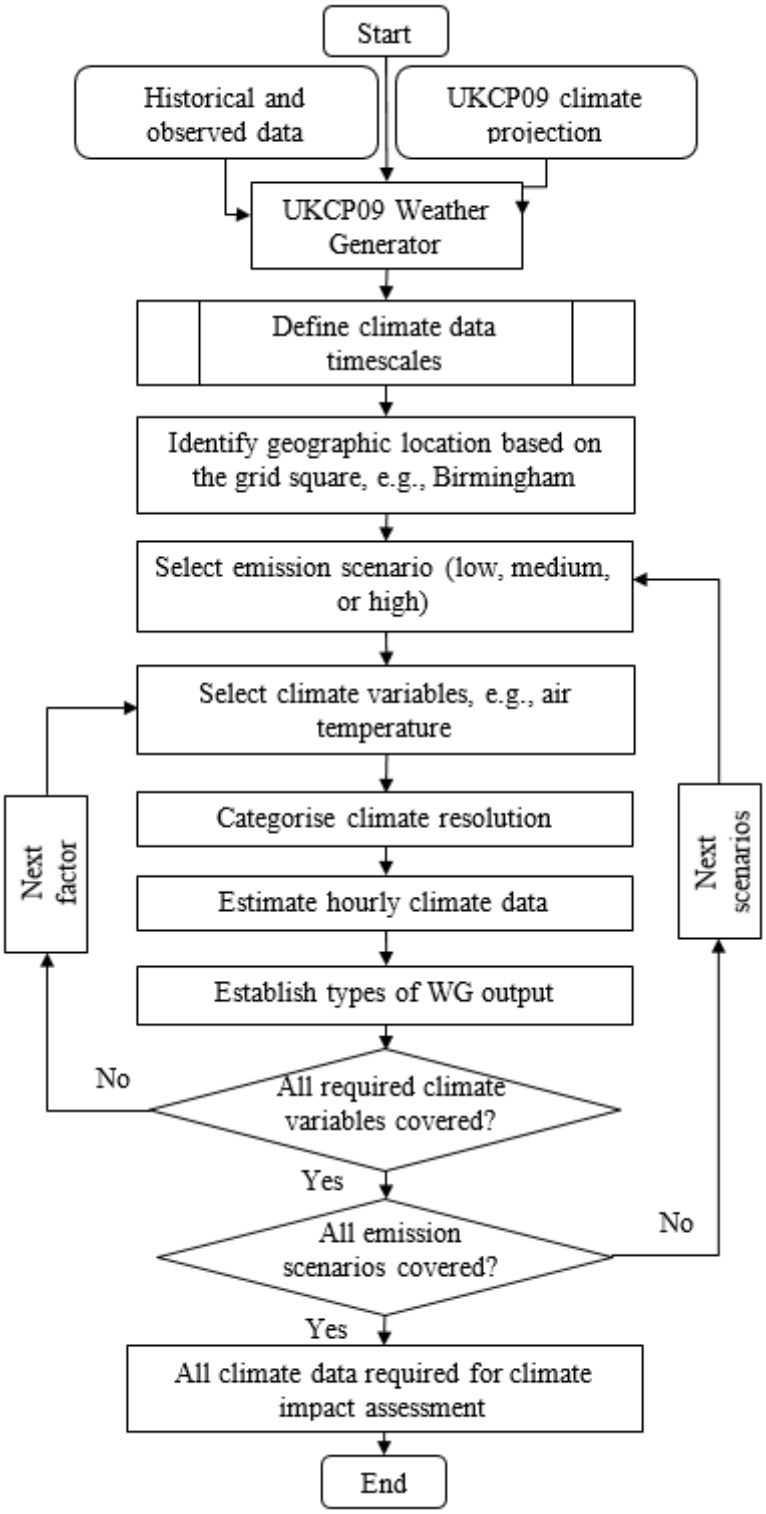


**Figure 4.4.** Flowchart of the main approach to long-term climate change simulation for the purpose of assessing the impact on the reliability of a PV-integrated power system

#### 4.3.2.5 WG Sample Output

The simulation approach outlined in **Figure 4.4** comprises multiple WG runs; for each run, data are provided for a 30-year time period for the selected emission scenario. The WG

model also furnishes two types of simulated weather data: control scenarios and emission scenarios. Control scenario data refer to baseline climate data without the application of any GHG emission scenario while emission scenario data refer to future climate change that includes consideration of a GHG emission scenario. Control scenario data are baseline historical data but are generated stochastically based on observed historical data with minor variations. In contrast, emission scenario data are generated based on assumed GHG emissions associated with future climate change for the specific scenario selected. The difference between the generated control data and the scenario data indicates future climate change. The output from each UKCP09 WG run reveals different climate change outcomes based on a probability distribution function (PDF). For this research, the factor considered was the central PDF estimate of climate variables.

Climate change data were simulated for Birmingham, UK, at 52.48° N latitude and 1.89° W longitude. The most important climate variables for the work discussed in this chapter are ambient air temperature and global horizontal irradiance (GHI), which reflects the total amount of direct and diffuse solar irradiation. **Figure 4.5** provides a comparison of the hourly air temperature (a) and solar irradiation (b) results for a sample high-emission scenario simulated over two different days: January 1, 2070, and January 1, 2099. The variations in temperature indicate possible effects of global warming due to GHG emissions. Fluctuations in solar irradiation are the result of rainfall, cloud movement, and varied cloud cover. It should be noted that the number of hours of sunshine remains exactly the same for both years: only the amount of solar irradiation changes.

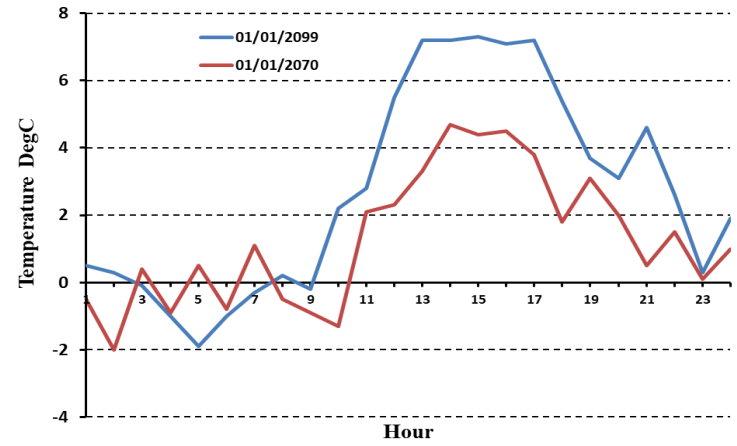


(a)

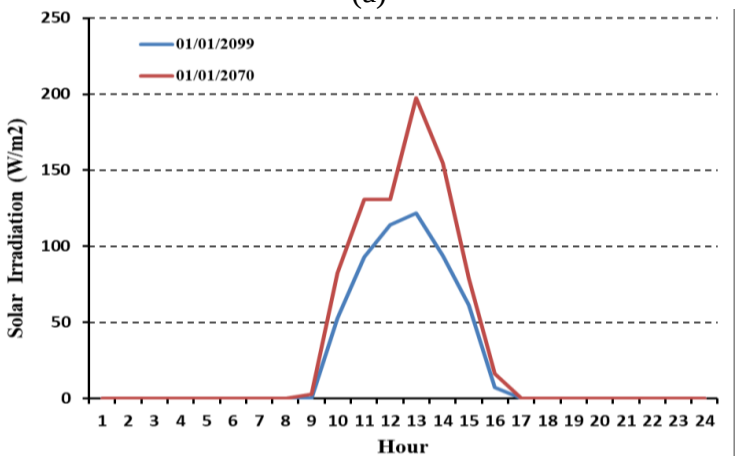


(b)

**Figure 4.5.** Example indicating (a) ambient temperature (°C) and (b) direct solar irradiation ($W/m^2$) for a single day (January 1st) in 2070 (red) and in 2099 (blue)

**Figure 4.6** presents PDFs of long-term climate change with respect to ambient temperature and solar irradiation for low, medium, and high emission scenarios. The PDFs reveal a clear image of climate change and future weather for 2020, 2050, and 2080. Small fluctuations in the climate variables translate into enormous differences with respect to integrated PV power systems.

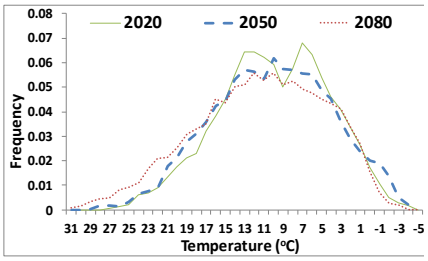


(a) Low emissions (temperature, in °C)

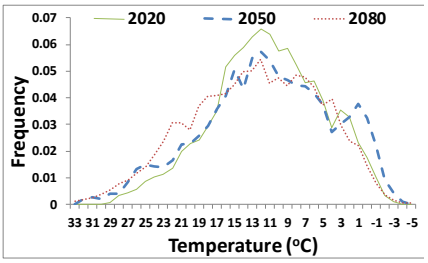


(b) Medium emission (temperature in °C)

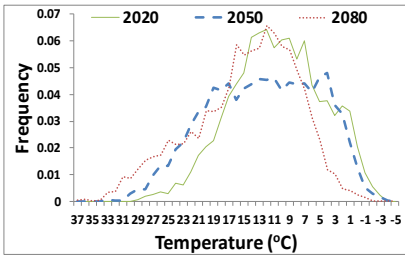


(c) High emissions (temperature, in °C)

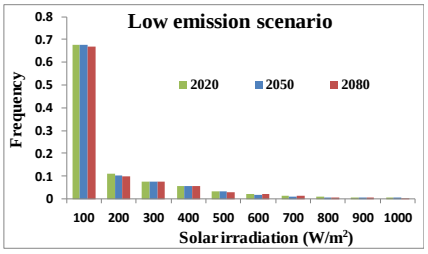


Low emissions (solar irradiation, in W/m$^2$ )

(d)

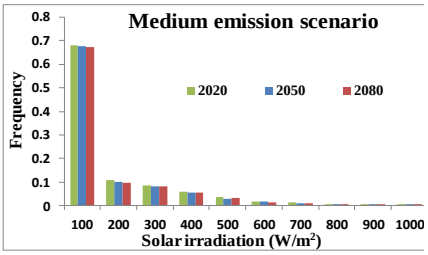


Medium emissions (solar irradiation, in W/m$^2$)

(e)

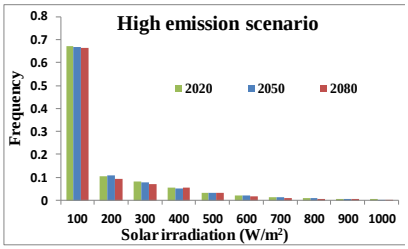


High emissions (solar irradiation, in W/m$^2$ )

(f)

**Figure 4.6**. Climate change PDFs: (a), (b), (c) ambient temperature for low emissions, all 2080 emission levels, and high emissions, respectively; (d), (e), (f) solar irradiation for low-, medium-, and high-emission scenarios, respectively

The probabilities associated with the ambient temperatures indicated in **Figure 4.6** (a), 4.6 (b), and 4.6 (c) for some emission scenarios for 2020, 2050, and 2080 vary due to the occurrence of climate change, with all curves slightly following a Gaussian distribution. However, in **Figure 4.6** (d), 4.6 (e), and 4.6 (f), it can be seen that, compared to the variations in ambient temperature, only minor differences are evident in solar radiation values across all scenarios.

## 4.4 PV System Modelling

A PV farm consists of a number of PV systems that, in turn, comprise subsystems and their components, including inverters and converters, which transform solar radiation into electricity, as illustrated in **Figure 4.7.** The key subsystem in a PV power generation system is the PV array, which constitutes the power conversion unit. A PV array is composed of strings

connected to the grid either in series or in parallel, depending on the specific design. Each string encompasses multiple PV modules with each module containing a number of PV cells. The high degree of uncertainty associated with a PV system output arises from many factors, including the specific technology and the ambient conditions.

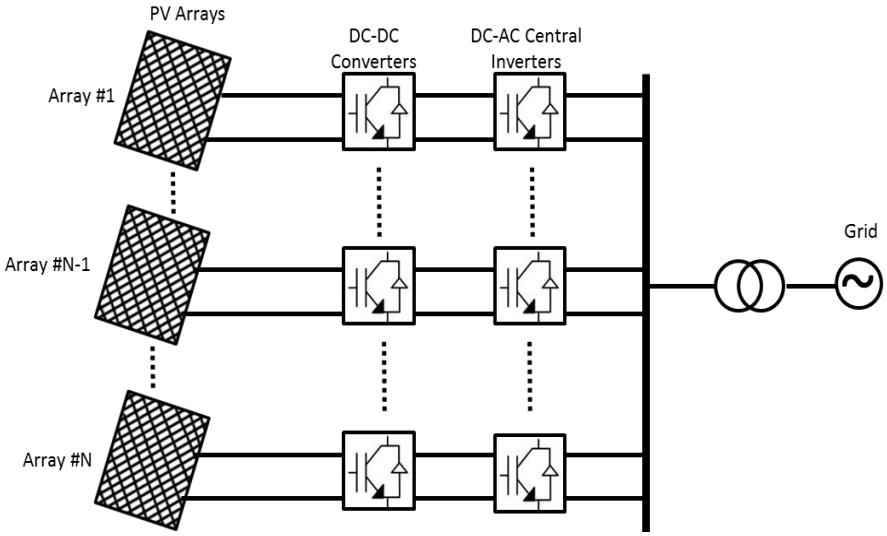


**Figure 4.7**. Schematic of a PV farm with N PV systems

In this chapter, the focus is on ambient conditions, the aging of a PV system, and the possible long-term impact of climate change on PV systems integrated into a power system. The power generation profile model in the context of climate variables, primarily solar irradiation and ambient conditions, is presented in the next section.

### 4.4.1 PV Power Generation Model

Chapter 2 introduced a method that uses an analytical model for estimating the output power of a PV system based only on solar irradiation while neglecting other climate variables. However, the analytical model presented in this chapter was designed to incorporate the effects of ambient temperature, operating temperature, and PV system efficiency along with multi-level solar irradiation. In addition, because PV system efficiency has been based on multiplied solar irradiation, for an accurate climate-impact assessment, the ambient and operating temperatures have therefore also been taken into account. **Figure 4.8** illustrates the PV output

power model with multiplied solar irradiation, since it is the key governing factor in PV output power. $G_{STC}$ represents the global standard solar irradiation, which is 1000 *W/m*$^2$, while $R_c$ indicates the solar irradiation point, which is selected based on the simulation results.

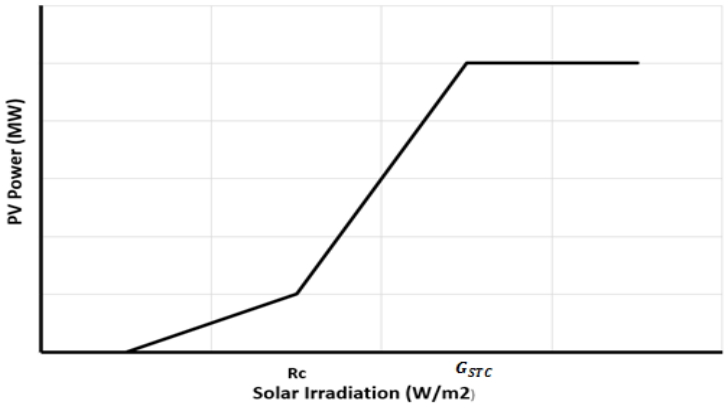


**Figure 4.8.** PV output power model that incorporates multiplied solar irradiation

The calculation of PV power generation as expressed in equation (2.17) has therefore been further extended to incorporate the ambient and operating temperatures, with consideration of efficiency as given in [231]. The PV power generation model $P_{pv}$ can thus be computed as follows:

$$P_{pv} = \begin{cases} \sum_{t=0}^{t=period} \frac{P_{STC}\ {G_{bi}}^2}{R_c\ x\ G_{STC}} \left(1 - \frac{\delta}{100}\ (T_{STC} - T_{cell}\right) & 0 \leq\ G_{bi} < R_c \\ \sum_{t=0}^{t=period} \frac{P_{STC}\ G_{bi}}{G_{STC}} \left(1 - \frac{\delta}{100}\ (T_{STC} - T_{cell}\right) & R_c \leq\ G_{bi} <\ G_{STC} \end{cases} \quad (4.1)$$

where

$R_c$ a solar irradiation point set to be *150 W/m*$^2$;

$G_{STC}$ global solar irradiation in *W/m*$^2$, which is (1000 *W/m*$^2$ );

$G_{bi}$ solar irradiation in W/m2;

$P_{STC}$ rated power of the PV system;

$T_{amb}$ ambient temperature in °C;

$T_{STC}$ test condition temperature set at 20 °C;

$T_{cell}$ PV cell temperature in °C, which can be calculated using (4.2):

$$T_{cell} = T_{amb} + \frac{NOCT - 20}{1000} \tag{4.2}$$

$NOCT$ nominal operating cell temperature, which is the cell temperature for a standard reference open-circuit environment;

$\delta$ and $\eta_c$ temperature coefficient and rated efficiency of the PV system, respectively; PV efficiency also can be computed using (4.3):

$$Eff_{pv} = \begin{cases} \frac{\eta_c}{R_c} G_{bi}\left(1 - \frac{\delta}{100}(T_{STC} - T_{cell}\right) & 0 \leq G_{bi} < R_c \\ \eta_c \times \left(1 - \frac{\delta}{100}(T_{STC} - T_{cell}\right) & R_c \leq G_{bi} \end{cases} \tag{4.3}$$

### 4.4.2 PV Power Generation Profile

A sample generation profile is presented in **Figure 4.9**. The readily observable changes in power generation for different $CO_2$ emission scenarios are clearly due to varying weather conditions. For example, with low-emission scenarios, the power level is high, especially during the summer, while the power level associated with a high-emission scenario is low, especially during the winter.

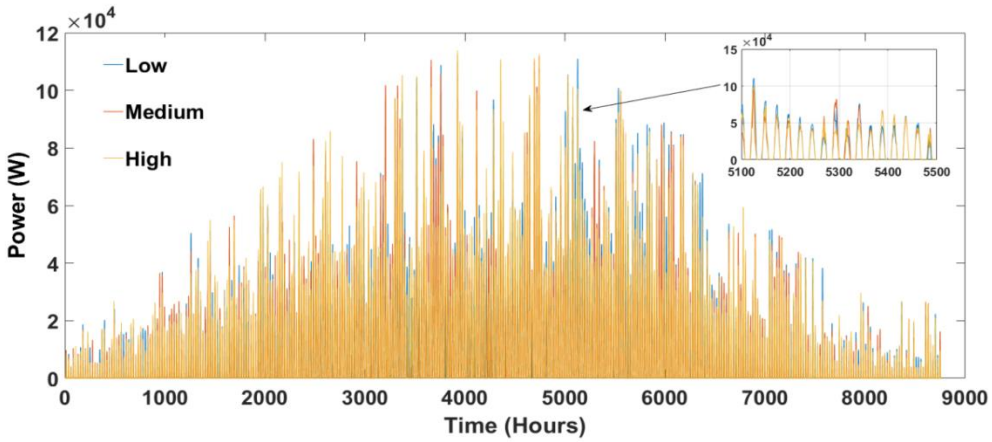


**Figure 4.9**. Generation profiles for 2020

## 4.5 Test System

The IEEE Reliability Test System (IEEE-RTS) 1996 was modelled and utilised for the work presented in this chapter in order to demonstrate the impact of climate change on the reliability of a PV-integrated power system. **Figure 4.10** shows a diagram of the IEEE 24-Bus Reliability Test System with the integration of PV systems. The system contains 24 buses, 38 branches, and 11 generators. System technical data, including the parameters of branches (lines and transformers) and generators, as well as reliability data, are provided in Appendix A. The system details were derived from [232] with adjustments appropriate for each case study.

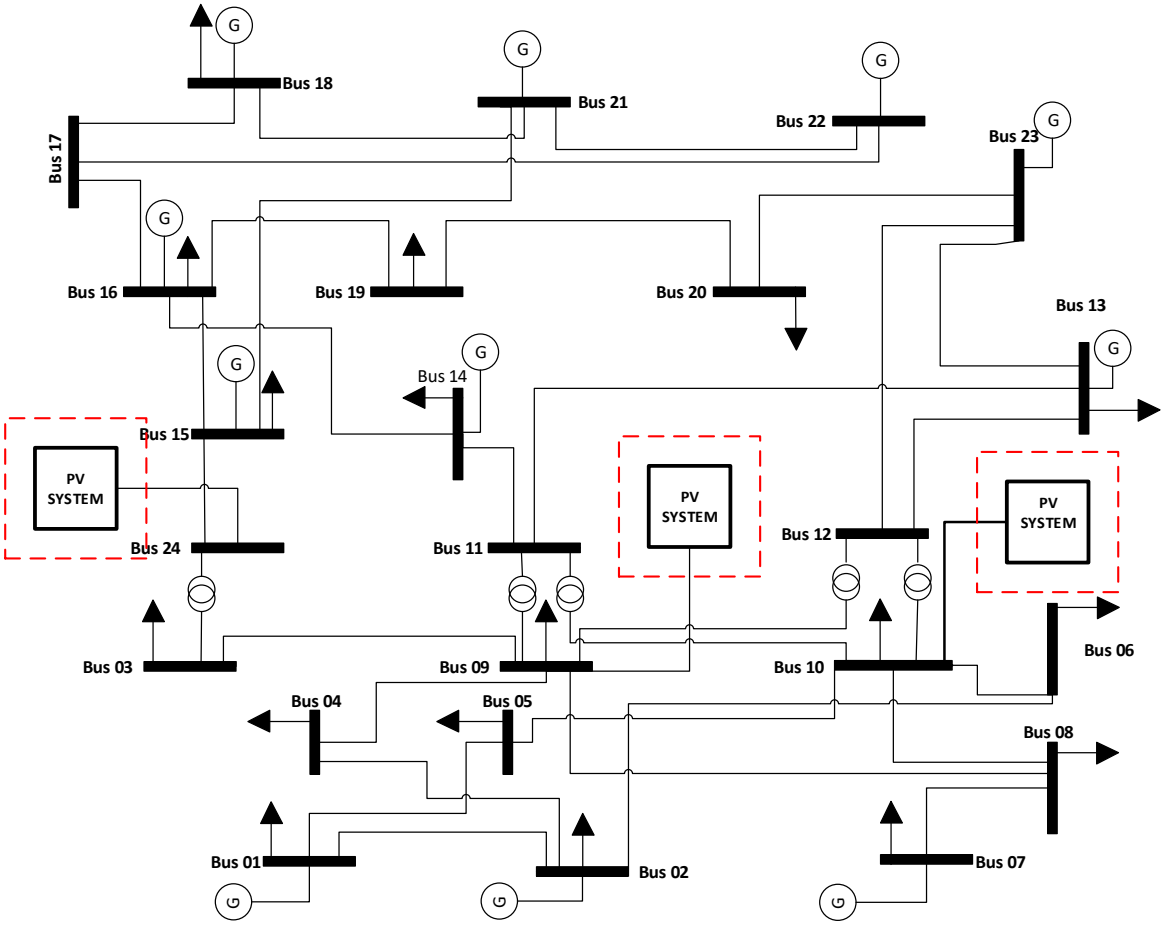


**Figure 4.10**. IEEE 24-Bus Reliability Test System diagram

## 4.6 PV System Reliability

The aim of the work presented in this section was to establish correlations with respect to the reliability of an integrated PV system, climate change, and PV module aging. The impact of long-term climate change on solar units can affect the power demand and overall reliability of the system, which requires assessment. The following subsections first discuss the incorporation of the effects of aging PV modules on reliability, followed by an examination of reliability assessment under climate change conditions.

### 4.6.1 PV System Aging

Environmental factors and operating conditions affect PV generators in ways that could impact their dynamics, leading to accelerated degradation. Climate change variables such as humidity, temperature, and irradiance can influence the aging process and result in a reduction in output power. Age-related deterioration decreases the overall reliability of these modules and thus diminishes their output power over time. In general, despite the fact that common Crystalline silicon PV module products can have life cycles as long as 25 years, the life-cycle limits associated with PV modules vary based on operating conditions [233]. An additional factor is that manufacturers normally provide a warranty that covers PV module output power, which usually guarantees at least 90 % output power after 10 to 12 years of operation and at least 80 % output power after 20 to 25 years. The common power tolerance for a PV module is 5 % [233]. PV system output power degrades linearly and can be computed as given in (4.4), (4.5), and (4.6):

$$P_{total=} P_{initial} \ [1 - (K - L)d] \tag{4.4}$$

$$\text{K=1,2,…L} \tag{4.5}$$

$$P_{PV,K=-} P_{total} + 2\, P_{initial} \tag{4.6}$$

where

$P_{initial}$ initial power capacity of the PV module;

$K$ specified year;

$L$ life cycle power of the PV module;

$d$ constant slope, as given in [69].

### 4.6.2 PV-Integrated Power System Reliability in Light of Climate Change

A large grid-connected PV system can fail due to random disturbances and during extreme events such as excessive flooding, heat waves, severe lightning, and storms. Adverse effects can occur in the form of reduced output, damage to infrastructure, and component failure. Climate change and its impact can therefore have negative ramifications for a large-scale PV system as a result of changes in the ambient conditions surrounding that PV system over an extended period. A small change in temperature, cloud cover, or direct or indirect solar irradiation can alter the potential of the PV system and, consequently, overall system reliability. The variation in these climate variables over the long-term represent climate change fluctuations in large-scale atmospheric circulation patterns, the simulation of which requires a method normally used with a large and complex network. For this reason, a non-sequential MCS has been employed because of its suitability for use in analysing the impact of weather. This method was adopted because it involved no necessity to increase the size of the system space and because the computing time is independent of the size of the system, i.e., the number of integrated renewables.

For evaluating the level of reliability, one of the most common reliability indices is the expected energy not supplied (EENS), which can be applied for measuring the variable impact of climate on an integrated PV system over time. The EENS index quantifies the energy that cannot be supplied to a system (MWh/y) due to the failure of the components in the entire system.

The accuracy of the reliability index is estimated through the simulation of a large number of experiments/iterations, with correspondingly significant computation time. However, a convergence criterion can be quantified in order to estimate the optimum number of these simulation experiments within an acceptable computation time. **Table 4.2** shows the base EENS values for the IEEE-RTS reliability evaluation for different numbers of MCS experiments and the respective computation time required. It can be seen from the table that both the computational time and the accuracy of the results increase with additional iterations. The limit of this variation in the reliability index decreases with the increase in the number of iterations simulated. Since the EENS simulation results for 20,000 iterations and 80,000 iterations do not differ significantly relative to a substantial difference in the computational time, 20,000 iterations have been employed so that the simulation stops within an acceptable computation time.

This study involved consideration of only the impact of climate change on the PV system and excluded the effects on the PV system due to other events that can occur in a power system. Any dissimilarity in the reliability index values for the different cases is therefore due to variations in the impact of climate change.

**Table 4.2.** EENS values for a number of MCS experiments relative to their computation times

| Number of iterations | EENS (MWh/yr) | Time (h:min) |
|---|---|---|
| 5000 | 5259.14 | 00:38 |
| 10,000 | 5211.91 | 01:07 |
| 20,000 | 5197.01 | 1:53 |
| 40,000 | 5187.78 | 02:49 |
| 80,000 | 5195.56 | 04:11 |

### 4.6.3 PV-Integrated Power System Reliability without PV Component Failure

To estimate the EENS indexes, reliability performance analyses were implemented using a non-sequential MCS technique because of its speed and suitability for weather impact studies. The EENS reliability indexes for the PV-integrated power system were established based on an assumption of the absence of any failure not due to the impact of climate change. **Figure 4.11** illustrates the reliability assessment procedure that addresses the impact of climate change on a PV-integrated power system, given an extreme assumption of fully reliable PV components. The reliability assessments were performed using DIgSILENT PowerFactory and MATLAB according to the following steps: Simulate future climate change patterns based on the emission scenarios selected for the chosen future year, as outlined in the steps shown in Figure 4.4. The simulated hourly climate change variables for the elapsed years are used as input for the next steps.

- Model and design the PV power generation model to be integrated into the reliability test system.
- Build the adapted IEEE-RTS model to be used for the validation and demonstration of the robustness of the proposed framework.
- For the reliability assessment, apply the simulated climate change scenarios in the PV-integrated power system and repeat the steps for each emission scenario and future year, as previously indicated.
- Initialise the number of occurrences and mount of load curtailment and insert the reliability data for each power system component (transformers, power lines, busbars, etc.).

- Generate a random number in the interval (0,1) for each power system component $i$. If the generated number is less than the forced outage rate (FOR), then the component is considered to be in a down state, and vice versa, as given in (4. 7):

$$State_i = \begin{cases} 1, & \text{Up state} \\ 0, & \text{Down state} \end{cases} \quad (4.\ 7)$$

- Perform load flow analysis and initialise the power balance within the voltage limits at the buses and within the thermal limits of the lines during the simulation.
- Calculate the load curtailment $C_i$ of each system state sampled.
- Repeat these steps for N, number of iteration
- Estimate the reliability analyses by calculating the demand not supplied (DNS) and energy not supplied (ENS) at each iteration. Then estimate the expected demand not supplied (EDNS) in MW and the EENS in MWh/y for all of the iterations using (4. 8) and (4. 9) [22]:

$$EDNS = \sum_{i \in S_i} C_i \times P_i \quad (4.\ 8)$$

$$EENS = \sum_{i \in S_i} C_i \times P_i \times 8760 \quad (4.\ 9)$$

where $C_i$ is the load curtailment in system state $i$, $P_i$ is the system state probability, and $S$ is the set of all system states associated with load curtailment.

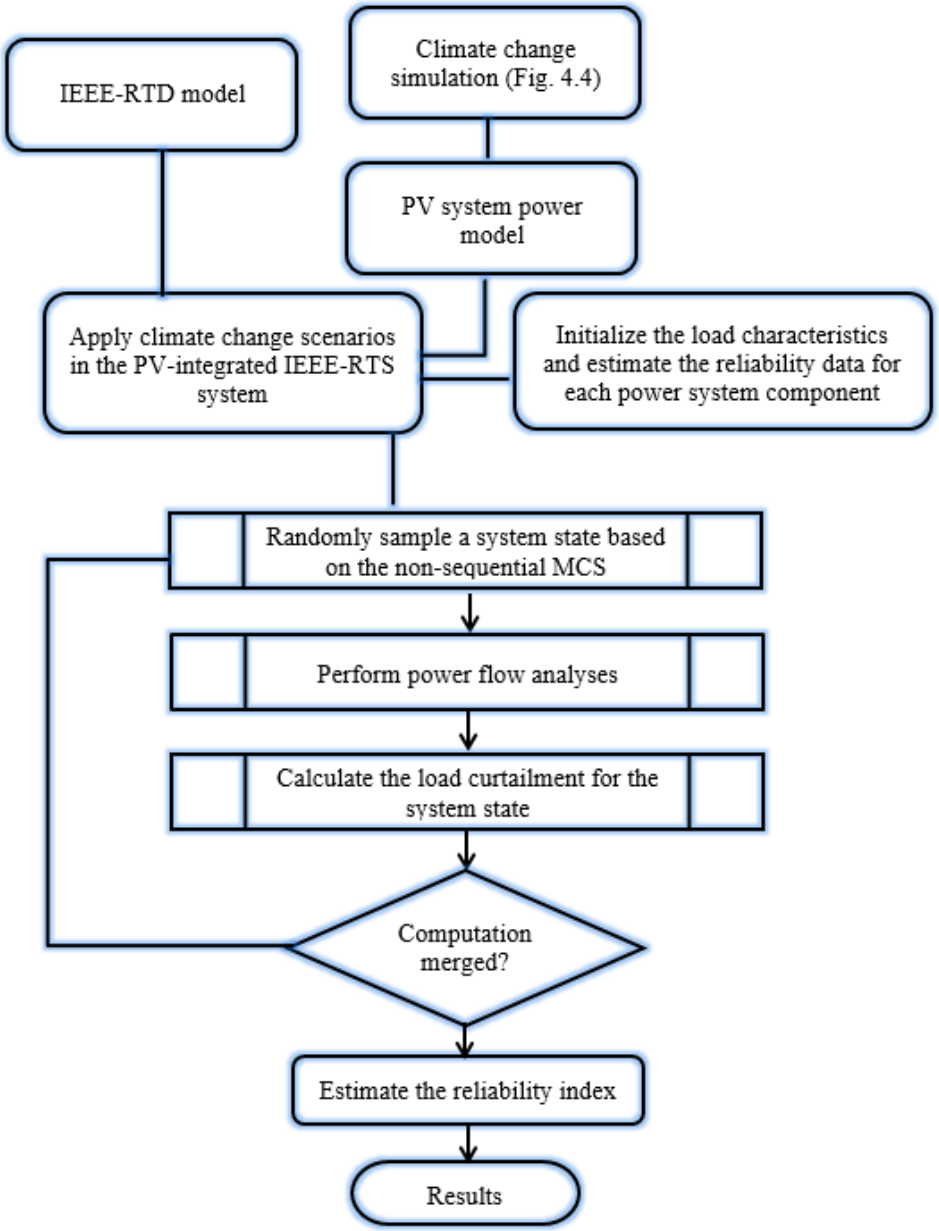


**Figure 4.11**. Reliability assessment procedures for establishing the impact of climate change on a PV-integrated power system with fully reliable PV components

## 4.7 Case Studies

To demonstrate the effect of climate change on future PV-integrated power systems for different emission scenarios, the proposed framework has been applied in a number of case studies. To this end, MATLAB was employed for the design of a large PV system with a 40 MW capacity to enable grid-connected operation. This PV system constituted the foundation for the assessment of the reliability of a power system under different climatic conditions.

Because real power system data corresponding to the Birmingham, UK, area were unavailable, this study relied on the IEEE 24-bus test system [234] as the power system to be investigated with respect to the effects of climate change patterns. To this end, MATLAB was employed for the design of a large PV system with a 40 MW capacity to enable grid-connected operation. The penetration level of the centralized PV system supplies roughly 23% of the customers connected at busbars 9 (load bus) within line rating limit. To simulate effect of centralized generation near load centre, the load bus is chosen to centralized integration with significant penetration level of PV generation. This penetration level is further increased into the doubled in decentralized case at busbar 10 and 24 in order compare. The centralized and decentralized PV systems are integrated at different busbars including medium voltage level (138 kV) at busbar 9 and 10, and high-level voltage (230 kV) at busbars 24 in order to assess the impacts of PV system on different connection levels and busbars types. Diverse topology of the network essentially provides more realistic scenarios which are likely to be observed in future smart grids. Baseline load scenarios were assumed in these case studies, which means that no changes in the load profile were attributable to climate change. The designed PV system was integrated into the power system at the resource locations identified in the following sections.

Four cases were simulated in order to assess the impact of climate change:

- **Case 1**: The first case was the base case without the integration of a PV system.
- **Case 2**: In the second case, the power system included a centralized PV system integrated at bus 10 for low, medium, and high emission scenarios.
- **Case 3**: For the third case, the power system was augmented by adding decentralized PV systems integrated at busbars 24 and 9 along with the centralized PV system already integrated at busbar 10. All of the systems were run with the high-emission scenario.
- **Case 4**: In addition to the impact of climate change on the centralized and decentralized integrated PV systems, the fourth case incorporated the influence of aging on reliability.

### 4.7.1 Case 1: Base Case (without PV Integration)

In the first scenario, the IEEE-RTS was simulated with no PV system and no climate change effects taken into consideration. This case provided a means of demonstrating the feasibility of the framework and of enabling a comparison with other scenarios in which climate change conditions were applied. MCSs were therefore employed for different iterations, and the optimum iteration established from **Table 4.2** was employed. The reliability of the IEEE-RTS performance for the base case was assessed, and the EENS reliability index was determined to be 5197 MWh/y, which then established a reference point for evaluating the results from the other scenarios.

### 4.7.2 Case 2: Impact of Climate Change with a Centralized PV System

The objective of the second case study was to determine the impact of climate change on the reliability of a centralized PV system. A PV system was centralized and integrated into busbar 10. For this case study, low, medium, and high GHG emission scenarios were simulated for the three years of under investigation: 2020, 2050, and 2080. The climate change model was merged with the PV power generation model in order to assess the IEEE-RTS reliability with the integration of the centralized PV system. The effect was then captured through the MCS in order to estimate the EENS. In this manner, the reliability values resulting from the application of each of the three emission scenarios could be compared in the following ways: with the outcome from the reference case, with the results produced by the other two emission scenarios, and with future-year values for that scenario itself. In this way, any changes in reliability performance are due to the different levels of GHG emissions while the effects of any other factors on the PV system other than climate change are neglected. The impact of PV module aging on the reliability performance was also ignored, meaning that it was assumed to be a new installation. Any change in the EENS reliability index compared to the base case and

the other cases can therefore confidently be concluded to be a consequence of the impact of climate change on the integrated PV system.

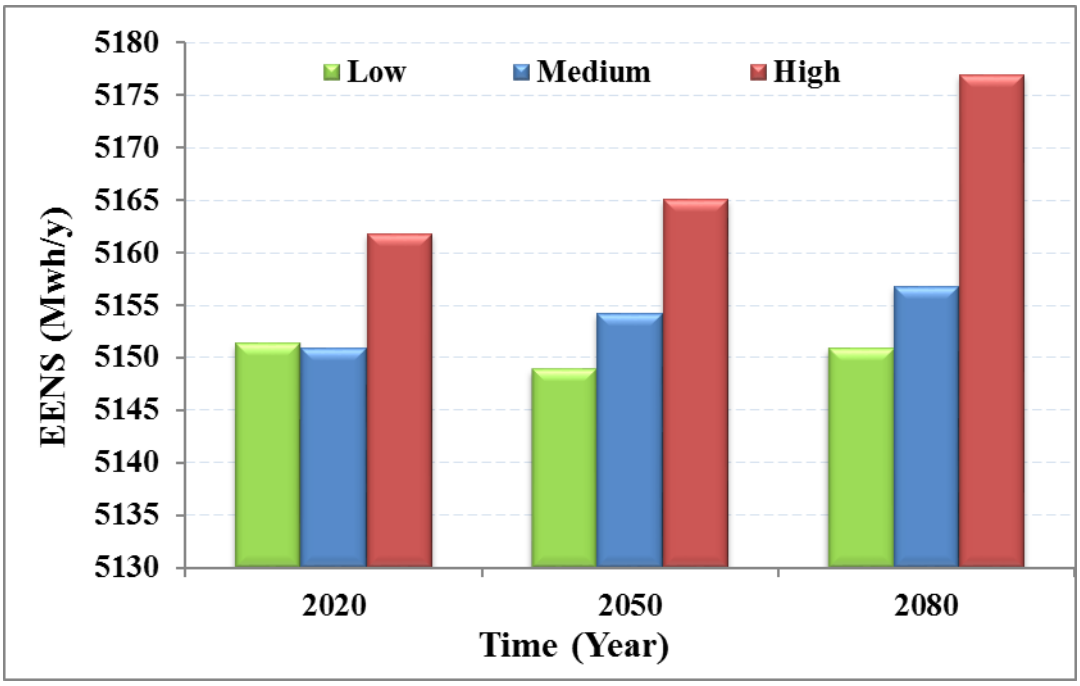


**Figure 4.12**. 2020, 2050, and 2080 EENS values for the integrated centralized PV system with different emission scenarios

**Figure 4.12** shows the EENS values for 2020, 2050, and 2080 as a function of time for the IEEE-RTS with a centralized PV system for the three $CO_2$ emission scenarios. Relative to the base case, all of the 2020, 2050, and 2080 reliability performance outcomes in this case exhibit considerable improvement, which can be attributed to the integration of the centralized PV system. When the results for each emission scenario are compared separately with the base-case level, the low-emission scenario significantly enhances reliability performance. The improvement degrades proportionally with increased GHG emissions, mainly $CO_2$, because the power flow pattern of the PV system is affected by the uncertainty associated with shifts in temperature and solar insolation, i.e., climate change. However, even with the less-enhanced EENS resulting from the medium- and high-emission scenarios, a substantial upgrade is still evident compared to the base case. The high-emission scenario produces the least increase in reliability over the base case because, in that scenario, GHG emissions remain high when

society fails to make concerted efforts to cut them. Reliability thus decreases with the greater levels of GHGs that characterize the medium- and high-emission scenarios, while the negative effect on reliability enhancement of the less-climate-sensitive low-emission scenario is not as great as with the other two scenarios.

With respect to timescale, small variations in the EENS reliability index could be distinguished with the low-emission scenario for all three years. On the other hand, as a result of the high GHG emissions and anticipated changes in weather conditions, the medium- and high-emission scenarios led to a significant increase in the EENS values for longer time-ahead periods, especially for 2080. Even though reliability decreases farther into the future with both the medium- and high-emission scenarios, the reduction resulting from medium emissions is less than with high emissions.

### 4.7.3 Case 3: Impact of High Emissions with Decentralized PV Systems

This case exemplifies the scenarios featuring the highest levels of emissions for the IEEE-RTS with decentralized PV farms integrated at buses 10, 24, and 9. It was thus intended to investigate the impact of climate change on a decentralized PV system for the 2020, 2050, and 2080 future time spans. As an extension of the previous case involving a single centralized PV farm, the EENS reliability index was also measured for an additional second and then a third decentralized PV farm with the same IEEE-RTS capacity, based on the merging of the climate change model with all three PV power generation models. For high-emission scenarios, there are thus three sets of circumstances in this case: the first involves the centralized PV farm and the second and third correspond to the addition of the decentralized PV farms. As with the second case, this case is also reliant on the assumption that the PV system components are fully available so that any changes in the level of reliability can credibly be attributed to the influence of climate change on the decentralized PV farms.

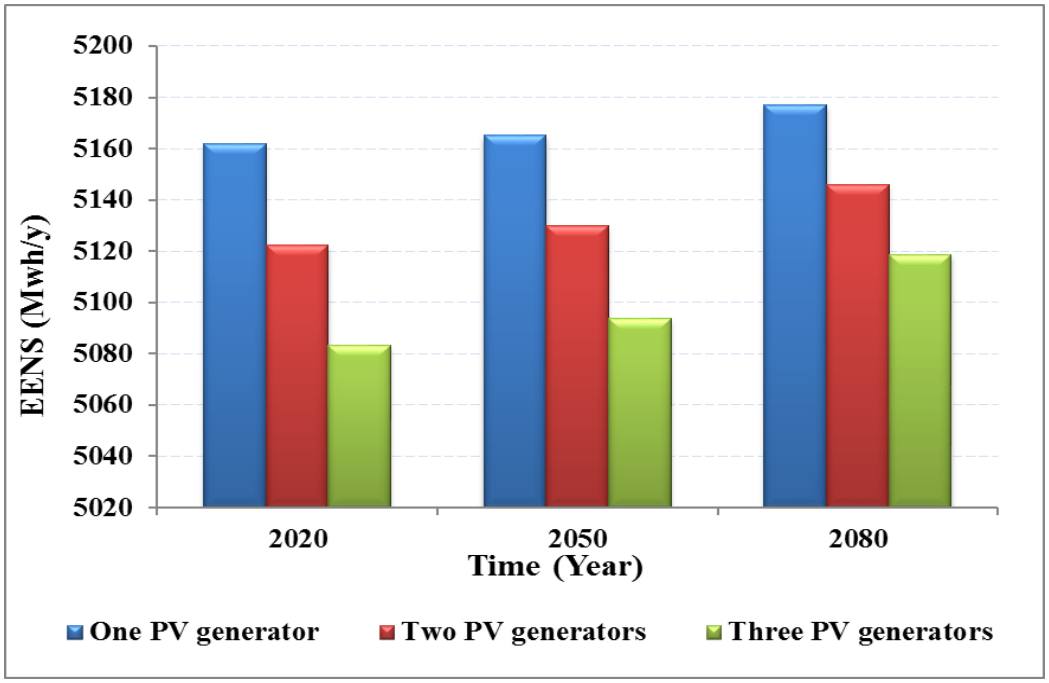


**Figure 4.13**. High emissions with decentralized integrated PV Systems

**Figure 4.13** depicts the reliability values with the decentralized integrated PV farms under high-emission conditions for 2020, 2050, and 2080. As in the second case, the significant EENS reductions with the first centralized PV system scenario rise proportionally with the 2050 and 2080 timescales. The addition of the decentralized PV systems into the IEEE-RTS in the second and third instances could substantially improve system reliability compared to the inclusion of just the centralized PV system. However, the second and third scenarios also exhibit a problematic decrease in EENS improvement over time: progressive reductions from 2020 to 2050 and then to 2080. **Figure 4.13** reveals that expanding the number of decentralized PV farms that are integrated into the power system enhances the improvement in the EENS reliability index.

The EENS improvement drops over time because the PV system output is affected by the altered temperatures and solar irradiation that accompany extended climate change, making the consistent output the PV system was designed to deliver no longer feasible. The results thus indicate that a PV system is vulnerable to the effects of the conditions arising from long-term

climate change. This situation becomes exacerbated over the long run with increased penetration levels of PV power generation and with a centralized PV system. Furthermore, although the EENS values are more advantageous with a decentralized PV system, the collective effect of the degradation in EENS improvement due to climate change also rises enormously with the integration of augmented PV capacity. However, the reliability evaluation in these results did not include consideration of the effect of PV aging, a factor that was incorporated into the fourth case study.

### 4.7.4 Case 4: Effects of Climate Change and Aging with Centralized and Decentralized PV Systems

In addition to conditions related to climate change, the aging of PV components can also impair power grid performance. For this reason, the fourth case study was targeted at assessing the impact of long-term climate change and age-related degradation on an integrated power grid featuring both centralized and decentralized PV systems. Centralized and decentralized PV systems were integrated at buses 10, 24, and 9. As additional factors, the case study includes consideration of a high-emission scenario only, as a benchmark, as well as a different range of selected future years: 2020, 2030, 2040, 2050, 2070, 2080, and 2095. The high GHG emission conditions and the centralized and decentralized PV farms define three scenarios for this case. Scenario one represents a PV system in which a new installation will be implemented in 2020, with an end-of-life date of 2045 (PV1). In scenario two, the PV2 system installed in 2045 will last until 2075, thus simulating a lifetime extended by technological advances in PV system materials, fabrication, and other features. Similarly, the PV3 installation activated in 2075 will also have a 30-year lifespan. In all three scenarios, the PV output power decreases due to aging as calculated in equations (4.4) to (4.6), based on consideration of maintenance and PV cleaning during their lifespans. In this way, any changes

in long-term reliability throughout the lifetime of the centralized and decentralized PV systems will be traceable to the effects of both climate change and age-related deterioration.

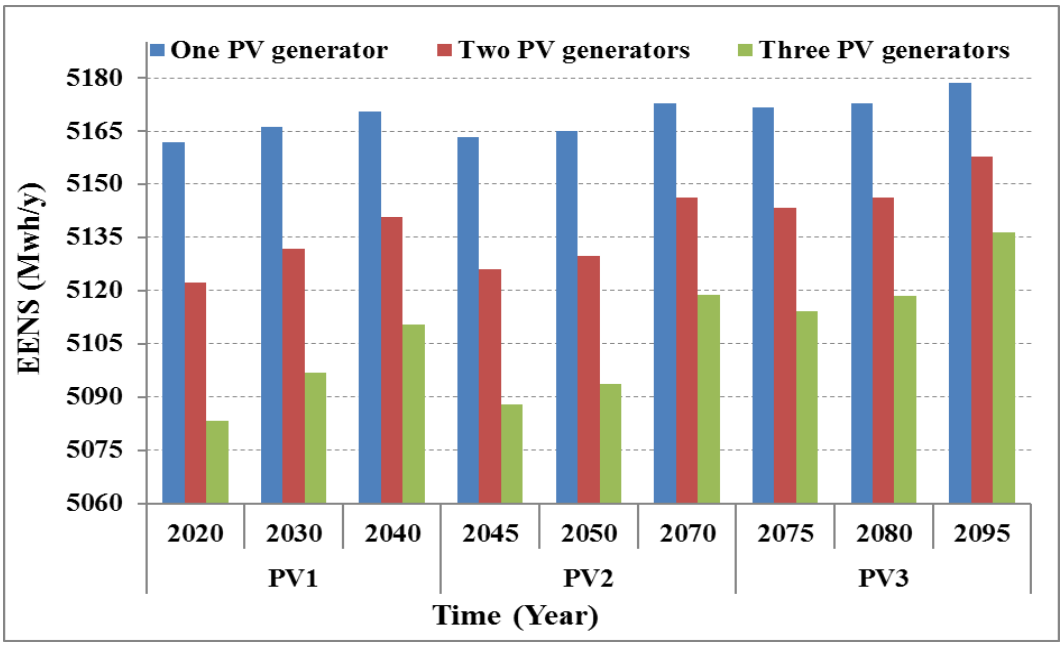


**Figure 4.14**. EENS values for the power system with integrated centralized and decentralized PV systems, incorporating consideration of PV degradation as a result of aging

**Figure 4.14** shows the long-term influence of both PV age-related degradation and climate change conditions with respect to the reliability performance of a power grid with PV system integration. Variations in reliability are evident during the aging process. For example, in 2050, the EENS is superior to that for 2040 as a result of the installation of the new PV2, which takes place in 2045. The findings thus suggest that taking into account the effects of both age-related deterioration and climate change on power grid reliability yields a nonlinear outcome for future time periods. It is therefore apparent that the consequences of climate change and aging with respect to the reliability of a power system should be assessed quantitatively since the impact on reliability is not linear and does not necessarily escalate with time. However, over the very long run, PV-integrated power systems could be subject to more significant challenges than at present with respect to maintaining the reliability of the power supply.

## 4.8 Summary

This chapter has introduced a framework for assessing the impact of climate change on a large-scale PV-integrated system over the long term. The framework applies climate models on both centralized and decentralized PV systems, with climate-related consequences for the power system being captured through an MCS. In addition, the framework also enables an examination of the influence of PV system aging on overall power system reliability. The framework incorporates high-resolution UKCP09 weather projection and WG climate models for different emission scenarios over long-term. The climate change simulations enable the implementation of meteorological data sets for investigating the impact of climate on the reliability performance of PV-integrated power systems.

Power system reliability assessments were performed in conjunction with PV system integration and climate change simulations. The IEEE-RTS Reliability Test System was implemented as the test network, and the PV power systems were integrated into it. A reliability procedure framework was also presented in order to demonstrate the influence of climate change and aging on the integrated PV system. A non-sequential MCS was employed for capturing the outcomes of the climate simulations for the PV-integrated system. In all cases, the EENS value was used as a benchmark for measuring the level of impact.

The results suggest that the reliability performance of a power system can be impacted by the response of any PV system due to climate change and aging. The impact on a power system is not necessarily heightened with time; however, over the very long run, establishing the reliability of PV-integrated power systems can be challenging, requiring a quantitative assessment in order to estimate the ramifications.

# Chapter 5: Reliability Studies on Wind Power Generation System with Climate Change

## 5.1 Introduction

### 5.1.1 Background

The rising levels of greenhouse gases in the atmosphere and their effect on climate is one of the major environmental concern. This in turn can potentially have impact on renewable energy generation. Among Renewable Energy Sources (RES), wind power generation system is reliant on prevailing weather conditions and can be vulnerable to change in ambient weather in a number of ways. Thus, the goals of the work presented in this chapter are to assess the effects of climate change on wind power generation system, and then to assess long-term impact of climate change on the reliability performance of a power system with integrated large onshore wind farms (WFs). The primary contribution of this chapter is the modelling and simulation of climate change based on different emission scenarios and the application of that simulation in a wind power generating model. Monte Carlo simulation (MCS) is employed for the quantification and assessment of the influence of climate change on WF integrated power system. Quantification of the intermittent characteristics associated with a large WF and the effect of climate change on the reliability of a WF-integrated power system are vital for in long-term system and operational planning.

### 5.1.2 Wind Power, Climate Change, and Drivers

Advances in the wind power industry have led to its rapid development around the world, with massive numbers of new wind turbines being integrated into electricity grids every year as a result of the significant role they play in reducing dependence on fossil fuels. According to the International Energy Agency Technology Roadmaps, it is anticipated that by

2050 about 12 % of the global demand for electricity will be obtained from wind power [235]. For the year from July 2012 to June 2013, the offshore and onshore wind power generation system capacity of the UK was increased by almost 2.6 GW, making the total installed capacity for wind power generation system 15.1 GW [235]. These figures indeed indicate the enormous amount of progress made over recent years with respect to the development of wind turbines.

There is no doubt that increasing the adoption of wind power generation system has a major role to play in mitigating the levels of carbon dioxide ($CO_2$) and other greenhouse gas (GHG) emissions [236]. However, one of the main challenges associated with the implementation of wind power technology is that the availability and reliability of such power is highly dependent on weather and climatic phenomena, with potentially negative repercussions for power system reliability. Conditions resulting from climate change can cause turbine failure and consequently poor turbine reliability, thus adversely affecting the behaviour of the power grid, which can eventually require increased maintenance. Of the multiple factors involved, wind speed constitutes a fundamental one because of the associated high degree of uncertainty and the resultant immense impact on the reliability of wind turbine power.

Studying the impact of long-term climate change on wind power generation system is important for acquiring an understanding of future challenges that could be encountered with respect to power system reliability. While it has been demonstrated that $CO_2$ emissions and geographic location have a direct effect on wind speed and its variability [107, 185], methods of assessing the impact of long-term climate change on the reliability of wind power generation system had not until now been fully investigated.

For these reasons, the research reported in this chapter was directed at proposing a framework for a detailed study of the ramifications of climatic change for WFs that are connected to a power system. The climate change simulation employed in the study were generated from a set of high-resolution weather data derived from a multi-model database, and

an ensemble of multi-GHG scenarios based on regional climate projections are also taken into account. The proposed framework also includes consideration of both the short-term and the long-term power planning required for accommodating fluctuations in wind power output. To this end, climate change simulations, a wind power generation system model, and a power system model are all incorporated as part of the framework.

For the climate change simulations, wind speeds associated with three representative concentration pathways (RCPs) for GHG emission scenarios (RCP2.6, RCP4.5, and RCP8.5) for the selected geographic location were simulated using a high-resolution multi-model ensemble of Coordinated Regional Downscaling Experiment (EURO-CORDEX) projections [237]. The climate change simulations were applied to the modelling of a large-scale WF integrated into a power grid, and the influence of the simulated conditions was quantified using a non-sequential MCS in order to establish performance levels of grid reliability. An adapted Roy Billinton Test System (RBTS) was developed in order to conduct the case studies that would demonstrate the efficacy of the proposed framework. This chapter include some parts have been published by the candidate in [238] throughout this Ph.D. work.

The next sections are structured as follows. The main methodology is presented in section 5.2, followed by a description of CORDEX and the EURO-CORDEX climate change model in section 5.3, along with its simulation, emission scenarios, structure, timescales, and output samples. In section 5.4, the WF model and wind power generation system model are introduced. The adapted RBTS is detailed in section 5.5 while the impact of climate change on the reliability of wind power generation system is explained in section 5.6. The case studies conducted for validating the proposed framework are detailed in section 5.7. The final section summarizes the chapter and offers conclusions.

## 5.2 Methodology

This section presents the main methodology for the proposed framework for the reliability assessment as a mean of quantifying the impact of climate change on a WF-integrated power system. As set out in **Figure 5.1**, the framework involves three key steps: climate change simulation, wind power generation system and power system modelling, and a reliability analysis and impact studies. In the first step, a stochastic model of climate change over the long term and for different emission scenarios, including RCP2.6, RCP4.5 and RCP8.5 emission scenarios, is developed using the World Climate Research Programme (WCRP) EURO-CORDEX projections [237].

The simulated climate change model based on wind speeds for diverse emission scenarios is applied in the next stage of the wind power generation system model, while the WFs are integrated into the power system model. The effects of climate on WF-integrated power system performance and the associated fluctuations are captured for use in the reliability analysis and impact study that constitute the third step, which involves the use of a non-sequential MCS in order to identify the levels of the long-term impact.

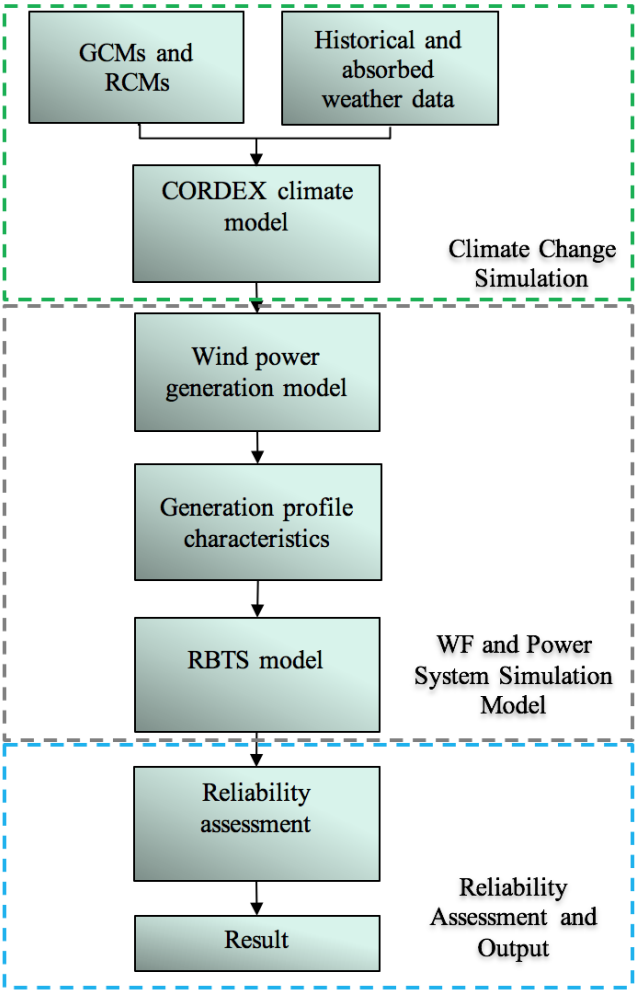


**Figure 5.1**. Overview of the methodology

## 5.3 Climate Change Simulation

With increasing GHG emissions, climate change is expected to escalate. The anticipated changes in climate variables can be obtained from global circulation models (GCMs) and regional climate models (RCMs), which provide a range of estimated future emission scenarios. This section details the climate change simulations that were carried out for assessing the long-term impact on wind power generation system. Due to the limited weather factors that were included in the UK Climate Projections 2009 (UKCP09) simulation described in Chapter 4, CORDEX Europe domain projections were employed for the climate simulation presented in this section, which describes the simulation framework, including

CORDEX, EURO-CORDEX, the simulation procedure, emission scenarios, and sample outcomes.

CORDEX represents WCRP frameworks developed with the goal of downscaling global climate projections to high-resolution regional versions. Global CORDEX models contain multi-domain ensembles of worldwide regional climate projections, including the EURO-CORDEX framework, which provides high-resolution climate projections for the European region. These projections cover weather factors for different emission scenarios. The scenarios considered are identified as RCP scenarios, such as the RCP2.6, RCP4.5, and RCP8.5 scenarios employed in this study [239]. Such long-term climate simulations enable the use of meteorological data sets for the investigation of the impact of climate change on the reliability performance of WF-integrated power systems.

### 5.3.1 The CORDEX Model

CORDEX was generated by the Task Force for Regional Climate Downscaling (TFRCD), established by the WCRP. CORDEX is able to downscale the Coupled Model Intercomparison Project Phase 5 (CMIP5) global climate projections in order to generate high-resolution multi-model ensembles based on regional climate projections for all terrestrial regions of the world, including Europe, within the Fifth Assessment Report (AR5) timeline [137]. The primary output of the CORDEX model is a core set of comprehensive climate projection frameworks and coordinated model evaluation frameworks applicable for most of the CORDEX domains. One of these domains, designated EURO-CORDEX, provides regional climate projections for Europe at a variety of resolutions. These are the projections that were employed in this research, as explained in the next section.

### 5.3.2 EURO-CORDEX Structure

The EURO-CORDEX weather simulations entail consideration of nine different global and regional climate model chains. The multi-model ensemble of GCMs and RCMs listed in **Table 5.1** is based on historical and GHG emissions. The weather simulation outcomes from the EURO-CORDEX ensemble have been matched with ENSEMBLES project findings in the Special Report on Emission Scenarios (SRES) in) [239], the results show that at the large scale, the patterns of weather changes are quite similar while they differ at the regional scale for all emission scenarios.

Regional climate projections constitute a useful tool for assessing the impact of climate on power systems that incorporate WFs. EURO-CORDEX provides two sets of regional climate projections for Europe at different resolutions: 50 km (EUR-44) and 12.5 km (EUR-11) [239]. Compared to the lower projection resolution of EUR-44, the EUR11 resolution offers more accurate projections because of its additional GCM values. For this research, regional climate projections from EUR-11 were therefore used for obtaining wind speed data.

**Table 5.1.** Overview of GCMs and RCMs used in EURO-CORDEX

| GCM | GCM member | RCM |
|---|---|---|
| CNRM-CM5-LR | r1i1p1 | RCA4 |
| EC-EARTH | r12i1p1 | RCA4 |
| ERA-Interim | r1i1p1 | RCA4 |
| HadGEM2-ES | r1i1p1 | RCA4 |
| IPSL-CM5A-MR | r1i1p1 | RCA4 |
| MPI-ESM-LR | r1i1p1 | RCA4 |
| CNRM-CM5-LR | r1i1p1 | CCLM4-8-17 |
| EC-EARTH | r12i1p1 | CCLM4-8-17 |
| ERA-Interim | r1i1p1 | CCLM4-8-17 |
| HadGEM2-ES | r1i1p1 | CCLM4-8-17 |
| MPI-ESM-LR | r1i1p1 | CCLM4-8-17 |

### 5.3.3 EURO-CORDEX Weather Simulation

It has been previously reported that possible future changes in climate variables could arise from increased $CO_2$ and other GHG emissions. Among these variables, the wind speed, for which a future shift is predicted based on the current climate change projections, is reported in [209]. For the work presented here, near-surface wind speeds (m/s) were simulated using multi-model and multi-scenario ensembles for future periods. The scenarios considered for the simulated wind speeds are representative concentration pathway (RCP) scenarios (RCP2.6, RCP4.5 and RCP8.5), which follow the A1 family designated by the Intergovernmental Panel on Climate Change (IPCC). The simulation is based on historical and absorbed weather data and on GHG emissions in order to project future wind speeds. The simulated wind speeds are three-hourly for near-surface winds (10 m above ground level) only, which must then be precisely interpolated into hourly values and at higher altitudes of up to 100 m, as explained in later sections.

#### 5.3.3.1 EURO-CORDEX Emission Scenarios

This study involves three GHG emission scenarios: RCP2.6, RCP4.5, and RCP8.5. These scenarios represent the complex developments and interactions affecting the climate system due mainly to GHG emissions, which alter radiative forcing. Each RCP pathway is defined by particular levels of emissions and consequent radiative forcing, which is based on measurements of incoming and outgoing solar irradiation in the earth-atmosphere system [240]. Changes in the radiative forcing relative to the preindustrial condition for the three RCP scenarios are illustrated in **Figure 5.2**.

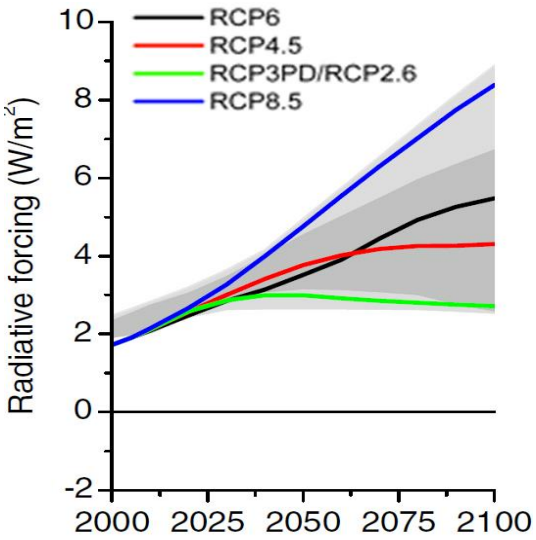


**Figure 5.2.** Changes in radiative forcing relative to pre-industrial conditions for the four RCP emission scenarios [240]

It can be observed that the worst-case scenario, i.e., the RCP8.5 pathway emission scenario, is based on the assumption that increases in radiative forcing due to GHG emissions will continue to rise beyond 2100. On the other hand, with the RCP2.6 pathway scenario, the assumption is that radiative forcing increases up to half of the amount with the RCP8.5 pathway because the GHG emissions are less than with RCP8.5, with the result that the radiative forcing begins to decline immediately before 2100. The amount of radiative forcing with the RCP4.5 and RCP6.0 pathways lies between the values for the RCP2.6 and RCP8.5 pathways. From the perspective of GHG emissions and radiative forcing, minor discrepancies are evident between the SRES scenarios presented in Chapter 4 and these RCP scenarios.

In order to investigate all impact possibilities with respect to the reliability of wind power generation system, future climate projections were determined for the RCP2.6, RCP4.5, and RCP8.5 emission scenarios, which are categorised based on the level of GHG emissions

and radiative forcing associated with each. For this study, the RCP8.5 pathway indicates high-emission scenarios, RCP4.5 represents medium-emission scenarios, and RCP2.6 refers to low-emission scenarios.

#### 5.3.3.2 EURO-CORDEX Timescale

The EURO-CORDEX domain can be used for simulating climate variables for future periods. The baseline data are established from historical and absorbed data, which for this study were taken from 1960 to 1990, with the generated data representing 2006 to 2100. To provide future weather data, the GHG emissions and radiative forcing factors were applied to the stochastic weather data generated based on the historical data. **Table 5.2** indicates the selected future periods from 2020 to 2080. These years have been considered for the reliability assessment of a power system incorporating WFs in order to investigate and compare the impact of climate change over the long term and for different timespans.

**Table 5.2.** Selected future periods from 2020 to 2080

<table>
<tr><td>No.</td><td></td><td colspan="2">1960 2006</td><td>2020</td><td>2050</td><td>2080</td></tr>
<tr><td>1</td><td></td><td colspan="2" rowspan="3">Baseline (1961-1990)</td><td>2010</td><td></td><td></td></tr>
<tr><td>2</td><td></td><td></td><td>2050</td><td></td></tr>
<tr><td>3</td><td></td><td></td><td></td><td>2080</td></tr>
</table>

#### 5.3.3.3 Temporal Disaggregation of Wind Speeds to an Hourly Timescale

The EURO-CORDEX model provides near-surface wind speeds for 3 h period; however, to improve the accuracy of the assessment, wind speeds at higher resolutions are required, which can be acquired through the interpolation of the three-hourly wind speeds into

hourly wind speeds. Numerous linear and nonlinear techniques are available for disaggregating wind speeds into hourly values. For example, sinusoidal and random techniques were used in [241], and a Gaussian distribution function was employed in [220] for disaggregating wind speeds from daily into hourly values. In this study, because the fluctuation during three hours of wind speed is not very large, a linear disaggregation can be employed. The hourly wind speed is thus calculated using the linear interpolation expressed in equations (5.1) and (5.2):

$$U_{h(2+3i)} = \left(\frac{U_{h(4+3i)} - U_{h(1-3i)}}{3}\right) + U_{h(1-3i)} \quad (5.1)$$

$$U_{h(3+3i)} = -\left(\frac{U_{h(4+3i)} - U_{h(1+3i)}}{3}\right) + U_{h(4+3i)} \quad (5.2)$$

where is *U* the hourly wind speed in (m/s) at hour i (i = 0, 1, 2, 3…n). **Figure 5.3** shows the temporal disaggregation of wind speeds from a three-hourly into an hourly timescale for the near-surface wind speeds from the RCP8.5 emission scenario during the first week of 2020.

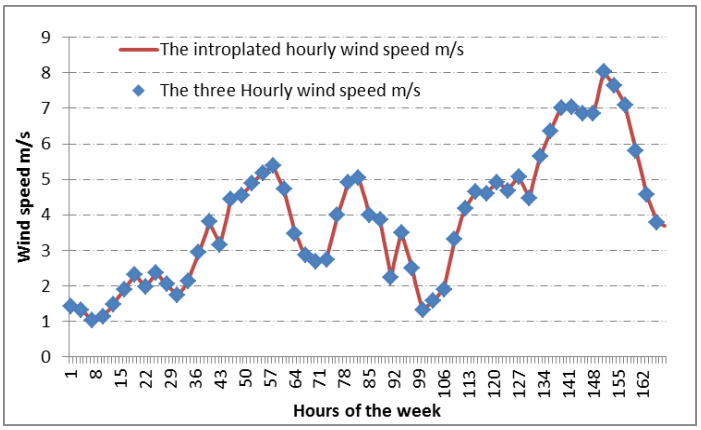


**Figure 5.3**. Disaggregation of wind speeds from a three-hour into an hourly timescale

#### 5.3.3.4 Extrapolated Hourly Wind Speeds at the Turbine Level

Near-surface wind speeds are generated by the EURO-CORDEX model at a height of 10 m above ground. However, to simulate accurate scenarios, the wind speeds used for the simulation must be at the level of the turbine hub, which is typically 100 m above ground. Near-surface hourly wind speeds must therefore be extrapolated so that they correspond to the

hub height for all-time series and grid points. Wind speeds at turbine hub level can be calculated using equations (5. 3) and (5. 4) [242]:

$$U_T = U_S \cdot (\frac{T}{S})^{\alpha} \alpha \tag{5. 3}$$

$$\alpha = 0.37 - 0.881 \cdot \ln(U_S) \tag{5. 4}$$

where

$U_T$ extrapolated hourly wind speed in m/s at wind turbine hub height

T wind turbine hub height: 100 m

$U_S$ original hourly wind speed in m/s at the near-surface level

$S$ highest near-surface level: 10 m

**Figure 5.4** indicates the extrapolated hourly wind speed in m/s at turbine hub level for the first week of March 2020 for the RCP8.5 emission scenario.

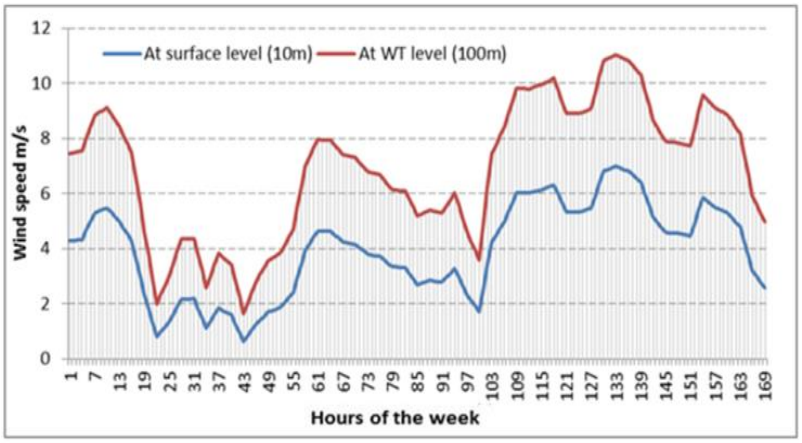


**Figure 5.4**. Extrapolated hourly wind speeds in m/s at turbine hub level

### 5.3.4 Steps in the Climate Change Simulation

The first step towards assessing how the impact of climate change on wind power generation system influences the reliability of a power system containing WFs is to simulate climate change under a variety of GHG emission levels. **Figure 5.5** provides the main approach employed for such a simulation of long-term climate change. Near-surface wind speeds are generated stochastically using the EURO-CORDEX climate model based on historical data and

on GHG emission scenarios. Spatial resolution, temporal resolution, and geographic location were all selected and identified according to the specific requirements of the study. Output samples were then generated based on the selection of the type of climate data. The next section describes those output samples and identifies key findings.

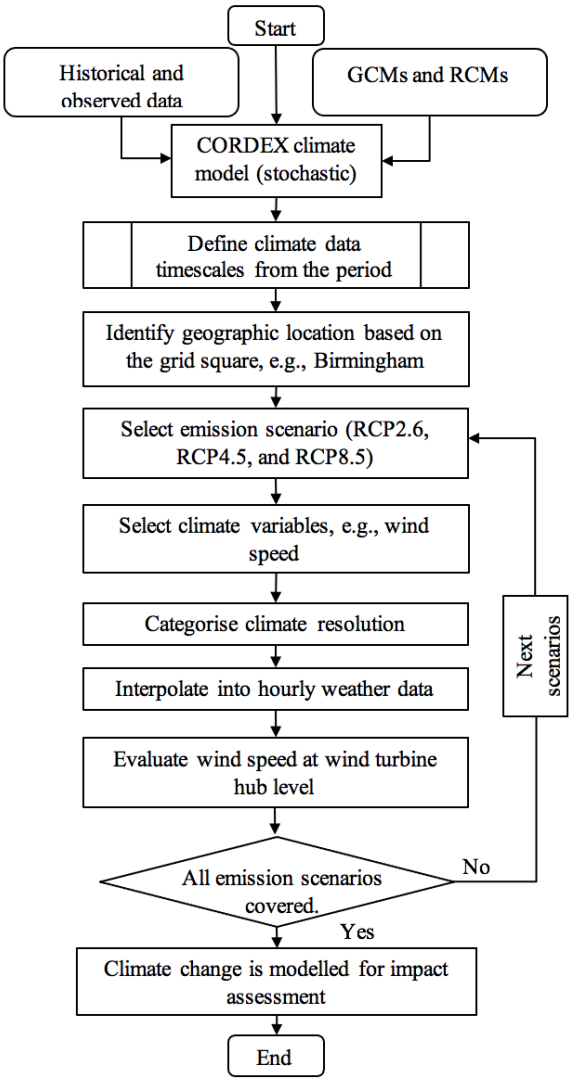


**Figure 5.5.** Overview of the approach to long-term climate change modelling for the purpose of assessing its impact on the reliability of a power system encompassing WFs

### 5.3.5 Output Samples of the Generated Wind Speeds for Different Emission Scenarios

Climate change data were simulated for the location of Birmingham, UK, at 52.48° N latitude and 1.89° W longitude. The weather data is simulated under three emission scenarios

over period ranging from the year 2007 to 2100. The emission scenario data were generated based on assumed GHG emissions associated with future climate change. Each emission scenario indicates different climate change level from other scenarios over long-term. In addition, climate change level can also be different within same scenario at different year.

In this chapter, the most important climate variables are wind speed (m/s) and wind direction. Wind direction has not been considered in this study due to the high degree of uncertainty associated with it, which makes it very difficult for either GCMs or RCMs to predict. On the other hand, wind speed for different emission scenarios is considered as it plays a significant role in wind power generation system. **Figure 5.6** provides a comparison of the hourly wind speeds with RCP2.6 (a), RCP4.5 (b), and RCP8.5 (c) for 2020, 2050, and 2080. These represent the wind speed at the turbine hub heights level. Variations in wind speed indicate possible effects of GHG emissions on weather patterns.

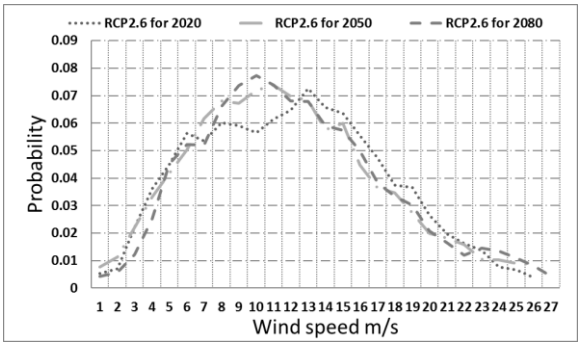


(a) RCP2.6

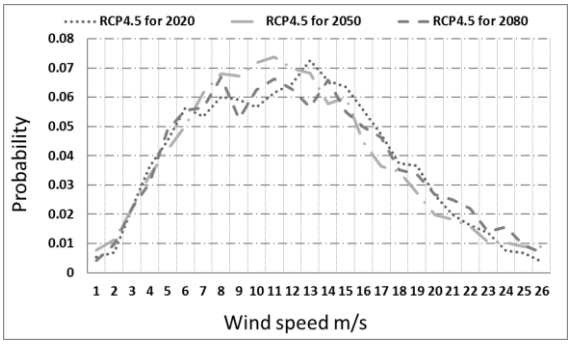


(b) RCP4.5

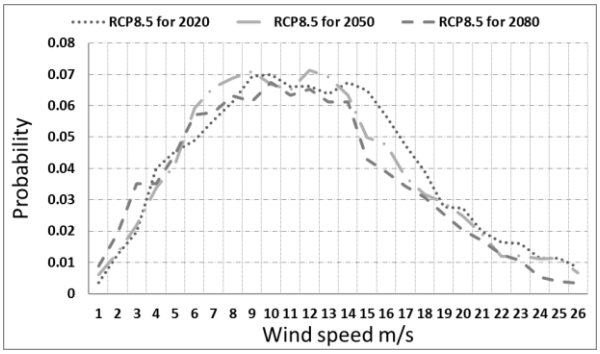


(c) RCP8.5

**Figure 5.6.** Probability distributions for hourly wind speeds for three emission scenarios: (a) RCP2.6, (b) RCP4.5, and (c) RCP8.5

## 5.4 Wind Farm Modelling

Wind turbines have two basic types of axes: horizontal and vertical. Horizontal-axis wind turbines are the most commonly used and are normally employed for large capacities, which are considered in this study. Wind turbines consist of different systems, such as mechanical and electrical, with each system comprising a number of interdependent subsystems. Mechanical subsystems include rotors, drive trains, and nacelle structures, while electrical systems comprise mainly power converters and generators. The kinetic energy of the wind is rotating the rotor blades of the wind turbine which are connected to each other through the hub. The gearbox increases the rotational speed of the rotor in the generator for the desired speed required for electrical power generation. The nacelle and rotor rotate according to the wind direction by the yaw system. The pitch mechanism helps to act as aerodynamic brake and adjust the blades position according to the wind speed.

Generators are categorised based on whether they are fixed or variable speed. For example, doubly fed induction generators (DFIGs), which are the most commonly and widely used, are based on variable speeds with a partial-scale frequency converter. In order to improve the power quality, the variable-speed wind turbine is designed to accomplish maximum aerodynamic efficiency over a variety of wind speeds. This type of generator efficiently converts mechanical power into electrical power that can be fed into the grid at a constant frequency, in contrast to a traditional WF generator that operates at a fixed speed. The fix-speed wind turbine has the pros and cons. It is simple and reliable but it has uncontrollable reactive power consumption and mechanical stress.

**Figure 5.7** shows a schematic and the structure of a DFIG-equipped wind turbine which include aerodynamic, mechanical and electrical system. The DFIG stator is connected directly to the grid whereas the rotor circuit is connected to the partial-scale frequency power converter. The pitch-controlled aerodynamic system is coupled to the generator through a multi-stage

gearbox. A wound rotor induction generator is used for coupling the converter via slip rings to the rotor. The converter system also controls the rotor voltage, thus providing reactive power compensation by smoothing the grid connection at a speed range of ± 30 % around the synchronous speed [243, 244]. A WF encompasses a number of wind turbine generators over a specific geographic location.

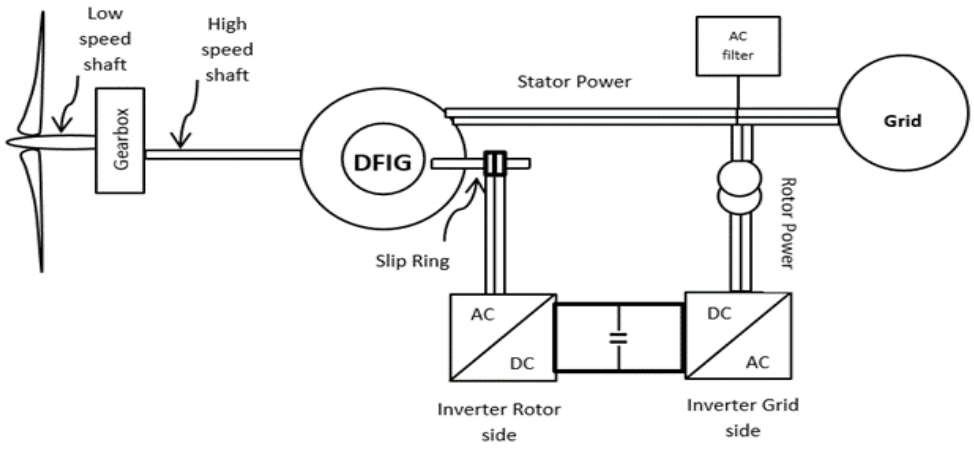


**Figure 5.7.** Schematic and structure of a DFIG-equipped wind turbine generator [243]

### 5.4.1 Wind Power Model

The nonlinear relation between the power generated from a wind turbine and the wind speed considered over a time series t can be affected by climatic conditions [105]. Wind speed and wind turbine generator characteristics are important factors which effect the generated power at any given time. To determine this effect of these factors, the amount of power $P_{WT}(t)$ generated by a wind turbine at time t can be estimated in MW as follows:

$$P_{WT}(t) = \begin{cases} 0 & 0 \le U_O(t) \ge U_{ci} \\ \left(A + BU_O + CU_O{}^2\right)P_r & U_{c\_i} \le U_O(t) \ge U_r \\ P_r & U_r \le U_O(t) \ge U_{co} \\ 0 & U_O(t) \ge U_{co} \end{cases} \quad (5.5)$$

where $P_r$ is the rated power (MW) of the wind turbine; $U_O(t)$, $U_r$, $U_{ci}$, and $U_{co}$ are the operating wind speed (m/s) at time t as well as the rated, cut-in, and cut-out wind speeds (m/s),

respectively. The constants A, B, and C can be computed as a function of $U_r$ and $U_{ci}$, as in equations (5.6), (5.7), and (5.8) [105]:

$$A = \frac{1}{(U_{c_i} - U_r)^2}\left[U_{c_i}(U_{c_i} + U_r) - 4(U_{c_i}U_r)\left[\frac{U_{c_i} + U_r}{2U_r}\right]^3\right] \quad (5.6)$$

$$B = \frac{1}{(U_{c_i} - U_r)^2}\left[4(U_{c_i} + U_r)\left[\frac{U_{c_i} + U_r}{2U_r}\right]^3 - (3U_{c_i} + U_r)\right] \quad (5.7)$$

$$C = \frac{1}{(U_{c_i} - U_r)^2}\left[2 - 4\left[\frac{U_{c_i} + U_r}{2U_r}\right]^3\right] \quad (5.8)$$

The generated power from WFs are obtained using (5.5)-(5.8) for each hour to simulate the entire wind capacity mode in form of time series.

## 5.5 Roy Billinton Test System

Due to the lack of real power system data for the selected geographic location, the proposed approach are applied to Roy Billinton Test System (RBTS) [245]. The RBTS was employed for the work presented in this chapter in order to demonstrate the impact of climate change on the reliability of a power system with integrated wind power generation system. The RBTS contains 11 generators with seven hydro plant units and four thermal plant units for a total installed capacity of 240 MW, as shown in **Figure 5.8.** For the reliability evaluations, the load models have been adjusted according to a specific load variation pattern using the annual peak load demand, which has been modified based on the RBTS. The load models vary according to the type of consumer (residential, commercial, or industrial), the temperature, and the season. The load models comprise the variation in system load level with time in a quantified period normally one year in power system reliability planning studies. However, the load models are similar for all scenarios, which means that the impact of climate change on the load is not considered so that only the effect of climate on the reliability of a WF-integrated power system is highlighted. The RBTS details, including branches, line parameters,

transformer and generator unit parameters, and reliability data, are provided in the Appendix. The system details were derived from [245], with adjustments appropriate for each case study.

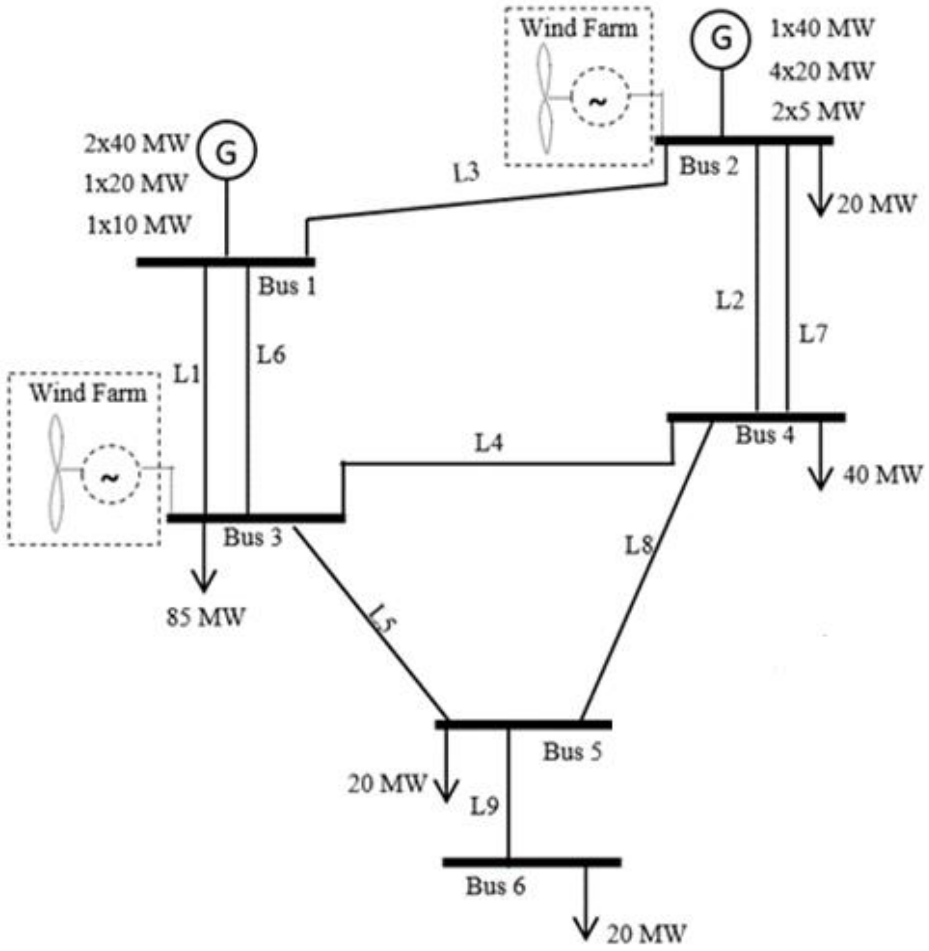


**Figure 5.8.** Shortened form of a single-line diagram of the RBTS [245]

## 5.6 Wind Farm Reliability with Consideration of Climate Change

Climate change may influences wind speed fluctuations and wind availability, which can affect the operation and reliability of a power system when WFs are integrated. The work presented in this study investigates the contribution of wind power to future power system reliability under a variety of climate change scenarios.

### 5.6.1 Wind Farm Reliability with Consideration of Climate Change

The goal of the work presented in this section was to establish the reliability of a WF-connected power system when climate change is taken into account. A large wind turbine can fail for many reasons, including random disturbances and extreme events such as intense storms, heat waves, wildfires, and lightning. This impact can manifest in a number of ways, such as a reduction in output or failure of the components. Climate change can also impact wind power by altering the geographic distribution of the variabilities inherent in a wind resource.

Since the failure rate of different types of wind turbines components have been addressed in [242], this study considers only the impact of climate change on wind turbine integrated power system while the effects of any other factors were excluded. Going back to chapter three, it was eminent that climate is determined mainly by the inward and outward balance of solar irradiation flux, which means that wind regime is highly vulnerable to any changes in factors that affect that balance. Climate change over long periods has an effect on the climate variables that govern the operation of a WF-integrated power system. Since wind speed constitutes the most significant wind power variable, in this study, the reliability evaluation involved consideration of long-term wind speeds at the turbine hub level for three emission scenarios as a means of investigating the effects of changes in wind speed. The wind regime is affect the wind turbine operation and can be completely absent when it is most needed resulting in a wide variation in the wind power output and reliability. For example, a wind turbine will stop operating at the higher and lower cut-out and cut-in wind speeds, respectively. Variability and variations in of wind speeds have enormous consequences for the reliability of a WF-connected power system.

The effect on power system reliability with different climate scenarios over the long term has been quantified using the expected energy not supplied (EENS) reliability index.

EENS is one of the most common reliability indictors for assessing the reliability performance of a power system, which provides substantial measure for generation adequacy and reliability performance. The EENS reliability index coefficient of variation has less convergence rate than other reliability indices. The EENS index represents the expected energy that could not be supplied to the grid (MWh/y) for any reason, including component failure or changes in climatic conditions, which can lead to wind turbine derating or an outage, thus making it an appropriate metric for assessing the impact of climate change. Any change in the EENS for any scenario is therefore attributable to the ramifications of climate change.

In order to reduce the sample variance of MCS and to improve the effectiveness of MCS, simulating a large number of experiments is required. Thus, to enhance the accuracy of the EENS measurement, a large number of experiments/ iterations based on a non-sequential MCS were simulated with correspondingly significant computation time. However, a convergence criterion can be quantified in order to estimate the optimum number of these simulation iterations with consideration of an computation time. The simulation results show that 12,000 iterations is the optimum value of iterations, thus 12,000 iterations have been employed so that the simulation stops within an acceptable computation time.

### 5.6.2 Wind Farm Reliability Procedures

Once long-term climate change has been simulated for different emission scenarios and applied to WFs, the reliability index for the power system can be calculated for each time frame and emission scenario. To obtain the average index values of the expected energy not supplied (EENS), a non-sequential MCS is utilized for 12,000 iterations. This method produces an estimate of the reliability level of the power system based on forced outage rates and wind-production-based climate change.

For an investigation of the impact of long-term climate change, reliability analyses of the WF-integrated power system were performed based on an assumption of fully reliable wind turbine system components. **Figure 5.9** outlines the procedures for assessing the reliability of a WF-integrated power system along with the impact of climate change when the failure of wind turbine components is not taken into account. MATLAB and DIgSILENT PowerFactory were employed for the reliability assessment that performed according to the following steps:

- Execute the climate change simulation as set out in **Figure 5.5** for three emission scenarios, RCP2.6, RCP4.5 and RCP8.5, and for three future years, 2020, 2050, and 2080. The simulated wind speed is also interpolated into hourly wind speed data and is extrapolated for the turbine hub level.
- Model the WFs to be integrated into the power system based RBTS and initialize the load demand.
- Configure the adapted RBTS model in order to validate the robustness of the proposed framework. This step includes establishing the load demand characteristics and estimating the reliability data for each power system component (transformers, power lines, busbars, etc.).
- Apply the simulated climate change scenarios to the wind turbine generators that are integrated into the RBTS for reliability assessment, and repeat this step for each emission scenario and future year.
- Insert the reliability data for each power system component (transformers, power lines, busbars, etc.).
- Select randomly the system state based on the non-sequential MCS in the interval (0,1) and compare the power system components to the probability of component failure, which is known as the forced outage rate (FOR), in order to estimate the component state: either up or down.

- Perform a load flow analysis and initialise the power balance within the voltage limits at the buses and within the thermal limits of the lines during the simulation.
- Evaluate the system state with the system overloading and fulfil load flow. If not, go to step (6).
- Calculate the load curtailment $C_i$ for each system state sampled and repeat these steps for N number of iterations.
- Estimate the ENS by computing the demand not supplied (*DNS*) and the ENS at each iteration. Then estimate the expected demand not supplied (*EDNS*) in MW and the EENS in MWh/y for all of the iterations using equations (5.9) and (5.10) [22]:

$$EDNS = \sum_{i \in S_i} C_i \times P_i \tag{5.9}$$

$$EENS = \sum_{i \in S_i} C_i \times P_i \times 8760 \tag{5.10}$$

where $C_i$ is the load curtailment for system state $i$, $P_i$ represents the system state probability, and $S$ denotes the set of all system states associated with load curtailment.

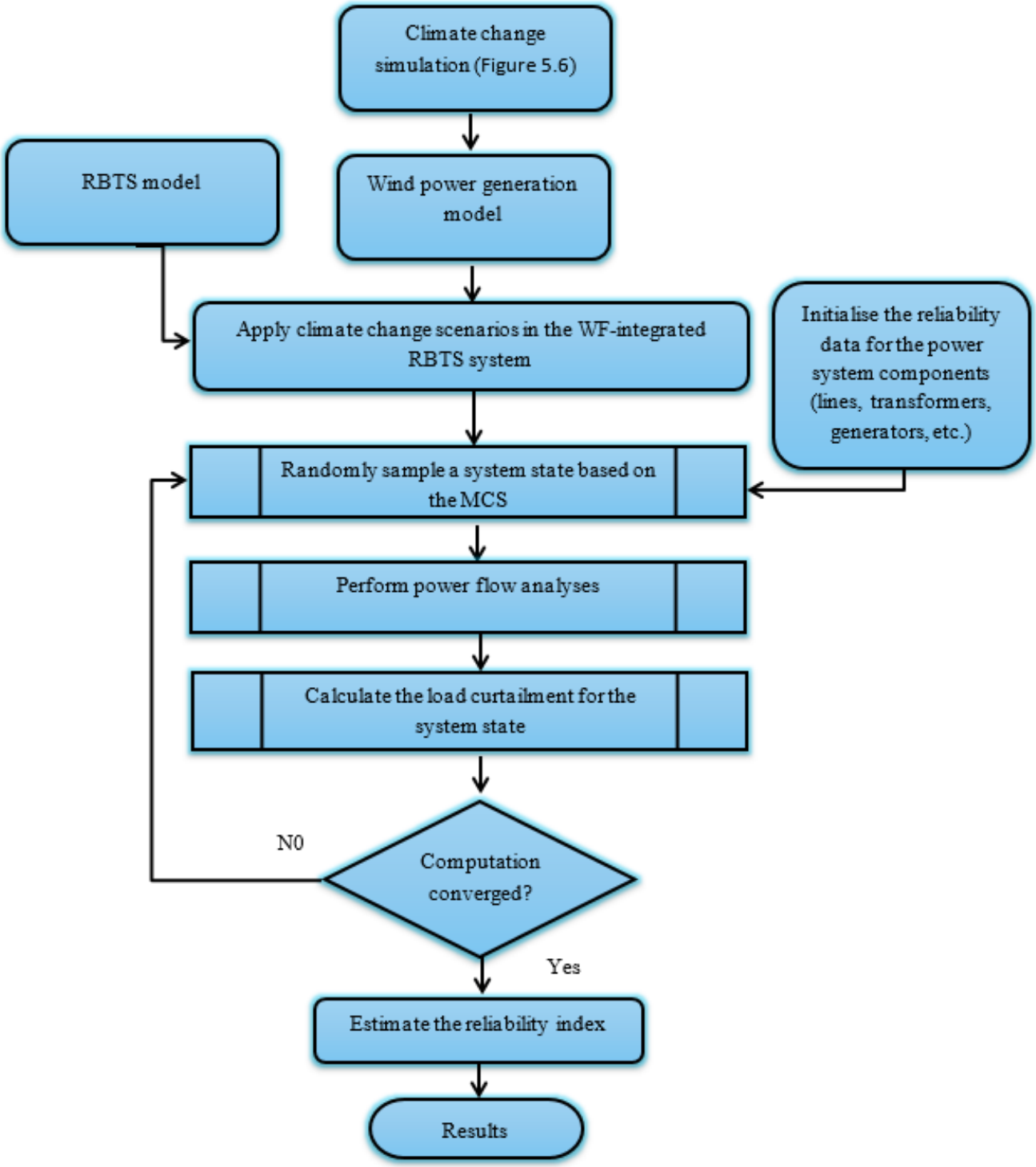


**Figure 5.9.** Reliability assessment procedures for establishing the impact of climate change on a WF-integrated power system with fully reliable turbine components

## 5.7 Case studies

To validate the proposed framework, it has been applied in a number of case studies designed to determine the effect of climate change on a future WF-integrated power system for different emission scenarios. Ambient and climate change conditions were applied to the wind power generation system model in order to simulate the influence of specific parameters on the WF output power and operating status. An MCS was used for assessing the reliability performance of the power system. The climate change data were simulated for the selected geographic location of Birmingham, UK, at 52.48° N latitude and 1.89° W longitude. Due to the unavailability of real power system data for the selected geographic location, the RBTS [245] was incorporated for the validation of the proposed framework. A WF with a 3 MW capacity was simulated for the case-study investigation which is supplying roughly less than 20% of the customers connected at busbar 2 of the RBTS. The penetration level of wind farms is increased into the doubled in further cases to supply the costumers connected at busbars 3 and 5 and to assess the reliability at different location of wind integration. The busbars used have different type of customers and this includes busbar 5 (government and office buildings), 2 (industrial buildings), and 3 (large industrial and commercial users). For the reliability assessment, DIgSilent power factory software, which is commonly used by utilities for reliability studies, was integrated with a MATLAB operating environment. MATLAB provided the required input to the power system model simulated on DIgSilent. In this study, four types of cases were examined, with each case involving multiple scenarios, as listed in **Table 5.3**.

**Table 5.3.** Case Studies with WFs Integrated into the RBTS

| Case | Explanation |
|---|---|
| 1 | The first case was the base case in which no WFs are integrated to the RBTS. |
| 2 | The second case represents the reliability performance of the climate change impact on centralized WF integrated into the RBTS at busbar 5. The three emission scenarios considered in this case are RCP2.6, RCP4.5, and RCP8.5 for the year 2020, 2050, and 2080. |
| 3 | The third case study illustrates the power system reliability performance with three decentralized WFs incorporated into busbars 5, 2, and 3. For comparison purposes, all emission scenarios were considered over 2020, 2050, and 2080 timelines, as in the second case study. |
| 4 | The fourth case exemplifies the levels of power system reliability when thermal power generation is removed from the system and wind turbines are added to meet the demand previously supplied by the thermal units. |

### 5.7.1 Base Case without WF Integration

In the first case, the reliability evaluations were carried out for the RBTS without either WF or climate change integration, thus it provides a benchmark for comparison with other scenarios and cases. To calculate the average EENS for the system, 12,000 experiments were carried out. The average EENS resulting from the case study was 824 MWh/year, which established a reference point for evaluating the outcomes of the other scenarios.

### 5.7.2 Case Study 2: Impact of Climate Change with Centralized Integrated WFs

The second case demonstrates the reliability performance of a centralized WF integrated into the RBTS at busbar 5 for different climate change scenarios based on GHG emission: RCP2.6, RCP4.5, and RCP8.5. **Figure 5.10** gives the EENS values for each of these three emission scenarios for 2020, 2050, and 2080. In comparison with the base case, a

significant improvement in reliability can be seen for all scenarios and all years. This is mainly due to the increase of power supplied in the grid from WF integration and therefore leading to improvement in reliability in the system. Moreover, the enhancements with WF integration are nonlinear, the EENS index decreases up to 2050. However, the EENS index increases in 2080 due to the impact of climate change on wind speeds, and ultimately on WF power generation. The loss in power generation occurs because the variations in wind speed means that the wind turbine stands inactive when wind speeds are either below the cut-in speed or above the cut-out speed. The wind turbine outage is not due to any failure but instead is attributable to the direct effect of conditions related to climate change, which have a negative impact on wind turbine operation and thus on the reliability index of EENS.

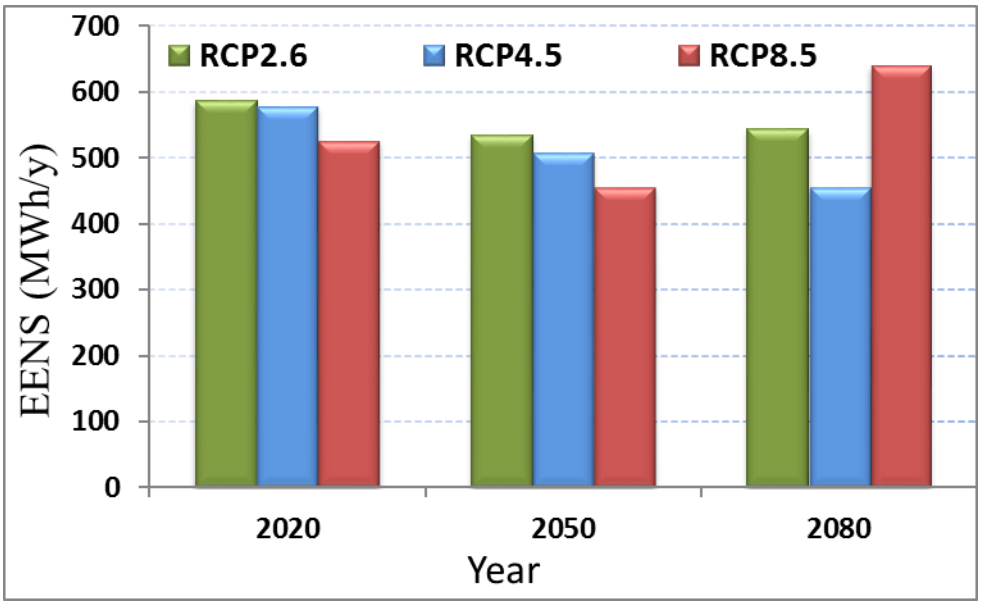


**Figure 5.10.** EENS values of climate change impact for emission scenarios: RCP2.6, RCP4.5, and RCP8.5

In 2020 and 2050, the EENS values are anticipated to be lowest for the third emission scenario: RCP8.5. These estimates are the result of the average wind speed at the specific geographic location being near the rated speed. However, the EENS value is expected to be the highest in 2080 since GHG emissions continue to rise, with a corresponding impact on radiative

forcing. The result indicate a significant impact of climate change on power system reliability with high emission scenario by the year 2080.

In 2080, the lowest EENS value is associated with the second scenario, which means that over the long term, the RCP4.5 scenario is likely to be the optimum scenario because wind speed might not be greatly affected by climate change. In addition, the strategy associated with this scenario entails no overshooting of GHG emissions so that emissions will be reduced before 2100. However, the second scenario also involves a reduction in GHG-based $CO_2$ emissions, which might negatively affect wind speed at the selected location, leading to a reduction in output power generation and a further decline in reliability performance compared with the third scenario.

### 5.7.3 Case Study 3: Impact of Climate Change on Decentralized Integration WFs

This case encompasses three scenarios, so that the impact of climate change on the reliability performance of a power system with integrated decentralized WFs can be evaluated for the three emission scenarios. These scenarios were investigated in order to determine the benefit of adding additional wind turbine generators to the power system grid. The first scenario of this case represents the power system with one WF generator connected at busbar 5. The second exemplifies the power system with two WFs integrated at busbars 2 and 5. In the third scenario, three WFs are integrated into the power system at busbars 2, 3, and 5.

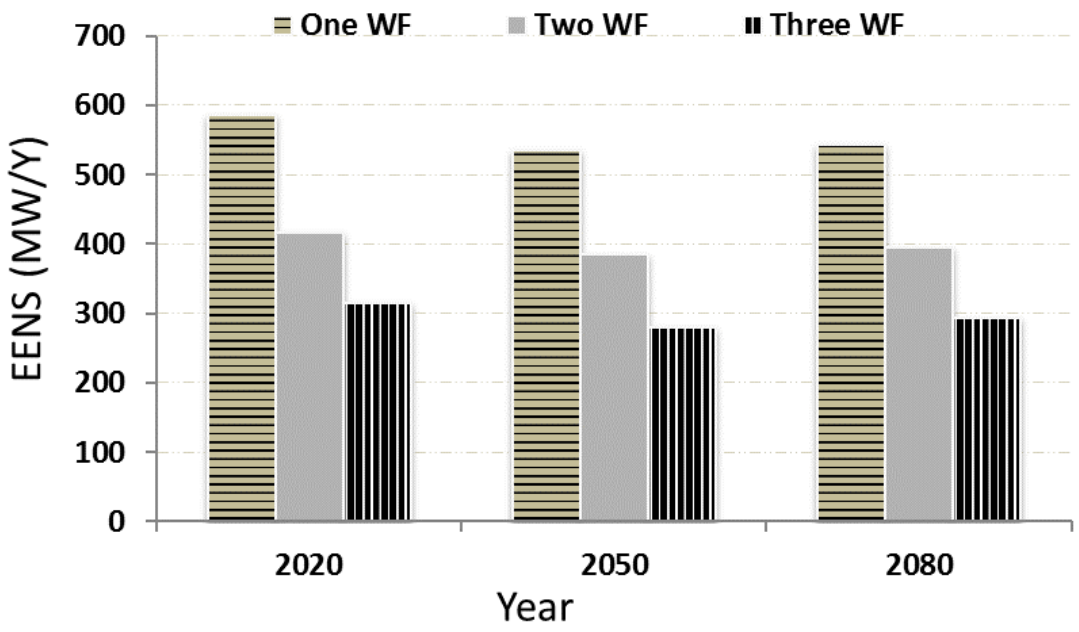


**Figure 5.11**. EENS values when additional WFs are integrated at different buses with the RCP4.5 scenario

**Figure 5.11** shows EENS values for the RCP4.5 scenario in which more WFs are added at different buses. In the case of the first scenario, in comparison with the base case, a monotonic increment in reliability can be observed from 2020 to 2050 and to 2080. This result shows that, with the first scenario, integrating further WFs into the power system enhances power system reliability.

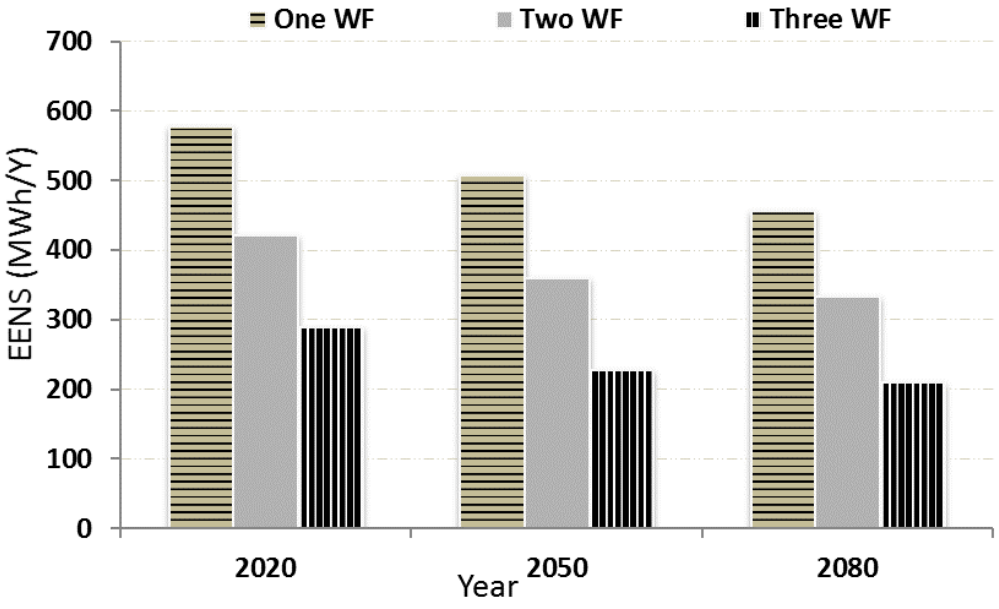

**Figure 5.12.** EENS values when additional WFs are integrated at different buses with the RCP2.6 scenario

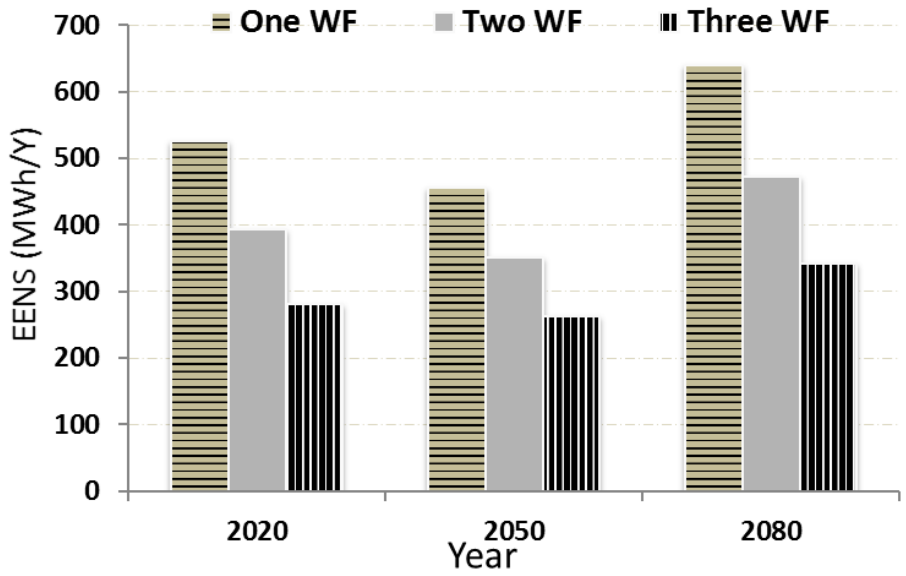


**Figure 5.13**. EENS values when additional WFs are integrated at different buses with the RCP8.5 scenario

The results for the other two scenarios, RCP2.6 and RCP8.5, exhibit a trend similar to the one revealed in the case study results shown in **Figure 5.11**, as can be seen from **Figure 5.12** and **Figure 5.13**, respectively. **Figure 5.13** indicates that the overall EENS values for the RCP8.5 scenario deteriorated to their lowest level during the year 2080, making it the worst of all the scenarios. This result confirms the impact of climate change on wind speed, which leads to a decline in reliability, as discussed in relation to the second case study.

### 5.7.4 Case Study 4: Replacement of Thermal Generators with WFs

To assess the reliability of a power system with wind power integration, 10 % (24 MW) of the total installed capacity initially supplied from thermal units is replaced by eight WF generators in the RBTS. **Figure 5.14** portrays the EENS values when 24 MW, i.e., 10 % of the thermal generation capacity, is replaced with wind turbine generators. This substitution reduces the reliability of the system, as evidenced by the sharp increase in the EENS value. To assess the penetration level of wind generation required in order to achieve the reliability level of the

base system, i.e., the reliability level without wind generation, in addition to the one for a 10 % replacement, reliability assessments were also carried out with additional wind power integration, ranging from 20 % of the total generation capacity through 30 %, 40 %, and 50 % to 100 %, as indicated in **Figure 5.14**. It can be observed that replacing 10 % of the thermal power generation required quite a large percentage from wind power generation system in order to maintain the EENS value. Even raising the installed wind power generation system to 100 % of the generation capacity might not provide a level of reliability performance equivalent to that of the base system. This outcome is attributable chiefly to the effects of the intermittent nature of wind generation and the geographic location. Integration beyond 100 % of the total capacity resulted in only negligible improvement in the EENS value.

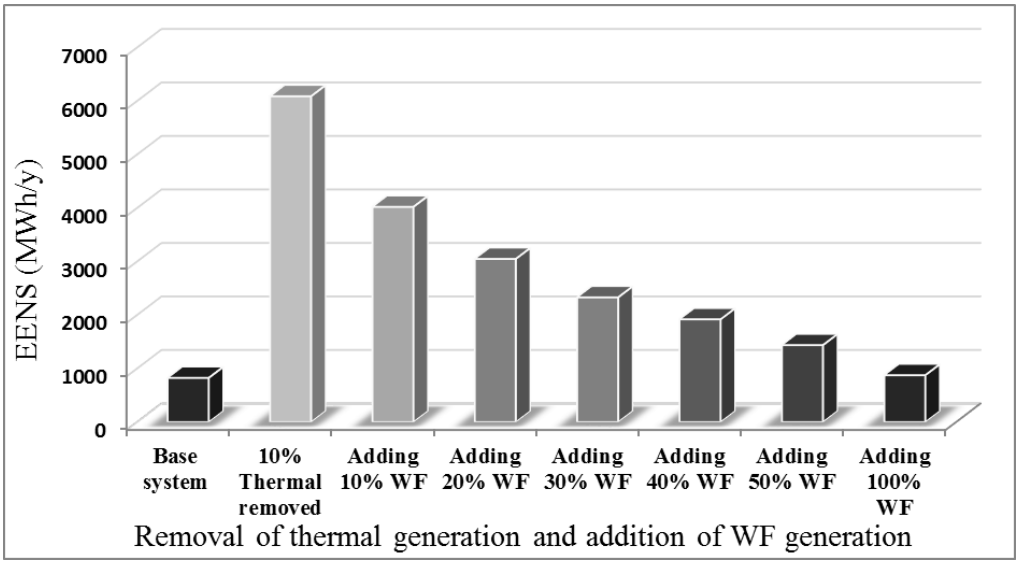


**Figure 5.14.** Replacement of 10 % of the thermal generation with increasing amounts of wind power generation

## 5.8 Summary

The uncertainties associated with climate change and its impact on WF-integrated power systems highly critical. This chapter has presented a framework for assessing the long-term effects of climate change on WF-integrated power systems. A detailed long-term climate

change simulation for a different of emission scenarios was applied to a wind power generation system model, and the influences of both elements on power system reliability were estimated using an MCS. The framework incorporate a high-resolution RCMs from EURO-CODRX for modelling a number of emission scenarios based on GHG emissions over long-term.

The reliability assessment is performed to assess the long-term impact of climate change for large-scale WFs integrated power system. In order to demonstrate and validated the proposed framework, it was applied on an adapted RBTS while the WFs were integrated into the RBTS. The climate change simulations were applied to WFs integrated power system at the selected geographic location and the MCS technique was employed to capture the outcomes over the long term. The developed reliability assessment procedures have been presented.

The findings suggest that climate change would potentially have a considerable impact on power system reliability. The effects are substantial for the long-term RCP8.5 emission scenario for 2080, when the EENS value sharply increases due to climatic conditions characterized by increased $CO_2$ emissions over the long run. Although WF integration into a power system and efforts to render a system smarter, are beneficial with respect to addressing concerns related to power generation based on fossil fuels, the impact of climate change on WFs should be specifically considered in order to limit new problems that might arise in the future. Such study would be a vital for the planning and operation of future power systems.

# Chapter 6: Impact Assessment of a Power System with Climate Change on Wind and PV Power Generation

## 6.1 Introduction

The climate change effect on the reliability performance of PV and wind power generation system were investigated in chapter 4 and 5, respectively. In this chapter, the climate change models are combined and employed to develop a stochastic model for generating future climate scenario with the aim of assessing their impact on power systems containing both wind and PV units. The importance and originality of this study are that it explores the proposed stochastic climate change models with respect to the effects of different emission scenarios on the long-term operation of future power systems. The proposed framework incorporates Likelihood Based Markov Chain (LBMC) modelling of climate change scenarios into PV and wind power generation system models, with stochastic variations being captured through Monte Carlo simulation (MCS).

With the growing consciousness of climate change and its impact, future power systems are most likely to be smarter than at present, and the primary source of power generation will probably shift from fossil fuels to renewable resources. Because integrated renewable power generation is dependent mainly on the ambient conditions surrounding a generating system, some reports as in [12-15], they suggest that the impact of long-term climate change on renewable power generation could be significant. Incorporating the detailed effects of this factor is therefore crucial for future power system planning and operation.

### 6.1.1 Status Quo

The operational performance of a power system can often be threatened by extreme weather, shifts in weather patterns, catastrophic events, and other occurrences. The influence

on power system operation of the uncertainties associated with these types of weather events is inevitable, and a great deal of research has been focussed on the assessment of power system security and control strategies for dealing with extreme weather [246]. The authors of [247] emphasize the substantial impact on the operation of transmission and distribution facilities due to climate effects. Thus, transmission and distribution facilities are more susceptible to change in the weather patterns, which might trigger component or system outages, cascading failures or blackouts.

To capture the stochasticity and impact of wind events, the researchers in [13] proposed a time-series MCS-based model for assessing power system resilience. Another study [248] was targeted at including consideration of weather factors in an examination of the operation risk assessment of a power system with wind-farm (WF) integration. The researchers proposed a combined model subjected to an overload outage on the line and the effects of time-variant weather. They concluded that the influence of inclement weather increases the level of risk. The integrated approach suggested in [72] took into account stochastic variations in weather patterns and dynamic thermal limits for the evaluation of insecurity in an active distribution network. The outcomes suggested a greater impact on supply security resulting from the stochastic variations in weather patterns than from the dynamic thermal limits. To investigate the effects of weather with respect to the reliability analysis of practical transmission and distribution systems, the authors of [249] and [250] presented a variety of weather models, including a three-state version. The work reported in [251] led to the proposal of a reliability and cost evaluation model for achieving optimal operation of renewable energy resources in a small isolated power system. The long-term climate change impact on the PV and wind power generation system and the influence of diverse GHGs emission scenarios are overlooked.

### 6.1.2 Research Problem

In the previous chapters, climate change effect of three possible future emission scenarios were applied on PV and wind power generation system independently. In fact there are high uncertainties in future emission scenarios i.e. which one will take path in future and this depends how human are responding to GHGs emission. Therefore, a stochastic model is required to have one possible emission scenarios based on diverse GHGs emission scenario. In addition, the PV and wind power generation systems were investigated separately whereas considering both in same power system may highlight the combined long-term impact on power system. Therefore, this study developed a stochastic climate change future scenarios and applied on both PV and wind power generation systems integrated power system for reliability assessment. Firstly, a new LBMC is proposed for capturing future weather scenarios derived from GHGs emission scenarios for two climate models: EURO-CORDEX and UKCP09. The future climate scenarios are then applied to grid-integrated renewable power generation in order to estimate the impact of climatic conditions on power grid reliability. A MCS technique is employed for capturing the influence of these impacts. Parts of this chapter have been published previously in [251] during the course of this Ph.D. work.

The chapter is structured as follows. The methodology for evaluating the effects of climate change on wind and PV power generation is introduced in section 6.2. Section 6.3 presents the climate change simulation, including the emission scenarios, and the steps in the simulation. The LBMC is explained in section 6.4, and the PV and wind power generation systems model is detailed in section 6.5. The IEEE Reliability Test System (IEEE-RTS) is outlined in section 6.6. Sections 6.7 and 6.8 discuss reliability performance and the case studies, respectively. A summary and the conclusions are given in section 6.9.

## 6.2 Methodology for Evaluating the Effects of Climate Change on Wind and PV Power Generation

The study in this chapter was carried out in four stages: climate change simulation, development of the proposed LBMC model for generating future climate scenarios, modelling of power system with integrated wind and PV power units, and reliability assessment with the use of the MCS technique. **Figure 6.1** shows the main stages of the proposed framework for assessing the effects of future climate change on a power system that includes integrated renewable PV and WF power generation. The first stage involves the simulation of two stochastic climate change projections representing different long-term emission scenarios including UK Climate Projection 2009 (UKCP09) [230] and World Climate Research Program Coordinated Regional Downscaling Experiment (EURO-CORDEX)[237]. In the second stage, the simulated future climate change scenarios are applied to the LBMC in order to generate a single probable future scenario. This scenario is next incorporated into the third stage, which entails the modelling of PV and WF generation that is connected to the power system grid. To capture the influence of the LBMC output scenario on the integrated renewable power generation, a non-sequential MCS is employed for power system reliability assessment.

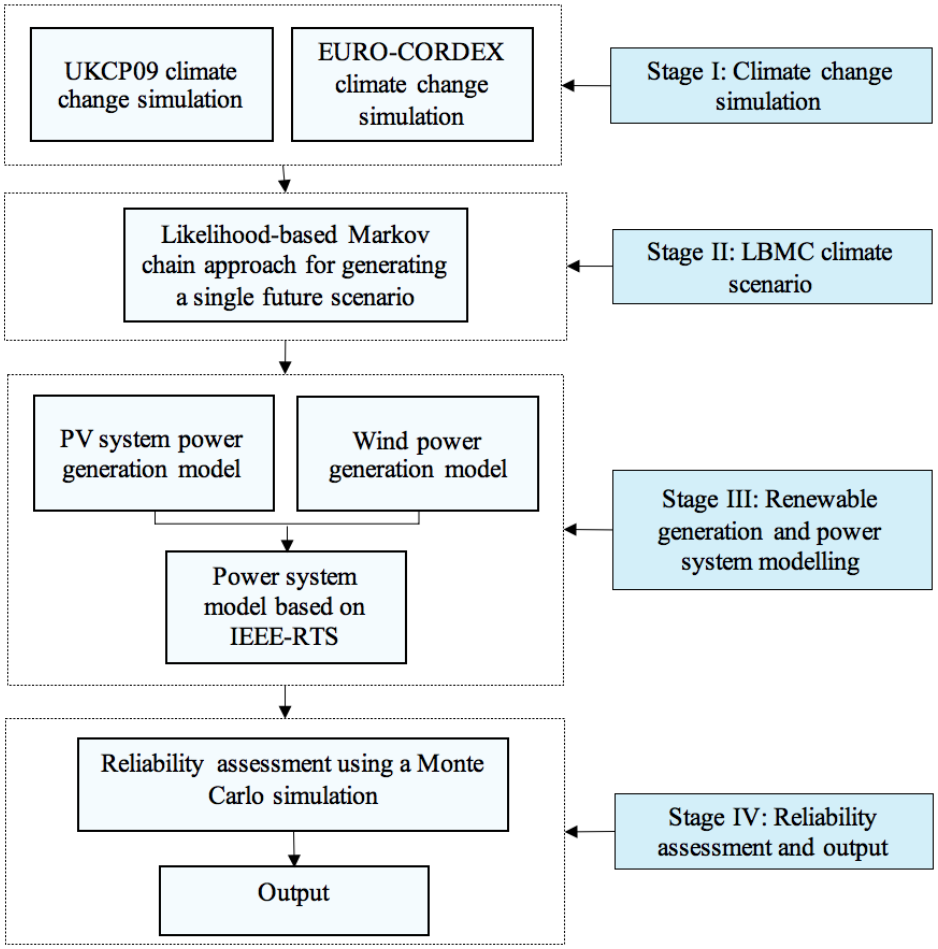


**Figure 6.1.** Overview of the main methodology

## 6.3 Climate Change Simulation

This section simulates the long-term climate change to assess its influence on PV and WF power generation and the consequent repercussions for the reliability of the power system. In the simulation, different climate change models are implemented in order to simulate the necessary hourly time series of future weather factors based on emission scenarios and recorded historical data. The climate models used were the UK Climate Projection 2009 (UKCP09) [230] and a comprehensive climate change model of Europe taken from the World Climate Research Program Coordinated Regional Downscaling Experiment (EURO-CORDEX) [237].

Climate change models were simulated at high resolution in order to produce long-term simulations according to different emissions scenarios for the selected geographic location.

UKCP09 and EURO-CORDEX are presented in detail in Chapter 4 and Chapter 5, respectively.

### 6.3.1 Climate Change Emission Scenarios and Timescales

The degree of influence of future climate change and its implications for renewable integrated power system reliability are dependent on the level of future greenhouse gas (GHG) emissions. Future weather is projected to change from time to time due to anthropogenic effects, which are believed to be perhaps the greatest cause of substantial increases in GHG emissions [138]. The UKCP09 emission scenarios are based on the Intergovernmental Panel on Climate Change (IPCC) *Special Report on Emissions Scenarios* (SRES), which are designated B1, A1B, and A1FI. On the other hand, the EURO-CORDEX emission scenarios are based on representative concentration pathway (RCP) scenarios, denoted RCP2.6, RCP4.5, and RCP8.5. Combining the scenarios from the two models enables them to be categorised based on the level of GHG emissions: B1 and RCP2.6 indicate low emission scenarios; A1B and RCP4.5 indicate medium emission scenarios; and A1FI and RCP8.5 indicate high emission scenarios, which are the most pessimistic scenarios, with no attention being paid to reducing GHG emissions.

The UKCP09 weather generator scenarios were simulated for 2010 to 2099 while the EURO-CORDEX ones were simulated for 2007 to 2099. For this study, however, three representative years were selected: 2020, 2050, and 2080 to quantify the impacts of climate change over long-term. The emission scenarios based on climate change data were simulated from historical and baseline weather data related to the period from 1961 to 1990

### 6.3.2 Climate Change Simulation Procedures

The climate change simulation involved two different models: the UKCP09 weather generator and the EURO-CORDEX climate model. The steps in the method employed for this

long-term simulation are outlined in **Figure 6.2**. The climate variables included in this simulation are wind speed, ambient air temperature, and solar irradiation for the selected geographic location of Birmingham, UK, at 52.48 N latitude and -1.89 W longitude.

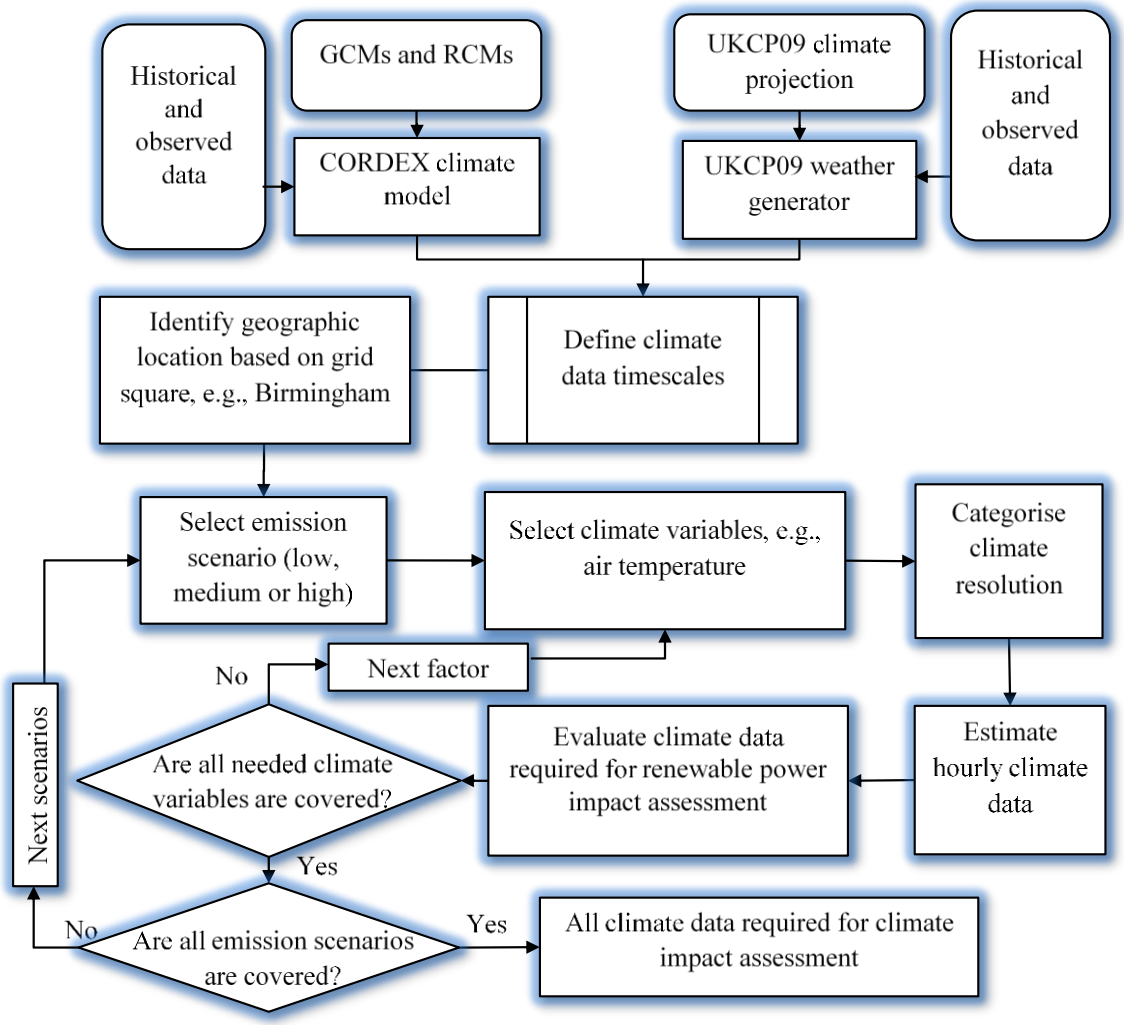


**Figure 6.2.** Methodology for simulating climate change for different GHG emission scenarios

## 6.4 Likelihood-Based Markov Chain

Given the uncertainty associated with future climate scenarios, a new LBMC approach is proposed for capturing a reasonable future weather scenario based on $CO_2$ emissions. Thus, the six emission scenarios simulated were considered in order to generate one future scenario based on the probabilities.

### 6.4.1 LBMC-Derived Future Scenarios

LBMC theory is based on random performance with a conditional probability of a self-state in the Markov chain. As illustrated in **Figure 6.3**, the technique is applied for three climate change states based on low, medium, and high GHG emissions.

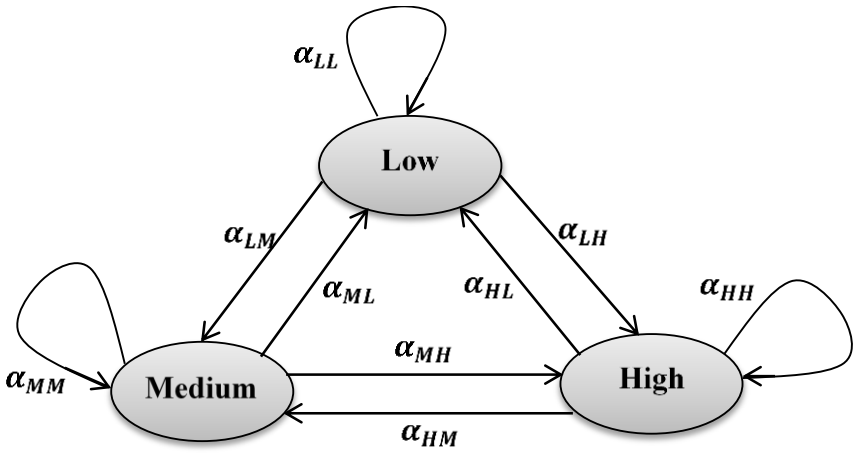


**Figure 6.3.** Three Markov states for the low, medium, and high emission scenarios

However, based on the probability of the self-states (λii) and the probability of the transitions between the states (λij), where *i* and *j* respectively represent self and transition states, a future single scenario is generated for each time duration (i.e., every hour) for each of the weather factors: ambient temperature, solar irradiation, and wind speed. The transition between states represented by $\alpha_{ij}$ where $i$ and $j$ represent by L(low), M(medium) and H(high). An additional factor is that the total probability of the self and transition states must be equal to one. However, a single future weather scenario can be generated based on a determination of which scenario would be most likely to occur in the future, given consideration of the levels of probability associated with all three scenarios (e.g., emission scenarios with a high (0.5) probability, a medium (0.3) probability, and a low (0.2) probability.

### 6.4.2 Climate-Change-Based LBMC Procedures

The LBMC algorithm employed for evaluating future weather scenarios is set out in Figure 6.4. A random number in the interval (0,1) is generated and compared with the self-state.

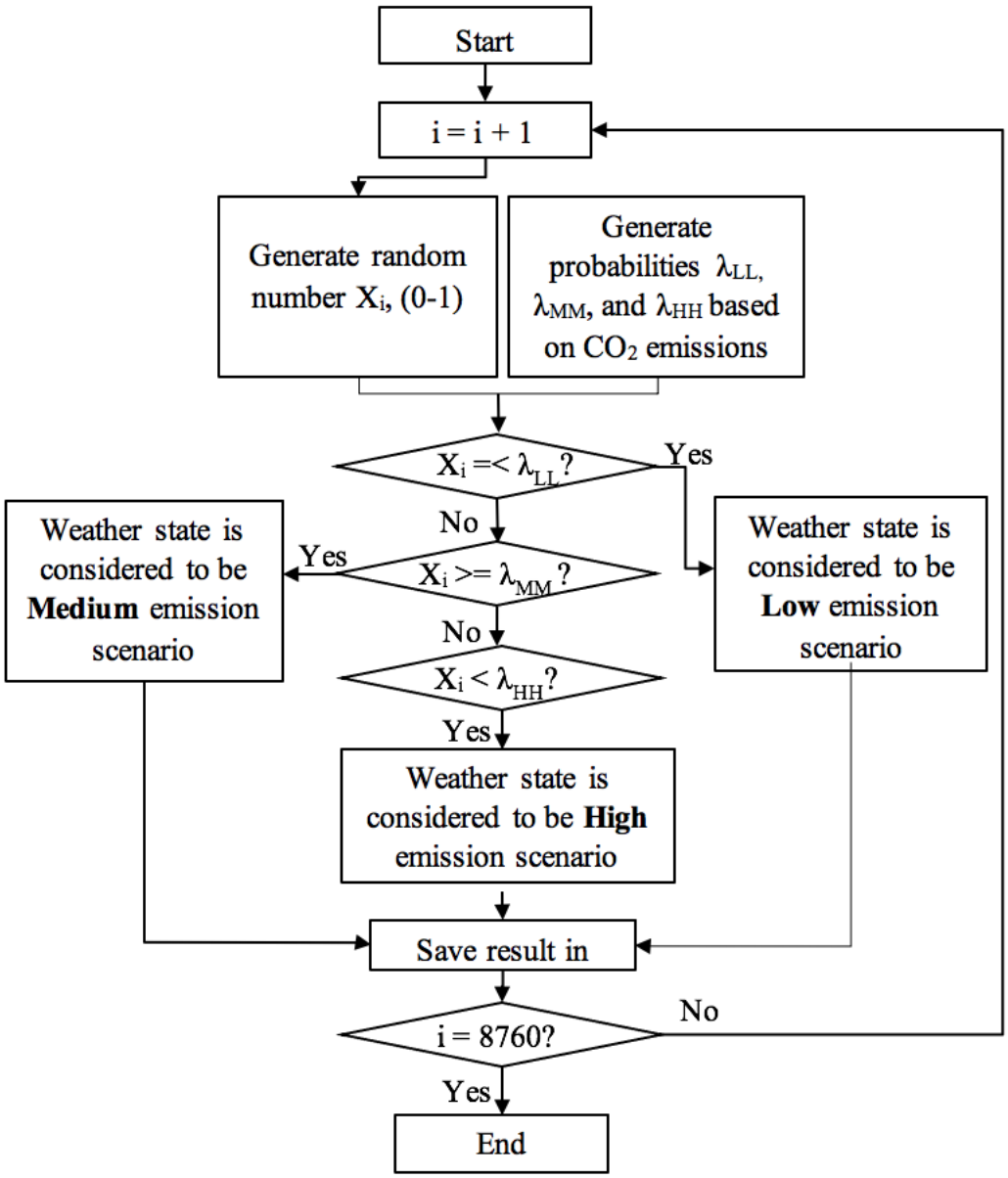


**Figure 6.4.** Algorithm for the LBMC evaluation of future weather scenarios

If the number generated is, e.g., smaller than or equal to the self-state $\lambda_{LL}$ probability, then, at that point, the weather data (e.g., ambient temperature) is considered to be a low-emission scenario for that hour. The algorithm is applied to all states over all of the time series. This

approach is implemented for all of the time series during the year, and the same technique is applied for the solar irradiation and wind speed weather data.

## 6.5 PV Systems and Wind Farms Modelling

The power generation models of the hybrid PV and WF generation considering of climate variables, primarily solar irradiation, ambient temperature, and wind speed, are utilized as described in Chapter 3 and Chapter 4. The PV power generation model based on analytical method, which was designed to incorporate the effects of ambient temperature, operating temperature, and PV system efficiency, along with multi-level solar irradiation. PV power generation is calculated as expressed in equation (6.1), which has therefore been further extended to incorporate the ambient and operating temperatures, taking efficiency into account as given in [231]. The PV power generation model $P_{pv}$ can thus be computed as follows:

$$P_{pv} = \begin{cases} \sum_{t=0}^{t=period} \frac{P_{STC}\ {G_{bi}}^2}{R_c\ x\ G_{STC}} \left(1 - \frac{\delta}{100}\ (T_{STC} - T_{cell}\right) & 0 \leq\ G_{bi} < R_c \\ \sum_{t=0}^{t=period} \frac{P_{STC}\ G_{bi}}{G_{STC}} \left(1 - \frac{\delta}{100}\ (T_{STC} - T_{cell}\right) & R_c \leq\ G_{bi} <\ G_{STC} \end{cases} \tag{6.1}$$

$$T_{cell} =\ T_{amb} + \frac{NOCT - 20}{1000} \tag{6.2}$$

The details of the equation are provided in Chapter 4. On the other hand, the WF power generation model can be estimated with the incorporation of wind speed, which has a nonlinear relation with power generation. The amount of power $P_{WT}(t)$ generated by a wind turbine at time *t* can therefore be determined in MW using (6.3) [105]:

$$P_{WT}(t) = \begin{cases} 0 & 0 \leq U_O(t) \geq U_{ci} \\ \left(A + BU_O + C{U_O}^2\right)P_r & U_{c\_i} \leq U_O(t) \geq U_r \\ P_r & U_r \leq U_O(t) \geq U_{co} \\ 0 & U_O(t) \geq U_{co} \end{cases} \tag{6.3}$$

Details of the equation are furnished in Chapter 5. The output weather data of LBMC are applied to the PV and WF generation models in order to compute the generation profile, while the renewable generation models are integrated into the power system for the purposes of reliability assessment.

## 6.6 Test System Network

The proposed framework was validated using the IEEE-RTS 1996. **Figure 6.5** shows a diagram of the 24-Bus IEEE-RTS with the integration of renewable power generation.

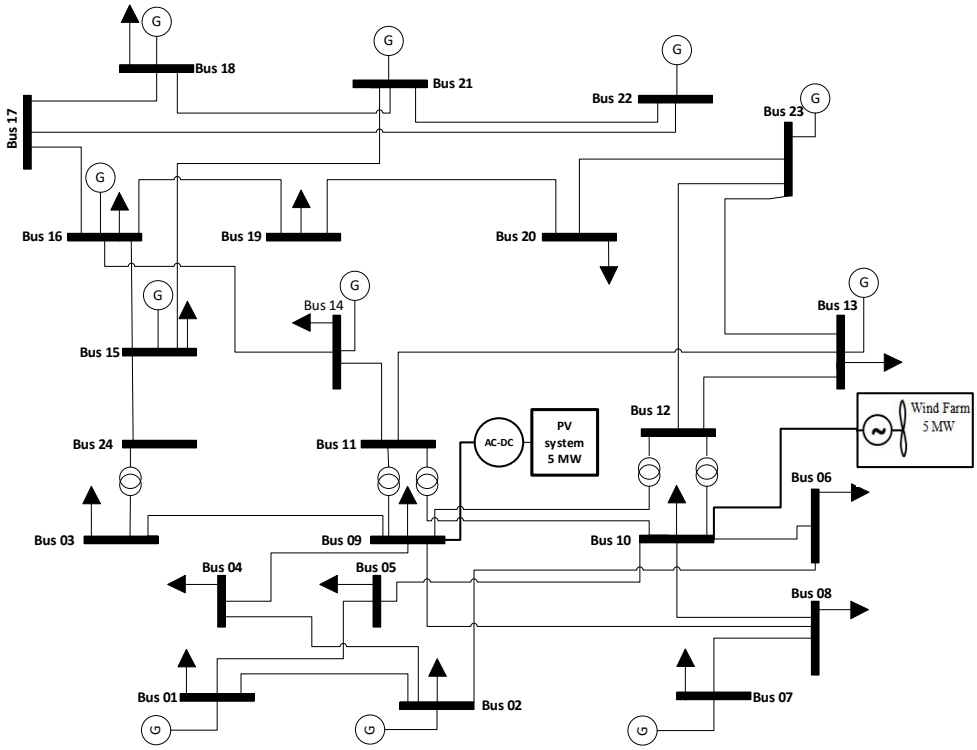


**Figure 6.5.** IEEE-RTS with the incorporation of renewable power generation

The IEEE-RTS was modelled and adapted for the work presented in this chapter in order to demonstrate the impact of climate change on the reliability of a PV- and WF-integrated power system. The system contains 24 buses, 38 branches, and 11 generators. Technical system data, including the parameters of the branches (lines and transformers) and generators, as well

as the reliability data, are provided in Appendix A. The system details were derived from [232] and [234], with adjustments appropriate for each case study.

## 6.7 PV and Wind Units Reliability

The reliability assessment procedures presented in this section was conducted in order to establish the correlations between renewable power integration with and without the effects of climate change. The impact of long-term climate change on PV and WF installations can affect the power demand and overall reliability of the connected system of these power generators and must therefore be assessed effectively. The following subsections first explore the climate change effects on renewable power generators' reliability, followed by a reliability assessment under LBMC climate model.

### 6.7.1 Reliability Assessment with Integrated Wind Farms and PV Power Generators Applying the Impact of Climate Change

For the reliability assessment, both PV and wind power generation systems were integrated into the IEEE-RTS power system. Large PV and WF facilities can be significantly affected by ambient weather conditions and therefore by the effects of long and short term climate change, such as heat waves, solar irradiation, ambient temperature and storms. The impact on PV and wind units can take the form of damage to infrastructure, component failure, or reduced output power production of PV and wind units. A small change in temperature, degree of cloud cover, amount of direct or indirect solar irradiation, or wind speed can have significant ramifications with respect to potential PV and wind power generation systems. When such sources of generation are integrated into a power system, these consequences of shifts in ambient conditions will have repercussions for the overall reliability of the power system.

The influence of climate change variables on PV and wind power generators integrated into a power system can be assessed with the use of non-sequential MCS because of its suitability for use in analysing the impact of weather. Since the reliability assessment of the PV and wind power generation systems model and its components has been investigated previously in [88, 242], this study involved only the assessment of the impact of climate change variables based LBMC model on PV and wind power generation and their consequent influence on the reliability of the power system.

For the evaluation of the reliability level of the system, the expected energy not supplied (EENS) index was considered as the assessment metric due its low rate of convergence. Based on literature in chapter 2, the coefficient of variation of the EENS is the lowest convergence rate. The EENS index quantifies the energy that cannot be supplied to a system (MWh/y) due to the failure of components throughout the entire system. Any change in the power system EENS compared to those without the incorporation of the effects of climate change can then potentially be due to the impact of climate change on the PV and wind power generation systems. The confidence of the reliability index was examined based on the simulation of a large number of experiments/iterations, with a correspondingly significant computation time. The sample variance of MCS decreases with increase in number of experiments, and therefore improves the effectiveness of MCS. Thus, using a practical and appropriately large number of samples depends on the system unavailability. The convergence criterion can be quantified in order to estimate the optimal number of these simulation experiments within an acceptable computation time.

### 6.7.2 Reliability Procedures

This section presents the reliability assessment procedures for the impact LBMC climate scenarios to the PV and wind power generation models. To estimate the ENS index, the level of the reliability performance was determined using a non-sequential MCS technique to capture

LBMC impact and based on an assumption of the absence of any failure not due to the impact of climate change. **Figure 6.6** outlines the reliability assessment procedures for establishing the impact of the proposed climate change scenarios on a PV- and WF-integrated power system. The reliability assessments were accomplished using DIgSILENT PowerFactory and MATLAB, which followed following steps:

- Simulate the proposed future climate change scenarios for different years, as outlined in the steps shown in Figure 6.2. The simulated hourly climate change variables are then used as input for the LBMC approach and the output of them are applied to the renewable power generation integrated power system.
- Build the modified power system model of IEEE-RTS for validation if the proposed framework with integration of PV and wind power generation for reliability assessment.
- Apply the simulated LBMC climate change scenarios into the designed and modelled PV and wind power generation integrated power system and repeat the steps for each emission scenario considering future years, as previously indicated.
- Initialise and insert the reliability data for each power system component.
- Generate a random number in the interval (0,1) for each power system component $i$ (i.e. generating units, transmission lines/transformers, etc.,). If the number generated is less than the forced outage rate (FOR), then the component is considered to be in a down state, and vice versa, as given in (6.4):

$$State_i = \begin{cases} 1, & \text{Up state} \\ 0, & \text{Down state} \end{cases} \tag{6.4}$$

- Perform load flow analysis and initialise the power balance within the voltage limits at the buses and within the thermal limits of the lines during the simulation.
- When the system $State_i$is not zero, then the system in a contingency state due to component outage and therefore it is required to determine curtailed load using the minimization model of load curtailment.

- Repeat these steps for N number of iterations, for each iteration if the curtailed load is not zero, then system states contribute to the unreliability indices.
- Estimate the reliability index by calculating the demand not supplied (DNS) and the ENS at each iteration. From the average of iterations, estimate the expected demand not supplied (EDNS) in MW and the EENS in MWh/y, using (6.5) and (6.6) [22]:

$$EDNS = \sum_{i \in S_i} C_i \times P_i \tag{6.5}$$

$$EENS = \sum_{i \in S_i} C_i \times P_i \times 24 \times 365 \tag{6.6}$$

where $C_i$ is the load curtailment in system state $i$, $P_i$ represents the system state probability, and $S$ denotes the set of all system states associated with load curtailment.

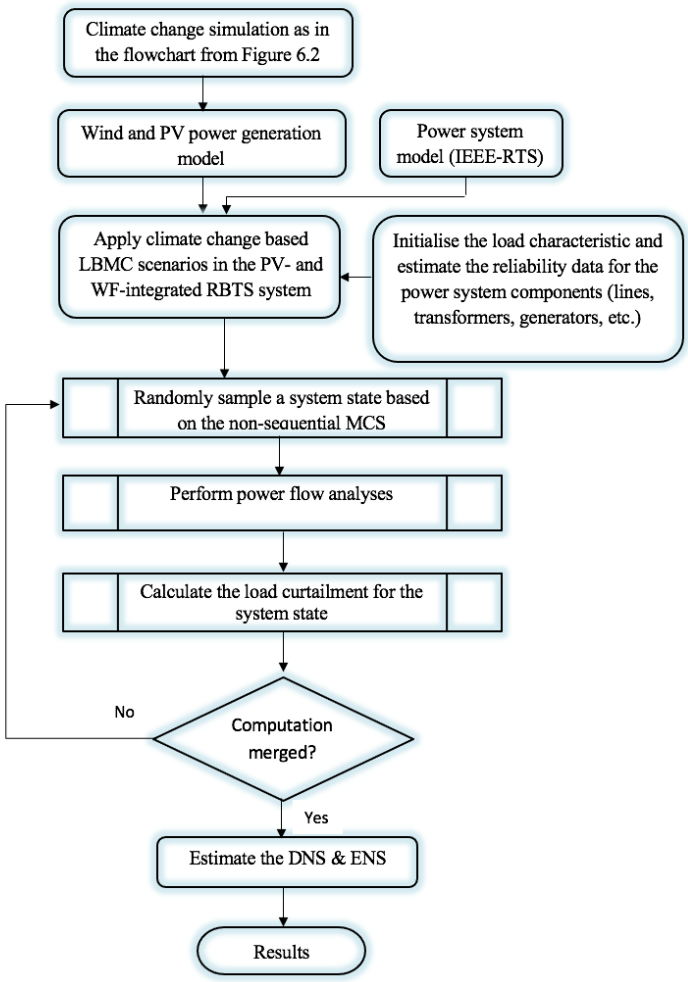


**Figure 6.6.** Reliability assessment procedures for establishing the impact of the proposed climate change scenarios on PV and WF generation systems

## 6.8 Case Studies

To assess the impact of climate change on PV and WF installations, each with a 5 MW capacity, was integrated to the power system. The ambient weather conditions for renewable power generation were simulated using a stochastic model for a variety of long-term $CO_2$ emission scenarios. These weather conditions were then applied to the proposed LBMC algorithm in order to evaluate the impact of future weather scenarios on the models.

Due to the unavailability of real power system data for the selected geographic location, the IEEE-RTS was considered for this study. DIgSILENT PowerFactory software, which is frequently used as a software platform for reliability assessment, was integrated with MATLAB. DIgSILENT provides essential input for MCS to perform reliability assessment of power system while MATLAB provides the necessary DIgSILENT input in the form of generation profiles that take into account the effects of climate change. PV and WF generation were integrated at buses 9 and 10, respectively, as indicated in **Figure 6.5**. Due to the effects of the large random variables inherent in integrated renewable power systems, non-sequential MCS was used for estimating reliability performance. For this study, the reliability assessment was conducted based on estimates of the ENS reliability index for different cases in order to validate the proposed approach. Any change in the EENS reliability index (compared to the results without climate change modelling) occurs because of the impact of climate change on the PV and wind generation, thus affecting the reliability performance of the power system. The study includes consideration of the following cases for which climate change data are incorporated into the PV units and wind turbines for different selected years, with the results then being compared with those of the first case, in which no renewable power generation is integrated.

- The first case represents the base case when no renewable power generation is integrated.

- The second case enables an examination of reliability performance when PV and WF units are integrated into bus 9 and bus 10, respectively. This case incorporates two proposed LBMC future climate change scenarios: “very likely” and “reasonably likely”.
- The third case involves the incorporation of climate change models that include consideration of very likely scenarios. Two sets of versions are analysed in order to assess the benefit with respect to power grid reliability when renewable energy penetration is increased under these scenarios.
- The fourth case provides a comparison of the reliability improvement for two sets of scenarios when increases of the same amount of PV and wind power capacity in the same year and geographic location.

### 6.8.1 Case 1: Base Case without the Integration of PV and Wind Units

In first case, reliability assessments were carried out for the IEEE-RTS with no PV and wind power generation systems being integrated and no climate change effects taken into consideration. The results from this case provided a reference point for demonstrating the feasibility of the proposed framework and for enabling a comparison with other scenarios in which LBMC climate scenarios were applied. In this case, the EENS reliability index for the power system was estimated as 5632.26 MWh/y.

### 6.8.2 Case 2: Two Different $CO_2$ Emission Scenarios

This case examines the reliability performance of power system when PV and WF generation is integrated at buses 9 and bus 10 and two different future weather scenarios are incorporated. The two future weather scenarios, exemplifying very likely and reasonably likely probabilities of occurring, were simulated using the proposed LBMC algorithm, and the

findings were compared with the base case. The two future weather scenarios were simulated considering the probability of the occurrence of low, medium, and high emission scenarios. The first scenario (very likely) indicates future weather data when the probabilities of the occurrence of low, medium, and high emission scenarios are 0.2, 0.3, and 0.5, respectively. The second scenario (reasonably likely) represents the future weather data with a lower probability of occurrence (reasonably likely), based on equal probabilities for low, medium, and high emission scenarios.

**Figure 6.7** depicts the EENS values for both scenarios "very likely" and "reasonably likely" compared with the base case results for 2020, 2050, and 2080. The first scenario exhibits decreased EENS performance compared to the second scenario. This reduction is caused primarily by the changes in the weather patterns since the high-emission scenario has the greatest probability of occurrence within first scenario. Compared to the outcomes of second scenario with the base case and the first scenario, a significant improvement in reliability leading to a reduction in the EENS value can be observed, which is less sensitive to climate effect and therefore its impact in PV and wind power generation systems less. For 2050 and 2080, the reliability improvement in both scenarios decreased proportionally with time leading to increase in EENS as a result of fluctuating weather conditions. The output power of the PV and wind power model is therefore reduced, resulting in an inferior reliability performance for the entire system.

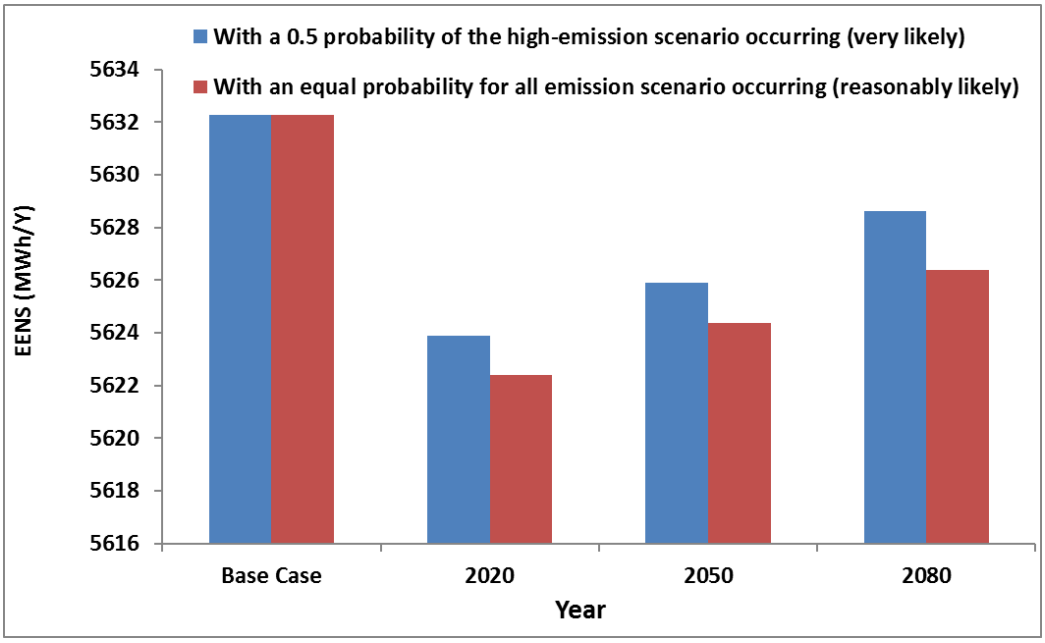


**Figure 6.7.** EENS values for the different $CO_2$ emission scenarios and their probability of occurrence (blue: very likely; red : reasonably likely)

### 6.8.3 Case 3: Effect of Increasing Renewable Generation Capacity

In this case, two sets of scenarios were studied in order to assess the benefits of increase the renewable energy penetration with respect to power grid reliability in conjunction with the incorporation of climate change models that include consideration of very likely scenarios. The first set represents the power system with different percentages of increased wind power capacity while the PV power capacity is remains unchanged. The second set represents the power system with increases in PV power capacity while the wind power capacity remains unchanged. A reliability assessment was then carried out for both sets, producing the results shown in **Figure 6.8** and **Figure 6.9**. It can be observed that in the first set, the EENS for the power system decrease with further additions of wind power in comparison with the base case, although the time-ahead EENS values are higher in 2050 and 2080 as a result of changes in climate leading to variation in weather pattern. The greater wind power capacity is likely to be more sensitive to the effects of long-term climate change.

The second set depicted in **Figure 6.9** that the reliability performance of the power system improves with additional contributions of PV power generation. This improvement in reliability lead to a reduction in EENS can be clearly seen with the 10 %, 20 %, and 30 % additions of PV power capacity. The EENS reduction is then slightly less with further additions of PV power. This outcome is particularly attributable to the higher probability of failure as a result of the intermittent nature of PV systems, which precipitates varying PV output power and leads to less reduction in the EENS reliability index.

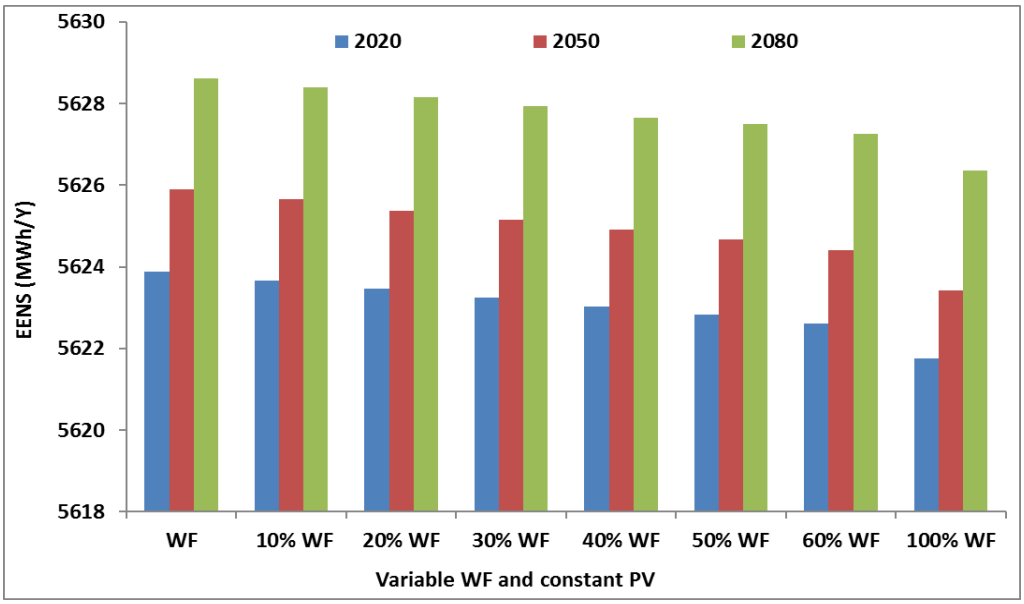


**Figure 6.8.** EENS values with constant PV capacity and variable WF capacity

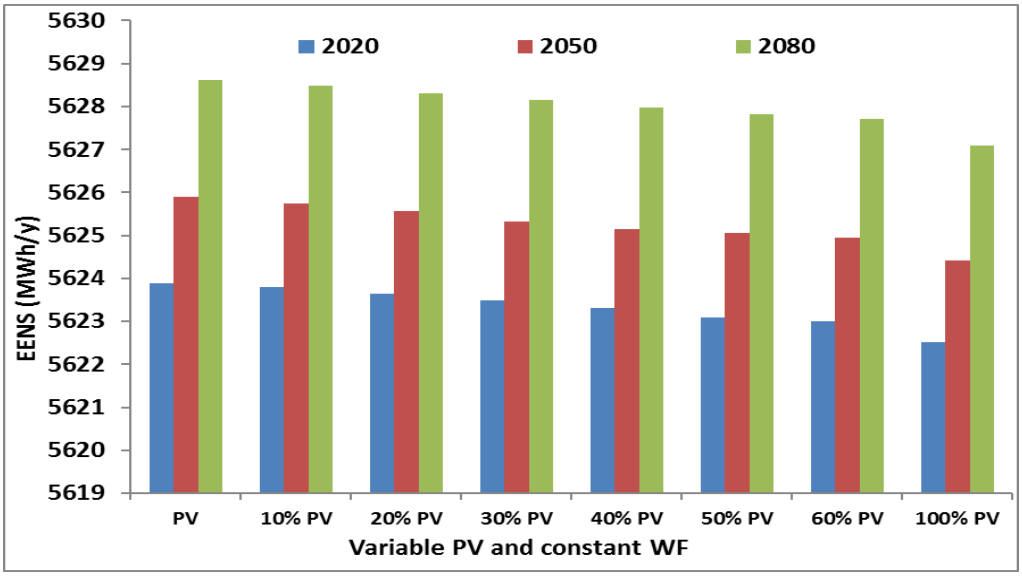


**Figure 6.9**. EENS values with constant WF capacity and variable PV capacity

### 6.8.4 Case 4: Comparison of the EENS Reduction with Added PV and Wind Power

This case enabled a comparison of the improvement in reliability between two scenarios that involved increases in PV and wind power capacity by the same amount during the same year. **Figure 6.10** compares the percentage improvement in EENS performance for two scenarios involving additions of renewable energy for 2020. It can be seen that the addition of greater PV and WF capacity potentially improves the EENS performance, although the enhancement of the EENS is less with additional PV power than with additional wind power. The system is thus rendered more resilient with larger increments of wind power because higher capacity is required from the PV systems in order to maintain the improved EENS levels. The results indicate that PV systems are more vulnerable to future climate model parameters than are wind generators. For both scenarios, the change in EENS improvement is more significant with greater increases in power capacity.

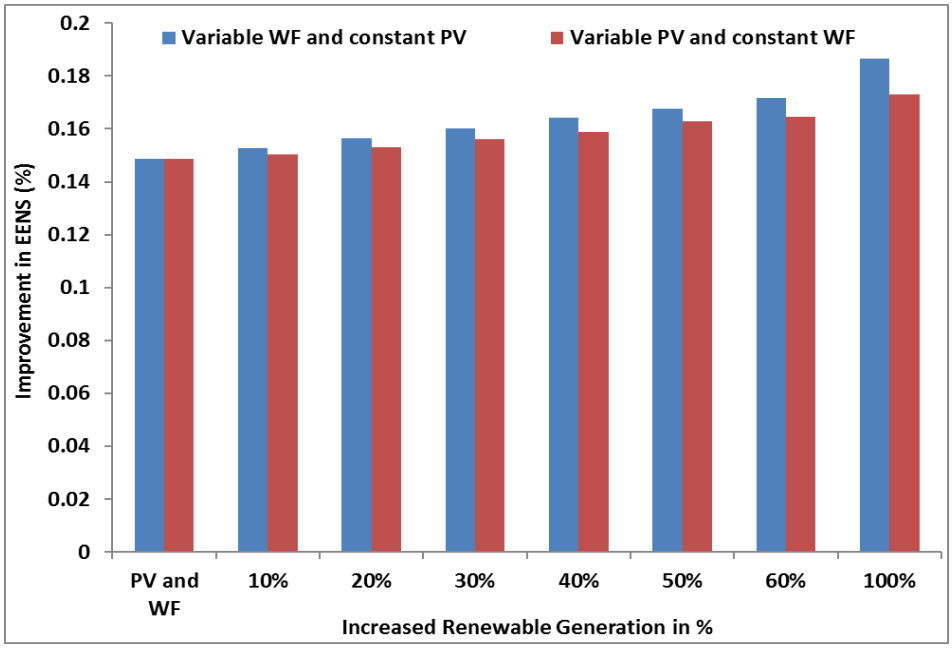


**Figure 6.10**. Percentage improvement in the 2020 EENS performance with increasing renewable generation capacity

## 6.9 Summary

This chapter has presented a framework that incorporates models of future climate change scenarios with the goal of determining their impact on the long-term reliability performance of a power system characterized by integrated PV and wind power generation systems. The framework employs an LBMC technique for generating future weather scenarios based on two different high-resolution climate change models: UKCP09 and EURO-CORDEX. The reliability process for demonstrating the influence of climate change on integrated PV and WF units is also presented. In reliability assessment, MCS technique was used to capture the impact of LBMC climate future scenario on the PV- and WF-integrated power system. In all cases, the EENS value was used as a benchmark for measuring the level of impact.

Two future climate scenarios were implemented in the case study using the proposed LBMC, which are "very likely" and "reasonably likely". These scenarios were generated based on occurring probabilities of GHGs emission. The findings demonstrated that the first scenario is more sensitive to the effects of climate change, as indicated by higher EENS, and therefore a greater impact is likely more than second scenario. The results suggest that consideration of impact of long-term climate change is vital for enhanced operational planning since the effects of climate change have a substantial impact on the reliability performance of PV and wind integrated power system. In both scenarios, the EENS suffer from increases with time in the year 2050 and 2080 more than 2020 as a result of ongoing changes in climate and continuing the GHGs emission, which required reduction on fossil fuel aiming prevent GHGs emission. The results also indicate that the reliability performance of the power system improves with the addition of greater amounts of PV and wind power capacity, although the enhancement is less pronounced with PV power system than with wind power generation system, as the PV system is more sensitive to climate change than wind turbine.

# Chapter 7: Reliability of Power Systems with Climate Change Impacts on Hierarchical Levels of PV Systems

## 7.1 Introduction

Chapter 4 presented a methodology to assess the impact of climate change on the reliability performance of PV integrated power system excluding the impact on PV components and subsystem. This chapter presents the proposed a long-term reliability assessment approach for PV integrated power systems considering the climate change effects on hierarchical levels of PV systems. Hierarchical levels in the PV systems were formed considering components in a PV system, subsystems in a PV system, whole PV system, and the power grid level. The approach suggests a way of mitigating the impact of climate change on PV systems through proactive design and the application of maintenance strategies for averting progressive component failure initiated by the effects of climate change. The approach takes into account different climatic factors including temperature, solar irradiation and wind speed as well as performance affecting factors including thermal stress, aging and degradation due to internal faults within the reliability evaluation framework. The approach drives through Monte Carlo simulation and Markov chain. The ability of identifying the critical components and subsystems in a PV system that lead to climate associated failures is one of the key features of the approach.

Climate change concerns are likely to drive the increased adoption of renewable energy, which is being developed around the world to mitigate greenhouse gases (GHGs) emissions and subsequentially global warming. Photovoltaics (PVs) power generation is considered as one of the most promising alternative sources of energy that can be integrated into a power system as rooftop PVs in bulk quantities or as a centralised connection depending on the

connection standards and regulatory scheme [228]. Climate uncertainties could have a direct impact on PV systems' performance and their components. The operating voltage of a PV cell can be affected by the rise of ambient temperature due to climate change. According to independent analyses by NASA and the National Oceanic and Atmospheric Administration (NOAA), the year 2018 was the fourth warmest year since 1880 with regard to the earth's global temperature [7]. On the other hand, the PV output power can also be affected by the level of solar irradiance, cleanness, and shading effects.

### 7.1.1 Status Quo

Numerous research advances have been made in the literature with regard to the reliability assessment of a power system with integrated PV systems. Among them the majority of assessments applied Monte Carlo simulation [228, 238], Markov chain [73] and fuzzy logic [76] concepts in their impact assessments with the integrated PV systems. Literature also reports that the power electronics related failures are the common course of most PV system failures [82-84, 88]; For example, the subsystem reliability evaluated in [83, 87]; the DC-AC inverter and the DC-DC converter in [80, 81]; and in some other studies the components such as the IGBT [84, 88], diode [87, 88] and capacitor [88] were susceptible to failures leading to a PV system outage. In [88, 89], the reliability assessment of the power electronic system, e.g. the DC-DC converter in [89] and DC-AC inverter in [88], is used based on the FIDES approach. The FIDES approach predicts the reliability of the components taking into account the acceleration of different stress factors and time sequence. Similarly, other studies, as in [81, 83], investigated the reliability of power electronics based on the Military-Handbook-217F [90]; which presents an analytical method to estimate the inherent reliability of military electronic components to increase the reliability of the system. However, these studies are focused only on power electronics and not the entire PV system; likewise, the impact of weather on components is not evaluated.

Other studies are focused on the PV system and geographic locations. In [61], the lifetime of the grid-integrated PV system inverter is evaluated considering the PV module's degradation and location. The study highlighted the impact of a hot climate on the PV inverter's lifetime. A multi-state Markov process was used in [73] to assess the reliability performance of photovoltaic module failure. Monte Carlo simulation (MCS) approach is used in [72] to assess the reliability performance of a power system with weather conditions. In [228, 238] the effect of climate change on the inputs of a PV system and a wind turbine are assessed using MCS. The authors in [88] propose a reliability performance evaluation method for an integrated PV system in a power system. In [252], a systematic reliability modelling and evaluation approach was proposed for the on-board power system in an electric aircraft using a hierarchical approach. The approach consists of three hierarchical levels (HLs): component level (HL1), subsystem level (HL2), and system level (HL3). Public domain research does not evidence a hierarchical application to a PV power generating system. However, these studies did not consider the internal power electronic components of the system.

### 7.1.2 Research Problem

Most previous research studies have focused on the reliability assessment of a PV system by estimating the failure rate of the main components. For instance, some studies in the literature considered a simplified assumption of constant failure rates and lifetime failures sequences were not considered. In addition, stress factors were lightly considered, and in most studies, the reliability of components in PV modules was not considered and abstracted the system. Further, the long-term impact of climate change, thermal stress factors of PV system components, or aging and degradation of the PV system components are not addressed comprehensively. Hence, a comprehensive framework to simulate a futuristic climate scenario accounting these factors is a need. Such a framework could play a key role in shaping the planning and operating standards of the future power grid.

Therefore, considering the research gab, this chapter proposes an advanced holistic framework for the reliability evaluation of a PV integrated power system incorporating impacts of climate change and subsequent variations in parameters.

### 7.1.3 Significance and the Study Framework

The uniqueness of the approach is that it comprehensively captures PV system components that could be vulnerable to climate change effects by extending the traditional component models to capture climate change sensitive features and then embed them into the system reliability assessment through Markov Chain integrated Monte Carlo simulation. The impacts of climate change are incorporated at four hierarchical levels in a PV system to ascertain the effects of component failure that can lead to progressive failure. The four hierarchical levels (HLs) are the component level (HLI), the subsystem level (HLII), the level that covers the entire PV system (HLIII), and the level that includes consideration of the influences on a PV-integrated power system (HLIV). The reliability assessment model captures weather factors including temperature, solar irradiation and wind speed together with the failure rate due to stress factors, aging and lifetime degradation. This framework provides more comprehensive platform for the reliability assessment incorporating detailed effects of vulnerable components in a PV system. The chapter also presents sensitivity studies of degradation and failures of PV system's components due to climate change over reliability performances of the entire system.

Two established climate models are incorporated to generate climate change factors for the years 2020, 2050 and 2080. Parts of this chapter have been submitted to [253], the work is part of the course of this Ph.D.

The chapter is divided into six sections. Section 7.1 present the introduction, status quo, significance of the study and research problem. The main methodology illustrated in section 7.2. The climate change simulation is presented in section 7.3. Section 7.4 formulate the

mathematical of hierarchical reliability model including PV system components level, PV system subsystem level, whole PV system and grid level. Section 7.5 and 7.6 expose the reliability evaluation, its procedure, and the conducted case studies. Finally, the summary is given in section 7.6.

## 7.2 Methodology

**Figure 7.1** shows a brief overview of the proposed approach to investigate the reliability performance of PV integrated power systems with climate change effects. In the first step, the climate change effects are simulated and then the outcome is fed to the second and third steps simultaneously. The second step of the approach assesses reliability of the PV system considering hierarchy levels without applying climate change effects on the PV system. In the third step, the influences of climate change are applied to the PV power generation model. The outputs of the third step are combined with the outputs from the second step which is then fed to the reliability assessment of the whole power system in the fourth step.

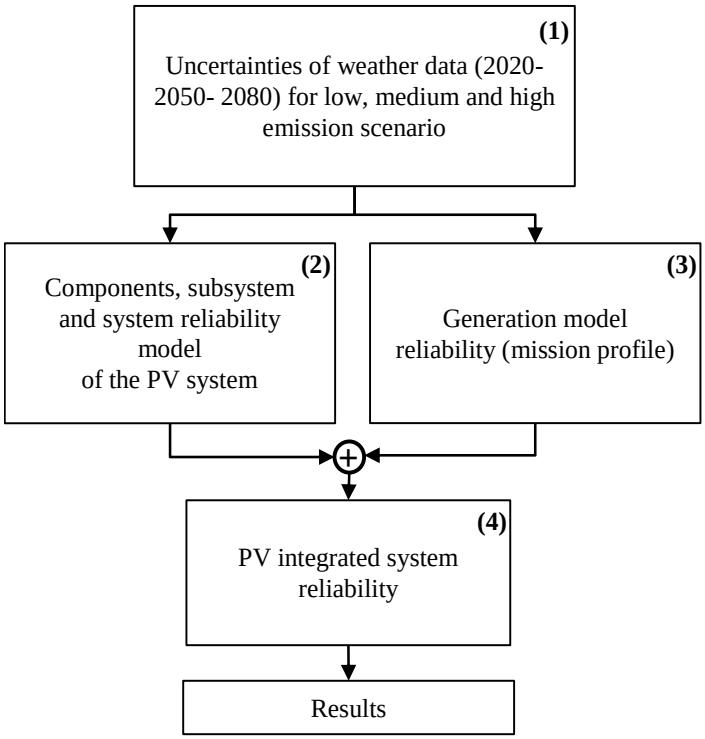


**Figure 7.1**. Methodology in brief

## 7.3 Weather Simulation

In order to assess climate change impacts that may harm a power system, two different climate models were incorporated in this study. A regional climate model for Europe within the World Climate Research Program Coordinated Regional Downscaling Experiment (EURO-CORDEX) [220, 237], and UK Climate Projection 2009 (UKCP09) [229] are simulated for low, medium and high $CO_2$ emission scenarios and for different future time horizons including the years of 2020, 2050 and 2080. The identified climate changes have a high probability of occurrences in the future as they are supported by 30 years of historical weather data. They provide a time series of weather data at a resolution of 5 km for UKCP09 and 12 km for EURO1-CORDEX. The weather parameters including air temperature, solar irradiation and wind speed are modelled to investigate their impact on the PV system's components. More details of the climate change simulation, it's procedures and emission scenario are given in chapter 6.

## 7.4 Reliability assessment considering Hierarchical Levels

The impact of ambient weather conditions on PV system reliability must be considered as part of a comprehensive model. As ambient conditions may influence the individual PV system components, subsystem reliability and component lifetime, the framework considers ambient weather impacts at each hierarchical level, as given in **Figure 7.2**.

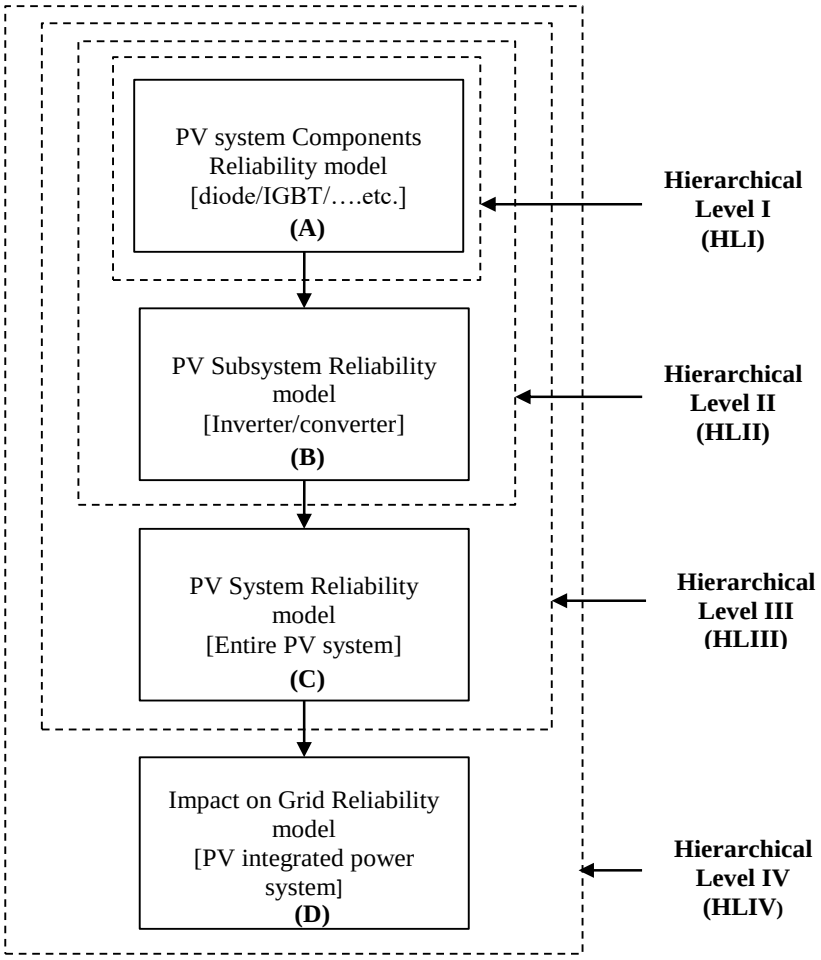


**Figure 7.2**. Hierarchical levels with integrated PV systems' reliability assessment

HLI represents the PV system components' failure rate (e.g., the failure rate model of the IGBT, diode, capacitor, fuse and PV panel); HLII represents the reliability model of the PV subsystem which comprises of HLI components and includes the DC-DC converter, DC-AC inverter, and PV array. The failure rates of both HLI and HLII are dependent on the ambient and operating conditions, which means that HLI and HLII failures due to these conditions also lead to failure at the HLIII and HLIV levels. HLIII represents the reliability assessment of the entire PV system, including HLI and HLII; HLIV represents the reliability performance of the PV system integrated with the power grid. The failure rate of components during their useful lifetime and wear-out stage is described in [22, 254]. The details of the hierarchical levels are given in **Figure 7.3**.

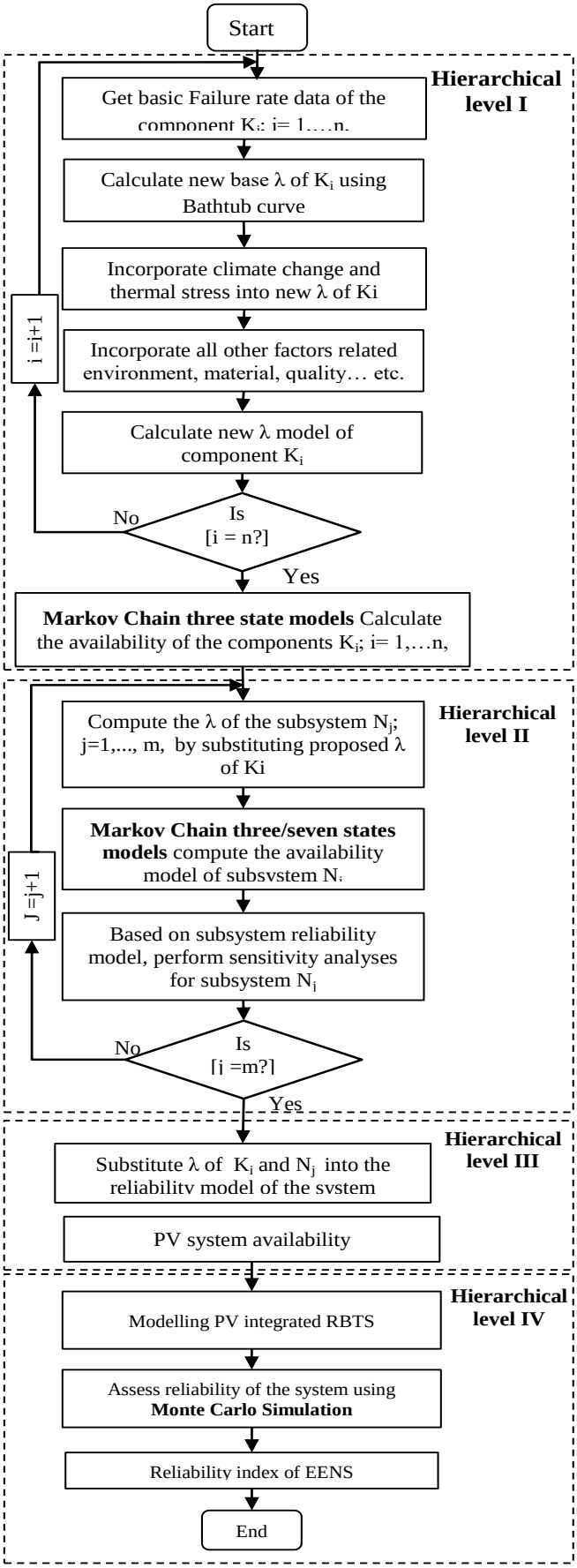


**Figure 7.3.** PV system hierarchical level-based reliability assessment

### 7.4.1 Components Level I (HLI)

One of the reliability prediction approaches applied in electronic components is MIL-HDBK-217 [90] referred to as a parts count prediction. MIL-HDBK-217 provides failure estimation for the components based on statistical analyses, basic failure, stress factors, and simplified assumptions. The reliability of a system and power grid can be estimated more accurately by estimating the failures of the individual components and subsystems. As shown in **Figure 7.4** , in the proposed approach, an extended parts count prediction based on the failure rates of individual components is estimated. In addition, a Markov chain is formed, considering the failure rates over components' lifespan based on bathtub curve. The failures of the components in the subsystem is characterized by a probability density function (pdf) and expressed by f(t) [22]:

$$F(t) = \int_0^t f(t)\, dt \tag{7.1}$$

Then, the reliability $R(t)$and failure rate $\lambda(t)$ of the components are estimated using (7.2) and (7.3):

$$R(t) = 1 - F(t) \tag{7.2}$$

$$\lambda(t) = \frac{f(t)}{R(t)} \tag{7.3}$$

The reliability of the system with $n$ components can be calculated using (7.4):

$$R(t) = \prod_i^n R_i(t) \tag{7.4}$$

For the work presented in this chapter, the failure rate of component $k$ is calculated using (7.5) and for the subsystem, using (7.6):

$$\lambda_k(t) = \lambda_{Base\_K} \times \prod_N \tag{7.5}$$

$$\lambda_{System}(t) = \sum_N \lambda_k\,(t) \tag{7.6}$$

where $\lambda_{Base}$ is the base failure rate of the specific component $k$, and $\prod_N$ stands for $n$ number of stress factors that have an impact on the failure rate of a specific component.

As depicted in **Figure 7.4**, the base failure rate of a component can be estimated using a bathtub curve with the Weibull distribution in combination with the Gumbel distribution, as given in (7.7) [254]. This technique enables consideration of both useful life ($T_U \leq t < T_W$ ) and the wear-out stages ( $t \geq T_W$), while failure during the infant period ( $\lambda_I$) $0 \leq t < T_U$ is neglected. $T_U$ and $T_W$ represent the time covered by a guarantee and the end of the lifetime of the components, respectively. The infant period normally extends from days to months, during which failure is due to manufacturing defects; therefore, any component that fails is replaced or repaired by the manufacturer within the guarantee period. For this study, the assumption was that the time of the guarantee $T_U$ is 3 months and that $T_W$ indicates different values based on each component, e.g., 25 years for a PV module.

$$\lambda_{Base} = \begin{cases} \lambda_I & ;\ 0 \leq t < T_U \\ \lambda_C & ; T_U \leq t < T_W \\ \infty & ; t \geq T_W \end{cases} \tag{7.7}$$

where, $\lambda_I$ is the failure rate during infant period as in (7.8) and $\lambda_C$ is the failure during both useful life and wear out stages and can be estimated using (7.9). The new base failure rate is then calculated using (7.10):

$$\lambda_I = \alpha e^{-\beta t} + \varepsilon \tag{7.8}$$

$$\lambda_C = a + \delta e^{\delta(t-\eta)} \tag{7.9}$$

$$\lambda_{P\_base} = a + \delta e^{\delta(t-\eta)} \tag{7.10}$$

here $\lambda_{P\_base}$ is the proposed base failure rate, $a$ indicates the failure rate displacement parameter (1/yr), δ denotes the failure rate scale, β represents the failure rate scale during the infant period, and η corresponds to the failure rate location parameter.

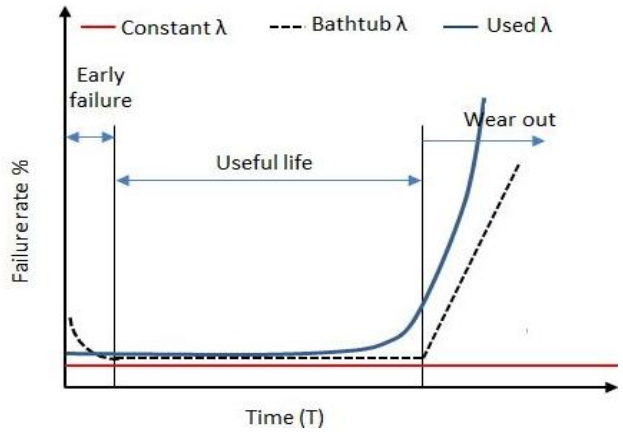


**Figure 7.4.** Failure rate propagation of a component's life

However, the failure rate of component i can be estimated using (7.11), but not all of the stress factors in (7.11) are applicable for all of the components [90]:

$$\lambda_i = \lambda_{P\_base} \times ( \pi_T \, \pi_Q \, \pi_S \, \pi_E \, \pi_{SR} \, \pi_v \, \pi_{C)} \tag{7.11}$$

where $\pi_T$ is the thermal factor; $\pi_Q$ is the quality factor, ranging from 0.7 up to 8 depending on the components [90]; $\pi_S$ is the electrical stress factor; $\pi_E$ is the environmental factor quantified within each part of the failure rate model, which varies depending on the material used; $\pi_C$ is the contact construction factor; $\pi_{SR}$ is the series resistance factor for capacitors only, which varies between 0.66 and 3.3 depending on the circuit resistance $(CR)$ [90]; and $\pi_v$ is the voltage stress factor.

#### 7.4.1.1 Failure Rate of a Diode

The power diode is a critical component in a DC-AC inverter, and it can fail under various conditions. Common failures include an open or a short circuit due to an external disconnection, reverse blocking state, reverse recovery transition and overstress, i.e. overvoltage, overcurrent and overheating [89]. The failure rate of the Schottky power diodes can be estimated using (7.12):

$$\lambda_D = \lambda_{P\_base\_Diode} \times (\pi_T \, \pi_Q \, \pi_E \, \pi_v \, \pi_C) \tag{7.12}$$

where $\pi_V$ and $\pi_T$ is the voltage stress and thermal factor and can be expressed as in (7.13);

$$\pi_V = \begin{cases} \dfrac{V_{out}}{V_{rate\_diode}} & ,for\ 0.3 < \left(\dfrac{V_{out}}{V_{rated_{diode}}}\right) \leq 1 \\ 0.054 & ,for \quad \left(\dfrac{V_{out}}{V_{rated_{diode}}}\right) \leq 0.3 \end{cases} \tag{7.13}$$

$$\pi_T = exp\left(-3091\left(\frac{1}{T_J + 273} - \frac{1}{298}\right)\right) \tag{7.14}$$

where the $T_J$ is the junction temperature of the diode. A typical inverter consists of a connection of IGBTs and diodes, thus, the temperature rise in both components can be estimated using linear heat transfer equations using (7.18) and (7.19) in Section 7.4.1.2.

#### 7.4.1.2 Failure Rate of the Switches

The failures of the semiconductor switches such as the insulated gate bipolar transistor (IGBT) and MOSFET are common in power electronic circuits. They can fail due to various reasons and under different circumstances. They may fail due to high voltage, high current, extreme temperature, or high junction temperatures [255]. In addition, switches may fail due to electrical faults and mechanical degradation [256]. The lifetime of switches is expected to be between 21 to 60 years with a 90% confidence level [84]. The failure of the semiconductor switches can be estimated using (7.15):

$$\lambda_S = \lambda_{P\_base\_Switch} \times (\pi_T\, \pi_Q\, \pi_E\, \pi_A) \tag{7.15}$$

The thermal factor $\pi_T$ can be expressed as in (7.16):

$$\pi_T = exp\left(-1925\left(\frac{1}{T_J + 273} - \frac{1}{298}\right)\right) \tag{7.16}$$

The junction temperature $T_J$ of both switch and diode is modelled as in [88] and can be estimated using (7.17):

$$T_J = \begin{cases} T_c + \Delta T_S & for\ Switch \\ T_c + \Delta T_{Diode} & for\ diode \end{cases} \tag{7.17}$$

where $T_c$ and $\Delta T$ are the case temperature and linear heat transfer respectively, and can be calculated as in (7.18) and (7.19):

$$T_c = T_a + \theta_a(P_{S\_loss} + P_{D\_loss} + P_{add}) \tag{7.18}$$

$$\Delta T = \begin{cases} \theta_{11}P_{S\_loss} + \theta_{12}P_{S\_loss} & for\ Switch \\ \theta_{21}P_{S\_loss} + \theta_{22}P_{D\_loss} & for\ Diode \end{cases} \tag{7.19}$$

where $\theta_a$ is the thermal resistance from ambient to case (top of the package) and $P_{S-loss}$ and $P_{D-loss}$ are the power dissipations in the switch and diode; $P_{add}$ is the power dissipated by other mounted devices including the switch and diode; $\theta_{11,22}$ and $\theta_{12,21}$ are the thermal resistance coefficients of the switch and diode and the coefficients' thermal resistance between the switch and diode, respectively.

#### 7.4.1.3 Failure Rate of the Coil

The failure of the coil can be estimated using (7.20):

$$\lambda_L = \lambda_{P\_base\_Coil} \times ( \pi_T \, \pi_Q \, \pi_E ) \tag{7.20}$$

The thermal temperature $\pi_T$ of the coil can be estimated by using (7.21):

$$\pi_T = exp\left( -\frac{-0.11}{8.617x10^{-5}} \left( \frac{1}{T_{HS} + 273} - \frac{1}{298} \right) \right) \tag{7.21}$$

The $T_{HS}$ is the hot spot temperature which is based on the ambient temperature (°C) and average temperature rise above ambient $\Delta$T (°C) and can be found from the device specification. The $T_{HS}$ can be estimated using (7.22):

$$\pi_{HS} = T_a + 1.1\ (\Delta T) \tag{7.22}$$

#### 7.4.1.4 Failure Rate of the Capacitor

The aluminium electrolytic and film capacitors are normally preferred for PV inverter applications, although the film capacitor is more reliable and expensive than the electrolytic [255]. The estimated lifetime of the capacitors can vary depending on the type of capacitor, operating and ambient conditions, but for the standard capacitor, it is around 20,000 hours, operating at 85 °C [255, 257]. Others capacitors, such as discrete dry polypropylene film have a life expectancy of around 115,000 hours [257]. Capacitors in a PV inverter normally fail due to power and temperature cycling, and high internal capacitor temperature [255]. Failure due

to temperature may increase when the inverter is installed outdoors or in a microinverter application. This may lead to vaporization or leads to a catastrophic failure, which consequently could affect other components' performance. The failure of the capacitor can be estimated using (7.23):

$$\lambda_C = \lambda_{P\_base\_C} \times (\pi_T \, \pi_Q \, \pi_E \, \pi_C \pi_{SR} \pi_V) \tag{7.23}$$

The thermal factor $\pi_T$ can be expressed using (7.24):

$$\pi_T = exp\left(\frac{-0.15}{8.617\ x\ 10^{-5}}\left(\frac{1}{T+273} - \frac{1}{298}\right)\right) \tag{7.24}$$

where the $\pi_{SR}$ is the series resistance factor and it varies from 0.66 to 3.3 depending on the circuit resistance values. $\pi_V$ and $\pi_C$ are the voltage stress and capacitance factors, respectively.

$$\pi_V = \left(\frac{s}{0.6}\right)^5 + 1 \tag{7.25}$$

$$\pi_C = C^{0.09} \tag{7.26}$$

The $s$ variable represents the operating voltage over the rated voltage of the system.

#### 7.4.1.5 Failure Rate of the Fuse

The fuse is connected in a PV string as series with PV panels. **Figure 7.5** shows PV system configuration incorporating fuses. Any failure on the fuse means failure on one string, while the rest of the strings is functional. The reverse current in a string could be due to shading or a short circuit causing a failure of a string fuse. The failure of the fuse is calculated according to (7.27):

$$\lambda_F = \lambda_{P\_base\_Fuse} \times \pi_E \tag{7.27}$$

### 7.4.2 Subsystem Level II (HLII)

At this level, the failure and reliability of each subsystem, the inverter, converter, and PV string and array are modelled

#### 7.4.2.1 DC-AC Inverter

The PV inverter is the most critical subsystem in a PV power generation system - a reliable inverter leads to more energy yield. Lifetime of the central inverter is less than 15 years (e.g. SolarEdge provides a 12-year warranty) [61, 255]. The lifetime and failure of the PV inverter are affected by the ambient conditions directly and indirectly. The temperature and solar irradiation influence the thermal load directly due to the rise in the junction temperature of the power devices such as switches and capacitors. In addition, there is also indirect impact on it due to the power losses dissipated in the power devices [61, 258]. For this study, a traditional three-phase full-bridge inverter is used, with several components including diodes, IGBTs and capacitors. The inverter has series connection; thus, any failure of these components causes failure on the PV inverter and consequently, the whole of the PV system. Failure rate of an inverter can be calculated using (7.28):

$$\lambda_{Inverter} = \sum_{N} (\lambda_D + \lambda_S + \lambda_C) \tag{7.28}$$

#### 7.4.2.2 DC-DC Converter

The DC-DC converter consists of different power electronics devices and has a lifetime around 15 years [255]. A converter is normally used to implement the maximum power point tracking which is used to maximize power extraction under all conditions. The DC-DC converter is based on a multiphase traditional boost converter that consists of diodes, capacitors, inductors and MOSFETs [259]. Since the converter's components are connected with the inverter in series; the failure of one component leads to the failure on the converter, and therefore failure on the whole PV system. The failure rate of a converter can be calculated using (7.29):

$$\lambda_{Converter} = \sum_{N} (\lambda_L + \lambda_D + \lambda_S + \lambda_C) \tag{7.29}$$

#### 7.4.2.3 PV String and Array

PV panel commercial products (e.g. SunPower offers a 25-year panels warranty) [61, 255]. The PV array is made up of a number of PV modules (panels) connected in series and parallel; while the PV string consists of a number of PV modules (panels) connected in in series as shown in **Figure 7.5**. A PV panel can fail for different reasons, such as due to a short circuit, broken connections, corrosion or failure in a junction box; while a failure in a bypass diode leads the system to operate at a reduced capacity [88]. The shading effects can be represented by ambient conditions including temperature, solar irradiation, and wind speed. Increased temperature resulting from climate change mostly increases the PV panel failure rate by raising thermal stress and junction temperature of the photo diode [260] . Furthermore, other climate factors have an impact on reduction of power and are represented by the mission profile (the generation profile). The failure rate of the panel can be expressed by (7.30):

$$\lambda_P = \lambda_{P-base\_Panel} \times \pi_E \, \pi_T \tag{7.30}$$

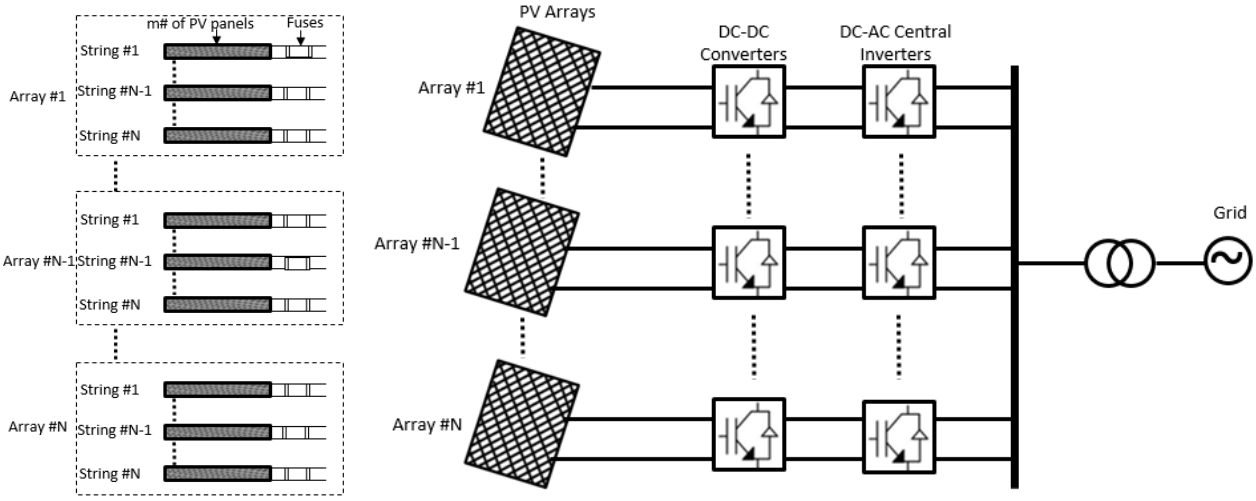


**Figure 7.5.** PV system configuration

The thermal stress of the panel can be calculated as in (**7.31)** where junction temperature $T_J$of the panel is higher than ambient temperature by 15 ºC based on [260] whereas the failure rate of the strings can occur when all PV panels have failed or a failure in the fuse.

$$\pi_T = exp\left(2790\left(\frac{1}{298} - \frac{1}{T_J + 273}\right)\right) \quad \textbf{(7.31)}$$

Otherwise, failure in n of the PV panels with at least one panel in operation does not count as a failure because the string could partially work. Therefore, the failure of m states can be calculated using (7.32):

$$\lambda_{String_m} = \lambda_F + \sum_{i}^{n} \lambda_P \quad \textbf{(7.32)}$$

where $\lambda_{String_m}$ is failure in state 1, 2,.., m-1. PV array can be in operation when one or more PV strings are in operation, while failures in all strings cause failure on the PV array. Therefore, the PV array's probability can be estimated by considering the number of strings in the array, which are estimated by forming a Markov chain model presented in section 7.4.2.4.

#### 7.4.2.4 Markov Chain Model, Availability and Reliability

The Markov chain is a stochastic model used to estimate the probability of possible states *S* being held in a transition matrix. Transition matrix gives the transitions between different states which can be used to estimate the probability of each state as in (7.33**)**:

$$S = \{1, 2, \dots, m\}Z \quad \text{for matrix} \quad m \times m \quad (7.33)$$

where $m$the is the number of states and *S* is the size of the matrix. The availability and unavailability of all components in a two-state model can be estimated using the Markov chain approach with UP and DOWN. The probability and the transition $P_{i,j}$ can be expressed as in 7.34) and 7.35), respectively

$$P = \left[P_{i,j}(t)\right] \text{ where } P_{i,j}(t) \geq 0 \quad (7.34)$$

$$\sum_{j \in S} P_{i,j}(t) = 1 \quad (7.35)$$

In [261], a Markov chain model with an obsolescence state was proposed for defining and

quantifying the lifetime and degradation rate of a component. For the study presented in this chapter, three Markov chains are proposed for the PV system components and are extended to seven states for the PV string.

**Figure 7.6** shows the schematic diagram of the Markov chain block used in the proposed approach. In this model, the transition between states can be due to a failure, repair, or degradation, where $\lambda_{ij}$ is the failure rate for a transition from state $i$ to state $j$. In the case of seven states, state one exemplifies all of the PV panels in one string being in full operation in an up state, which means that 100 % of the total number of panels are functioning, while in state six, the PV panels in that string are down, which means that 0 % of the total number of panels are working. State seven represents the end-of-life state in which the PV panels cannot be repaired and need a replacement. The final cases, from the second to the fifth state, signify derated states at different percentages ranging from 80 % to 20 %, which represent a reduction in capacity due to the failure of individual panels, (e.g., 80 % of the individual panels functioning, with 20 % having failed). On the other hand, the three states that are applied to all components except the PV panel represent up, down, and end-of-life states. The end-of-life state denotes the system at the end of its life, at which point it cannot be repaired.

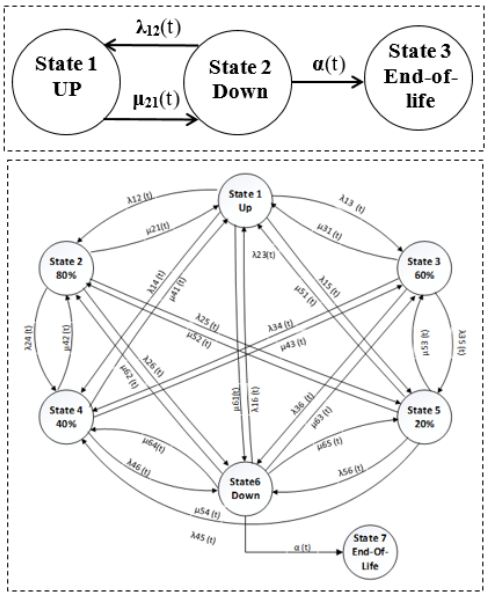


**Figure 7.6.** Markov chain model

The matrix of the three and seven states shown in **Figure 7.6** can be presented in canonical form as G=H+I where the matrix G for three states is given in (7.36) and for the seven states is given in (7.37). The end-of-life of the PV system components such as the diode, IGBT and capacitor represents the end of life for the entire subsystem, i.e., the inverter. The degradation rate is a function of time and can be estimated using the subsystem system/components' failure and lifetime as given in (7.39).

$$G_3 = \begin{bmatrix} 1-\lambda_{12} & \lambda_{12} & 0 \\ \mu_{21} & 1-\mu_{21}-\lambda_f & \lambda_f \\ 0 & 0 & 0 \end{bmatrix} \tag{7.36}$$

$$G_7 = \begin{bmatrix} A_1 & \lambda_{12} & \lambda_{13} & \lambda_{14} & \lambda_{15} & \lambda_{16} & 0 \\ \mu_{21} & A_2 & \lambda_{23} & \lambda_{24} & \lambda_{25} & \lambda 26 & 0 \\ \mu_{31} & \mu_{32} & A_3 & \lambda_{34} & \lambda_{35} & \lambda_{36} & 0 \\ \mu_{41} & \mu_{42} & \mu_{43} & A_4 & \lambda_{45} & \lambda_{46} & 0 \\ \mu_{51} & \mu_{52} & \mu_{53} & \mu_{54} & A_5 & \lambda_{56} & 0 \\ \mu_{61} & \mu_{62} & \mu_{63} & \mu_{64} & \mu_{65} & A_6 & \lambda f \\ 0 & 0 & 0 & 0 & 0 & 0 & 0 \end{bmatrix} \tag{7.37}$$

where the transition $A_i$ is expressed as

$$\begin{cases} A_1 = 1-\lambda_{12}-\lambda_{13}-\lambda_{14}-\lambda_{15}-\lambda_{16} \\ A_2 = 1-\lambda_{23}-\lambda_{24}-\lambda_{25}-\lambda_{26}-\mu_{21} \\ A_3 = 1-\lambda_{34}-\lambda_{35}-\lambda_{36}-\mu_{31}-\mu_{32} \\ A_4 = 1-\lambda_{45}-\lambda_{46}-\mu_{41}-\mu_{42}-\mu_{43} \\ A_5 = 1-\lambda_{56}-\mu_{51}-\mu_{52}-\mu_{53}-\mu_{54} \\ A_6 = 1-\lambda_f-\mu_{61}-\mu_{62}-\mu_{63}-\mu_{64}-\mu_{65} \end{cases} \tag{7.38}$$

In the case of $\lambda_f$, its value for both three states and seven states can be calculated by following the steps set out in reference [261] for solving the *G3* and *G7* matrices, as given in (7.36) and (7.37), respectively. For example, the value of $\lambda_f$ for G3 can be calculated using (7.39):

$$\lambda_f = \frac{\lambda_{12} + \mu_{21}}{Lifetime \times \lambda_{12} - 1} \tag{7.39}$$

The $G_3$and $G_7$ matrices can be employed for defining the system state probability vector for the 3-state $G_3$ components, subsystem, and system, and for the 7-state $G_7$ string/array as in (7.40) [261]:

$$\overline{P(t)} = \sum_{i=1}^{n} C_i \, \overline{V_i} e^{V_i t} \tag{7.40}$$

where $V$ and $\bar{V}$ are the eigenvalues and eigenvector of matrix $G$; while $C$ represents the constant values of the initial conditions. For the n-state Markov chain, the probabilities of all n-states are expressed as in (7.41):

$$\begin{aligned} P_1(t) &= C_1\overline{V_{11}}e^{V_1 t} + C_2\overline{V_{12}}e^{V_2 t} + \ldots + C_n\overline{V_{1n}}e^{V_n t} \\ P_2(t) &= C_1\overline{V_{21}}e^{V_1 t} + C_2\overline{V_{22}}e^{V_2 t} + \ldots + C_n\overline{V_n}e^{V_n t} \\ &\vdots \qquad\quad \vdots \qquad\quad \vdots \qquad\quad \vdots \\ P_n(t) &= C_1\overline{V_{n1}}e^{V_1 t} + C_2\overline{V_{n2}}e^{V_2 t} + \ldots + C_n\overline{V_{nn}}e^{V_n t} \end{aligned} \tag{7.41}$$

Therefore, the availability $A_i$ can be represented by operational states which include a derated state and unavailability $U_i$ can be represented by a non-operational state; $i$ denotes the components and subsystem.

$$A_i(t) = \sum_{i \in operational\ state} P_i\,(t) \tag{7.42}$$

$$U_i(t) = \sum_{i \in non-operational\ state} P_i\,(t) \tag{7.43}$$

The main steps of the proposed Markov Chain approach can be summarized as follows:

**Step1.** Design $m \times m$ matrix where m is number of states as in equation (**7.33**) and 7.35) accounting for the number of components, states and all relevant parameters.

**Step2.** Incorporate climate change effect for different years and emission scenarios by modelling the effect of thermal stress on the failure rate as in (7.11) - (7.31).

**Step3.** Build a state diagram using the transitions between states; the transitions are formulated in terms of failure rate (λ) and repair rate (μ) of the components as in (7.36) and (7.37).

**Step4.** Construct a transition matrix based on step 1. The dimension of the Markov Chain is m ×m. In this study m= 7 and 3 (two Markov models) while the transition rate goes into the ith row and jth column of the built matrix.

**Step5**. Define the system state probability vector using eigenvalues and eigenvector of matrices as in (7.40).

**Step6**. Calculate probabilities of all n-states matrices as in (7.41), to calculate the availability and unavailability of the system.

**Step7.** Calculate the availability and unavailability of the system. Availability is characterized by operational states which include de-rated states. Unavailability is characterized by a non-operational state as in (7.42) and (7.43).

#### 7.4.2.5 Scalability of the Proposed Seven state Markov-Chain Model

Real PV systems may involve a large number of individual panels and therefore the framework should be scalable. In the proposed framework, rather than modelling the state of each panel, the Markov chain model is constructed with each state reflecting a percentage of the total panels currently in that state. For instance, at state 1 (UP) and 6 (DOWN), 100% and 0% of PV panels are working, respectively. The de-rated states represent a reduction in capacity due to failure of individual panels, (e.g., 80% of the individual panels are in function where 20% have failed) leading to a reduction in the capacity. The de-rated states are based on the average failure rate of the PV panel in addition the effect of climate on failure as in (7.30).
The main advantage of this method is the scalability which can be applied for both large and small PV systems. By using a percentage, the model is agnostic to the number of PV panels allowing the analysis to be easily scalable. Therefore, the application of this approach with a real PV system consisting of many panels is feasible. However, for large PV systems, the integration with the system could be limited by the capacity of the point of interconnection.

### 7.4.3 System Level III (HLIII)

In system level III, the reliability of the PV system is evaluated by taking into account both levels HLI and HLII. A failure of a PV array, inverter, or converter leads to a failure in the whole PV system, although a failure on the PV string can cause a reduction in the

availability of the PV array capacity and the PV system output. The total system reliability can be estimated using (7.44):

$$R_{system} = \sum_{i=1}^{n} R_i \tag{7.44}$$

where $R_i$ is the reliability of the subsystem. Therefore, the availability and unavailability of the PV system can be calculated using (7.45) and (7.46), respectively:

$$A_{systen}(t) = \sum_{i \in} A_i(t) \tag{7.45}$$

$$U_{system}(t) = \sum_{i \in} U_i(t) \tag{7.46}$$

## 7.4.4 Grid Level IV (HLIV)

### 7.4.4.1 Power Generation Model

In this level, the hierarchical levels of HLI, HLII, HLIII and HLIV are considered with the mission profile of the PV system reflecting ambient conditions including air temperature, solar irradiation and wind speed. The PV power generation model in [231] was developed using the cell temperature as in [262] to consider the PV system ambient condition. The developed model of the mission profile calculates the output power $P_{pv}$ and the efficiency $Eff_{pv}$ based on the solar irradiation level, where the temperature and wind speed are incorporated as in (7.47):

$$P_{pv} = \begin{cases} \sum_{t=0}^{t=period} \frac{P_{STC}\ {G_{bi}}^2}{R_c\ x\ G_{STC}} \left(1 - \frac{\delta}{100}\ (T_{STC} - T_{cell}\right) & 0 \leq\ G_{bi} < R_c \\ \sum_{t=0}^{t=period} \frac{P_{STC}\ G_{bi}}{G_{STC}} \left(1 - \frac{\delta}{100}\ (T_{STC} - T_{cell}\right) & R_c \leq\ G_{bi} <\ G_{STC} \end{cases} \tag{7.47}$$

$$Eff_{pv} = \begin{cases} \frac{\eta_c}{R_c}\ G_{bi} \left(1 - \frac{\delta}{100}\ (T_{STC} - T_{cell}\right) & 0 \leq\ G_{bi} < R_c \\ \eta_c\ x\ \left(1 - \frac{\delta}{100}\ (T_{STC} - T_{cell}\right) & R_c \leq\ G_{bi} \end{cases} \tag{7.48}$$

$$T_{cell} = G\ x\ (e^{a+b\ x\ V_{Wind}}) + T_{amb} \quad (7.49)$$

where $R_c$ is a irradiation point set as *150 W/m²*; and $G_{bi}$ is global solar irradiation in *W/m²*; $T_{cell}$ , $T_{amb}$ and $T_{STC}$ are PV cell temperature, ambient temperature and standard test condition temperature at 25 °C, respectively; $P_{STC}$ is the rated power of the PV power and $\delta$ and $\eta_c$ are temperature coefficient and the rated efficiency of the PV cell. A sample of the mission profile is presented in **Figure 7.7**. It can be clearly seen that the change in power generation for different $CO_2$ emission scenarios is due to change in weather conditions. For instance, under low emission scenarios, the power level is high especially in the summer while in the high emission scenario the power level is low, especially in the winter.

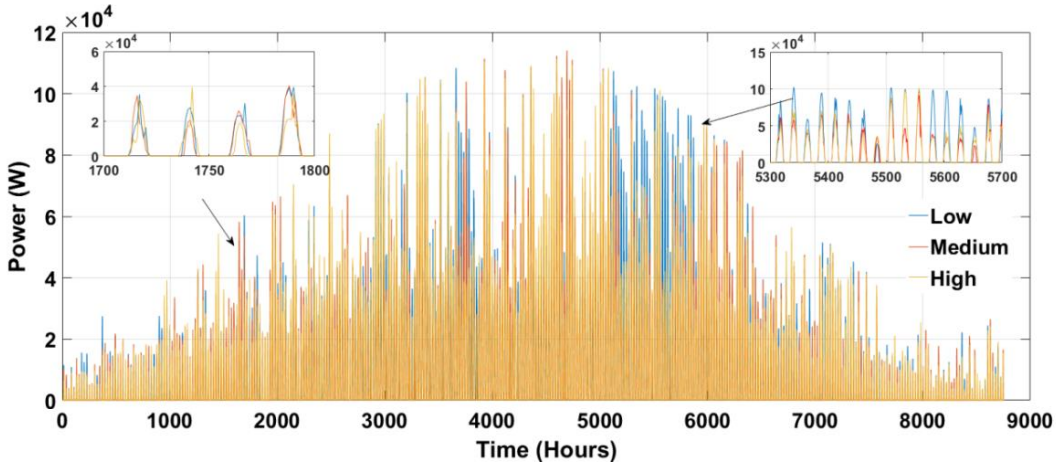


**Figure 7.7.** Mission profile for the year 2080

### 7.4.4.2 Reliability Evaluation

Monte Carlo simulation (MCS) uses a sampling process to obtain numerical results by simulating the system behaviour using a statistical approach. Therefore, in this study, MCS is applied in the reliability assessment considering expected energy not served (EENS) as the metric of impact on the system [22]. MATLAB-DIgSILENT integrated platform has been used to implement the proposed reliability evaluation framework. MATLAB is used to model the availability, failure rates, thermal stress, aging and Markov Chain of the components. The

Markov chain probabilities in MATLAB are fed into DIgSILENT with muti-state stochastic power generation model for the reliability evaluation of the entire system. The following steps are required to accomplish the proposed reliability evaluation framework:

***Step1.*** Generate the mission profile for the PV system considering timescale and emission scenarios using (7.47) which incorporates the ambient temperature, solar irradiation and wind speed.

***Step2.*** Determine the impact of the ambient condition and thermal stress factors on the failure rates of the PV system components using (7.11) to (7.30).

***Step3***. Employ the bathtub curve to the components considering both useful life and wear out stages using (7) to (10).

***Step4.*** Apply Markov chain model with obsolescence state to determine the probabilities of the components, subsystems and PV arrays using (7.32) to (7.42), as stated previously. The output of these steps is fed into the DIgSIlENT platform for the next steps.

***Step5.*** Model the power system considering failure-repair rates of power system components and define load demand by classifying them as agricultural, domestic, commercial or industrial as relevant

***Step6.*** Integrate PV system model into power system with multi-state stochastic power generation model and define the PV availabilities and mission profiles for different scenarios as indicated previously.

***Step7***. Perform load flow analysis and initialise the power balance within voltage limits at buses and thermal limits of lines during the simulation.

***Step8.*** Run Monte Carlo simulation and in the events of load shedding, apply the optimum power flow to curtail the minimum load and then to calculate the reliability index at a sample in the MCS. EENS in MWh/y is used as the metric of impact on the system. ENS (energy not served) can be estimated using (7.50) and(7.51) [22]:

$$EDNS = \sum_{i \in S_i} C_i \times P_i \tag{7.50}$$

$$EENS = \sum_{i \in S_i} C_i \times P_i \times 24 \times 365 \tag{7.51}$$

$EDNS$ is Expected Demand Not Supplied in MW, where $C_i$ is the load curtailment in system state $i$, $P_i$ is the system state probability and $S$ is the set of all system states associated with load curtailment.

## 7.5 Case Studies

A PV farm with a capacity of 1 MW (10 PV systems 100 kW each) is simulated to investigate the impact of climate change. The climate change was simulated considering Birmingham, UK weather at the location of latitude 52.4862 N and longitude -1.8904 W. The Roy Billinton Test System (RBTS) was used for the case studies due to the unavailability of the power system data of Birmingham [245]. The RBTS contains six buses, eleven generating units with a total installed capacity of 240 MW and peak load of 185 MW. **Figure 7.8** shows the single line diagram of RBTS with a PV system connected at Bus 2 and 3. The base failure rates for the components in the PV system are given in **Table 7.1** [83], [88], [87], [260] and the stress factors are listed in **Table 7.2** [90], [260]. Some of the stress factors vary based on the equations indicated.

**Table 7.1.** Components Reliability Data

| Components | | $\lambda$ (1/y) | | | $\mu$ (1/y) |
|---|---|---|---|---|---|
| | | $\delta$ | $a$ | η | |
| Diode | | 0.025 | 0.015 | 32 | 18.75 |
| Switch | IGBT | 0.030 | 0.027 | 28 | 20 |
| | MOSFET | 0.0023 | 0.021 | 35 | 20 |
| Coil | | 0.0015 | 0.008 | 35 | 17.92 |
| Capacitor | | 0.013 | 0.015 | 19 | 26.071 |
| Fuse | | 0.0042 | 0.007 | 17 | 52.143 |
| PV panel | | 0.0018 | 0.007 | 25 | 48 |

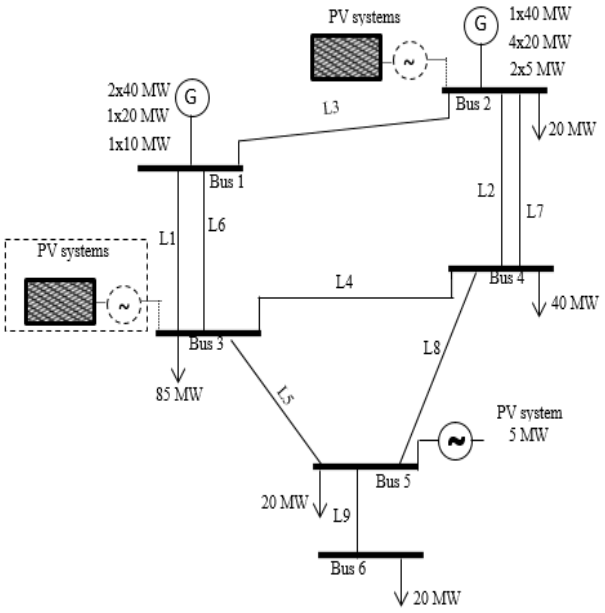


**Figure 7.8.** Single line diagram of the adapted RBTS integrated PV system

**Table 7.2.** Component Stress's Factors

| Component | $\pi_T$ | $\pi_E$ | $\pi_Q$ | $\pi_C$ | $\pi_v$ | $\pi_A$ | $\pi_{SR}$ |
|---|---|---|---|---|---|---|---|
| Diode | Eq.(7.14) | 1 | 5.5 | 1 | Eq.(7.13) | × | × |
| Switch | Eq.(7.16) | 1 | 5.5 | × | × | 10 | × |
| Coil | Eq.(7.21) | 1 | 3 | × | × | × | × |
| Capacity | Eq.(7.15) | 1 | 10 | Eq.(7.26) | Eq.7.25) | | 1.1 |
| Panel | Eq.(7.31) | 1 | × | × | × | × | × |
| Fuse | × | 1 | × | × | × | × | × |

### 7.5.1 Reliability of the PV Components, Subsystem, and System

**Figure 7.9** (a) gives the estimated reliability performance for the component level HLI and the subsystem level HLII is given in **Figure 7.9** (b), (c), and (d); while system level HLIII is given in **Figure 7.9** (e) and (f). Reliability of the component level in **Figure 7.9** (a) implies that the unavailability of the capacitor and switches is significantly larger than other components. Consequently, it is reflected in at the failure of the subsystem level (power converter). The DC-DC converter is more reliable than the DC-AC inverter as illustrated in

**Figure 7.9** (b). This is due to the high stress of the IGBT and the inverter topology consisting of six IGBTs, which cause a higher forced outage rate (FOR). Accordingly, the inverter has lesser lifetime by one year than the converter as noticed in **Figure 7.9** (c). This also indicates that the DC-DC system components have lesser stress than the DC-AC power components. The PV array is the most reliable subsystem level as suggested in **Figure 7.9** (d). This is because there is a bypass diode on the PV panel and string which can reduce the output rather than causing an outage on the entire string. It can be observed that the PV array maintains consistent reliable and then it sharply decreases after 15 years due to the aging.

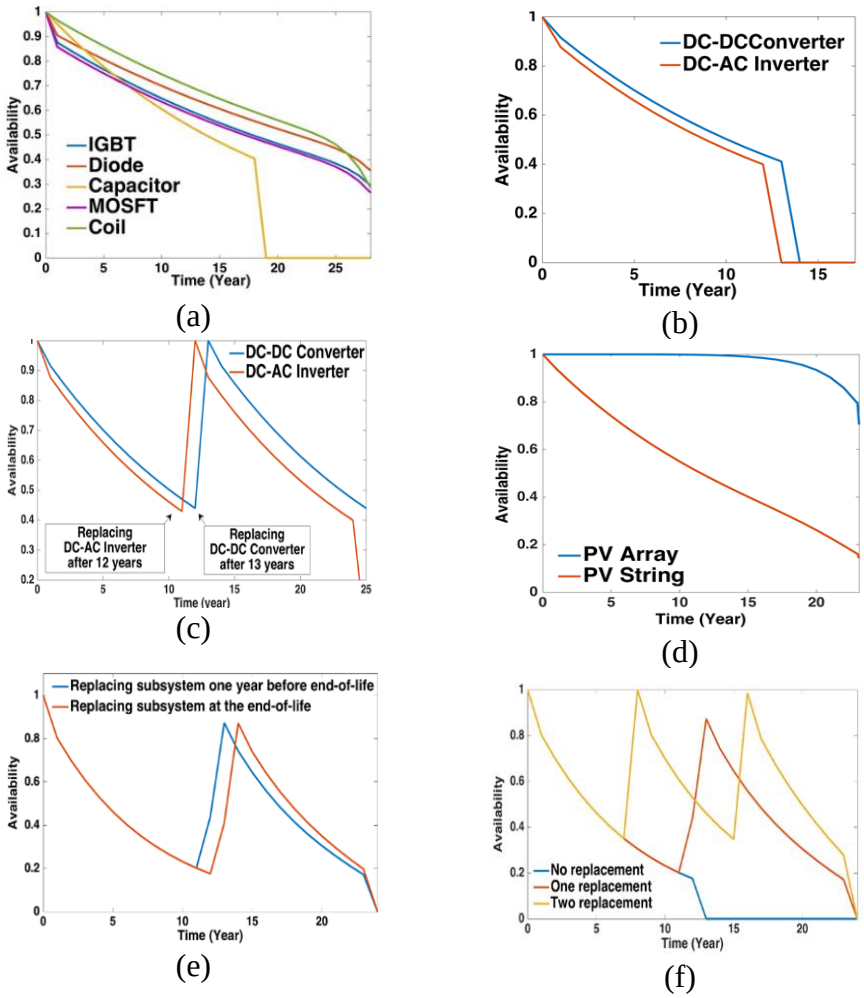


**Figure 7.9.** Unavailability with respect to (a) the components level, (b) the inverter and converter subsystem level, (c) the replacement of the power electronic subsystem, (d) the array and string subsystem level, (e) the PV system with the replacement of one subsystem, and (f) two replacements

The unavailability of the system level is given in **Figure 7.9** (e) for a single PV system at two different years: subsystem replacement at the end-of-life and one year before. Replacing the inverter and converter one year before the end-of-life could improve the entire PV system's availability by 6%. However, replacing the inverter and converter twice as in **Figure 7.9** (f) at 7 years and 14 years can significantly improve the reliability of the system, although the cost of the power electronics could be high. Based on the reliability evaluation of HLI, HLII, and HLIII, higher failure is shown in the subsystem level due to higher failures in individual components.

### 7.5.2 PV System Sensitivity and Availability/Reliability for Different Temperatures

The reliability analyses of HLI, HLII and HLIII levels are conducted for different temperatures to obtain the sensitivity of them. In the sensitivity analysis, it is assumed that the power electronics including the inverter and converter are located outdoors and are sensitive to the ambient conditions. The ambient temperature is assumed to vary between 20 $^{o}$C and 50 $^{o}$C, while in the temperatures below 20 $^{o}$C the change is considered as very small. The temperature has a direct impact on the junction temperature of the IGBT, diode, MOSFET and capacitor; while solar irradiation has an indirect impact through the input power, causing a power loss and therefore increases the junction and core temperature. The sensitivity analyses' results are depicted in **Figure 7.10.** In fact, the change in reliability in this case is only due to uncertainties of the ambient conditions while the degradation on the components due to aging is neglected. The stress in the HLI level for critical components is given in **Figure 7.10** (a) for the diode, (b) for the IGBT, and (c) for the capacitor. It can be observed that the decrease in availability of the components varies from 1% to 5.5 % due to the thermal stress leading to a higher FOR. It observed that the capacitor could be the most sensitive PV components and this is due to the

fact that rise in thermal temperature leads to a reduction in capacitance, and therefore increasing voltage and current ripples cause increasing core temperatures. The ripple current increase the internal temperature and thus causes a reduction in the availability of the capacitor thereby the overall reliability of the converter. This emphasises the robustness required in the capacitor designed and the appropriateness of applying remedial actions in the events of stress on the capacitor.

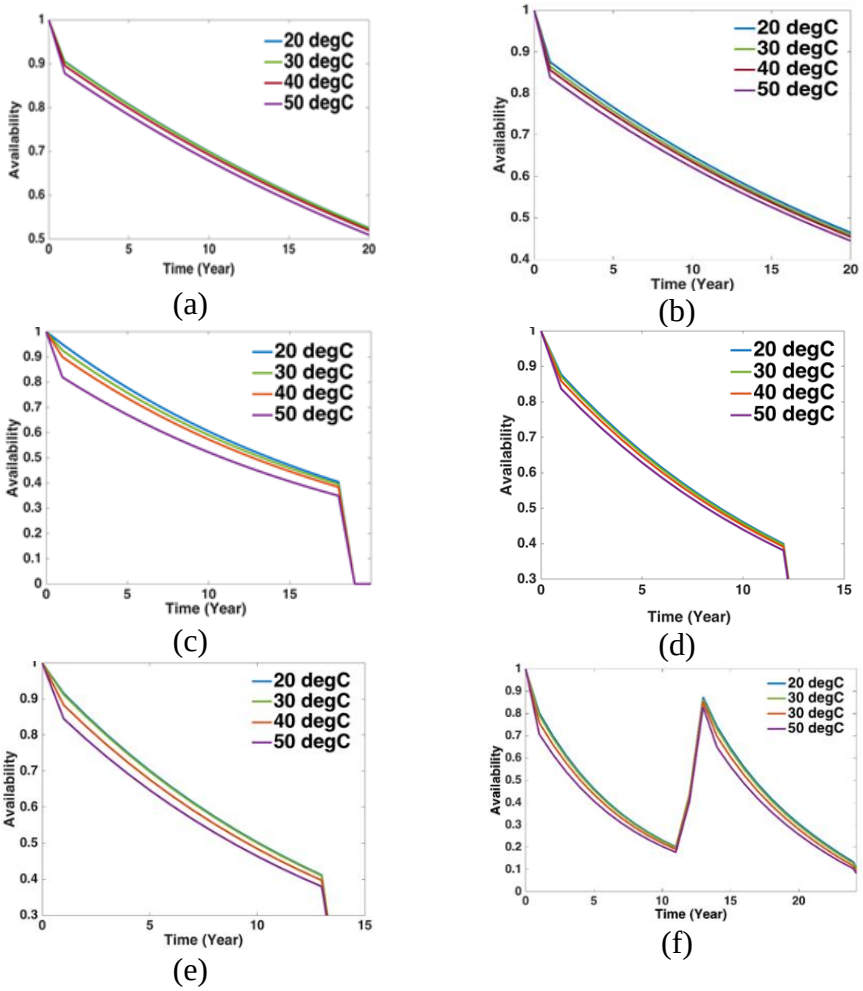


**Figure 7.10**. Sensitivity analyses of different temperatures for: (a) diode; (b) IGBT; (c) capacitor; (d) DC-AC inverter; (e) DC-DC converter and (f) PV system

Furthermore, the inverter and converter consist of a number of complex components, failure of any of the components causes failure in the entire inverter or converter and consequently in the entire PV system. This can be noticed in **Figure 7.10 (**d) DC-AC inverter

and (e) DC-DC converter. The influence of the temperature-related stress on the DC-DC converter is higher due to the numbers of capacitors in the converter are more than the inverter. In a comparison of the subsystem, the converter is more reliable than the inverter but it is also more sensitive to ambient temperature. Finally, the reliability reduction due to an ambient temperature of HLIII level (PV system) is illustrated in **Figure 7.10** (f). With increasing the temperature, the FOR increases, causing a reduction in the availability of the PV system. The sensitivity analyses of the availability of PV system components is quite minor for the temperatures 20 $^{o}$C and 30 $^{o}$C, but the availability threshold decreases when the temperature reaches 44 $^{o}$C and higher. Although this study suggests that impact of temperature-related stress can affect the reliability of components, the effect of the temperature-related stress on the lifetime of the components is a vital part to be studied.

Despite some uncertainties, there remains a high degree of confidence in the occurrence of climate change due to the global warming and the continue emissions of greenhouse gases. The simulation results shown in **Figure 7.9** and **Figure 7.10** are based on high-resolution RCM and GCM data: 5 km for UKCP09 and 12 km for EURO-CORDEX, resolutions that reinforce confidence in the results for comprehensive assessment . It should also be noted that the level of confidence might differ for other climate change models, which could result from minor changes due to discrepancies with respect to resolution and the type of climate model.

### 7.5.3 PV-Integrated RBTS System

#### 7.5.3.1 Base and Emissions' Scenarios without Considering PV System Availability

In this case, the reliability studies are performed for the integrated PV system in RBTS, applying the climate change model to the PV power generation model. The influence is then captured through the MCS to estimate the EENS. Therefore, a comparison of EENS of the base case (without integrating the PV system) and integrated PV system for the years 2020, 2050

and 2080 is presented in this case. In this case different $CO_2$ emission scenarios from climate change were considered despite the fact that the failures rates of the components are ignored to investigate the effect of climate change on entire PV system with neglecting degradation and aging. In other words, the PV system is assumed to be fully available such a new installation. Therefore, any change in the reliability index of the EENS compared to the base case and other cases is due to the climate change impact the PV input (mission profile). In the base case, the EENS of the power system is 16249.8 MWh/y. The base case provides a reference for comparison with other cases.

**Figure 7.11** corresponds the reliability index of the EENS as a function of time for the integrated PV system over different $CO_2$ emission scenarios. It can be noticed that the EENS decreased compared with the base case for the years 2020, 2050 and 2080 due to integration of the PV system. The reduction in reliability improvement over time is due to the fact that the power flow pattern of the PV system is affected by changing of temperature, solar insulation and wind speed, these changes are due to the emission of GHG. Consequently, the reliability decreases with time in medium and high emission scenarios; while the low emission scenario is less sensitive to climate and therefore reduction in reliability improvement is less compared with the other two scenarios. High emission scenarios suffer from a significant increase in EENS, especially in the year 2080 as a result of changes in weather conditions and high emissions of $CO_2$.

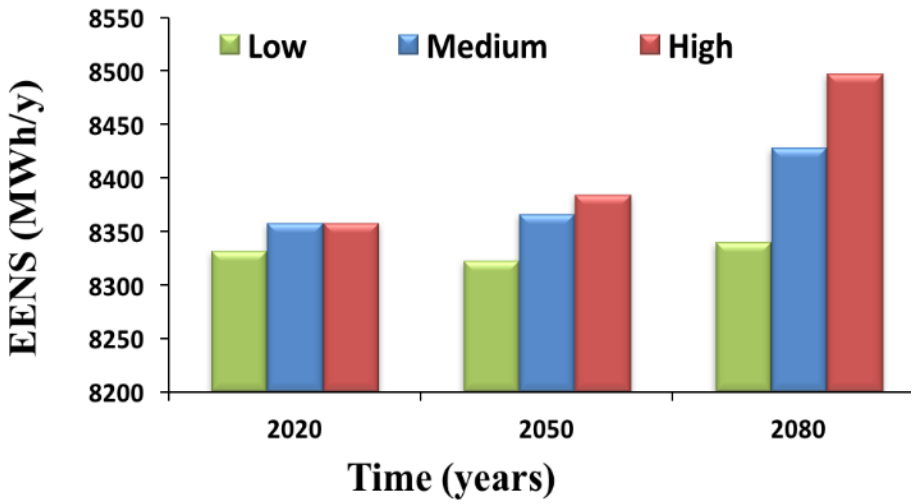


**Figure 7.11.** EENS for the PV system for different emission scenarios without PV system components' failure

#### 7.5.3.2 Consideration of PV Systems under Different Emission Scenarios for 2020, 2050, and 2080 vis-à-vis the Reliability of the Components

This case represents the HLIV level, investigating the reliability of the integrated PV system considering both the climate change model and the reliability models (HLI, HLII, and HLIII). Because temperature, solar irradiation, and wind speed climate variables are all considered at the hourly level, in this case, the temperature cycles was considered. First, the average availability of the PV system for different emission scenarios was obtained. Climate models of different emission scenarios were then applied to the mission profile of the PV power generation model. Subsequently, the influences of both are quantified through Monte Carlo simulation to estimate EENS. Broader set of input parameters are required for the long-term strategic assessment.

**Figure 7.12** illustrates the EENS the PV system for different emission scenarios and average PV system availability for the years 2020, 2050 and 2080. All scenarios suffer from a significant increase in EENS with time from 2020 through 2050 toward 2080 due to the act that GHGs emission increase with all emission scanrio causing a change in climate. Also, there is a substantial reduction in reliability as the $CO_2$ emission scenario increases from low to high.

The increase in EENS is mainly due to increases in temperature and the ambient condition which compound the impact on both the mission profile and the availability of the PV system causing a reduction in overall reliability.

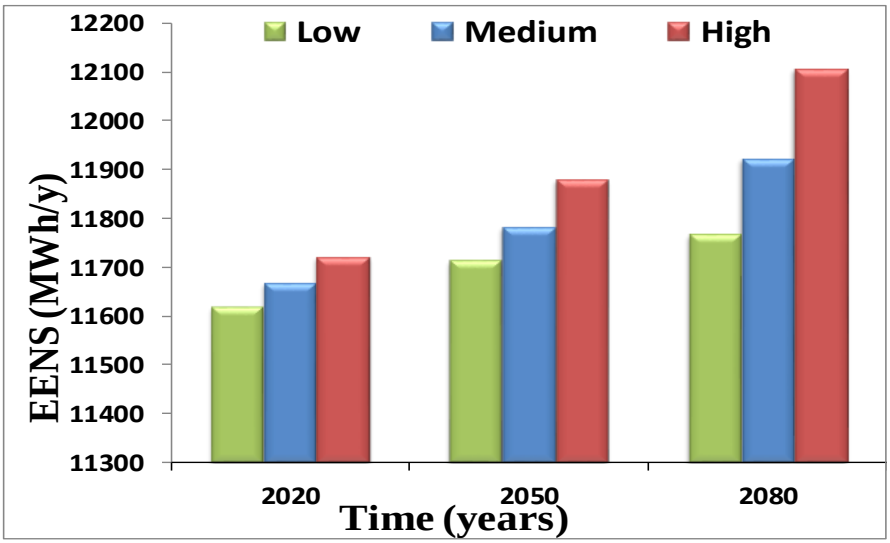


**Figure 7.12.** EENS values for the PV system for different emission scenarios considering PV system's availability

Compared with the results in **Figure 7.11** and **Figure 7.12,** the results in **Figure 7.13** depict that a change in the EENS values for the PV system, with and without PV system components' availability. The changes in EENS varies between 39% and 42.5%, which is due to the reduction in the system's reliability. For instance, in the high emission scenario in the year 2080, the increase in EENS is the highest at 42.5%; while in the year 2020 in the same emission scenario it is 40 %, making a difference as high as 2.5% due to the GHG emission over years. Therefore, reduction in the availability of the PV system is due to the increase in ambient temperature and therefore increase in thermal stress.

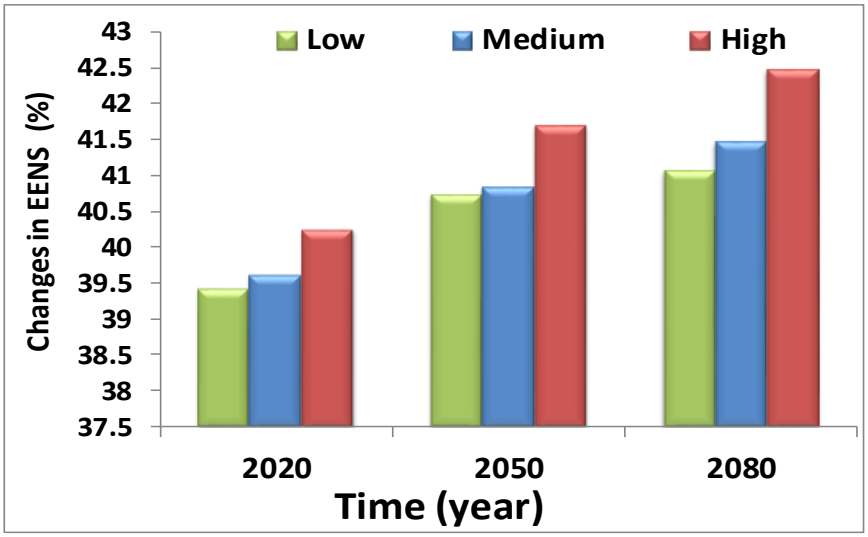


**Figure 7.13**. Changes in the EENS values for the PV system with and without consideration of PV system availability

#### 7.5.3.3 Reliability Analyses Considering System Availability and Aging

This case presents the reliability performance of the HLIV level integrated PV generation incorporating availability and aging of the HLI, HLII and HLIII levels. In this case, the PV systems are assumed to be installed and replaced three times during this century, i.e. installed in 2020 and replaced in 2045 and 2070, respectively. **Figure 7.14** shows EENS for the three PV systems installed at different times considering climate change, availability and aging. In this case, only the low emission scenario is presented. It can be perceived that the EENS is inconsistent with time. This is mainly due to the degradation of aging of the components, i.e. the highest EENS is in year 2044. The main reason for that is the failure rate increases due to combination of climate related effect, aging and degradation over years till the end-of-life of the PV system, which is after 24 years of installation; this means a increment repair rate is required over years to maintain the availability of the components. However, in 2020 and 2070, the EENS is expected to be the lowest (8000 MWh/y), as the degradation rate is zero and the availability of the PV system is high (new installation). The performance PV components, subsystem and system as a function of time towards the end-of-life are vulnerable and sensitive to the aging and degradation. Nevertheless, the impacts are inconsistent with time

when climate change, availability and aging is considered over the long run. This is mainly due to the new replacement of the PV system from 2020 through 2050 toward 2080.

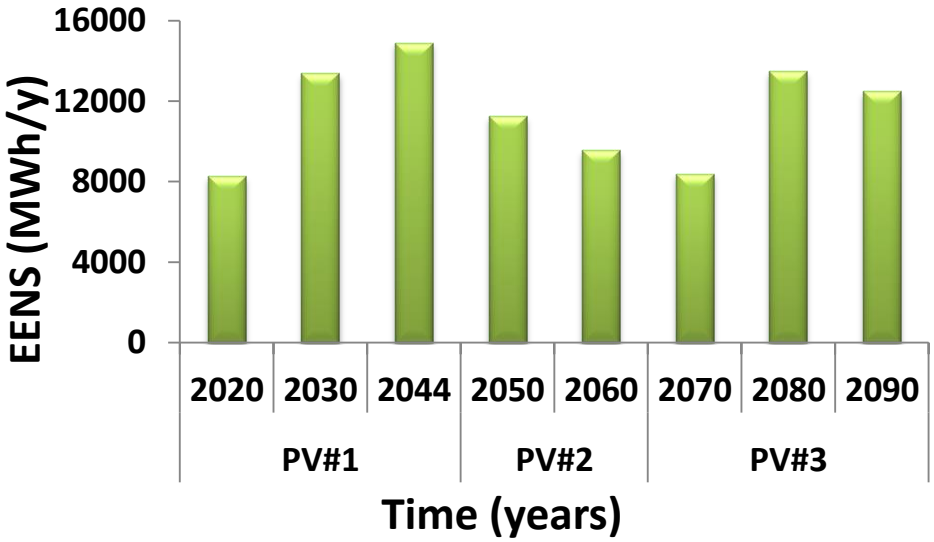


**Figure 7.14.** EENS for the three PV systems considering climate change, availability and aging

#### 7.5.3.4 Reliability and Sensitivity Analyses at Different Temperature Levels

**Figure 7.15** shows the change in availability when only variations of temperature are applied to the PV system, using 30 $^{o}$C as a reference. The results indicate that the change in the availability of the PV system increases with temperature increases. Because the temperatures that were considered in this study were at a constant level, temperature cycles were neglected. However, the changes that occur between temperatures of 20 $^{o}$C and 30 $^{o}$C are quite small, although the amount of change increases noticeably as the temperature rises toward and above 50 $^{o}$C. These parameters were applied to the PV system with the solar irradiation kept constant in order to explore the impact of temperature on the EENS value. **Figure 7.16** illustrates the change in reliability for different temperatures and constant solar irradiation when 30 $^{o}$C is set as a reference. The EENS is slightly decrease at a temperature of 20 $^{o}$C compared to the reference of 30 $^{o}$C. However, the EENS slightly increase for a temperature of 40 $^{o}$C, then decreases sharply at a temperature of 50 $^{o}$C. This effect is attributable to the fact that the

component and subsystem failure rate increases as a result of the increase in the temperature of the junction and in the core temperatures of the diode, IGBT, coil and capacitor, all of which lead to a reduction in reliability. The reliability modelling framework can be further extended by including other power system components at the connection points, including at the connecting point of transformer and the relevant circuit breakers.

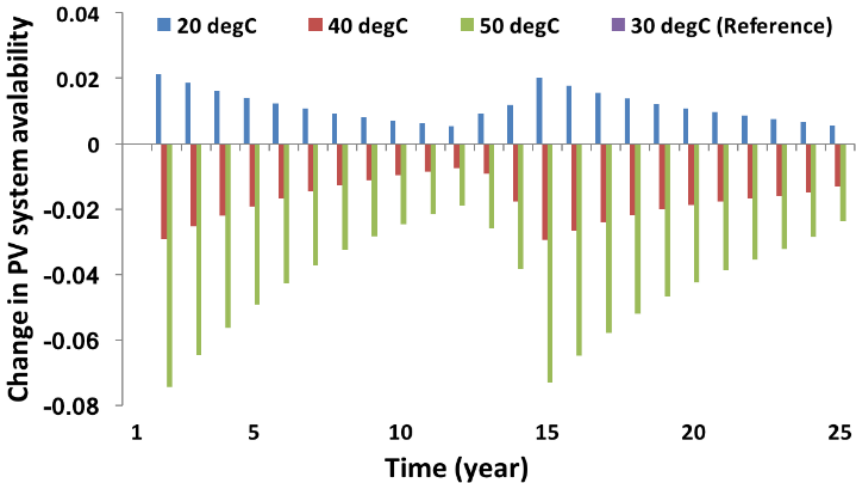


**Figure 7.15.** Change in PV system availability at different temperature level when 30 ºC set as a reference

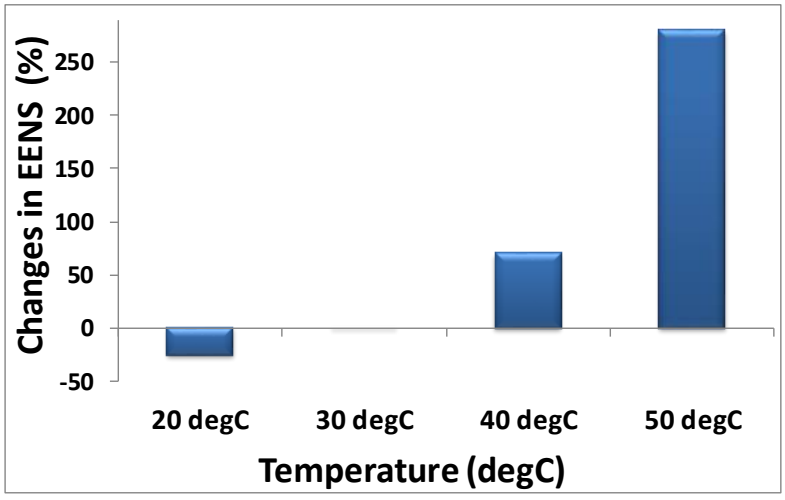


**Figure 7.16.** Changes in the EENS at different temperature levels when 30 ºC was set as a reference

## 7.6 Summary

An innovative framework for assessing the impact of the reliability for PV integrated power systems considering the long-term climate change effects on hierarchical level of PV systems

was presented in this chapter. The proposed framework capable of analysing the climate impacts on hierarchical level of PV systems. To evaluate the system reliability, an innovative analytical methodology to assess the climate impact on hierarchical levels in the PV systems including components in a PV system, subsystems in a PV system, whole PV system, and the power grid level is presented. Two different climate models were incorporated in climate simulation and the case study is carried out on the Roy Bilinton Test System (RBTS) to simulate the impact climate on the hierarchical level of PV systems.

Overall results suggest that the reliability performance of a power system with integrated PV systems can potentially be affected by climate change and the effects are noticeable over the long run. The high emission scenario with the year 2080 presents the worst impact on availability of the PV system components due to high level of GHG emission and subsequently resulting increased level of EENS. The IGBTs and capacitors are identified as critical components in a PV system that impact the reliability performance of a PV system mostly and they are sensitive to thermal stresses of climate change effects. Results further suggests that the reliability of a PV integrated power system decreases due to impacts of climate change in long-term however, the decrements are inconsistent due to lifetime and aging effects of macro level components in the PV system. The proposed approach can be used for the power system preventive maintenance planning applications with the aim of reducing impacts on a PV system integrated power system. The findings reported from results shed new light to the identification of critical components and subsystems within a PV system that lead to climate-associated failure. The proposed framework can offer a way of mitigating the impact of climate change on PV systems through proactive design and the application of maintenance strategies for averting progressive component failures initiated by the effects of climate change.

# Chapter 8: Conclusions and Future Work

## 8.1 General Overview

Growing concerns over the climate change are resulting in a rise in penetration of renewable power generation as a mitigating factor. PV and wind power generation systems are subject to impacts from future climate changes with potential implications on the reliability and performance of a power system. Foregoing the above, this thesis was aimed at providing insight into the future climate change impact on the wind power generation system and hierarchy levels of a PV system, and to assess power systems reliability resulting from impacted PV and wind power generation system. In achieving the aim, this thesis presents comprehensive methodologies to assess the reliability of a RE integrated power system by considering future climate change models and PV and wind power generation systems availability.

## 8.2 Conclusions

### 8.2.1 Climate Change Impact on Integrated PV System Reliability

PV power generation is dependent on weather and climate, this dependency could affect their availability. Therefore, a novel framework for assessing the impact of climate change and aging on a large-scale PV-integrated system over the long term is proposed in chapter 4. Investigations suggest that decentralized PV systems could substantially improve system reliability compared to that of the centralized PV system. The low emission scenario based GHGs significantly enhances reliability performance of both centralized and decentralized PV systems compared to the medium and high emission scenario. The reliability improvement degrades proportionally with increased GHG emissions, mainly CO2, because the power flow

pattern of the PV system is affected by the uncertainty associated with shifts in weather pattern mainly solar insolation, ambient temperature and cloud cover. The increase in temperature and decrease in solar irradiations resulted in an overall decrease in photovoltaic systems and therefore in power system reliability. Accordingly, it is expected that the declines in reliability of the system take place for all three emission scenarios and is expected to become more severe at high emission scenario. These findings provide an understanding of the future climate effects on the reliability PV integrated power system over three possible emission scenarios.

It was also found that the reliability performance of the system decreases correspondingly with time and the decrement in 2080 is expected to be the worst. This is mainly due to cumulative GHGs emission over time causing variation in climate variables and weather patterns. Although both the climate change and aging have an adverse impact, the impacts are inconsistent with time; however, establishing the reliability of PV-integrated power systems could be challenging. This also highlights the need of climate change effect consideration during PV integration and during the overall system planning. Further it enables power system planners and operators to quantify the potential impacts of future climate change and develop relevant strategies to mitigate the impact on integrated PV systems.

### 8.2.2 Climate Change Impact on Wind Farm Integrated Power System Reliability

Wind energy could potentially be vulnerable to climate change as it reliant on prevailing weather and climate conditions such as wind speed, which are prone to be impacted by climate change. A comprehensive reliability assessment to investigate the long-term effects of climate change on WF-integrated power systems is proposed in chapter 5. The key findings of the assessment suggest that climate change would potentially have a considerable impact on power

system reliability with the presence of wind farm. The impacts are considerable for RCP8.5 emission scenario for the year 2080, where the EENS value sharply increases due to climatic conditions, mainly the wind speed which characterized by increased CO2 emissions over the long run. However, the RCP2.6 scenario also involves a sharp variation in GHG-based CO2 emissions, which might adversely affect wind speed at the selected location, leading to a reduction in output power generation and a further decline in reliability compared with the RCP4.5 scenario. The effects of wind speed depend on GHGs and other climate related factors including geographic location and land-sea thermal gradient.

Accordingly, the power system reliability with wind farm integration is noticeably affected by the significant variations in GHGs in long-term whereas the RCP4.5 scenario is likely to be less impacted as wind speed pattern might not be greatly affected by climate change and therefore improvement on the entire system reliability. It can be concluded that, RCP4.5 scenario is more favourable over long-term compared to the RCP2.6 and RCP8.5 scenarios due to their adverse impact on the system reliability. The climate change needs to be adapted on safety borders in the design and operation of wind turbines. The result also show that a significant amount of wind power generation system is required to maintain the reliability of the system with removing 10% of thermal power generation. This is mainly due to the effects of the intermittent nature of wind power generation system on the geographic location. The assessment results help to understand the performance with WF integration against climate change over long run. The implications of adverse impact of climate change should be integrated and reflected into policies and planning for adaptation strategies to mitigate the possible effect of climate change.

### 8.2.3 Stochastic Future Climate Scenario Based GHG on the Reliability PV and wind power generation

Recognising that climate change may have impact into the future of power system reliability with PV and wind energy integration, its impact toward the reliability varies based on the diverse future GHGs emission scenario. Hence, a stochastic model for generating future climate scenarios to assess their impact on reliability of power systems with PV and WF power integration is developed in chapter 6. The methods offer a new set of future scenarios to be used in assessment based on the current and future GHGs emission.

Two sets of future scenarios were generated as ‘very likely’ and ‘reasonably likely’ probabilities of the occurrence of low, medium, and high emission scenarios. The generated ‘very likely’ scenario is more sensitive to the effects of climate change than ‘reasonably likely’ scenario, and therefore a greater impact is expected. The sensitivity referred to high-emission scenario as it has the greatest probability of occurrence within the ‘very likely’ scenario. This scenario is expected to have a greater impact in weather patterns of including wind speed, ambient temperature and solar irradiation. The reliability performance decreases proportionally with time for both scenarios as a result of higher CO2 emission. The output power of the PV and wind power model is therefore reduced, resulting in an inferior reliability performance for the entire system. Increasing the penetration of the PV and wind generation with same capacity potentially improves the EENS, although the enhancement of the EENS is less with additional PV power than with additional wind power. This indicates that the system is rendered more resilient with larger increments of wind power because higher capacity is required from the PV systems in order to maintain the improved EENS levels.

The findings of these results suggest that in an integrated power system, PV systems are more vulnerable to future climate model parameters than with wind energy systems. Right

strategy for energy mix considering climate effect on penetration of wind and PV energy would lead to substantial reliability improvement in a power system.

### 8.2.4 Sensitivity, Availability and Reliability of PV System Hierarchical Levels with Climate change Integration

The availability of PV system components and subsystem may be affected by climate related stresses and their impact towards the reliability may affect the entire power system. Therefore, a holistic framework for the reliability evaluation of a PV integrated power system incorporating impacts of climate change and subsequent changes on the components is proposed in chapter 7. The proposed framework is significant toward power system operation and planning strategies as it represents a realistic method by incorporating components' failure, thermal stress factors, aging and degradation.

The framework results suggest that the reliability of a PV integrated power system decreases due to the impacts of climate change and the effects are noticeable over the long run. However, the decrements are inconsistent due to lifetime and aging degradation effects of macro level components in the PV system. Sensitivity analyses indicate that some components may be affected significantly by the thermal stresses than others, leading to a reduction in the entire system's reliability. For example, the IGBT and capacitor are identified as critical components in a PV system that disturb the reliability performance of a PV system mostly and they are sensitive to thermal stresses of climate change effects. The reliability performance reduction of the components varies from 1% to 5.5 % due to the stresses of the temperature leading to a higher force outage rate.

The sensitivity analyses of the availability of PV system components is found a quite minor effect for the temperatures 20 oC and 30 oC, but the availability threshold decreases when the temperature reaches 44 oC and higher. The analyses demonstrated that replacing the

inverter and converter one year before the end-of-life could improve the entire system's reliability by 6%. This emphasises the robustness required in the designed components and the appropriateness of applying remedial actions in the events of stress on components.

The results highlight the importance of the proposed framework toward the reliability improvement of the PV system components with consideration of future climate effect. The findings reported from results shed new light to the identification of critical components and subsystems within a PV system that lead to climate-associated failure. Policies and incentives can be initiated to ensure that the climate change effect and related stress do not adversely affect the PV components availability and future power system reliability. The obtained assessment results could assist power system operators in long-term planning. The proposed methodology offers a way of mitigating the impact of climate change on PV systems through proactive design and the application of maintenance strategies for averting progressive component failure initiated by the effects of climate change.

Overall, the proposed assessment methodologies throughout this thesis have investigated the long-term climate change effects on power system reliability with PV system and/or wind farms; and the hierarchical of the PV system. The long-term climate impacts on renewable energy integration are significant and reflect on the power system reliability in such a way that it requires a change of strategy for the power utilities. Climate change is expected to effect the PV system and wind farm and the effect become more severe from 2020 to 2080 with respect to the emission scenarios while high emission scenario will have higher impact on the reliability of both PV and wind power generation as described in chapter 4 and 5. Integration of wind farms may have less climate impact than PV system over long-term and climate change should be adapted on safety borders in the design and operation of wind turbines as revealed in chapter 6.

The effect of thermal stress on PV system components availability is major leading to higher force outage rate and therefore reduction in entire system reliability as exposed in chapter 7. This accentuates the robustness required in the designed components and the appropriateness of applying corrective actions for averting the components' failure initiated by the effects of climate change. Inclusive evaluation of climate effect in future power system reliability is continuously required due to the uncertainty associated with climate. The right strategy for utilities to consider the techniques, outcomes, and the effect of climate change on the power system reliability can lead to substantial reliability improvement. This thesis has provided deeper insight, allowing power system planners to take into account the effect of climate change in their planning process that involve wind and PV power generation Therefore, greater efforts must be made to mitigate the climate effect on power system reliability - by strengthening the need for thorough reliability assessments, vulnerability analysis for climate related stress, encouraging planning strategies, consider robustness in the components designed and cutting the GHG emissions and implement the carbon capture and storage.

## 8.3 Future Research

There are several suggestions for future work based on the work presented in this thesis. The suggested future work is categorised into framework development or applicatory extensions.

- A new climate model of UKCP18 with higher resolution and more accurate weather factors at small scale 2.5 Km, could be used for impact assessment and will be available to researchers by end of 2020. In addition, more geographic locations can be included in the impact assessment for comparison i.e. south of England, Midland and Scotland. It would be appropriate to include different geographic location in the study for a more practical reliability assessment and to allow the power industries to response the climate

impact on renewable within the UK for power strategies and planning. Moreover, the use of additional high-resolution RCMs and GCMs would be beneficial in understanding the uncertainty in future climate change. This will enhance the confidence level in climate change simulation and the proposed framework.

- The proposed framework with hierarchical levels of PV systems could be extended and applied to other renewable power generation to assess their reliability performance with climate effect. The hierarchical levels of the renewable power generation can be formed considering components, subsystems, whole system and/or the power grid level. This would reveal methodology to mitigate the impacts of climate on renewable power generation components and further improve the system reliability.
- In this thesis, the reliability assessment is carried out taking into consideration PV and Wind power generation systems with climate change effect. However, it would be valuable to extend the research to investigate the complex interactions between renewable energy including PV, wind, hydro geothermal, and solar thermal energy with considering future climate change. It would be appropriate to include these complexities in the study for a more practical and comprehensive reliability assessment
- The framework can be further improved by including the improvement in future technologies and the effect of climate on electricity demand in parallel with impact in power generation. This can be achieved by modelling reliability data of future PV system technology along with applying the long-term climate simulation in the future demand. This would be significant for strategies of power planning.

# References


[1] M. Čepin, *Assessment of power system reliability: methods and applications*: Springer Science & Business Media, 2011.

[2] "City of Dallas news," [Online], 29 July, 2020. Available: http://www.dallascitynews.net/ .

[3] "Azerbaijan Press," [Online], 29 July, 2020. Available : https://www.rferl.org/.

[4] O. Edenhofer, R. Pichs-Madruga, Y. Sokona, K. Seyboth, S. Kadner, T. Zwickel, P. Eickemeier, G. Hansen, S. Schlömer, and C. von Stechow, *Renewable energy sources and climate change mitigation: Special report of the intergovernmental panel on climate change*: Cambridge University Press, 2011.

[5] W. Li, *Risk assessment of power systems: models, methods, and applications*: John Wiley & Sons, 2014.

[6] C. Fant, B. Boehlert, K. Strzepek, P. Larsen, A. White, S. Gulati, Y. Li, and J. Martinich, "Climate change impacts and costs to US electricity transmission and distribution infrastructure," *Energy,* vol. 195, pp. 1-11, 2020.

[7] NASA. "Global Climate Change by NASA," [Online], July, 2019. Available: https://climate.nasa.gov.

[8] K. Ohlenforst, and G. W. E. Council, "Global Wind Report 2018," Recuperado, 2019.

[9] "UK Energy Statistics, Q2 2019," Department for Business, Energy and Industrial Strategies, 2019.

[10] K. Solaun, and E. Cerdá, "Climate change impacts on renewable energy generation. A review of quantitative projections," *Renewable and Sustainable Energy Reviews,* vol. 116, pp. 1-16, 2019.

[11] P. Zhang, W. Li, S. Li, Y. Wang, and W. Xiao, "Reliability assessment of photovoltaic power systems: Review of current status and future perspectives," *Applied Energy,* vol. 104, pp. 822-833, 2013.

[12] D. Burnett, E. Barbour, and G. P. Harrison, "The UK solar energy resource and the impact of climate change," *Renewable Energy,* vol. 71, pp. 333-343, 2014.

[13] M. Panteli, and P. Mancarella, "Modeling and evaluating the resilience of critical electrical power infrastructure to extreme weather events," *IEEE Systems Journal*, vol.11, No.3, pp.1733-1742, 2015.

[14] M. Davis, and S. Clemmer, "Power failure: How climate change puts our electricity at risk—and what we can do," *Union of Concerned Scientists*, 2014.

[15] J. Wachsmuth, A. Blohm, S. Gößling-Reisemann, T. Eickemeier, M. Ruth, R. Gasper, and S. Stührmann, "How will renewable power generation be affected by climate change? The case of a Metropolitan Region in Northwest Germany," *Energy,* vol. 58, pp. 192-201, 2013.

[16] P. Wang, and R. Billinton, "Reliability cost/worth assessment of distribution systems incorporating time-varying weather conditions and restoration resources," *IEEE Transactions on Power Delivery,* vol. 17, no. 1, pp. 260-265, 2002.

[17] H. E. Murdock, R. Adib, C. Lins, F. Guerra, A. Misra, L. Vickery, U. Collier, P. Le Feuvre, E. Bianco, and S. Mueller, "Renewable Energy Policies in a Time of Transition," IAEA, 2018.

[18] F. Urban, and T. Mitchell, "Climate change, disasters and electricity generation," Strengthening Climate Resilience Discucssion Paper No.8, 2011.

[19] S. N. Rezaei, L. Chouinard, S. Langlois, and F. Légeron, "Analysis of the effect of climate change on the reliability of overhead transmission lines," *Sustainable Cities and Society,* vol. 27, pp. 137-144, 2016.

[20] M. R. Allen, S. J. Fernandez, J. S. Fu, and M. M. Olama, "Impacts of climate change on sub-regional electricity demand and distribution in the southern United States," *Nature Energy,* vol. 1, no. 8, pp. 16103, 2016.

[21] N. NERC, "Operating Manual,"Glossary of Terms Used in Reliability Standards" [Online], July, 2020. Available: https://nerc.ukri.org/.

[22] W. Li, *Reliability assessment of electric power systems using Monte Carlo methods*: Springer Science & Business Media, 2013.
[23] R. Billington, and R. N. Allan, “Reliability evaluation of power systems: Springer Science & Business Media 1984.
[24] R. Billinton, and W. Li, "Basic concepts of power system reliability evaluation," *Reliability Assessment of Electric Power systems Using Monte Carlo Methods*, pp. 9-31: Springer, 1994.
[25] C. T. Force, ” *Power System Reliability Analysis-Composite Power System Reliability Evaluation,*" *Cigre Publication*, 1992.
[26] R. Billinton, and R. N. Allan, “Power-system reliability in perspective,” *Electronics and Power,* vol. 30, no. 3, pp. 231-236, 1984.
[27] R. Billinton, *Power system reliability evaluation*: Taylor & Francis, 1970.
[28] R. Allan, “Power system reliability assessment—A conceptual and historical review,” *Reliability Engineering & System Safety,* vol. 46, no. 1, pp. 3-13, 1994.
[29] R. E. Brown, *Electric power distribution reliability*: CRC press, 2017.
[30] Transmission, and D. Committee, “IEEE Guide for Electric Power Distribution Reliability Indices,” *IEEE Std 1366™-2003*, 2003.
[31] P. S. E. Committee, “Reliability indices for use in bulk power supply adequacy evaluation,” *IEEE Transactions on Power Apparatus and Systems*, no. 4, pp. 1097-1103, 1978.
[32] C. Singh, P. Jirutitijaroen, and J. Mitra, *Electric power grid reliability evaluation: models and methods*: John Wiley & Sons, 2018.
[33] R. Billinton, and R. N. Allan, "Reliability Evaluation of Power Systems: Springer Science & Business Media, 1996.
[34] I. Marneris, P. Biskas, and A. Bakirtzis, “Stochastic and deterministic unit commitment considering uncertainty and variability reserves for high renewable integration,” *Energies,* vol. 10, no. 1, pp. 140, 2017.
[35] D. AlAli, H. Griffiths, L. Cipcigan, and A. Haddad, “Assessment of line overloading risk for transmission networks,” In 11th IET International Conference on AC and DC Power Transmission, IET, 2015, pp. 1-6.
[36] D. Elmakias, *New computational methods in power system reliability*: Springer Science & Business Media, 2008.
[37] R. Allan, A. L. Da Silva, A. Abu-Nasser, and R. Burchett, “Discrete convolution in power system reliability,” *IEEE Transactions on Reliability,* vol. 30, no. 5, pp. 452-456, 1981.
[38] M. Mazundar, and D. Gaver, “A comparison of algorithms for computing power generating system reliability indices,” *IEEE Transactions on Power Apparatus and Systems*, vol. 41, no. 1, pp. 92-99, 1984.
[39] R. Chanda, and P. Bhattacharjee, “A reliability approach to transmission expansion planning using fuzzy fault-tree model,” *Electric Power Systems Research,* vol. 45, no. 2, pp. 101-108, 1998.
[40] V. Khare, S. Nema, and P. Baredar, “Reliability analysis of hybrid renewable energy system by fault tree analysis,” *Energy & Environment,* vol. 30, no. 3, pp. 542-555, 2019.
[41] J. Hanes, and R. P. Wiegand, “Analytical and Evolutionary Methods for Finding Cut Volumes in Fault Trees Constrained by Location,” *IEEE Transactions on Reliability*, vol. 68, no. 4, pp1214-1226, 2019.
[42] Y.-Y. Hong, and L.-H. Lee, “Reliability assessment of generation and transmission systems using fault-tree analysis,” *Energy Conversion and Management,* vol. 50, no. 11, pp. 2810-2817, 2009.
[43] S. Patra, K. Soman, and R. Misra, “Event tree analysis of a power system using Bayesian and fuzzy set approach,” *Journal-Institution of Engineers India Part Et Electronics and Telecommunications Engineering Division*, pp. 11-18, 1995.

[44] F. P. García Márquez, I. Segovia Ramírez, and A. Pliego Marugán, “Decision Making using Logical Decision Tree and Binary Decision Diagrams: A Real Case Study of Wind Turbine Manufacturing,” *Energies,* vol. 12, no. 9, pp. 1753, 2019.
[45] A. Pregelj, M. Begovic, and A. Rohatgi, "Impact of inverter configuration on PV system reliability and energy production." In the 29th IEEE Photovoltic Specialists Conference, IEEE, 2010, pp. 1388-1391.
[46] T. Vrana, and E. Johansson, “Overview of power system reliability assessment techniques,” *CIGRE 2011*, pp. 51-62, 2011.
[47] A. S. Dobakhshari, and M. Fotuhi-Firuzabad, “A reliability model of large wind farms for power system adequacy studies,” *IEEE Transactions on Energy Conversion,* vol. 24, no. 3, pp. 792-801, 2009.
[48] R. Billinton, and Y. Gao, “Multistate wind energy conversion system models for adequacy assessment of generating systems incorporating wind energy,” *IEEE Transactions on Energy Conversion,* vol. 23, no. 1, pp. 163-170, 2008.
[49] R. Karki, and R. Billinton, “Cost-effective wind energy utilization for reliable power supply,” *IEEE Transactions on Energy Conversion,* vol. 19, no. 2, pp. 435-440, 2004.
[50] R. Billinton, H. Chen, and R. Ghajar, “A sequential simulation technique for adequacy evaluation of generating systems including wind energy,” *IEEE Transactions on Energy Conversion,* vol. 11, no. 4, pp. 728-734, 1996.
[51] P. Hu, “Reliability evaluation of electric power system including wind power and energy storage,” University of Saskatchewan, 2009.
[52] A. A. Kadhem, N. I. A. Wahab, I. Aris, J. Jasni, and A. N. Abdalla, “Computational techniques for assessing the reliability and sustainability of electrical power systems: A review,” *Renewable and Sustainable Energy Reviews,* vol. 80, pp. 1175-1186, 2017.
[53] R. Billinton, and L. Gan, “Use of Monte Carlo simulation in teaching generating capacity adequacy assessment,” *IEEE Transactions on Power Systems,* vol. 6, no. 4, pp. 1571-1577, 1991.
[54] A. Almutairi, M. H. Ahmed, and M. Salama, “Probabilistic generating capacity adequacy evaluation: Research roadmap,” *Electric Power Systems Research,* vol. 129, pp. 83-93, 2015.
[55] C. L. Borges, and D. M. Falcão, "Power system reliability by sequential Monte Carlo simulation on multicomputer platforms." In International Conference on Vector and Parallel Processing, Springer, Berlin, 2000, pp. 242-253.
[56] B. S. Dhillon, *Applied reliability and quality: fundamentals, methods and procedures*: Springer Science & Business Media, 2007.
[57] G. J. Anders, “Probability concepts in electric power systems,” U.S. Department of Energy, 1989.
[58] R. H. M. Zargar, and M. H. Y. Moghaddam, “Development of a Markov-Chain-Based Solar Generation Model for Smart Micro-grid Energy Management System,” *IEEE Transactions on Sustainable Energy*, vol. 11, no. 2, pp. 736-745, 2019.
[59] K. Hou, H. Jia, X. Xu, Z. Liu, and Y. Jiang, “A continuous time Markov chain based sequential analytical approach for composite power system reliability assessment,” *IEEE Transactions on Power Systems,* vol. 31, no. 1, pp. 738-748, 2015.
[60] V. Tyagi, N. A. Rahim, N. A. Rahim, A. Jeyraj, and L. Selvaraj, “Progress in solar PV technology: Research and achievement,” *Renewable and sustainable energy reviews,* vol. 20, pp. 443-461, 2013.
[61] A. Sangwongwanich, Y. Yang, D. Sera, and F. Blaabjerg, “Lifetime evaluation of grid-connected PV inverters considering panel degradation rates and installation sites,” *IEEE Transactions on Power Electronics,* vol. 33, no. 2, pp. 1225-1236, 2017.
[62] T. E. Hoff, and R. Perez, “Modeling PV fleet output variability,” *Solar Energy,* vol. 86, no. 8, pp. 2177-2189, 2012.

[63] A. Sayed, M. EL-Shimy, M. El-Metwally, and M. Elshahed, “Impact of subsystems on the overall system availability for the large scale grid-connected photovoltaic systems,” *Reliability Engineering & System Safety,* vol. 196, pp. 106742, 2020.
[64] R. A. Shayani, and M. A. G. de Oliveira, “A new index for absolute comparison of standalone photovoltaic systems installed at different locations,” *IEEE Transactions on Sustainable Energy,* vol. 2, no. 4, pp. 495-500, 2011.
[65] M. Mahmud, H. Pota, and M. Hossain, “Nonlinear current control scheme for a single-phase grid-connected photovoltaic system,” *IEEE Transactions on Sustainable Energy,* vol. 5, no. 1, pp. 218-227, 2013.
[66] A. Bonfiglio, M. Brignone, F. Delfino, and R. Procopio, “Optimal control and operation of grid-connected photovoltaic production units for voltage support in medium-voltage networks,” *IEEE Transactions on Sustainable Energy,* vol. 5, no. 1, pp. 254-263, 2013.
[67] L. Hassaine, E. OLias, J. Quintero, and V. Salas, “Overview of power inverter topologies and control structures for grid connected photovoltaic systems,” *Renewable and Sustainable Energy Reviews,* vol. 30, pp. 796-807, 2014.
[68] Y. Yang, H. Wang, A. Sangwongwanich, and F. Blaabjerg, "Design for reliability of power electronic systems," *Power Electronics Handbook*, pp. 1423-1440: Elsevier, 2018.
[69] Y. Wang, P. Zhang, W. Li, and N. H. Kan'an, "Comparative analysis of the reliability of grid-connected photovoltaic power systems." In IEEE Power and Energy Society General Metting, IEEE, 2012, pp. 1-8.
[70] R. M. Moharil, and P. S. Kulkarni, “Reliability analysis of solar photovoltaic system using hourly mean solar radiation data,” *Solar Energy,* vol. 84, no. 4, pp. 691-702, 2010.
[71] R. Billinton, “Generating capacity adequacy evaluation of small stand-alone power systems containing solar energy,” *Reliability Engineering & System Safety,* vol. 91, no. 4, pp. 438-443, 2006.
[72] D. Jayaweera, and S. Islam, “Security of energy supply with change in weather conditions and dynamic thermal limits,” *IEEE Transactions on Smart Grid,* vol. 5, no. 5, pp. 2246-2254, 2014.
[73] L. Cristaldi, M. Khalil, and M. Faifer, “Markov process reliability model for photovoltaic module failures,” *ACTA IMEKO,* vol. 6, no. 4, pp. 121-130, 2017.
[74] L. Cristaldi, M. Khalil, M. Faifer, and P. Soulatiantork, "Markov process reliability model for photovoltaic module encapsulation failures." In International Conference on Renewable Energy Research and Applications, IEEE, 2015, pp. 203-208.
[75] E. Collins, M. Dvorack, J. Mahn, M. Mundt, and M. Quintana, "Reliability and availability analysis of a fielded photovoltaic system."In IEEE 34th Photovoltic Specialists Conference, IEEE,2009, pp. 2316-2321.
[76] H. H. El-Tamaly, and A. A. E. Mohammed, “Impact of interconnection photovoltaic/wind system with utility on their reliability using a fuzzy scheme,” *Renewable Energy,* vol. 31, no. 15, pp. 2475-2491, 2006.
[77] S. V. Dhople, A. Davoudi, P. L. Chapman, and A. D. Domínguez-García, "Integrating photovoltaic inverter reliability into energy yield estimation with Markov models." pp. 1-5.
[78] S. V. Dhople, and A. D. Domínguez-García, “Estimation of photovoltaic system reliability and performance metrics,” *IEEE Transactions on Power Systems,* vol. 27, no. 1, pp. 554-563, 2011.
[79] Z. Esau, and D. Jayaweera, “Reliability assessment in active distribution networks with detailed effects of PV systems,” *Journal of Modern Power Systems and Clean Energy,* vol. 2, no. 1, pp. 59-68, 2014.
[80] S. Peyghami, H. Wang, P. Davari, and F. Blaabjerg, "Mission profile based power converter reliability analysis in a DC power electronic based power system." In IEEE Energy Conversion Congress and Exposition, IEEE, 2018, pp. 4122-4128.

[81] S. E. De Leon-Aldaco, H. Calleja, F. Chan, and H. R. Jimenez-Grajales, “Effect of the mission profile on the reliability of a power converter aimed at photovoltaic applications—a case study,” *IEEE Transactions on Power Electronics,* vol. 28, no. 6, pp. 2998-3007, 2012.

[82] S. Sulaeman, M. Benidris, and J. Mitra, "Modeling and assessment of PV solar plants for composite system reliability considering radiation variability and component availability." iN IEEE Power Ssystem Computation Conference, IEEE, 2016, pp. 1-8.

[83] A. Ristow, M. Begovic, A. Pregelj, and A. Rohatgi, “Development of a methodology for improving photovoltaic inverter reliability,” *IEEE Transactions on Industrial Electronics,* vol. 55, no. 7, pp. 2581-2592, 2008.

[84] P. D. Reigosa, H. Wang, Y. Yang, and F. Blaabjerg, “Prediction of bond wire fatigue of IGBTs in a PV inverter under a long-term operation,” *IEEE Transactions on Power Electronics,* vol. 31, no. 10, pp. 7171-7182, 2015.

[85] J. H. Wohlgemuth, D. W. Cunningham, P. Monus, J. Miller, and A. Nguyen, "Long term reliability of photovoltaic modules." In 4th World Conference on Photovoltaic Energy, IEEE, 2006, pp. 2050-2053.

[86] N. G. Dhere, N. Shiradkar, E. Schneller, and V. Gade, "The reliability of bypass diodes in PV modules." In International Society for Optics and Photonics, SPIE, 2013, pp. 88-94.

[87] F. Chan, and H. Calleja, “Reliability estimation of three single-phase topologies in grid-connected PV systems,” *IEEE Transactions on Industrial Electronics,* vol. 58, no. 7, pp. 2683-2689, 2010.

[88] P. Zhang, Y. Wang, W. Xiao, and W. Li, “Reliability evaluation of grid-connected photovoltaic power systems,” *IEEE Transactions on Sustainable Energy,* vol. 3, no. 3, pp. 379-389, 2012.

[89] S. E. De León-Aldaco, H. Calleja, and J. A. Alquicira, “Reliability and mission profiles of photovoltaic systems: A FIDES approach,” *IEEE Transactions on Power Electronics,* vol. 30, no. 5, pp. 2578-2586, 2014.

[90] D. o. Defense, *Reliability prediction of electronic equipment*: Departement of Defense, 1991.

[91] S. Beeson, and J. D. Andrews, “Importance measures for noncoherent-system analysis,” *IEEE Transactions on Reliability,* vol. 52, no. 3, pp. 301-310, 2003.

[92] H. Wang, D. Zhou, and F. Blaabjerg, "A reliability-oriented design method for power electronic converters.", In 28th IEEE Applied Power Electronic Conference and Exposition, IEEE, 2013, pp. 2921-2928.

[93] S. Tao, C. Li, L. Zhang, and Y. Tang, “Operational Risk Assessment of Grid-connected PV System Considering Weather Variability and Component Availability,” *Energy Procedia,* vol. 145, pp. 252-258, 2018.

[94] X. Chu, Y. Zhu, J. Shi, and J. Song, "Method of image segmentation based on fuzzy C-means clustering algorithm and artificial fish swarm algorithm." In International Conference on Intelligent Computing and Integrated System, IEEE, 2010, pp. 254-257.

[95] S.-T. Cha, D.-H. Jeon, I.-S. Bae, and I.-R. Lee, "Reliability evaluation of distribution system connected photovoltaic generation considering weather effects." In Internnational Conference on Intelligent Computing and Integrated System, IEEE, 2010, pp. 451-456.

[96] J. Park, W. Liang, J. Choi, A. El-Keib, M. Shahidehpour, and R. Billinton, "A probabilistic reliability evaluation of a power system including solar/photovoltaic cell generator." In IEEE Power & Energy Society General Metting, IEEE, 2009, pp. 1-6.

[97] H. Wang, N. Zhu, and X. Bai, “Reliability model assessment of grid-connected solar photovoltaic system based on Monte-Carlo,” *Applied Solar Energy,* vol. 51, no. 4, pp. 262-266, 2015.

[98] P. B. Eriksen, T. Ackermann, H. Abildgaard, P. Smith, W. Winter, and J. R. Garcia, “System operation with high wind penetration,” *IEEE Power and Energy Magazine,* vol. 3, no. 6, pp. 65-74, 2005.

[99] P. Zhou, R. Jin, and L. Fan, “Reliability and economic evaluation of power system with renewables: A review,” *Renewable and Sustainable Energy Reviews,* vol. 58, pp. 537-547, 2016.
[100] S. Zhang, G. Li, and M. Zhou, "Calculation and analysis of capacity credit of wind farms based on Monte-Carlo simulation." In IEEE PES General Meeting, IEEE, 2010, pp. 1-6.
[101] A. Van Wijk, N. Halberg, and W. Turkenburg, “Capacity credit of wind power in the Netherlands,” *Electric Power Systems Research,* vol. 23, no. 3, pp. 189-200, 1992.
[102] "The Wind Power and UK Wind Speed Database programs: Wind Turbine Characteristics." [Online], June, 2020. Available: https://www.renewableuk.com/
[103] T. Ackermann, *Wind power in power systems*: John Wiley & Sons, 2005.
[104] Z. Gao, P. Wang, and J. Wang, "Impacts of energy storage on reliability of power systems with WTGs." In 11th International Conference on probabilistic Methods Applied to Power Systems, IEEE, 2010, pp. 65-70.
[105] P. Giorsetto, and K. F. Utsurogi, “Development of a new procedure for reliability modeling of wind turbine generators,” *IEEE Transactions on Power Apparatus and Systems*, no. 1, pp. 134-143, 1983.
[106] C. Singh, and A. Lago-Gonzalez, “Reliability modeling of generation systems including unconventional energy sources,” *IEEE Transactions on Power Apparatus and Systems*, no. 5, pp. 1049-1056, 1985.
[107] R. Billinton, and G. Bai, “Generating capacity adequacy associated with wind energy,” *IEEE Transactions on Energy Conversion,* vol. 19, no. 3, pp. 641-646, 2004.
[108] S. Wang, Y. Chen, W. Liu, Z. Liu, X. Chen, and Q. Chen, "A multistate model of wind farm in mountainous land considering ice coating." In 43rd Annual Conference of the IEEE Industrial Electronics Society, IEEE, 2017, pp. 2344-2349.
[109] A. Ghaedi, A. Abbaspour, M. Fotuhi-Firuzabad, and M. Moeini-Aghtaie, “Toward a comprehensive model of large-scale DFIG-based wind farms in adequacy assessment of power systems,” *IEEE Transactions on Sustainable Energy,* vol. 5, no. 1, pp. 55-63, 2013.
[110] N. Nguyen, S. Almasabi, and J. Mitra, “Impact of correlation between wind speed and turbine availability on wind farm reliability,” *IEEE Transactions on Industry Applications,* vol. 55, no. 3, pp. 2392-2400, 2019.
[111] T. Manco, and A. Testa, "A Markovian approach to model power availability of a wind turbine." In IEEE Lausanne Power, IEEE, 2007, pp. 1256-1261.
[112] H. Kim, and C. Singh, "Three dimensional clustering in wind farms with storage for reliability analysis." In IEEE Grenoble Conference, IEEE, 2013, pp. 1-6.
[113] M. A. Abdullah, K. M. Muttaqi, A. P. Agalgaonkar, and D. Sutanto, “A noniterative method to estimate load carrying capability of generating units in a renewable energy rich power grid,” *IEEE Transactions on Sustainable Energy,* vol. 5, no. 3, pp. 854-865, 2014.
[114] X. Liu, S. Islam, A. Chowdhury, and D. Koval, "Reliability evaluation of a wind-diesel-battery hybrid power system." In IEEE Industrial and Commerical Power System Technical Conference, IEEE, 2008, pp. 1-8.
[115] L. Cradden, D. Burnett, A. Agarwal, and G. Harrison, “Climate change impacts on renewable electricity generation,” *Infrastructure Asset Management,* vol. 2, no. 3, pp. 131-142, 2015.
[116] R. Karki, P. Hu, and R. Billinton, “A simplified wind power generation model for reliability evaluation,” *IEEE Transactions on Energy Conversion,* vol. 21, no. 2, pp. 533-540, 2006.
[117] N. B. Negra, O. Holmstrom, B. Bak-Jensen, and P. Sorensen, “Aspects of relevance in offshore wind farm reliability assessment,” *IEEE Transactions on Energy Conversion,* vol. 22, no. 1, pp. 159-166, 2007.
[118] D. Zhou, F. Blaabjerg, T. Franke, M. Tonnes, and M. Lau, “Reduced cost of reactive power in doubly fed induction generator wind turbine system with optimized grid filter,” *IEEE Transactions on Power Electronics,* vol. 30, no. 10, pp. 5581-5590, 2014.

[119] R. Cardenas, R. Peña, S. Alepuz, and G. Asher, “Overview of control systems for the operation of DFIGs in wind energy applications,” *IEEE Transactions on Industrial Electronics,* vol. 60, no. 7, pp. 2776-2798, 2013.
[120] J. Chivite-Zabalza, C. Gironés, A. Cárcar, I. Larrazabal, E. Olea, and M. Zabaleta, "Comparison of power conversion topologies for a multi-megawatt off-shore wind turbine, based on commercial power electronic building blocks." In 39th Annual Conference of the IEEE Industrial Electronics Society, IEEE, 2013, pp. 5242-5247.
[121] Y. Zhang, and S. Ula, "Comparison and evaluation of three main types of wind turbines." In IEEE/PES Tranmission and Distribution Conference, IEEE, 2008, pp. 1-6.
[122] J. Carroll, A. McDonald, and D. McMillan, “Reliability comparison of wind turbines with DFIG and PMG drive trains,” *IEEE Transactions on Energy Conversion,* vol. 30, no. 2, pp. 663-670, 2015.
[123] D. Zhou, F. Blaabjerg, T. Franke, M. Tønnes, and M. Lau, “Comparison of wind power converter reliability with low-speed and medium-speed permanent-magnet synchronous generators,” *IEEE Transactions on Industrial Electronics,* vol. 62, no. 10, pp. 6575-6584, 2015.
[124] F. Wang, J. Chen, B. Xu, and K. A. Stelson, “Improving the reliability and energy production of large wind turbine with a digital hydrostatic drivetrain,” *Applied Energy,* vol. 251, pp. 1-15, 2019.
[125] J. Carroll, A. McDonald, and D. McMillan, “Failure rate, repair time and unscheduled O&M cost analysis of offshore wind turbines,” *Wind Energy,* vol. 19, no. 6, pp. 1107-1119, 2016.
[126] F. Spinato, P. J. Tavner, G. J. Van Bussel, and E. Koutoulakos, “Reliability of wind turbine subassemblies,” *IET Renewable Power Generation,* vol. 3, no. 4, pp. 387-401, 2009.
[127] B. Hahn, M. Durstewitz, and K. Rohrig, "Reliability of wind turbines," *Wind energy*, pp. 329-332: Springer, 2007.
[128] C. Crabtree, Y. Feng, and P. Tavner, "Detecting incipient wind turbine gearbox failure: a signal analysis method for on-line condition monitoring." In European Wind Energy Conference,EWEC, 2008, pp. 154-156.
[129] M. Wilkinson, G. Hassan, S. Vincent, S. Lane, B. Bs, T. Van Delft, and K. Harman, “The effect of environmental parameters on wind turbine reliability,” *EWEA 2012*, pp. 174-178, 2012.
[130] A. P. Leite, C. L. Borges, and D. M. Falcao, “Probabilistic wind farms generation model for reliability studies applied to Brazilian sites,” *IEEE Transactions on Power Systems,* vol. 21, no. 4, pp. 1493-1501, 2006.
[131] H. Chao, B. Hu, K. Xie, H.-M. Tai, J. Yan, and Y. Li, “A Sequential MCMC Model for Reliability Evaluation of Offshore Wind Farms Considering Severe Weather Conditions,” *IEEE Access,* vol. 7, pp. 132552-132562, 2019.
[132] E. Byon, L. Ntaimo, and Y. Ding, “Optimal maintenance strategies for wind turbine systems under stochastic weather conditions,” *IEEE Transactions on Reliability,* vol. 59, no. 2, pp. 393-404, 2010.
[133] P. Tavner, R. Gindele, S. Faulstich, B. Hahn, M. Whittle, and D. Greenwood, "Study of effects of weather & location on wind turbine failure rates." In European Wind Energy Conference, EWEC, 2010, PP.1-6.
[134] "special report on the impacts of global warming of 1.5 C above pre-industrial levels and related global greenhouse gas emission pathways." In Intergovermental Panel in Climate Change, 2018.
[135] P. S. Molly Hellmuth, Judsen Bruzgul, Dana Spindler, and Heidi Pacini, *Assessment of Climate Change Risks to Energy Reliability in the WECC Region*, Washington, DC, 2014.
[136] K. E. Trenberth, K. Miller, L. Mearns, and S. Rhodes, *Effects of changing climate on weather and human activities*, University Science Books Sausalito, CA, 2000.
[137] "IPCC Fifth Assessment Report (AR5)," In Intergovernmental Panel on Climate Change, 2014.

[138] T. Stocker, *Climate change 2013: the physical science basis: Working Group I contribution to the Fifth assessment report of the Intergovernmental Panel on Climate Change*: Cambridge University Press, 2014.
[139] M. Sethi, *Climate change and urban settlements: A spatial perspective of carbon footprint and beyond*: Routledge, 2017.
[140] J. B. Smith, and D. A. Tirpak, *The potential effects of global climate change on the United States*: Office of Policy, Planning and Evaluation, US Environmental Protection Agency, 1989.
[141] M. Ranson, L. Morris, and A. Kats-Rubin, *Climate change and space heating energy demand: A review of the literature*." National Centre for Envrmental Economcs, US Environmenal Protection Agency, Vol. 216, pp.08-268, 2014.
[142] E. League, P. Kabat, P. Egerton, O. Baddour, L. Paterson, C. Nullis, S. Castonguay, and M. Walsh, "United in Science: High-level Synthesis Report of Latest Climate Science Information convened by the Science Advisory Group of the UN Climate Action Summit 2019," 2019.
[143] ESRL, "Earth System Research Laboratory." [Online], May, 2020,. Available: https://www.esrl.noaa.gov/
[144] R. Rasmussen, and M. Khalil, "Atmospheric trace gases: trends and distributions over the last decade," *Science,* vol. 232, no. 4758, pp. 1623-1624, 1986.
[145] N. Nakicenovic, J. Alcamo, A. Grubler, K. Riahi, R. Roehrl, H.-H. Rogner, and N. Victor, *Special report on emissions scenarios (SRES), a special report of Working Group III of the intergovernmental panel on climate change*: Cambridge University Press, 2000.
[146] B. Girod, A. Wiek, H. Mieg, and M. Hulme, "The evolution of the IPCC's emissions scenarios," *Environmental Science & Policy,* vol. 12, no. 2, pp. 103-118, 2009.
[147] N. W. Arnell, "Climate change and global water resources: SRES emissions and socio-economic scenarios," *Global Environmental Change,* vol. 14, no. 1, pp. 31-52, 2004.
[148] R. J. Nicholls, and R. S. Tol, "Impacts and responses to sea-level rise: a global analysis of the SRES scenarios over the twenty-first century," *Philosophical Transactions of the Royal Society A: Mathematical, Physical and Engineering Sciences,* vol. 364, no. 1841, pp. 1073-1095, 2006.
[149] R. Knutti, T. F. Stocker, F. Joos, and G.-K. Plattner, "Constraints on radiative forcing and future climate change from observations and climate model ensembles," *Nature,* vol. 416, no. 6882, pp. 719, 2002.
[150] C. Jones, E. Robertson, V. Arora, P. Friedlingstein, E. Shevliakova, L. Bopp, V. Brovkin, T. Hajima, E. Kato, and M. Kawamiya, "Twenty-first-century compatible CO2 emissions and airborne fraction simulated by CMIP5 earth system models under four representative concentration pathways," *Journal of Climate,* vol. 26, no. 13, pp. 4398-4413, 2013.
[151] Y. Ishizaki, H. Shiogama, S. Emori, T. Yokohata, T. Nozawa, T. Ogura, M. Abe, M. Yoshimori, and K. Takahashi, "Temperature scaling pattern dependence on representative concentration pathway emission scenarios," *Climatic Change,* vol. 112, no. 2, pp. 535-546, 2012.
[152] H.-J. Baek, J. Lee, H.-S. Lee, Y.-K. Hyun, C. Cho, W.-T. Kwon, C. Marzin, S.-Y. Gan, M.-J. Kim, and D.-H. Choi, "Climate change in the 21st century simulated by HadGEM2-AO under representative concentration pathways," *Asia-Pacific Journal of Atmospheric Sciences,* vol. 49, no. 5, pp. 603-618, 2013.
[153] D. P. Van Vuuren, J. Edmonds, M. Kainuma, K. Riahi, A. Thomson, K. Hibbard, G. C. Hurtt, T. Kram, V. Krey, and J.-F. Lamarque, "The representative concentration pathways: an overview," *Climatic change,* vol. 109, no. 1-2, pp. 5, 2011.
[154] J. T. Payne, A. W. Wood, A. F. Hamlet, R. N. Palmer, and D. P. Lettenmaier, "Mitigating the effects of climate change on the water resources of the Columbia River basin," *Climatic Change,* vol. 62, no. 1-3, pp. 233-256, 2004.
[155] A. Venäläinen, B. Tammelin, H. Tuomenvirta, K. Jylhä, J. Koskela, M. A. Turunen, B. Vehviläinen, J. Forsius, and P. Järvinen, "The influence of climate change on energy

production & heating energy demand in Finland," *Energy & Environment,* vol. 15, no. 1, pp. 93-109, 2004.
[156] N. L. Miller, K. Hayhoe, J. Jin, and M. Auffhammer, "Climate, extreme heat, and electricity demand in California," *Journal of Applied Meteorology and Climatology,* vol. 47, no. 6, pp. 1834-1844, 2008.
[157] S. Kulkarni, M. Deo, and S. Ghosh, "Evaluation of wind extremes and wind potential under changing climate for Indian offshore using ensemble of 10 GCMs," *Ocean & Coastal Management,* vol. 121, pp. 141-152, 2016.
[158] H. Kikumoto, R. Ooka, Y. Arima, and T. Yamanaka, "Study on the future weather data considering the global and local climate change for building energy simulation," *Sustainable Cities and Society,* vol. 14, pp. 404-413, 2015.
[159] G. S. Mohor, D. A. Rodriguez, J. Tomasella, and J. L. S. Júnior, "Exploratory analyses for the assessment of climate change impacts on the energy production in an Amazon run-of-river hydropower plant," *Journal of Hydrology: Regional Studies,* vol. 4, pp. 41-59, 2015.
[160] L. Gaudard, J. Gabbi, A. Bauder, and F. Romerio, "Long-term uncertainty of hydropower revenue due to climate change and electricity prices," *Water resources management,* vol. 30, no. 4, pp. 1325-1343, 2016.
[161] A. Miara, J. E. Macknick, C. J. Vörösmarty, V. C. Tidwell, R. Newmark, and B. Fekete, "Climate and water resource change impacts and adaptation potential for US power supply," *Nature Climate Change,* vol. 7, no. 11, pp. 793-798, 2017.
[162] R. L. Wilby, and T. Wigley, "Downscaling general circulation model output: a review of methods and limitations," *Progress in Physical Geography,* vol. 21, no. 4, pp. 530-548, 1997.
[163] C. Frei, R. Schöll, S. Fukutome, J. Schmidli, and P. L. Vidale, "Future change of precipitation extremes in Europe: Intercomparison of scenarios from regional climate models," *Journal of Geophysical Research: Atmospheres,* vol. 111, no. D6, 2006.
[164] S. Solomon, "IPCC (2007): Climate change the physical science basis." In Intergvernmental Panel On Climate Change, 2007, PP. 01-47.
[165] R. Pašičko, Č. Branković, and Z. Šimić, "Assessment of climate change impacts on energy generation from renewable sources in Croatia," *Renewable Energy,* vol. 46, pp. 224-231, 2012.
[166] G. J. Jenkins, J. M. Murphy, D. M. Sexton, J. A. Lowe, P. Jones, and C. G. Kilsby, "UK Climate Projections briefing report," [Online], July, 2020. Available: http://cedadocs.ceda.ac.uk/ .
[167] F. Feser, B. Rockel, H. von Storch, J. Winterfeldt, and M. Zahn, "Regional climate models add value to global model data: a review and selected examples," *Bulletin of the American Meteorological Society,* vol. 92, no. 9, pp. 1181-1192, 2011.
[168] M. Rummukainen, "State-of-the-art with regional climate models," *Wiley Interdisciplinary Reviews: Climate Change,* vol. 1, no. 1, pp. 82-96, 2010.
[169] M. Allen, P. Antwi-Agyei, F. Aragon-Durand, M. Babiker, P. Bertoldi, M. Bind, S. Brown, M. Buckeridge, I. Camilloni, and A. Cartwright, "Technical Summary: Global warming of 1.5° C. An IPCC Special Report on the impacts of global warming of 1.5° C above pre-industrial levels and related global greenhouse gas emission pathways, in the context of strengthening the global response to the threat of climate change, sustainable development, and efforts to eradicate poverty," December, 2019, [Online]. Available: http://pure.iiasa.ac.at/id/eprint/.
[170] J. Ospina Norena, C. Gay García, A. Conde, and G. SÁNCHEZ TORRES ESQUEDA, "A proposal for a vulnerability index for hydroelectricity generation in the face of potential climate change in Colombia," *Atmósfera,* vol. 24, no. 3, pp. 329-346, 2011.
[171] H. Koch, S. Vögele, F. F. Hattermann, and S. Huang, "The impact of climate change and variability on the generation of electrical power," *Meteorologische Zeitschrift,* vol. 24, no. 2, pp. 173, 2015.

[172] M. Zhu, Y. Pan, Z. Huang, and P. Xu, "An alternative method to predict future weather data for building energy demand simulation under global climate change," *Energy and Buildings,* vol. 113, pp. 74-86, 2016.
[173] V. Klimenko, E. Fedotova, and A. Tereshin, "Vulnerability of the Russian power industry to the climate change," *Energy,* vol. 142, pp. 1010-1022, 2018.
[174] I. Staffell, and S. Pfenninger, "The increasing impact of weather on electricity supply and demand," *Energy,* vol. 145, pp. 65-78, 2018.
[175] I. Popescu, L. Brandimarte, and M. Peviani, "Effects of climate change over energy production in La Plata Basin," *International Journal of River Basin Management,* vol. 12, no. 4, pp. 319-327, 2014.
[176] Q. Zhou, N. Hanasaki, S. Fujimori, S. Yoshikawa, S. Kanae, and T. Okadera, "Cooling water sufficiency in a warming world: Projection using an integrated assessment model and a global hydrological model," *Water,* vol. 10, no. 7, pp. 872, 2018.
[177] "Climate Change Risks & Adaptation Responses for UK Electricity Generation: A Sector Overview 2015," *Energy UK, London*, 2015.
[178] P. Berry, M. Rounsevell, P. Harrison, and E. Audsley, "Assessing the vulnerability of agricultural land use and species to climate change and the role of policy in facilitating adaptation," *Environmental Science & Policy,* vol. 9, no. 2, pp. 189-204, 2006.
[179] R. Contreras-Lisperguer, and K. de Cuba, "The potential impact of climate change on the energy sector in the Caribbean region," *Organization of American States, Washington DC*, 2008.
[180] J. Skea, and R. Moreno, "Industry, energy, and transportation: impacts and adaptation," IPCC *Climate change*, pp. 365-398, 1995.
[181] J. McFarland, Y. Zhou, L. Clarke, P. Sullivan, J. Colman, W. S. Jaglom, M. Colley, P. Patel, J. Eom, and S. H. Kim, "Impacts of rising air temperatures and emissions mitigation on electricity demand and supply in the United States: a multi-model comparison," *Climatic Change,* vol. 131, no. 1, pp. 111-125, 2015.
[182] "Electricity networks climate change adaptation report," *Engineering Rep*, 2011, [Online], June, 2017. Available: https://assets.publishing.service.gov.uk
[183] J. Cronin, G. Anandarajah, and O. Dessens, "Climate change impacts on the energy system: a review of trends and gaps," *Climatic Change,* vol. 151, no. 2, pp. 79-93, 2018.
[184] M. Panteli, and P. Mancarella, "Influence of extreme weather and climate change on the resilience of power systems: Impacts and possible mitigation strategies," *Electric Power Systems Research,* vol. 127, pp. 259-270, 2015.
[185] R. Schaeffer, A. S. Szklo, A. F. P. de Lucena, B. S. M. C. Borba, L. P. P. Nogueira, F. P. Fleming, A. Troccoli, M. Harrison, and M. S. Boulahya, "Energy sector vulnerability to climate change: a review," *Energy,* vol. 38, no. 1, pp. 1-12, 2012.
[186] M. New, D. Lister, M. Hulme, and I. Makin, "A high-resolution data set of surface climate over global land areas," *Climate Research,* vol. 21, no. 1, pp. 1-25, 2002.
[187] T. K. Mideksa, and S. Kallbekken, "The impact of climate change on the electricity market: A review," *Energy Policy,* vol. 38, no. 7, pp. 3579-3585, 2010.
[188] S. Jerez, I. Tobin, R. Vautard, J. P. Montávez, J. M. López-Romero, F. Thais, B. Bartok, O. B. Christensen, A. Colette, and M. Déqué, "The impact of climate change on photovoltaic power generation in Europe," *Nature Communications,* vol. 6, pp. 10014, 2015.
[189] S. N. Chandramowli, and F. A. Felder, "Impact of climate change on electricity systems and markets–a review of models and forecasts," *Sustainable Energy Technologies and Assessments,* vol. 5, pp. 62-74, 2014.
[190] H. J. Hovel, "Solar cells," *NASA STI/Recon Technical Report A,* vol. 76, 1975.
[191] A. Razak, Y. Irwan, W. Leow, M. Irwanto, I. Safwati, and M. Zhafarina, "Investigation of the effect temperature on photovoltaic (PV) panel output performance," *International Journal*

*on Advanced Science, Engineering and Information Technology,* vol. 6, no. 5, pp. 682-688, 2016.
[192] D. Thevenard, and S. Pelland, "Estimating the uncertainty in long-term photovoltaic yield predictions," *Solar Energy,* vol. 91, pp. 432-445, 2013.
[193] M. Wild, D. Folini, F. Henschel, N. Fischer, and B. Müller, "Projections of long-term changes in solar radiation based on CMIP5 climate models and their influence on energy yields of photovoltaic systems," *Solar Energy,* vol. 116, pp. 12-24, 2015.
[194] I. Huber, L. Bugliaro, M. Ponater, H. Garny, C. Emde, and B. Mayer, "Do climate models project changes in solar resources?," *Solar Energy,* vol. 129, pp. 65-84, 2016.
[195] F. Mavromatakis, E. Kavoussanaki, F. Vignola, and Y. Franghiadakis, "Measuring and estimating the temperature of photovoltaic modules," *Solar Energy,* vol. 110, pp. 656-666, 2014.
[196] P. C. Johnston, *Climate risk and adaptation in the electric power sector*: Asian Development Bank, 2012.
[197] A. Patt, S. Pfenninger, and J. Lilliestam, "Vulnerability of solar energy infrastructure and output to climate change," *Climatic Change,* vol. 121, no. 1, pp. 93-102, 2013.
[198] C. A. Gueymard, and S. M. Wilcox, "Assessment of spatial and temporal variability in the US solar resource from radiometric measurements and predictions from models using ground-based or satellite data," *Solar Energy,* vol. 85, no. 5, pp. 1068-1084, 2011.
[199] Z. Pan, M. Segal, R. W. Arritt, and E. S. Takle, "On the potential change in solar radiation over the US due to increases of atmospheric greenhouse gases," *Renewable Energy,* vol. 29, no. 11, pp. 1923-1928, 2004.
[200] J. A. Crook, L. A. Jones, P. M. Forster, and R. Crook, "Climate change impacts on future photovoltaic and concentrated solar power energy output," *Energy & Environmental Science,* vol. 4, no. 9, pp. 3101-3109, 2011.
[201] I. S. Panagea, I. K. Tsanis, A. G. Koutroulis, and M. G. Grillakis, "Climate change impact on photovoltaic energy output: the case of Greece," *Advances in Meteorology,* vol. 2014, 2014.
[202] D. Carvalho, A. Rocha, M. Gómez-Gesteira, and C. S. Santos, "Potential impacts of climate change on European wind energy resource under the CMIP5 future climate projections," *Renewable Energy,* vol. 101, pp. 29-40, 2017.
[203] S. Pryor, and R. Barthelmie, "Assessing the vulnerability of wind energy to climate change and extreme events," *Climatic Change,* vol. 121, no. 1, pp. 79-91, 2013.
[204] K. Solaun, and E. Cerdá, "Impacts of climate change on wind energy power–Four wind farms in Spain," *Renewable Energy,* vol. 145, pp. 1306-1316, 2020.
[205] S. Pryor, and R. Barthelmie, "Assessing climate change impacts on the near-term stability of the wind energy resource over the United States," *Proceedings of the National Academy of Sciences,* vol. 108, no. 20, pp. 8167-8171, 2011.
[206] R. Vautard, J. Cattiaux, P. Yiou, J.-N. Thépaut, and P. Ciais, "Northern Hemisphere atmospheric stilling partly attributed to an increase in surface roughness," *Nature Geoscience,* vol. 3, no. 11, pp. 756-761, 2010.
[207] S. C. Pryor, and R. Barthelmie, "Climate change impacts on wind energy: A review," *Renewable and Sustainable Energy Reviews,* vol. 14, no. 1, pp. 430-437, 2010.
[208] S. Greene, M. Morrissey, and S. E. Johnson, "Wind climatology, climate change, and wind energy," *Geography Compass,* vol. 4, no. 11, pp. 1592-1605, 2010.
[209] S. Pryor, and R. Barthelmie, "Climate change impacts on wind energy: A review," *Renewable and Sustainable Energy Reviews,* vol. 14, no. 1, pp. 430-437, 2010.
[210] T. Laakso, H. Holttinen, G. Ronsten, L. Tallhaug, R. Horbaty, I. Baring-Gould, A. Lacroix, E. Peltola, and B. Tammelin, "State-of-the-art of wind energy in cold climates," *IEA annex XIX,* vol. 24, pp. 15-24, 2003.

[211] W. Jasinski, S. Noe, M. Selig, M. Bragg, W. Jasinski, S. Noe, M. Selig, and M. Bragg, "Wind turbine performance under icing conditions." Solar and Energy Engineering- Transaction vol. 1, No. 1, pp. 60-65, 1998.
[212] P. Sarajčev, and R. Goić, "A review of current issues in state-of-art of wind farm overvoltage protection," *Energies,* vol. 4, no. 4, pp. 644-668, 2011.
[213] S. Shahid, "Vulnerability of the power sector of Bangladesh to climate change and extreme weather events," *Regional Environmental Change,* vol. 12, no. 3, pp. 595-606, 2012.
[214] G. P. Harrison, and A. R. Wallace, "Climate sensitivity of marine energy," *Renewable Energy,* vol. 30, no. 12, pp. 1801-1817, 2005.
[215] R. Baker, S. Walker, and J. Wade, "Annual and seasonal variations in mean wind speed and wind turbine energy production," *Solar Energy,* vol. 45, no. 5, pp. 285-289, 1990.
[216] D. J. Sailor, M. Smith, and M. Hart, "Climate change implications for wind power resources in the Northwest United States," *Renewable Energy,* vol. 33, no. 11, pp. 2393-2406, 2008.
[217] L. C. Cradden, G. P. Harrison, and J. P. Chick, "Will climate change impact on wind power development in the UK?," *Climatic Change,* vol. 115, no. 3-4, pp. 837-852, 2012.
[218] H. Hueging, R. Haas, K. Born, D. Jacob, and J. G. Pinto, "Regional changes in wind energy potential over Europe using regional climate model ensemble projections," *Journal of Applied Meteorology and Climatology,* vol. 52, no. 4, pp. 903-917, 2013.
[219] S. E. Haupt, J. Copeland, W. Y. Cheng, Y. Zhang, C. Ammann, and P. Sullivan, "A method to assess the wind and solar resource and to quantify interannual variability over the united states under current and projected future climate," *Journal of Applied Meteorology and Climatology,* vol. 55, no. 2, pp. 345-363, 2016.
[220] I. Tobin, R. Vautard, I. Balog, F.-M. Bréon, S. Jerez, P. M. Ruti, F. Thais, M. Vrac, and P. Yiou, "Assessing climate change impacts on European wind energy from ENSEMBLES high-resolution climate projections," *Climatic Change,* vol. 128, no. 1-2, pp. 99-112, 2015.
[221] D. Hdidouan, and I. Staffell, "The impact of climate change on the levelised cost of wind energy," *Renewable Energy,* vol. 101, pp. 575-592, 2017.
[222] I. Barstad, A. Sorteberg, and M. d.-S. Mesquita, "Present and future offshore wind power potential in northern Europe based on downscaled global climate runs with adjusted SST and sea ice cover," *Renewable Energy,* vol. 44, pp. 398-405, 2012.
[223] I. Tobin, S. Jerez, R. Vautard, F. Thais, E. Van Meijgaard, A. Prein, M. Déqué, S. Kotlarski, C. F. Maule, and G. Nikulin, "Climate change impacts on the power generation potential of a European mid-century wind farms scenario," *Environmental Research Letters,* vol. 11, no. 3, pp. 1-6, 2016.
[224] A. Ahadi, N. Ghadimi, and D. Mirabbasi, "Reliability assessment for components of large scale photovoltaic systems," *Journal of Power Sources,* vol. 264, pp. 211-219, 2014.
[225] S. Sulaeman, M. Benidris, and J. Mitra, "Modeling and assessment of PV solar plants for composite system reliability considering radiation variability and component availability." In Power System Computation Conference,IEEE ,2016, pp. 1-8.
[226] D. Jayaweera, and S. Islam, "Risk of supply insecurity with weather condition-based operation of plug in hybrid electric vehicles," *IET Generation, Transmission & Distribution,* vol. 8, no. 12, pp. 2153-2162, 2014.
[227] A. Ghaedi, A. Abbaspour, M. Fotuhi-Friuzabad, and M. Parvania, "Incorporating large photovoltaic farms in power generation system adequacy assessment," *Scientia Iranica. Transaction D, Computer Science & Engineering, Electrical,* vol. 21, no. 3, pp. 924, 2014.
[228] A. Altamimi, and D. Jayaweera, "Reliability performances of grid-integrated PV systems with varying climatic conditions." In IET International Conference on Resilience of Traansmission and Distribution Network. IET, 2017, pp. 1-6.
[229] "Weather Generators at UK climate projection 2009," UKCP09, [Online], September, 2016. Available: https://www.metoffice.gov.uk

[230] P. Jones, C. Kilsby, C. Harpham, V. Glenis, and A. Burton, “UK Climate Projections science report: Projections of future daily climate for the UK from the Weather Generator,” UKCP09, 2009.
[231] C. Correa-Betanzo, H. Calleja, and S. De León-Aldaco, “Module temperature models assessment of photovoltaic seasonal energy yield,” *Sustainable Energy Technologies and Assessments,* vol. 27, pp. 9-16, 2018.
[232] C. Grigg, P. Wong, P. Albrecht, R. Allan, M. Bhavaraju, R. Billinton, Q. Chen, C. Fong, S. Haddad, and S. Kuruganty, “The IEEE reliability test system-1996. A report prepared by the reliability test system task force of the application of probability methods subcommittee,” *IEEE Transactions on Power Systems,* vol. 14, no. 3, pp. 1010-1020, 1999.
[233] M. Vázquez, and I. Rey-Stolle, “Photovoltaic module reliability model based on field degradation studies,” *Progress in photovoltaics: Research and Applications,* vol. 16, no. 5, pp. 419-433, 2008.
[234] “Reliability test system task force, The IEEE reliability test system-1996,” *IEEE Trans. Power Syst,* vol. 14, no. 3, pp. 1010-1020, 1999.
[235] D. o. E. C. Change. "UK Renewable Energy Roadmap Update 2013," [Online], December, 2017. Available: https://www.gov.uk/government/uploads/.
[236] A. Altamimi, and D. Jayaweera, “Reliability Performances of Grid-Integrated PV Systems with Varying Climatic Conditions,” In IET International Conference on Resilience of Traansmission and Distribution Network. IET, 2017, pp. 1-6.
[237] "World Climate Research Program Coordinated Regional Downscaling Experiment EURO." Regional Environmental Change, vol. 12, no. 2, pp 563-578, 2014.
[238] A. Altamimi, and D. Jayaweera, "Long-Term Reliability Impacts of a Power System with Climate Change Effects on Wind Farms." In PES Innovative Smart Grid Technologies Conference Europ, IEEE, 2018, pp. 1-6.
[239] D. Jacob, J. Petersen, B. Eggert, A. Alias, O. B. Christensen, L. M. Bouwer, A. Braun, A. Colette, M. Déqué, and G. Georgievski, “EURO-CORDEX: new high-resolution climate change projections for European impact research,” *Regional Environmental Change,* vol. 14, no. 2, pp. 563-578, 2014.
[240] G. Wayne, “The beginner’s guide to representative concentration pathways,” *Skeptical Science,* vol. 25, pp. 1-6, 2013.
[241] M. Safeeq, and A. Fares, “Accuracy evaluation of ClimGen weather generator and daily to hourly disaggregation methods in tropical conditions,” *Theoretical and Applied Climatology,* vol. 106, no. 3-4, pp. 321-341, 2011.
[242] J. M. P. Pérez, F. P. G. Márquez, A. Tobias, and M. Papaelias, “Wind turbine reliability analysis,” *Renewable and Sustainable Energy Reviews,* vol. 23, pp. 463-472, 2013.
[243] L. Xu, and Y. Wang, “Dynamic modeling and control of DFIG-based wind turbines under unbalanced network conditions,” *IEEE Transactions on Power Systems,* vol. 22, no. 1, pp. 314-323, 2007.
[244] Y. Lei, A. Mullane, G. Lightbody, and R. Yacamini, “Modeling of the wind turbine with a doubly fed induction generator for grid integration studies,” *IEEE Transactions on Energy Conversion,* vol. 21, no. 1, pp. 257-264, 2006.
[245] R. Billinton, and S. Jonnavithula, “A test system for teaching overall power system reliability assessment,” *IEEE Transactions on Power Systems,* vol. 11, no. 4, pp. 1670-1676, 1996.
[246] Y. Liu, and C. Singh, “A methodology for evaluation of hurricane impact on composite power system reliability,” *IEEE Transactions on Power Systems,* vol. 26, no. 1, pp. 145-152, 2011.
[247] F. Xiao, J. D. McCalley, Y. Ou, J. Adams, and S. Myers, "Contingency probability estimation using weather and geographical data for on-line security assessment." In International Conference on Probabilistic Methods Applied to Power System, IEEE, 2006, pp.1-6.
[248] X. Li, and H. Wang, "Operation risk assessment of wind farm integrated system influenced by weather conditions." In IEEE Power & Energy Society General Metting, IEEE, 2013, pp. 1-5.

[249] R. Billinton, and G. Singh, “Application of adverse and extreme adverse weather: modelling in transmission and distribution system reliability evaluation,” *IEE Proceedings-Generation, Transmission and Distribution,* vol. 153, no. 1, pp. 115-120, 2006.
[250] R. Billinton, and J. Acharya, "Consideration of multi-state weather models in reliability evaluation of transmission and distribution systems." In Canadian Conference on Electrical and Computer Engineering, IEEE, 2005, pp. 916-922.
[251] A. Altamimi, Peju Oyewole, and Dilan Jayaweera, "Future Power System Study Models With Stochastic Climate Changes Imposed on Wind and PV Power generation." In IEEE PES Smart Grid Saudi Arabia, IEEE, 2018, pp. 1-6.
[252] Q. Xu, Y. Xu, P. Tu, T. Zhao, and P. Wang, “Systematic reliability modeling and evaluation for on-board power systems of more electric aircrafts,” *IEEE Transactions on Power Systems,* vol. 34, no. 4, pp. 3264-3273, 2019.
[253] A. Altamimi, and a. D. Jayaweera, “Reliability of Power Systems with Climate Change Impacts on Hierarchical Levels of PV Systems,” *Electric Power Systems Research*, 2020.
[254] M. S. Alvarez-Alvarado, and D. Jayaweera, “Bathtub curve as a Markovian process to describe the reliability of repairable components,” *IET Generation, Transmission & Distribution,* vol. 12, no. 21, pp. 5683-5689, 2018.
[255] T. J. Formica, H. A. Khan, and M. G. Pecht, “The effect of inverter failures on the return on investment of solar photovoltaic systems,” *IEEE Access,* vol. 5, pp. 21336-21343, 2017.
[256] J. D. Flicker, and R. Kaplar, *Reliability of Power Conversion Systems in Photovoltaic Applications*, Sandia National Lab.(SNL-NM), Albuquerque, NM (United States), 2015.
[257] M. Salcone, and J. Bond, "Selecting film bus link capacitors for high performance inverter applications." In IEEE International Electric Machines and Drives Conference, IEEE, 2009, pp. 1692-1699.
[258] S. Yang, A. Bryant, P. Mawby, D. Xiang, L. Ran, and P. Tavner, “An industry-based survey of reliability in power electronic converters,” *IEEE Transactions on Industry Applications,* vol. 47, no. 3, pp. 1441-1451, 2011.
[259] S. V. Dhople, A. Davoudi, A. D. Domínguez-García, and P. L. Chapman, “A unified approach to reliability assessment of multiphase DC–DC converters in photovoltaic energy conversion systems,” *IEEE Transactions on Power Electronics,* vol. 27, no. 2, pp. 739-751, 2010.
[260] M. Piri, M. Niroomand, and R.-A. Hooshmand, “A comprehensive reliability assessment of residential photovoltaic systems,” *journal of renewable and sustainable energy,* vol. 7, no. 5, pp. 1-8 , 2015.
[261] M. S. Alvarez-Alvarado, and D. Jayaweera, "Aging Reliability Model for Generation Adequacy." In IEEE International Conference on Power Systems, IEEE, 2018, pp. 1-6.
[262] J. Choi, J. Park, M. Shahidehpour, and R. Billinton, "Assessment of CO 2 reduction by renewable energy generators." In Innovative Smart Grid Technologies Conference, IEEE, 2010, pp. 1-5.

# Appendices

## Appendix A: IEEE Reliability Test System (IEEE-RTS)

This section provides information about the IEEE Reliability Test System (IEEE-RTS), which was utilised for demonstrating the use of the proposed frameworks introduced in Chapter 4 and Chapter 6. Figure A1 presents a schematic of the test system, and system parameters are listed in Tables A1, A2, A3, and A4 [232].

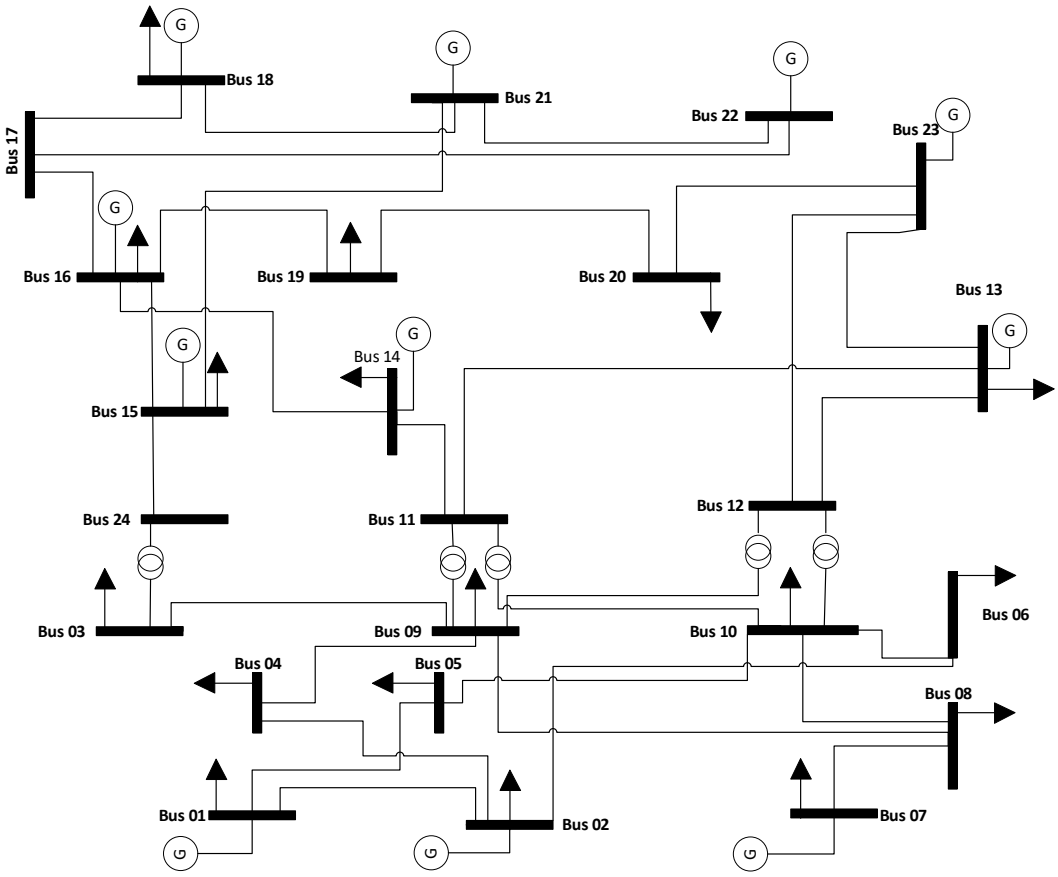


Figure A1. IEEE-RTS Reliability Test System (IEEE-RTS)

Table A1. IEEE-RTS generator reliability data

| Unit Group | Unit Size (MW) | Unit Type | Forced Outage Rate | MTTF (Hours) | MTTR (Hours) | Scheduled Maintenance Weeks per year |
|---|---|---|---|---|---|---|
| U12 | 12 | Oil/Steam | 0.02 | 2940 | 60 | 2 |
| U20 | 20 | Oil/CT | 0.10 | 450 | 50 | 2 |
| U50 | 50 | Hydro | 0.01 | 1980 | 20 | 2 |
| U76 | 76 | Coal/Steam | 0.02 | 1960 | 40 | 3 |
| U100 | 100 | Oil/Steam | 0.04 | 1200 | 50 | 3 |
| U155 | 155 | Coal/Steam | 0.04 | 960 | 40 | 4 |
| U197 | 197 | Oil/Steam | 0.05 | 950 | 50 | 4 |
| U350 | 350 | Coal/Steam | 0.08 | 1150 | 100 | 5 |
| U400 | 400 | Nuclear | 0.12 | 1100 | 150 | 6 |

Table A2. IEEE-RTS bus load data

| Area/Bus Number | | | % of System Load | Load | |
|---|---|---|---|---|---|
| 1 | 2 | 3 | | MW | MVar |
| 101 | 201 | 301 | 3.8 | 108 | 22 |
| 102 | 202 | 302 | 3.4 | 97 | 20 |
| 103 | 203 | 303 | 6.3 | 180 | 37 |
| 104 | 204 | 304 | 2.6 | 74 | 15 |
| 105 | 205 | 305 | 2.5 | 71 | 14 |
| 106 | 206 | 306 | 4.8 | 136 | 28 |
| 107 | 207 | 307 | 4.4 | 125 | 25 |
| 108 | 208 | 308 | 6.0 | 171 | 35 |
| 109 | 209 | 309 | 6.1 | 175 | 36 |
| 110 | 210 | 310 | 6.8 | 195 | 40 |
| 113 | 213 | 313 | 9.3 | 265 | 54 |
| 114 | 214 | 314 | 6.8 | 194 | 39 |
| 115 | 215 | 315 | 11.1 | 317 | 64 |
| 116 | 216 | 316 | 3.5 | 100 | 20 |
| 118 | 218 | 318 | 11.7 | 333 | 68 |
| 119 | 219 | 319 | 6.4 | 181 | 37 |
| 120 | 220 | 320 | 4.5 | 128 | 26 |
| Total | | | 100 | 2850 | 580 |

Table A3. IEEE-RTS branch data

| ID # | From Bus | To Bus | R (p.u.) | X (p.u.) | B (p.u.) | CON (MVA) | LTE (MVA) | STE (MVA) | Tr (p.u.) |
|---|---|---|---|---|---|---|---|---|---|
| 1 | 1 | 2 | 0.003 | 0.14 | 0.461 | 175 | 193 | 200 | 0 |
| 2 | 1 | 3 | 0.055 | 0.211 | 0.057 | 175 | 208 | 220 | 0 |
| 3 | 1 | 5 | 0.022 | 0.085 | 0.023 | 175 | 208 | 220 | 0 |
| 4 | 2 | 4 | 0.033 | 0.127 | 0.034 | 175 | 208 | 220 | 0 |
| 5 | 2 | 6 | 0.05 | 0.192 | 0.052 | 175 | 208 | 220 | 0 |
| 6 | 3 | 9 | 0.031 | 0.119 | 0.032 | 175 | 208 | 220 | 0 |
| 7 | 3 | 24 | 0.002 | 0.084 | 0 | 400 | 510 | 600 | 1.015 |
| 8 | 4 | 9 | 0.027 | 0.104 | 0.028 | 175 | 208 | 220 | 0 |
| 9 | 5 | 10 | 0.023 | 0.088 | 0.024 | 175 | 208 | 220 | 0 |
| 10 | 6 | 10 | 0.014 | 0.061 | 2.459 | 175 | 193 | 200 | 0 |
| 11 | 7 | 8 | 0.016 | 0.061 | 0.017 | 175 | 208 | 220 | 0 |
| 12 | 8 | 9 | 0.043 | 0.165 | 0.045 | 175 | 208 | 220 | 0 |
| 13 | 8 | 10 | 0.043 | 0.165 | 0.045 | 175 | 208 | 220 | 0 |
| 14 | 9 | 11 | 0.0002 | 0.084 | 0 | 400 | 510 | 600 | 1.03 |
| 15 | 9 | 12 | 0.0002 | 0.084 | 0 | 400 | 510 | 600 | 1.03 |
| 16 | 10 | 11 | 0.0002 | 0.084 | 0 | 400 | 510 | 600 | 1.015 |
| 17 | 10 | 12 | 0.0002 | 0.084 | 0 | 400 | 510 | 600 | 1.015 |
| 18 | 11 | 13 | 0.006 | 0.048 | 0.1 | 500 | 600 | 625 | 0 |
| 19 | 11 | 14 | 0.005 | 0.042 | 0.088 | 500 | 600 | 625 | 0 |
| 20 | 12 | 13 | 0.006 | 0.048 | 0.1 | 500 | 600 | 625 | 0 |
| 22 | 12 | 23 | 0.012 | 0.097 | 0.203 | 500 | 600 | 625 | 0 |
| 23 | 13 | 23 | 0.011 | 0.087 | 0.182 | 500 | 600 | 625 | 0 |
| 24 | 15 | 16 | 0.002 | 0.017 | 0.036 | 500 | 600 | 625 | 0 |
| 25 | 15 | 21 | 0.006 | 0.049 | 0.103 | 500 | 600 | 625 | 0 |
| 26 | 15 | 21 | 0.006 | 0.049 | 0.103 | 500 | 600 | 625 | 0 |
| 27 | 15 | 24 | 0.007 | 0.052 | 0.109 | 500 | 600 | 625 | 0 |
| 28 | 16 | 17 | 0.003 | 0.026 | 0.055 | 500 | 600 | 625 | 0 |
| 29 | 16 | 19 | 0.003 | 0.023 | 0.049 | 500 | 600 | 625 | 0 |
| 30 | 17 | 18 | 0.002 | 0.014 | 0.03 | 500 | 600 | 625 | 0 |
| 31 | 17 | 22 | 0.014 | 0.105 | 0.221 | 500 | 600 | 625 | 0 |
| 32 | 18 | 21 | 0.003 | 0.026 | 0.055 | 500 | 600 | 625 | 0 |
| 33 | 18 | 21 | 0.003 | 0.026 | 0.055 | 500 | 600 | 625 | 0 |
| 34 | 19 | 20 | 0.005 | 0.04 | 0.083 | 500 | 600 | 625 | 0 |
| 35 | 19 | 20 | 0.005 | 0.04 | 0.083 | 500 | 600 | 625 | 0 |
| 36 | 20 | 23 | 0.003 | 0.022 | 0.046 | 500 | 600 | 625 | 0 |
| 37 | 20 | 23 | 0.003 | 0.022 | 0.046 | 500 | 600 | 625 | 0 |
| 38 | 21 | 22 | 0.009 | 0.068 | 0.142 | 500 | 600 | 625 | 0 |

CON = continuous rating

LTE = long-term emergency rating (24 hour)

STE = short-term emergency rating (15 min)

Tr = transformer off-nominal tap ratio

Table A4. IEEE-RTS branch reliability data

| ID # | From Bus | To Bus | Permanent $\lambda_p$ | Duration | Transient $\lambda_t$ |
|---|---|---|---|---|---|
| 1 | 1 | 2 | 0.24 | 16 | 0.0 |
| 2 | 1 | 3 | 0.51 | 10 | 2.9 |
| 3 | 1 | 5 | 0.33 | 10 | 1.2 |
| 4 | 2 | 4 | 0.39 | 10 | 1.7 |
| 5 | 2 | 6 | 0.48 | 10 | 2.6 |
| 6 | 3 | 9 | 0.38 | 10 | 1.6 |
| 7 | 3 | 24 | 0.02 | 768 | 0.0 |
| 8 | 4 | 9 | 0.36 | 10 | 1.4 |
| 9 | 5 | 10 | 0.34 | 10 | 1.2 |
| 10 | 6 | 10 | 0.33 | 35 | 0.0 |
| 11 | 7 | 8 | 0.30 | 10 | 0.8 |
| 12 | 8 | 9 | 0.44 | 10 | 2.3 |
| 13 | 8 | 10 | 0.44 | 10 | 2.3 |
| 14 | 9 | 11 | 0.02 | 768 | 0.0 |
| 15 | 9 | 12 | 0.02 | 768 | 0.0 |
| 16 | 10 | 11 | 0.02 | 768 | 0.0 |
| 17 | 10 | 12 | 0.02 | 768 | 0.0 |
| 18 | 11 | 13 | 0.40 | 11 | 0.8 |
| 19 | 11 | 14 | 0.39 | 11 | 0.7 |
| 20 | 12 | 13 | 0.40 | 11 | 0.8 |
| 22 | 12 | 23 | 0.52 | 11 | 1.6 |
| 23 | 13 | 23 | 0.49 | 11 | 1.5 |
| 24 | 15 | 16 | 0.33 | 11 | 0.3 |
| 25 | 15 | 21 | 0.41 | 11 | 0.8 |
| 26 | 15 | 21 | 0.41 | 11 | 0.8 |
| 27 | 15 | 24 | 0.41 | 11 | 0.9 |
| 28 | 16 | 17 | 0.35 | 11 | 0.4 |
| 29 | 16 | 19 | 0.34 | 11 | 0.4 |
| 30 | 17 | 18 | 0.32 | 11 | 0.2 |
| 31 | 17 | 22 | 0.54 | 11 | 1.8 |
| 32 | 18 | 21 | 0.35 | 11 | 0.4 |
| 33 | 18 | 21 | 0.35 | 11 | 0.4 |
| 34 | 19 | 20 | 0.38 | 11 | 0.7 |
| 35 | 19 | 20 | 0.38 | 11 | 0.7 |
| 36 | 20 | 23 | 0.34 | 11 | 0.4 |
| 37 | 20 | 23 | 0.34 | 11 | 0.4 |
| 38 | 21 | 22 | 0.45 | 11 | 1.3 |

# Appendix B: Roy Billinton Test System (RBTS)

This section provide the Roy Billinton Test System (RBTS) information that was employed for validating the proposed framework of Chapter 5 and 7 [245].

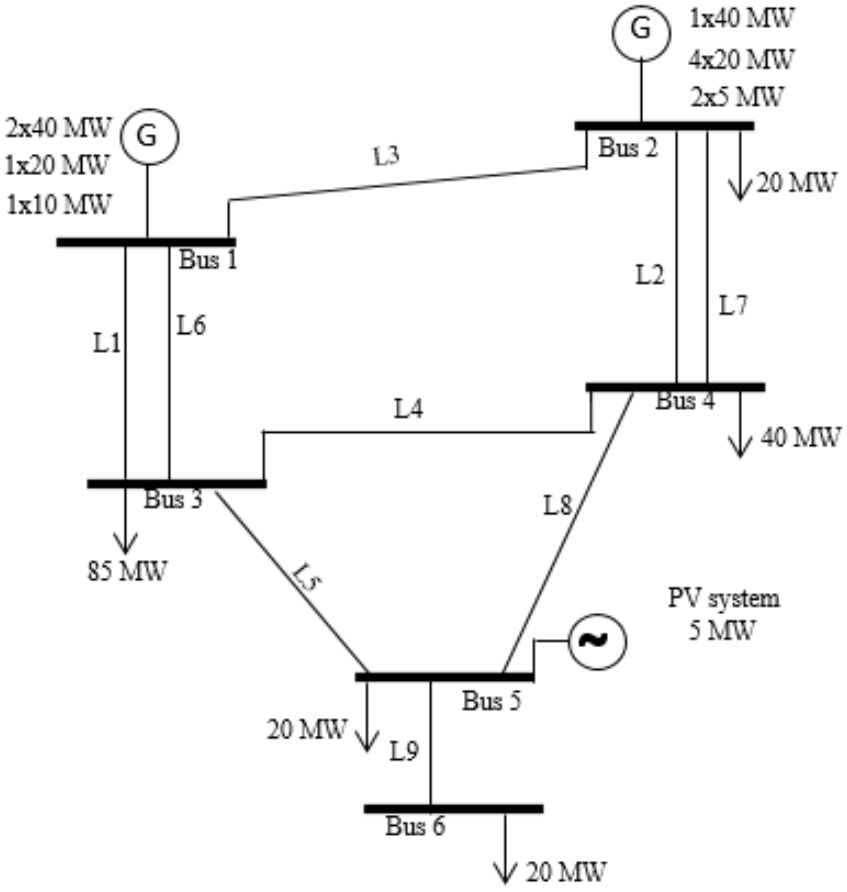


Figure B1. Roy Billinton Test System (RBTS)

Table B1 Load data for the RBTS

| Bus No. | Load | |
|---|---|---|
| | Active (MW) | Reactive (MVAR) |
| 1 | 0 | 0 |
| 2 | 20 | 7 |
| 3 | 85 | 28 |
| 4 | 40 | 13 |
| 5 | 20 | 7 |
| 6 | 20 | 7 |

Table B2 Line Data for the RBTS

| Line No. | Bus | | R | X | B/2 | Tap | Current Rating (p.u.) | Failure rate (occ/yr) | Repair rate (hrs) |
|---|---|---|---|---|---|---|---|---|---|
| | I | J | | | | | | | |
| 1 | 1 | 3 | 0.0342 | 0.1800 | 0.0106 | 1.00 | 0.85 | 1.50 | 10.0 |
| 2 | 2 | 4 | 0.1140 | 0.6000 | 0.0352 | 1.00 | 0.71 | 5.00 | 10.0 |
| 3 | 1 | 2 | 0.0912 | 0.4800 | 0.0282 | 1.00 | 0.71 | 4.00 | 10.0 |
| 4 | 3 | 4 | 0.0228 | 0.1200 | 0.0071 | 1.00 | 0.71 | 1.00 | 10.0 |
| 5 | 3 | 5 | 0.0228 | 0.1200 | 0.0071 | 1.00 | 0.71 | 1.00 | 10.0 |
| 6 | 1 | 3 | 0.0342 | 0.1800 | 0.0106 | 1.00 | 0.71 | 1.50 | 10.0 |
| 7 | 2 | 4 | 0.1140 | 0.6000 | 0.0352 | 1.00 | 0.85 | 5.00 | 10.0 |
| 8 | 4 | 5 | 0.0228 | 0.1200 | 0.0071 | 1.00 | 0.71 | 1.00 | 10.0 |
| 9 | 5 | 6 | 0.0228 | 0.1200 | 0.0071 | 1.00 | 0.71 | 1.00 | 10.0 |

Table B3 Generator data for the RBTS

| Unit No. | Bus No. | Rating (MW) |
|---|---|---|
| 1 | 1 | 40.0 |
| 2 | 1 | 40.0 |
| 3 | 1 | 10.0 |
| 4 | 1 | 20.0 |
| 5 | 2 | 5.0 |
| 6 | 2 | 5.0 |
| 7 | 2 | 40.0 |
| 8 | 2 | 20.0 |
| 9 | 2 | 20.0 |
| 10 | 2 | 20.0 |
| 11 | 2 | 20.0 |

# Appendix C: PV and Wind Power Generation Basic Profile

This appendix shows some of the basic simulated weather data that is used in this thesis. Table C1 shows the weather data which is simulated from the climate models for two days over February, 2030 for low emission scenarios and the generation profile for PV and wind power generation systems. The following steps are implemented to obtain the PV and wind power generation profiles.

I. Simulate the climate model of UKCP09 as on the procedure given on figure 4.4. The outcomes are a temperature ($C^O$) and solar irradiation ($W/m^2$) and other weather data for different emission scenarios over different years.

II. Simulate the climate model of EURO-CODEX using the steps given on figure 5.5. The outcomes are a wind speed over three hours at near surface level. Use the equations (5.1), (5.2) and (5.3) to interpolate the three hourly wind speed into hourly wind speed and to extrapolate the wind speed into turbine level.

III. Use the power generation model for both PV and wind power generation as given on equations (5.5), (5.6), (5.7), (5.8), (7.47), (7.48) and (7.49). This can be used over all emission scenarios over long-term.

C1: Basic weather data along with PV and Wind power generation system

| Day | Hours | Temperature ($C^O$) | solar irradiation ($W/m^2$) | Wind Speed (m/s) | PV Power (Kw) | Wind Power (Kw) |
|---|---|---|---|---|---|---|
| Day 1 | 0 | 5.8 | 0 | 12.61 | 0 | 98.31675 |
| | 100 | 6.3 | 0 | 12.95 | 0 | 85.37907 |
| | 200 | 6.7 | 0 | 13.30 | 0 | 87.15491 |
| | 300 | 6.3 | 0 | 13.63 | 0 | 93.34458 |
| | 400 | 5.8 | 0 | 13.39 | 0 | 88.8346 |
| | 500 | 6 | 0 | 13.14 | 0 | 84.41607 |
| | 600 | 6.1 | 0 | 12.89 | 0 | 80.09 |
| | 700 | 6.7 | 34.2 | 11.25 | 7.825381 | 54.25285 |
| | 800 | 6.9 | 94.2 | 9.54 | 59.37121 | 32.73208 |
| | 900 | 7.2 | 192.3 | 7.75 | 193.007 | 15.9948 |
| | 1000 | 7.5 | 233.4 | 8.00 | 234.2723 | 17.99508 |
| | 1100 | 7.8 | 259.2 | 8.25 | 260.1828 | 20.09656 |
| | 1200 | 7.9 | 256.6 | 8.50 | 257.5774 | 22.29724 |
| | 1300 | 8.2 | 217.2 | 8.75 | 218.0379 | 34.21842 |
| | 1400 | 8.5 | 195.8 | 9.00 | 196.5632 | 41.65036 |
| | 1500 | 8 | 121.9 | 9.24 | 99.44378 | 62.27236 |
| | 1600 | 7.9 | 48 | 8.26 | 15.41869 | 67.40293 |
| | 1700 | 7.7 | 5.2 | 7.26 | 0.18095 | 53.80333 |
| | 1800 | 7.5 | 0 | 6.21 | 0 | 41.49922 |
| | 1900 | 7.1 | 0 | 6.27 | 0 | 33.03482 |
| | 2000 | 7.1 | 0 | 6.33 | 0 | 15.98563 |
| | 2100 | 6.6 | 0 | 6.39 | 0 | 7.303428 |
| | 2200 | 7.1 | 0 | 6.77 | 0 | 9.398082 |
| | 2300 | 6.6 | 0 | 7.15 | 0 | 11.72486 |
| Day 2 | 0 | 6.2 | 0 | 7.52 | 0 | 14.27566 |
| | 100 | 5.8 | 0 | 7.72 | 0 | 15.81246 |

| | | | | | | |
|---|---|---|---|---|---|---|
| | 200 | 5.5 | 0 | 7.93 | 0 | 17.41719 |
| | 300 | 5 | 0 | 8.13 | 0 | 19.0887 |
| | 400 | 4.4 | 0 | 8.49 | 0 | 22.21746 |
| | 500 | 4.8 | 0 | 8.85 | 0 | 25.54773 |
| | 600 | 5.2 | 0 | 9.20 | 0 | 29.07434 |
| | 700 | 5.3 | 0.1 | 8.80 | 6.69E-05 | 25.15057 |
| | 800 | 5.7 | 0.1 | 8.41 | 6.69E-05 | 21.47215 |
| | 900 | 5.8 | 33.1 | 8.01 | 7.328119 | 30.64365 |
| | 1000 | 7 | 107.1 | 8.30 | 76.74733 | 33.70304 |
| | 1100 | 8.1 | 150.3 | 8.59 | 150.8782 | 36.88433 |
| | 1200 | 9.8 | 165.4 | 8.87 | 166.0594 | 40.18537 |
| | 1300 | 9.8 | 136 | 8.92 | 123.7985 | 40.74433 |
| | 1400 | 9.8 | 69.8 | 8.97 | 32.60998 | 41.30651 |
| | 1500 | 9.9 | 0.1 | 9.02 | 6.69E-05 | 41.87192 |
| | 1600 | 10 | 0 | 8.90 | 0 | 42.14143 |
| | 1700 | 9.5 | 0 | 8.79 | 0 | 56.04234 |
| | 1800 | 8.7 | 0 | 8.68 | 0 | 60.90069 |
| | 1900 | 7.3 | 0 | 9.03 | 0 | 78.86696 |
| | 2000 | 7.5 | 0 | 9.37 | 0 | 84.33721 |
| | 2100 | 7.4 | 0 | 9.71 | 0 | 89.9563 |
| | 2200 | 7 | 0 | 10.02 | 0 | 95.11187 |
| | 2300 | 6.7 | 0 | 10.31 | 0 | 78.58379 |